The multifaceted role of phosphatidylinositol-4-kinases beta in morphogenesis and defence responses of Arabidopsis thaliana

Anastasiia Starodubtseva

University of Chemistry and Technology, Prague

UNIVERSITÉ PARIS-EST, ÉCOLE DOCTORALE, Sciences de l'Univers et Environnement

Etude des multiples rôles des phosphatidylinositol-4-kinases betas dans la morphogenèse et les réponses de défense d'Arabidopsis thaliana

AUTEURE	Starodubtseva Anastasiia
SUPERVISEUSE	doc. Ing. Lenka Burketová, CSc.
SUPERVISEUR	Eric Ruelland, PhD
CONSULTANTE	MSc. Tetiana Kalachova, PhD Sciences
SPÉCIALITÉ	Sciences de l'Univers et Environnement
LA DATE DE SOUTENANCE	4 novembre 2022

LES NOMS ET PRENOMS DES MEMBRES DU JURY :

Rapporteur MARTINEC Jan

Rapportrice GUIVARCH Anne

Co-directeur de thèse RUELLAND Eric

Examinatrice VALENTOVA Olga

Co-directrice de thèse BURKETOVA Lenka

Examinateur PETŘIVALSKÝ Marek

University of Chemistry and Technology, Prague

University of Chemistry and Technology, Prague

UNIVERSITÉ PARIS-EST, ÉCOLE DOCTORALE, Sciences de l'Univers et Environnement

The multifaceted role of phosphatidylinositol-4-kinases in plant morphogenesis and defence responses

Génie Enzymatique et Cellulaire
Université de Technologie de Compiègne
Centre de Recherches
Rue Personne de Roberval
CS 60319, 60203 Compiègne Cedex France

Institute of Experimental Botany of the Czech Academy of Sciences
Laboratory of Pathological Plant Physiology
Rozvojová 313, 165 02 Praha 6 - Lysolaje, Česká republika

les mots clés en français: immunité des plantes, phospholipides, résistance non-hôte, récepteurs immunitaires, Phosphatidylinositol 4-kinase bêta

les mots clés en anglais: plant immunity, phospholipids, non-host resistance, immune receptors, Phosphatidylinositol 4-kinase beta

ABSTRACT

Plants adapt to changing environment by rapid adjustment of metabolic processes. One of the key regulatory hubs in plant cells is the vesicular trafficking, that ensures the correct and timely transport between plasma membrane and other cellular compartments. This is controlled by membrane phospholipid turnover, and executed by a tight cooperation of lipid kinases and phosphatases. Phosphatidylinositol 4-kinases (PI4Ks) are the first enzymes that commit phosphatidylinositol into the phosphoinositide pathway. Phosphoinositides (PPI) are the phosphorylated derivatives of phosphatidylinositol (PI), such as PI-4-phosphate (PI4P) and PI-4,5-bisphosphate (PI(4,5)P_2). The formation of membrane domains enriched in PI4P and PI(4,5)P_2 is a crucial component of plasma membrane dynamics. Besides, PI4P and PI(4,5)P_2 serve as substrates for enzymes, especially for PI-PLCs. Phosphoinositides can also act as ligands of many proteins via PPI-binding domains. In the *Arabidopsis thaliana* genome, twelve putative PI4K isoforms have been identified. Eight belong to type II and four belong to type III (*AtPI4Kα1* and *α2* and *AtPI4Kβ1* and *β2*). To study the role of the PI4Ks, I have worked with a double mutant defective plant in both the PI4Kβ genes. I have shown that the *pi4kβ1β2* double mutant exhibits several root phenotypes: impaired root growth, a lower sensitivity of roots to exogenous auxin, impaired gravistimulation, and misshapen root hair growth. These changes appeared to coincide with a less stable actin cytoskeleton and altered in intracellular trafficking dynamics in *pi4kβ1β2* roots. In the roots of this double mutant, gene expression was less responsive to exogenous auxin. These data, therefore, link altered PI4K activity to the modification of vesicular trafficking and actin filaments organization one the one hand to altered auxin response likely due to alteration in auxin homeostasis one the other hand. The second part of my thesis is related to the *Blumeria graminis* f. sp. *hordei* (*Bgh*) interaction with *pi4kβ1β2* double mutant. It is known that *A. thaliana* has non-host resistance to *Bgh*. Indeed, *A. thaliana* plants are able to form a special resistance structure - papillae - that acts as a barrier between fungi and plant cells. The *pi4kβ1β2* double mutant showed lower resistance to penetration of *Bgh* at 24 hpi (hour post inoculation). Here, I could show that the lack of PI4Kβ1β2 leads to a decreased accumulation of PI4P in the papillae. My hypothesis is that PI4Kβ1β2 are essential for the successful defense of the plant against *Bgh*, and more specifically for the formation of a successful papillae. The third part of my thesis concerns the mechanism leading to constitutively active immunity in *pi4kβ1β2* double mutant. It was shown that the 4-week-old *pi4kβ1β2* plants have a constitutive accumulation of SA that is responsible for the dwarfism of these plants. The question is now to understand the determinants of this constitutive accumulation. Therefore, I crossed the *pi4kβ1β2* double mutant with several mutants affected in different receptors or regulators of immunity. If any of these regulators act upstream of SA accumulation or play a role in SA signal transduction, I expected to obtain a reverted plant phenotype. The dwarf *pi4kβ1β2* phenotype was preserved for all mutants except one - *wrky70/pi4kβ1β2*. The rosette size of this triple mutant was WT-like, indicating a possible role of the WRKY70 factor in the constitutive SA accumulation or its transduction. In conclusion, in my thesis, I could describe the multifaceted effects of the *pi4kβ1β2* double mutation in *A. thaliana*. The obtained results open new perspectives on the roles of PPI in the non-host resistance to *Bgh* and on the mechanisms linking alteration in PI4Kbetas to overaccumulation of SA.

RÉSUMÉ

Les plantes s'adaptent aux changements de leur environnement en ajustant rapidement leurs processus métaboliques. L'un des principaux centres de régulation des cellules végétales est le trafic vésiculaire qui assure le transport correct et rapide entre la membrane plasmique et les autres compartiments cellulaires. Il est contrôlé par le renouvellement des phospholipides membranaires via une coopération étroite de lipide-kinases et de lipide-phosphatases. Les phosphatidylinositol-4-kinases (PI4Ks) sont les premières enzymes qui engagent le phosphatidylinositol (PI) dans la voie des phosphoinositides (PPI). Les PPI sont les dérivés phosphorylés du PI, comme le PI-4-phosphate (PI4P) et le PI-4,5-bisphosphate ($PI(4,5)P_2$). La formation de domaines membranaires enrichis en PI4P et $PI(4,5)P_2$ est un composant crucial de la dynamique des membranes plasmiques. En outre, PI4P et $PI(4,5)P_2$ servent de substrats à des enzymes, en particulier aux PI-PLCs. Les PPI peuvent aussi agir comme ligands de nombreuses protéines. Dans le génome d'*Arabidopsis thaliana*, douze isoformes de PI4K putatifs ont été identifiés dont quatre appartiennent au type III (*AtPI4Kα1* et *α2* et *AtPI4Kβ1* et *β2*). Pour étudier le rôle des PI4Ks, j'ai travaillé avec une plante double mutante défectueuse dans les deux gènes PI4Kβ. J'ai montré que le double mutant *pi4kβ1β2* présente une altération de la croissance des racines et une sensibilité plus faible des racines à l'auxine exogène. Ces changements semblaient coïncider avec un cytosquelette d'actine moins stable et une altération de la dynamique du trafic intracellulaire dans les racines *pi4kβ1β2*. Dans les racines de ce double mutant, l'expression génétique était moins sensible à l'auxine exogène. Ces données établissent donc un lien entre l'activité altérée de PI4K et la modification du trafic vésiculaire et de l'organisation des filaments d'actine, d'une part, et la réponse altérée à l'auxine, probablement due à une altération de l'homéostasie auxine, d'autre part. La deuxième partie de ma thèse est liée à l'interaction entre *Blumeria graminis* f. sp. *hordei* (*Bgh*) avec le double mutant *pi4kβ1β2*. On sait que *A. thaliana* a une résistance de type non-hôte à *Bgh*. Le double mutant *pi4kβ1β2* a montré une plus faible résistance -comparée au sauvage- à la pénétration de *Bgh* à 24 heures après l'inoculation. J'ai montré que la déficience den PI4Kbetas a conduit à une diminution de l'accumulation de PI4P dans les papilles, une structure qui agit comme une barrière entre le champignon et les cellules végétales. Mon hypothèse est que les PI4K sont essentielles pour la défense des plantes contre Bgh, et plus particulièrement pour la formation de papilles efficaces. La troisième partie de ma thèse concerne le mécanisme conduisant à une immunité constitutivement active dans le double mutant *pi4kβ1β2*. Les plantes *pi4kβ1β2* âgées de 4 semaines présentent une accumulation constitutive de SA qui est responsable du nanisme de ces plantes. La question est donc de comprendre l'origine de cette accumulation constitutive. Par conséquent, j'ai croisé le double mutant *pi4kβ1β2* avec plusieurs mutants affectés dans différents récepteurs ou régulateurs de l'immunité. Si l'un de ces régulateurs est placé en amont de l'accumulation du SA, ou joue un rôle dans la signalisation du SA, je m'attendais à obtenir un phénotype réversé. Le phénotype nain de *pi4kβ1β2* a été conservé pour tous les mutants sauf un - *wrky70/pi4kβ1β2*. La taille de la rosette de ce triple mutant est de type sauvage, ce qui indique un rôle possible du facteur WRKY70 dans l'accumulation constitutive du SA ou la transduction du SA. En conclusion, dans ma thèse, j'ai pu décrire de nombreux aspects des effets pléiotropiques de la double mutation *pi4kβ1β2* chez *Arabidopsis thaliana*. Les résultats obtenus ouvrent de nouvelles perspectives sur les rôles des PPI dans la résistance non-hôte à *Bgh* et sur les mécanismes liant l'altération des *PI4Kbetas* à la suraccumulation du SA.

ACKNOWLEDGEMENT

First and foremost, I would like to thank my supervisors who guided and helped me in doing these projects.

I would like to thank Lenka Burketová who gave me the golden opportunity to do this wonderful project and for invaluable patience and feedback.

I would like to thank Eric Ruelland who helped me in doing a lot of research in France, for scientific inspiration and active involvement during all the time.

I could not have undertaken this journey without my thesis committee, Anne Guivarch and Sylvie Collin, who generously provided knowledge and expertise. Thank you very much for your comments and ideas.

My sincere thanks to the members of the jury for their time and extreme patience.

I’m extremely grateful to Tetiana Kalachova for day-to-day support, for teaching plenty of biological methods and for great enthusiasm.

Special thanks to Katarzyna Retzer who guided me in gravitropic microscopy methods.

Many thanks to Romana Pospíchalová for technical collaboration.

I am also grateful to Lukáš Maryška, Hana Leontovyčová, Barbora Jindřichová, Daniel Stehlík, Marzieh Mohri, Nikoleta Rubil, Oksana Iakovenko, Anzhela Antonova and Natalie Kornienko for discussion and really a tight, unified team.

Last but not least, I thank my husband and parents, who always support me in science and life.

TITLE

1. INTRODUCTION

Plant health and productivity depend on root outgrowth, which allows water and nutrient uptake, and is equally crucial for efficient photosynthetic rates (Retzer and Weckwerth, 2021; Waldie and Leyser, 2018). Root morphogenesis is a complex process, orchestrated by a complex signaling crosstalk at different levels, from single-cell metabolism to hormone transport within plant organs. On-point spatial and temporal organization of cell organelles, the polar establishment of cell architecture and the directed shootward auxin transport are fundamental for correct root cell differentiation. Root hair cell priming and plasticity require fine-tuned, interconnected cellular processes driven by a properly established cytoskeleton that controls the polar delivery of membrane components to the root apex in order to enlarge the cell unidirectionally, and by the transport of auxin through the root tip (Retzer and Weckwerth, 2021). Auxin regulates cell polarity by activating ROPs (Rho-like GTPase), which control the polar localization of PIN-FORMED (PIN) family proteins. PIN family proteins are plasma membrane (PM)-integrated auxin efflux carriers responsible for the direction and intensity of auxin flow through the plant body. Their cellular localization and activity are regulated at many levels (Habets and Offringa, 2014; Luschnig and Vert, 2014; Semeradova et al., 2020), and depend on the lipid composition of the membrane in which they are located.

Phosphoinositides, minor components of PM, are phosphorylated derivatives of phosphatidylinositol (PI), such as phosphatidylinositol-4-phosphate (PI4P) and phosphatidylinositol-4,5-bisphosphate (PI(4,5)P_2). Phosphoinositides are important signaling molecules as they are substrates or cofactors of important signaling enzymes. In plants, both PI4P and PI(4,5)P_2 can be substrates to phospholipases C (PLCs) leading to a diacylglycerol and the corresponding phosphorylated inositol. PI(4,5)P_2 is a cofactor of some phospholipases D (PLDs), that catalyze the production of phosphatidic acid, a major plant signaling lipid (Pokotylo et al., 2018). More generally, phosphoinositides can directly interact with membrane proteins (such as ion channels or G protein-coupled receptors) or cytosolic proteins that they can recruit to membranes (Noack and Jaillais, 2020; Platre et al., 2018). Interestingly, specific relative levels of phosphoinositides are a characteristic feature of different membranes: PM, endoplasmic reticulum and Golgi membranes do not have the same relative composition of phosphoinositides (Gronnier et al., 2017; Noack and Jaillais, 2020). Besides, membrane nanoclusters enriched in certain proteins crucial for signal

transduction and transport proteins also have a specific composition of phosphoinositides (Galvan-Ampudia et al., 2020; Jaillais and Ott, 2020). Formation of membrane domains enriched in PI4P and PI(4,5)P_2 is a crucial component of PM dynamics. Such phosphoinositide-enriched domains are important for the localization of remorins, scaffold proteins governing PM–bound signaling (Ke et al., 2021), and FLS2, a pattern-recognition receptor that determines the specific perception of the bacterial protein flagellin (McKenna et al., 2019). Remorins are involved in plant-microbe interactions. Remorins are anchored by their C-terminal domain to the cytosolic leaflet of the plasma membrane upon interaction with PI4P and sterol. PI4P accumulates in response to pathogen infection. During infection of *A. thaliana* with the powdery mildew fungus *Erysiphe cichoracearum*, the PI(4,5)P_2 pools were dynamically upregulated at the pathogen infection sites and further integrated into the extrahaustorial membrane, while PI4P showed constant levels at the plasma membrane and was absent in the extrahaustorial membrane (Qin et al., 2020).

Composition of phosphoinositides is modified by the activities of lipid kinases. PI4Ks phosphorylate the 4th hydroxyl position in the inositol head group of PI to generate PI4P. PI4P can be further phosphorylated by phosphatidylinositol-4,5-kinases (PI(4,5)K) into PI(4,5)P_2. There are two types of PI4Ks according to their primary sequences and pharmacological sensitivities. Type II PI4Ks are inhibited by adenosine while type III PI4Ks are inhibited by micromolar concentrations of wortmannin, a steroid produced by the fungi *Penicillium funiculosum*. In the *A. thaliana* genome, twelve putative PI4K isoforms have been identified. Eight belong to type II (*At*PI4Kγ1-8), and four belong to type III (*At*PI4Kα1 and α2 and *At*PI4Kβ1 and β2) (Akhter et al., 2016). Not much is known about type II PI4Ks as they could actually be protein kinases and not lipid kinases (Akhter et al., 2016; Galvão et al., 2008). We have previously shown that type III PI4Ks are upstream of the PLC activity that controls the responses of tobacco BY2 cells to cryptogein, a fungal elicitor (Cacas et al., 2016). Type III PI4Ks are also upstream of PLC-mediated plant cold response (Delage et al., 2012) and of the PLC activity that controls basal gene expression in *A. thaliana* (Djafi et al., 2013). Type III PI4Ks have also been shown to be activated in response to a SA, whilst the consequent increase in a phosphoinositides content is an important part of the specific response of *A. thaliana* to this phytohormone (Kalachova et al., 2016; Krinke et al., 2007; Ruelland et al., 2014). Since *AtPI4Kα2* is a pseudogene and viable homozygous *PI4Kα1* mutants have never been obtained, we have opted to work on a double mutant defective in both *PI4Kβ* genes. Four-week-old *pi4kβ1β2* plants exhibited a constitutively high SA level that led to a stunted phenotype (Šašek et al., 2014). However, SA accumulation did not occur

in young *pi4kβ1β2* seedlings (Pluhařová et al., 2019; Šašek et al., 2014) and therefore, they appeared to be the material of choice to study the roles of PI4Ks and phosphoinositides in root development. Several aspects of the role of PI4Ks in plant cell biology have been discovered using *pi4kβ1β2* double mutant, such as the involvement of PI4K*β*1 in cell plate formation during cytokinesis (Lin et al., 2019), formation of secretory vesicles (Kang et al., 2011a) as well as root hair shaping and polar growth (Preuss et al., 2006).

2. LITERATURE REVIEW

2.1 PLANT PI4Ks

2.1.1 Phospholipids in plant cells

2.1.1.1 Distribution of phospholipids

Phospholipids are a class of lipids, contained in biological membranes. Their structure is based on two hydrophobic fatty acyl groups and a hydrophilic polar head group attached to the glycerol backbone by a phosphodiester link. Because of their amphiphilic nature, phospholipids can form a lipid bilayer, the fundament of the cellular membranes. According to the nature of the polar head, one distinguishes different phospholipid classes. The polar head group can be hydrogen, choline, serine, ethanolamine, inositol or glycerol molecule, forming phosphatidic acid (PA), phosphatidylcholine (PC), phosphatidylserine (PS), phosphatidylethanolamine (PE), phosphatidylinositol (PI) or phosphatidylglycerol (PG), respectively.

PI can be phosphorylated at the hydroxyl groups at different positions of the inositol ring. One distinguishes PI-3-phosphate (PI3P) or PI4P, PI-3,5-bisphosphate ($PI(3,5)P_2$) and $PI(4,5)P_2$.

The different phospholipid classes are unequally distributed between the various organellar membranes in eukaryotic cells. PC is the most abundant phospholipid in the majority of organelles. PE is the second most abundant phospholipid in eukaryotic membranes, located in the inner (cytoplasmic) leaflet of the plasma membrane. PE is absent from plastid membranes. PG is localized mainly in plastids (Fujii et al., 2021). In *A. thaliana* apical pollen tube, PS is mainly localized in the trans-Golgi network/early endosome, certain post-Golgi compartments, and the plasma membrane (Zhou et al., 2020). $PI(4,5)P_2$ is localized mainly at the plasma membrane and in the nucleus. PI4P is spread between the plasma membrane (the highest concentration), trans-Golgi network (TGN), and Golgi apparatus (Platre et al., 2018). $PI(3,5)P_2$ is localized in late endosomes.

The different phospholipid classes have distinct roles. In plastid membranes, besides its structural role, PC serves as a precursor for the synthesis of glycerolipids, such as monogalactosyldiacylglycerol, digalactosyldiacylglycerol and sulfoquinovosyldiacylglycerol

(Ohlrogge and Browse, 1995). PS plays a main role in participating in the negative surface charge to membranes due to the acidic nature of its headgroup (Yeung et al., 2009). PS is needed for root cytokinesis, by mediating vesicular trafficking for cell plate formation (Yamaoka et al., 2021). PG are present in thylakoid membranes in chloroplasts, and are important in photosynthesis, especially in photosystem II. It maintains the structural integrity of the quinone-binding site (Kobayashi et al., 2016). PA is a biologically active lipid molecule that activates defense responses during salt stress (Pokotylo et al., 2018). The physiological roles of phosphoinositides will be discussed in a separate section.

2.1.1.2 Phosphoinositides synthesis

The metabolism of phosphoinositides (PPIs) is regulated by specific kinases, phosphatases, and phospholipases. Phosphatidylinositol is the initial substrate for phosphorylating the hydroxyl groups along the inositol ring. During the biosynthesis of PPIs, the first phosphorylation occurs at the hydroxyl group at positions 3, 4 or 5 of the inositol ring giving rise to seven phosphoinositide derivatives. The six phosphoinositides found in plants: PI3P, PI4P, PI5P, PI(3,4)P_2, PI(3,5)P_2, PI(4,5)P_2. A seventh PI, PI(3,4,5)P_3, has so far only been reported in animal cells (**Fig. 1**) (Dieck et al., 2012).

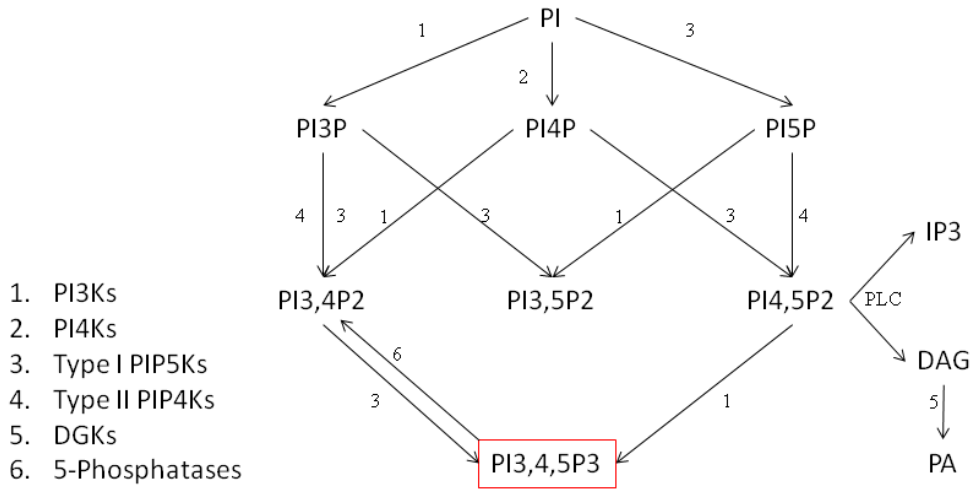

Fig. 1: Pathways for phosphoinositides synthesis. The six phosphoinositides found in plants: PI3P, PI4P, PI5P, PI(3,4)P_2, PI(3,5)P_2, PI(4,5)P_2. A seventh PI, PI(3,4,5)P_3, has so far only been reported in animal cells (in red frame) (Kusano et al., 2008).

The structures of PI4Ks will be detailed below. Concerning PI3K, it phosphorylates PI at its 3′-hydroxyl position thus forming PI3P (Raynaud et al., 2007). PI3Ks are localized in cytosol, plasma membrane, central vacuole of stomata, and in endosomal vesicles that are

close to Golgi stacks (Van Leeuwen et al., 2007). PI3Ks are involved in plant growth and development (Welters et al., 1994), normal stomatal movements in response to abscisic acid (Jung et al., 2002), root hair elongation (Lee et al., 2008), cytoskeleton arrangements (Dove et al., 1994).

$PI(4,5)P_2$ is synthesized from PI4P by PI4P5K. *A. thaliana* genome possesses 11 genes encoding PI4P5K isoforms (Mueller-Roeber and Pical, 2002). They can be clustered into two groups based on their structure, one group containing *AtPI4P5K1–9* and the other formed by *AtPI4P5K10–11* (Ischebeck et al., 2010). My PhD work concerns the role of PI4Ks, so the next part will be devoted to introducing the different types of this enzyme.

2.1.2 The PI4Ks

2.1.2.1 Diversity of PI4Ks

A lot of information on PI4Ks was derived from mammals and yeast (Barylko et al., 2001). The yeast genome has three genes that encode one type II PI4Ks (Lsb6) and two type III PI4Ks (Pik1, Stt4) (Strahl and Thorner, 2007). Stt4 is the yeast orthologue of the human PI4KIIIα while Pik1 is the yeast ortholog of mammalian PI4KIIIβ (Kapp-Barnea et al., 2003, p. 1).

There are indeed two types of PI4Ks according to their primary sequences and pharmacological sensitivities. Type II PI4Ks are inhibited by adenosine and calcium while type III PI4Ks are inhibited by wortmannin (WM) (inhibits PI3K at the nanomolar concentration and PI4K at the micromolar concentration), a steroid produced by the fungi *Penicillium funiculosum* (Balla, 1998). Phenylarsine oxide (PAO) inhibits type III PI4Ks, with relatively little effect on type II PI4K enzymes, and, among the type III enzymes, PI4KIIIα is more sensitive to PAO than PI4KIIIβ (Balla et al., 2005). LY294002 is a PI3K inhibitor (Takahashi et al., 2017).

Type II PI4Ks are smaller than type III PI4Ks, 70 kDa and 100-230 kDa respectively.

Eight *A. thaliana* putative type II PI4Ks (PI4Kγ1-PI4Kγ8) have been identified (S. Liu et al., 2012) (**Fig. 2**).

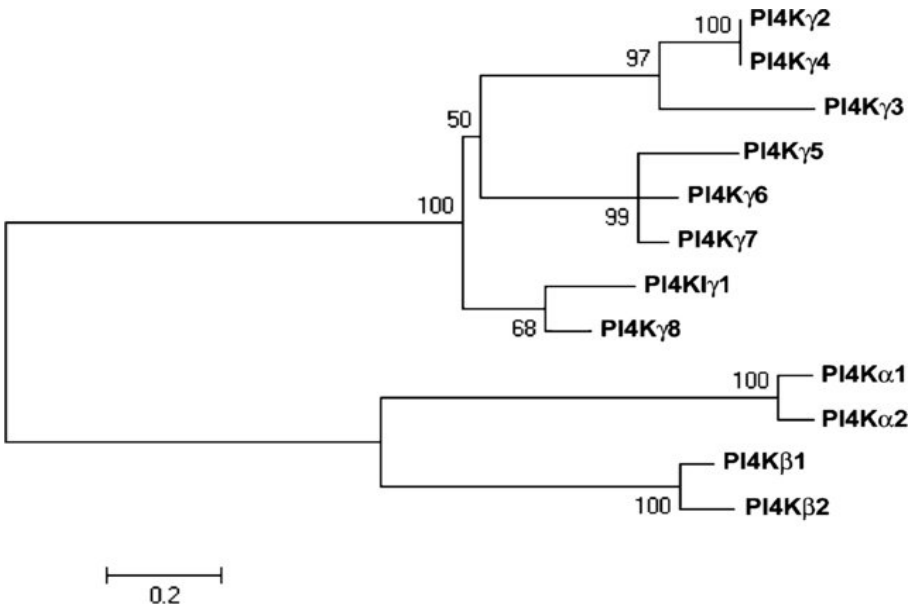

Fig. 2: Twelve predicted PI4K proteins of *Arabidopsis thaliana* (Szumlanski and Nielsen, 2010).

Concerning type III PI4Ks, *A. thaliana* genome encodes two PI4KIIIα and two PI4KIIIβ subtypes (Balla, 1998) that have different protein domain structure. PI4KIIIα1 contains LKU (lipid kinase unique), PH (Pleckstrin homology) and kinase domains while PI4KIIIα2 contains only the PI3/4 kinase domain. PI4KIIIβ1 and PI4KIIIβ2 have the same structure, consisting of a LKU domain followed by amphiphatic repeats (repetitive motif), an NH (novel homology) domain and the PI3/4 kinase catalytic domain (**Fig. 3**). The description of PH domains will be detailed below (section 1.3.2.1). LKU - lipid kinase unique domain is conserved in both PI4KIIIα and PI4KIIIβ types but has different locations. This domain is predicted to be helical and comprise about 100 residues. NH - novel homology domain, interacts with RabA4b GTPase (Preuss et al., 2006). A repetitive domain consists of 11 repeats of a charged core unit. It is unique for the plant β isoforms and is responsible for targeting PI4Kβs to the plasma membrane, possibly via binding to PA, PI, or PI4P (Ma et al., 2006). No clear function can be assigned to the LKU and NH; they may play a role in the interaction of PI4K with other proteins and/or membrane structures. *AtPI4KIIIα2* is likely to be a pseudogene (nonfunctional gene). *AtPI4KIIIβ2* is 83% identical to *AtPI4KIIIβ1* (Mueller-Roeber and Pical, 2002). Type II PI4Ks have a different primary structure from that of type III enzymes. Type II PI4Ks contain PI3/4 kinase catalytic domain and a variable number (none, one, or two) of ubiquitin-like (UBL) domains. They do not have the PI-binding domains such as the PH (that is present in the type III *AtPI4Kα*) or the repetitive domains (that are present in the type III *AtPI4Kβ*). The UBL domain is essential for protein-

protein interaction. According to the number of UBL domains, type II PI4Ks can be divided into three subgroups: no UBL (PI4Kγ1, γ2, γ8), one UBL (PI4Kγ5, γ6, PI4Kγ7) and two UBLs (PI4Kγ3, PI4Kγ4) (Yong Tang 2016).

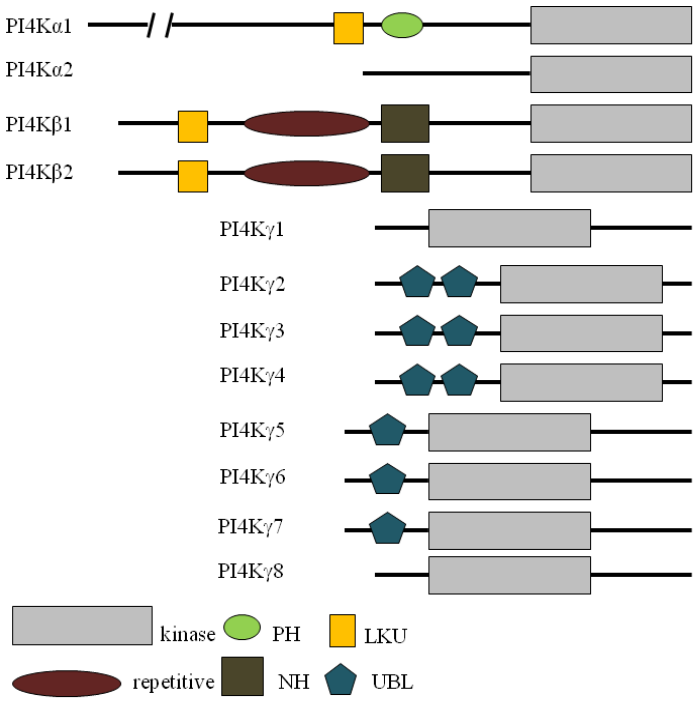

Fig. 3: Protein Domain Structure of PI4K-family members in *Arabidopsis thaliana*. A truncated image of PI4Kα1 is shown due to a large protein size and a lack of predicted domains in the N-terminal part of PI4Kα1. A space flanked by two slanted lines indicates the location of the truncation (Szumlanski and Nielsen, 2010).

Different types of PI4Ks have diverse subcellular localization and thus control different PI4P pools.

Mammalian type II PI4Ks are present in the TGN, subcompartments of the endoplasmic reticulum and endosomes especially in the case of the type IIα enzyme (Balla et al., 2005). PI4KIIα activity and association with membranes is dependent on palmitoylation (Barylko et al., 2009). Not much is known about *A. thaliana* type II PI4Ks; some data suggest that they could act as protein kinases and not lipid kinases (Galvão et al., 2008).

Mammalian PI4KIIIα is associated with the plasma membrane (Szentpetery et al., 2011), endoplasmic reticulum and Golgi apparatus. In mammalian cells, PI4KIIIα could shuttle from cytosol to plasma membranes. Mammalian PI4KIIIβ is mainly associated with the Golgi apparatus (De Matteis et al., 2013). Plant *AtPI4KIIIβ1* and *AtPI4KIIIβ2* localized on the

plasma membrane, Golgi apparatus and cytoplasmic vesicle membranes (Kang et al., 2011a; Lou et al., 2006). *AtPI4KIIIα1* localizes at the perinuclear region and plasma membrane (Noack et al., 2022). Plant PI4Ks are also expected to be present in the endoplasmic reticulum, but for now no confirmation is available.

2.1.2.2 Role of PI4Ks in trafficking

PI4Ks that synthesize PI4P are crucial regulators of membrane trafficking. PI4Ps are localized in different compartments of the *A. thaliana* endomembrane system (Simon et al., 2014). The highest concentration of PI4P is found at the plasma membrane; lower concentrations are detected in post-Golgi/endosomal compartments with the lowest concentrations of PI4P being detected in the Golgi. PI4P is involved in several secretory and endocytic trafficking pathways that will be described below (Kang et al., 2011a; Lee et al., 2008; Preuss et al., 2006).

The interaction between PI4Ks and small guanosine triphosphatases (GTPases) is a background mechanism required for expansion and remodeling of PI4P-containing membranes. In *A. thaliana*, PI4Kβ1 interacts with a small GTPase (RabA4b), and acts in the polarized exocytosis of cell wall materials such as pectin and xyloglucan in root hairs (Kang et al., 2011a; Preuss et al., 2006). The *A. thaliana* RabA4b has been detected in TGN-like compartments.

$PI(4,5)P_2$ is crucial for endocytosis. It functions as an important coreceptor regulating endocytic proteins by their selective recruitment to the plasma membrane. $PI(4,5)P_2$ commonly binds to endocytic clathrin adaptors (for example, AP-2, epsin) (Choi et al., 2015, p. 2). In addition $PI(4,5)P_2$ acts through the actin cytoskeleton, which universally controls all internalization pathways (Platre et al., 2018).

Cellulose microfibrils ensure plant cell wall structural and mechanical rigidity. In plants, cellulose is synthesized by cellulose synthase complexes (CSCs) that consist of cellulose synthase catalytic subunits (CESAs). Cellulose synthesis by CSCs occurs at the plasma membrane. However, CESAs were shown to be localized in several intracellular compartments including the Golgi apparatus, the TGN. Recent research has identified a few proteins involved in the intracellular trafficking of CSCs. PI4K inhibitors affect the internalization of CESA3, which should be due to an inhibitory effect on an early clathrin-mediated endocytosis (Fujimoto et al., 2015).

PI4P and $PI(4,5)P_2$ are involved in the regulation of clathrin-dependent endocytosis at the tips of pollen tubes. Maintaining the balance between PI4P and $PI(4,5)P_2$ accumulation in the

apical plasma membrane is important for a clathrin-dependent endocytosis. PI(4,5)P_2 induces the formation and invagination of clathrin-coated pits while PI4P plays a role at the last step of clathrin-dependent endocytosis at pollen tube tips (Zhao et al., 2010).

Salt stress leads to the internalization of a plasma membrane aquaporin (PIP2;1) from the plasma membrane to the vacuolar lumen that is mediated by a clathrin-mediated endocytosis. PI4K is a part of such activity as shown by using PAO. This inhibitor of type III PI4Ks significantly suppressed the salt-induced internalization of plasma membrane aquaporin in root epidermal cells (Ueda et al., 2016).

The formation of dot-like endosomal components in plasma membranes implicating GFP–PATROL1 is dependent on PI4K activity, as shown by WM and PAO treatments in *A. thaliana* cotyledon leaf epidermis. PATROL1 is a translocation factor of the plasma membrane proton pump ATPase (PM H^+-ATPase) and a key regulator of stomatal opening under low carbon dioxide conditions (Higaki et al., 2014). In *A. thaliana* guard cells, GFP-tagged PATROL1 localized in the cytoplasm and on dot-like endosomal components that became prominent during stomatal closure (Hashimoto-Sugimoto et al., 2013).

2.1.2.3 Role of type III PI4Ks in organelle physiology

PI4P negatively regulates the division of chloroplasts. The inhibition of type III PI4Ks by PAO caused an increase in chloroplast divisions in parallel with an increase in the amount of a chloroplast division machinery component - DYNAMIN-RELATED PROTEIN5B (DRP5B) localized on the surface of chloroplasts. PI4Kα1 is the main contributor to the regulation of chloroplast divisions. When PI4Kα1 expression was transiently knocked-down, the levels of PI4P decreased in chloroplasts, the number of chloroplasts increased, and their size was diminished compared with non-induced plants (Okazaki et al., 2015).

Changes in the PPI metabolism have been shown to be important for phototropin-mediated processes including phototropic responses and guard cell movements. Phototropin is a photoreceptor which is involved in regulating light dependent processes. Treatment with a PLC inhibitor leads to a dose-dependent inhibition of phototropin-mediated chloroplast movements. This suggests a PI(4,5)P_2-PLC involvement in such phototropin-mediated movements (Aggarwal et al., 2013).

PI4KIIIα1 is the main donor to the PI4P production required for chloroplast biogenesis in leaves (Okazaki et al., 2015), while PI4KIIIβ1 and PI4KIIIβ2 play redundant roles in root tissue trafficking (Preuss et al., 2006).

2.1.2.4 Role of type III PI4Ks in responses to stress

Throughout their development, plants can experience various types of stress. Those include abiotic ones such as light, temperature, soil water potential changes, or biotic ones comprising various interactions with microorganisms.

Phosphoinositides play a role as signaling molecules in stomatal responses to environmental signals. Application of PAO has led to specific inhibition of the stomatal response to CO_2, suggesting an intermediate role of PI4K (Takahashi et al., 2017).

In the experiments of Jung et al., (2002) an important role of PI3P and PI4P for stomatal movements in guard cells was suggested. By conducting *in vitro* assays with protein extracts from guard cell–enriched epidermal samples, they have shown that WM inhibits PI3K, PI4K and PI4P5K, whereas LY294002 inhibits PI3K and PI4K but not PI4P5K. In the presence of 1 to 10 μM WM, stomatal opening induced by the circadian clock-related treatments (darkness or white light) were greatly enhanced (Jung et al., 2002).

The enzyme activity of PI4K was measured in the vesicles enriched in plasma membrane fraction in seedlings treated with or without NaCl. NaCl treatment leads to increased PI4P content, while PAO treatment reduces PI4P content in NaCl-treated seedlings (Y. Yang et al., 2021).

Organic acids (malate, citrate, and oxalate) are secreted from the roots of some plants to protect their sensitive root tips from aluminum (Al) rhizotoxicity in acidic soils (Liu et al., 2009). The role of type III PI4Ks in Al-inducible malate secretion was shown in *A. thaliana* with the help of PAO inhibitor (Wu et al., 2019).

This is only a fraction of the experiments that document the involvement of type III PI4Ks in plant responses to stresses. Yet how phosphoinositides act in cell signaling, notably the direct product (PI4P) and by-product ($PI(4,5)P_2$) of type III PI4K, remains to be an open question.

2.1.3. Mode of action of phosphoinositides

As we have just seen, phosphoinositides have diverse functions and are essential for shaping the membranes, controlling vesicular trafficking and regulating plant physiology. Yet, what is known about the molecular mode of actions of phosphoinositides?

PI4P and $PI(4,5)P_2$ participate negatively charging membranes in which they are incorporated, thus triggering electrostatic interactions with positively charged amino acids in membrane-associated proteins and regulates ion channels. This can occur through phosphoinositide binding domains present in the proteins. Besides, phosphoinositides can act as substrates of enzymes, especially of PI-PLCs. This is what I am now going to detail.

2.1.3.1 Phosphoinositides acting through PI-PLC as substrates

2.1.3.1.1. PI-PLC

$PI(4,5)P_2$ is the substrate for the phosphoinositide specific phospholipase C (PI-PLC), which produces diacylglycerol (DAG) and inositol 1,4,5-trisphosphate (IP_3) as second messengers in a Ca^{2+}-dependent manner (Pokotylo et al., 2014). PI4P also serves as a substrate for PI-PLC in plants (Arisz et al., 2009). *A. thaliana* contains 9 genes that encode PI-PLC enzymes (Munnik and Testerink, 2009), all of them are structurally related to the PLCζ isoform, as they are formed by the succession of EF hand, X/Y and C2 domains (Wang et al., 2005). Seven PI-PLC are likely to be catalytically active (*AtPLC8* and *AtPLC9* lack the enzymatic activity) (Tasma et al., 2008). These isoforms are differentially expressed in response to drought, cold or salt stress (**Fig. 4**) (Pokotylo et al., 2014).

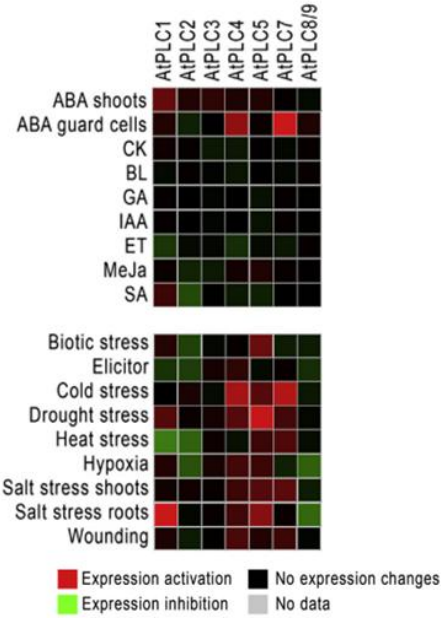

Fig. 4: Changes in *Arabidopsis thaliana* PI-PLC gene expression in response to hormone treatments and during stresses. Shown here are cumulative representative data concerning changes in PI-PLC gene expression in different growth conditions. When several expression data points with different time or different dose of treatment were available, the one with the most apparent and consistent changes in PI-PLC expression was chosen. ABA, abscisic acid; CK, cytokinins; Bl, brassinolide; GA, gibberellic acid; IAA, indolacetic acid; ET, ethylene; MeJa, methyl jasmonate; SA, salicylic acid (Pokotylo et al., 2014).

The X/Y domain is essential for enzymatic activity PI-PLC. Many residues are highly conserved in the X/Y domains of all eukaryotic PI-PLCs and they are involved in substrate binding and catalysis. The EF-hand domain includes four helix-loop-helix folding motifs. EF

hand has the ability to bind calcium (Kumar and Verma, 2013). However, plant PI-PLCs have no full length EF-hand domain since most of them have a truncated EF-hand consisting of only two helix-loop-helix motifs (Otterhag et al., 2001) while several plant PI-PLCs have no N-terminal EF-hand, such as *AtPLC2* (Hirayama et al., 1995). All identified plant PI-PLCs contain a C2 domain, which will be described below. The linker region between the X and Y domains is highly hydrophilic and extremely divergent and plays different roles in different PI-PLCs. Plant PI-PLCs linker region includes a high percentage of acidic residues that are exposed at the surface of the folded protein (Hirayama et al., 1995). The role of the linker in plant PI-PLC activity remains to be identified.

Ca^{2+} regulates activity, subcellular localisation and substrate preference of PLC. *In vitro* assays demonstrated that PI-PLC uses $PI(4,5)P_2$, PI(4)P, or PI as substrates, depending on Ca^{2+} concentrations. In plant PI-PLC could be soluble in cytosol or bind to the membrane (Nomikos et al., 2011). Soluble PI-PLC generally prefers PI to $PI(4,5)P_2$ and PI(4)P under millimolar levels of Ca^{2+}, whereas membrane-associated PI-PLC selects $PI(4,5)P_2$ and PI(4)P as substrates under micromolar Ca^{2+} (Hong et al., 2016).

2.1.3.1.2 Type III PI4Ks feed PI-PLC with substrates

Here I will give the experiments that indicate that type III PI4Ks are upstream PI-PLC and feed PI-PLC with their substrates. The roles of PI-PLC in responses to stresses will be detailed below.

Cryptogein is a MAMP protein from the oomycete *Phytophthora cryptogea*. The protein promotes cell death and systemic acquired resistance-inducing activities in *Nicotiana tabacum* (Cacas et al., 2005). After treatment cells with the cryptogein peptide production of PA increased and reached a maximum within the first 10 min and then plateaued. It was shown the role for a PI-PLC/DGK (diacylglycerol kinases) pathway in cryptogein-induced PA production in tobacco cell cultures. Application of PLC and DGK inhibitors (edelfosine and R59022 respectively) decreased cryptogein-induced PA accumulation in a dose-dependent manner. In addition, treatment with 30 μM WM resulted in a 46% inhibition of cryptogein-induced PA accumulation (Cacas et al., 2016). There was a functional coupling between type III PI4K and PI-PLC leading to the control of the expression of a cluster of genes. The transcriptome of the response to edelfosine (a PI-PLC inhibitor) was compared to that obtained with 30 μM WM (a concentration that inhibits type III PI4K activity). 596 genes had their expression similarly affected by edelfosine and WM, this being at least 10-fold more than expected in case of a random distribution (Djafi et al., 2013).

$PI(4,5)P_2$ can be substrates for PLD. The PLD role in responses to stress will be detailed below.

Treatment of suspension cells with WM before a cold shock leads to 80% reduction of PI4P labeling at 22°C and $PI(4,5)P_2$ was no longer detectable (Delage et al., 2012). Type III PI4Ks of *A. thaliana* feed PI-PLC pathway with substrate. PI-PLC activity at 0°C was reduced by 40% in a *pi4kIIIβ1β2* double-mutant whereas it was not significantly lowered in either *pi4kIIIβ1* or *pi4kIIIβ2* simple-mutants (Delage et al., 2012).

Metabolites derived from the PI4K pathway regulate early Al-inducible expression of *AtALMT1*. PI4K inhibitors PAO blocked Al-responsive events controlled by *AtALMT1*. PAO significantly inhibited early Al-inducible expression of *AtALMT1* (22%). PAO also suppressed the early Al-inducible expression of Al-biomarker genes. In addition, PAO reduced malate secretion to 21% by 35S:AtALMT1 plants. In contrast, there was no reduction of malate content of the root cells by inhibitor. It suggests PAO inhibits the process of Al-activated malate transport but not the synthesis of malate (Wu et al., 2019).

Another experiment is in favor of type III PIKs providing the substrate to PI-PLC pathway. In the above mentioned experiment (Jung et al., 2002), the authors showed that WM (10 μM) reduced the probability of ABA-induced $[Ca^{2+}]_{cyt}$ increases as well as the stomatal closing induced by ABA (Jung et al., 2002). As $[Ca^{2+}]_{cyt}$ is considered to be downstream PI-PLC this is consistent with type III PI4K being upstream PI-PLC pathway.

2.1.3.1.3 PI-PLC in plant response to stress

PI-PLC plays an important role in biotic and abiotic stress response in plants (Kalachova et al., 2016). PI-PLC is involved in plant adaptation to drought, heat, and cold conditions (Pokotylo et al., 2014).

Different salts (NaCl, KCl) and osmotic stress inducers (mannitol, sorbitol and mannose) induce an increase of IP_3, PI-PLC product. Increase of calcium level dependent on PI-PLC was observed in *A. thaliana* root tips (DeWald et al., 2001), seedlings (Perera et al., 2008) and tobacco cells (Cessna et al., 2007). The Ca^{2+} signal may mediate the function of PI-PLCs as part of the salt stress response (Han and Yang, 2021). Xia et al., (2017) showed that *AtPLC4* is a negative regulator of *A. thaliana* seedling growth under salt stress and Ca^{2+}. Cytosolic Ca^{2+} signal in animal cells is induced by IP_3, while in plant cells, IP_6 also mobilizes intracellular Ca^{2+}, thereby inducing the cytosolic Ca^{2+} signaling. The accumulation of $PI(4,5)P_2$ and $PI(3,5)P_2$ during salt stress, and further production of cytosolic Ca^{2+} can be a strategy for plant salt tolerance (Han and Yang, 2021). The IP_3-induced Ca^{2+} release is well

described for animals. The mammalian IP_3-receptor is a huge molecule (2700 amino acids) with a well-defined domain structure. Based on the presence of this domain, no homologous protein in plants has been found. The presence of an ion transport domain is more general, and several proteins possessing a similar domain can be found in *A. thaliana* and rice genomes, but those represent mostly the genes previously annotated as K^+ channels with a quite different domain architecture from what would be expected for a true IP_3-receptor homologue (Krinke et al., 2007). IP_3 gates plant endomembrane Ca^{2+} release channels, which might result from binding to a coupled receptor that shares some homology with the animal IP_3 receptor (Cousson, 2011). No functional plant receptor of IP_3 has yet been identified (Dong et al., 2012).

Plants accumulate proline for decreasing osmotic stress action. In *A. thaliana*, intracellular calcium level, mediated by IP_3-dependent calcium release, represents an essential and rate-limiting factor for proline accumulation in response to salt stress (Parre et al., 2007).

Dehydration responsive element binding protein 2 (*DREB2*) genes are essential for the response to environmental stresses, including dehydration (Ruelland et al., 2014). The expression level of *DREB2A* is negatively regulated by PI-PLC.

ABA is one of the main plant stress hormones that accumulate upon stress exposure and it controls many plant defence reactions including in the salt stress response (Yu et al., 2020). PI-PLCs are involved in plant ABA-dependent signaling. For example, external ABA application leads to IP_3 accumulation in *A. thaliana* seedlings (Xiong et al., 2001). *AtPI-PLC1* is induced during ABA-mediated salt stress response (Sanchez and Chua, 2001). ABA plays a key role during the response to dehydration stress and is known to induce stomatal closure to reduce water loss (Cutler et al., 2010). PI-PLCs (such as *AtPI-PLC7* and *AtPI-PLC3*) have been reported as regulators of stomatal opening that depend on ABA (Yu et al., 2020). The stomatal closure response was tested in leaf peels of the WT (wild type) and knock-down *plc3* mutants after treatment with different concentrations of ABA. Guard cells of *plc3* mutants were compromised in ABA-dependent stomatal closure (Zhang et al., 2018). In control conditions, the *plc5/7* double mutant has less open stomata compared to wild-type plants, while upon ABA treatment the *plc5/7* mutants were less responsive (Di Fino et al., 2017).

Heat stress induces the accumulation of $_{IP3}$ (within minutes) in *A. thaliana* (Liu et al., 2006). *AtPLC3* may affect the thermotolerance of *A. thaliana* through the Ca^{2+} content and the expression of heat shock proteins (Ren et al., 2017). The deletion of *AtPLC9* results in decreased thermotolerance while the overexpression of *AtPLC9* results in increased

thermotolerance (Gao et al., 2014). Cold stress also activates the PI-PLC signal pathway. IP_3 accumulation, paralleled with decreased levels of PI4P and $PI(4,5)P_2$, was observed in *A. thaliana* suspension cells submitted to chilling stress (Ruelland et al., 2002). The PI-PLC activation within the cold stress relies on calcium entry into the cells while substrates for PI-PLCs are supplied by type III PI4K (Delage et al., 2012).

Several other stresses activate the PI-PLC pathway. For example, hypoxia induces a rapid G-protein dependent IP_3 accumulation in rice roots. Kanehara et al., (2015) revealed that *AtPLC2* is responsible for the endoplasmic reticulum stress responses in *A. thaliana*.

In addition, PI-PLC-derived molecules are involved in plant defense reactions. *A. thaliana* mutants expressing a mammalian type I inositol polyphosphate 5-phosphatase have low levels of IP_3, IP_6 and had a reduced cytosolic Ca^{2+} increase in response to flagellin (Ma et al., 2012). As a result, PI-PLC regulates plant defense reactions through Ca^{2+} levels that are perceived by Ca^{2+} dependent protein kinases (Lin et al., 2013).

To conclude, plant PI-PLC plays an important role in signal transduction in response to different stresses. Type III PI4Ks that provide the substrates to these enzymes have therefore a major role. Moreover, PI-PLC also had a great impact on plant development.

2.1.3.1.4 PI-PLC in plant response to development

PI-PLC plays a role in regulating growth and development-related processes that are multifaceted. PI-PLCs involvement was shown for polarized pollen growth (Cole and Fowler, 2006). Such an asymmetric cell expansion is known to rely on several events including calcium signaling, vesicular trafficking and cytoskeleton rearrangements (Cole and Fowler, 2006). In the elongating pollen tube, PI-PLC accumulates in the plasma membrane specifically at the flanks of the tip. On the contrary, $PI(4,5)P_2$ accumulates at the apex of the pollen tube (Dowd et al., 2006). The PI-PLC inhibitor U73122 inhibited pollen tube growth and led to swollen tips, thus indicating that expansion is no longer polarized (Helling et al., 2006). Such effects as reduction of growth and swelling correlate with the spreading of $PI(4,5)P_2$ to the flanks of the tip. Consequently, PI-PLC has a major role to create and maintain a $PI(4,5)P_2$ gradient in the pollen tip, between the apical and lateral membranes, that is necessary for polarized growth (Helling et al., 2006). $PI(4,5)P_2$ controle apical pectin deposition and actin cytoskeleton dynamics through membrane trafficking including clathrin-dependent endocytosis (Ischebeck et al., 2011). In addition, $PI(4,5)P_2$ is involved in growth of root hair tips. *A. thaliana* mutants deficient in phosphatidylinositol-4-phosphate 5-kinase gene *PIP5K3* were significantly impaired in root hair development (Stenzel et al., 2008).

The role of IP_3, product of PI-PLC, has been established in the differentiation of xylem vessels (Zhang et al., 2002), asymmetric cell divisions that produce stomatal complexes in Zea mays (Apostolakos et al., 2008), cell cycle progression in tobacco, through DNA synthesis control (Apone et al., 2003).

Li et al., (2015) showed that *AtPLC2* is involved in auxin biosynthesis and signaling, thus modulating development of both male and female gametophytes in *A. thaliana*. Expression levels of the auxin reporters DR5:GUS and DR5:GFP were indeed elevated in *plc2* anthers and ovules. Expression of the auxin biosynthetic *YUCCA* genes was increased in *plc2* plants (Li et al., 2015). *AtPI-PLC2* has an impact on the polar distribution of PIN2 and regulates root development through auxin signaling (Chen et al., 2019). Cotyledons, rosette leaves, and the root tissues of *plc2* seedlings were smaller than those of WT. The primary roots of *plc2* seedlings were not only shorter but also curlier compared with those of WT seedlings.

AtPLC3 is involved in seed germination, root development, stomatal movement and ABA signaling while *AtPI-PLC5* is involved in root growth and development (Zhang et al., 2018). *plc3* mutants germinated slightly more slowly than WT seeds. *plc3* mutant seedlings exhibited significant differences in root system architecture compared with the WT, i.e. shorter primary roots (5–10%), fewer lateral roots (~10–20%) and reduced lateral root densities. In the absence of ABA, no significant differences in the stomatal aperture between the WT and *plc3* mutants were found. However, with increasing concentrations of ABA, the *plc3* mutant clearly exhibited reduced stomatal closure responses (Zhang et al., 2018).

2.1.3.2 Phosphoinositides binding domains as ligands

Phosphoinositides do not only act as substrates of PI-PLCs, they can also act as ligands of many proteins. PPI-binding domains are diverse and PPI can be bound by Pleckstrin Homology (PH), Phox homology (PX), Epsin N-Terminal Homology (ENTH), C2 (conserved region-2 of protein kinase C), FYVE and others domains (**Fig. 5**) (Kutateladze, 2010). PPI-binding domains act as effectors of lipid signaling via anchoring proteins to membranes where specific PPIs are present, or through activating proteins by a conformational change, induced under PPI binding (van Leeuwen et al., 2004).

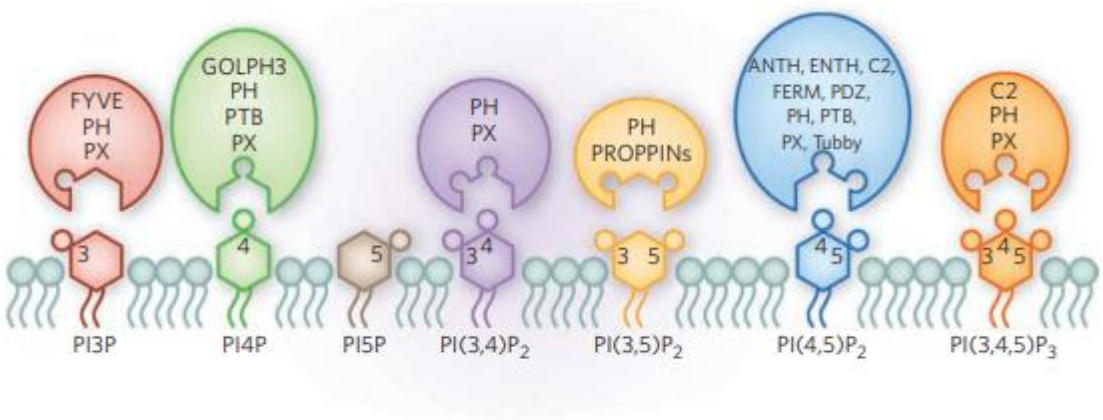

Fig. 5: PPI-recognizing effectors. Signaling domains and their target PPIs. For each PPI, the hydroxyl group that is phosphorylated is indicated by numbering. Mono- PI3P, PI4P, PI5P; poly-phosphorylated PIs: $PI(3,5)P_2$, $PI(4,5)P_2$, $PI(3,4,5)P_3$. The last one $PI(3,4,5)P_3$ is revealed for mammals. Above each PPI, the domains that can bind them are indicated (Kutateladze, 2010).

2.1.3.2.1 Pleckstrin homology domain

The PH domain is found in many proteins. It consists of about 100 amino acids (Maffucci and Falasca, 2001). The PH domain contains seven β-strands and one C-terminal α-helix (**Fig. 6**). Together these elements form a central hydrophobic core that stabilizes the consensus structure. The most conserved elements of PH domains are the hydrophobic residues of the secondary structures that contribute to the hydrophobic core of the domain. The central Trp of the helix is the most conserved residue, displaying 98.2% identity, with its mutation resulting in misfolding. The conserved secondary structure elements contrast with the much more variable loops which connect the β-strands (Lenoir et al., 2015).

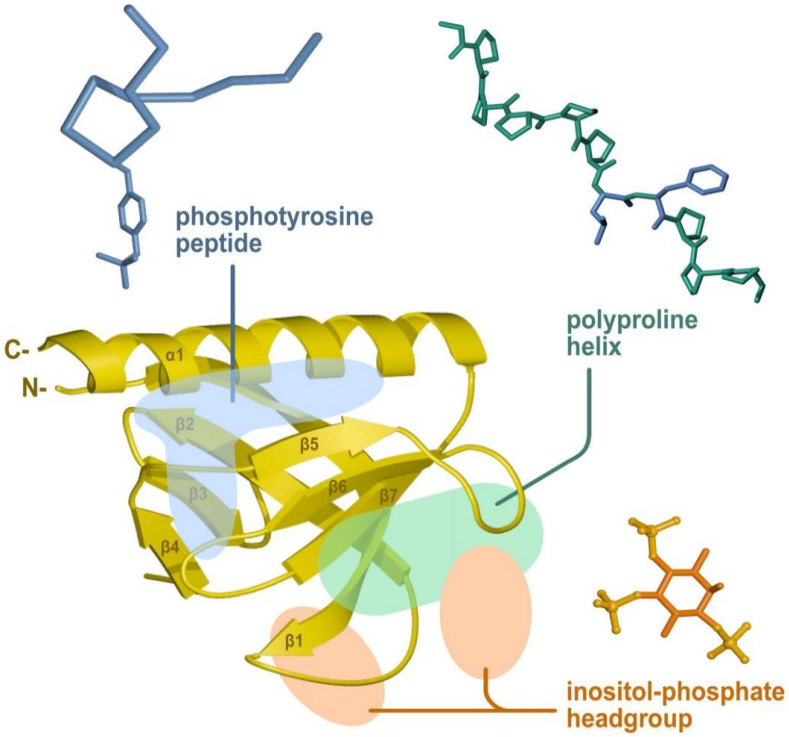

Fig. 6: The PH module and its canonical ligand binding sites. Besides protein interaction partners, the PH fold can accommodate binding sites for phosphorylated inositol head groups (orange), polyproline helices (green) and phosphotyrosine peptides (blue). The α-helix and β-strands of the PH module are labeled and numbered in dark yellow (Scheffzek and Welti, 2012).

The PH domains can have affinity to PI4P, PI(4,5)P_2, PI3P, PI(3,4)P_2 (Stevenson et al., 1998). Individual PH domains possess specificities for these different PPI. *A. thaliana* contains 53 proteins with a PH domain (**Table 1**). Among them are dynamin-related proteins (DRPs), EDR1 (enhanced disease resistance) kinase, 3-phosphoinositide-dependent protein kinase-1 (van Leeuwen et al., 2004). 3′-phosphoinositide-dependent kinase-1 (*AtPDK1*) has a PH domain that binds a wide spectrum of lipids (Deak et al., 1999).

Table 1. Proteins that contain PH domains in *A. thaliana* (van Leeuwen et al., 2004). Domain structures of *A. thaliana* proteins containing PH domains.
Abbreviations: OBP, oxysterol-binding protein; PH, pleckstrin homology; PLD, phospholipase D; RCC, regulator of chromosome condensation; ANK, ankyrin repeats; BAR, Bin/Amphiphysin/Rvs domain; GED, GTPase Effector Domain; START domain is a lipid/sterol-binding domain; OxysterolBP, oxysterol-binding protein; RhoGAP, Rho GTPase activating protein domain; ARFGAP, ARF GTPase–activating protein; S/T kinases, serine-threonine protein kinase catalytic domains.

No	Name	Domains	AGI
1	SWAP70	PH	*At2g30880*
2	AGD4	BAR+PH+ArfGap+2ANK	*At1g10870*

3	AGD2	BAR+PH+ArfGap+2ANK	*At1g60860*
4	AGD1	BAR+PH+ArfGap+2ANK	*At5g61980*
5	SFC	BAR+PH+ArfGap+3ANK	*At5g13300*
6	ADL6	DYN+PH+GED	*At1g10290*
7	DL3	DYN+PH+GED	*At1g59610*
8		PH	*At2g29700*
9		PH	*At5g05710*
10		PH	*At1g77730*
11	ORP1A	PH+OxysterolBP	*At2g31020*
12	ORP1C	PH+OxysterolBP	*At4g08180*
13	ORP1D	PH+OxysterolBP	*At1g13170*
14	ORP2B	PH+OxysterolBP	*At4g12460*
15	ORP2A	PH+OxysterolBP	*At4g22540*
16		PH+START	*At3g54800*
17	EDR2	PH+START	*At4g19040*
18		PH+START	*At5g45560*
19		PH+START	*At5g35180*
20		PH+START	*At2g28320*
21	REN1	PH+RhoGAP	*At4g24580*
22	PHGAP1	PH+RhoGAP	*At5g12150*
23	PHGAP2	PH+RhoGAP	*At5g19390*
24		PH	*At1g48090*
25		PH	*At4g17140*
26	PLD zeta1	PX+PH+2PLD	*At3g16785-90*
27	PLD zeta2	PX+PH+2PLD	*At3g05630*
28		PH	*At1g17820*
29		PH	*At1g73200*
30		PH+6RCC1+FYVE	*At1g65920*

31		PH+6RCC1+FYVE	*At3g47660*
32		PH+6RCC1+FYVE	*At1g69710*
33	PRAF1	PH+6RCC1+FYVE	*At1g76950*
34		PH+6RCC1+FYVE	*At5g42140*
35	RCC1	PH+6RCC1+FYVE	*At3g23270*
36	Disease resistance N like protein	PH+6RCC1+FYVE	*At4g14370*
37		PH+6RCC1+FYVE	*At5g12350*
38	RCC1	PH+7RCC1+FYVE	*At5g19420*
39	FLP5	PH	*At4g32780-85*
40	FKD1	PH	*At3g63300*
41	FL1	PH	*At5g43870*
42	FL2	PH	*At3g22810*
43	FL3	PH	*At4g14740*
44	FL7	PH	*At4g16670*
45	FL5	PH	*At4g17350*
46	F6	PH	*At5g47440*
47	PDK1-1	S/T-Kinase+PH	*At3g10540*
48	PDK1-2	S/T-Kinase+PH	*At5g04510*
49	VPS34	PH+PI3/4Kinase	*At1g60490*
50		PH+PI3/4Kinase	*At1g51040*
51		PH+PI3/4Kinase	*At1g49340*
52		PH+PI3/4Kinase	*At5g09350*
53		PH+PI3/4Kinase	*At5g64070*

In plants, the lipid-interacting properties of PH domain-containing proteins regulate cellular trafficking processes (Allen et al., 2022). PH domain-containing protein AtPH1 (*AT2G29700.1*) directly binds PI3P. The *atph1* mutation leads to accumulation of metal transporter, AtNRAMP1, on the vacuolar membrane (Agorio et al., 2017).

Proteins containing both a PH domain and START domain are rare. *A. thaliana edr2* mutants showed enhanced disease resistance to the biotrophic powdery mildew pathogen *Erysiphe*

cichoracearum. The EDR2 protein consists of a PH domain and a steroidogenic acute regulatory protein-related lipid-transfer (START) domain, and contains an N-terminal mitochondrial targeting sequence. The PH and START domains are implicated in lipid binding, suggesting that EDR2 may provide a link between lipid signaling and activation of programmed cell death mediated by mitochondria (Tang et al., 2005).

Arabidopsis dynamin-like 6 (ADL6) contains a conserved GTPase domain at the N terminus, a PH domain at the center, and a Pro-rich motif at the C terminus. ADL6 is involved in vesicle formation for vacuolar trafficking at the TGN (Jin et al., 2001). Other members of dynamin related proteins DRP2A (*At1g10290*) and DRP2B (*At1g59610*) involved in endocytosis in *A. thaliana*. A functional PH domain is crucial for dynamin activity and in localisation of dynamins (Bethoney et al., 2009).

2.1.3.2.2 Phox homology domain

The PX domain is a type of phosphoinositide binding module that preferentially binds PI3P but can also bind PA, PI(3,4)P_2, PI(3,5)P_2, PI(4,5)P_2, and PI(3,4,5)P_3 (Kanai et al., 2001). The PX domain can also interact with other domains and proteins. The PX domain is approximately 120 residues long, and consists of three antiparallel β-strands (β1-β3), followed by three α-helices (α1–α3) (**Fig. 7**). An extended sequence is found between helices α1 and α2; it is termed the PPK loop as it generally contains a conserved ΨPxxPxK motif (Ψ = large aliphatic amino acids V, I, L, and M). Side chains of residues from the β3 strand, α1 helix and PPK loop together form a binding pocket for the headgroup of the canonical lipid PI3P. PX domain contains a conserved Pro-rich motif that can bind phosphoinositides and SH3 domain.

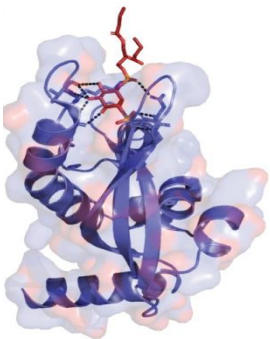

Fig. 7: Structure of PX domain of p40Phox interacting with phosphatidylinositol 3-phosphate (Allen et al., 2022).

In *A. thaliana,* eleven PX domain-containing proteins were identified. They are classified into four subgroups (van Leeuwen et al., 2004) (**Table 2**).

Table 2. *A. thaliana* Phox homology domain proteins. Domain structures of *A. thaliana* proteins containing PX domains.
Abbreviations: PH, pleckstrin homology; PLD, phospholipase D; PXA, PX-associated domain; SPEC, Spectrin repeats; SNX sorting nexin-like

No	**Name**	**Domains**	**AGI**
1	PLD zeta1	PX+PH+2PLD	*At3g16785-90*
2	PLD zeta2	PX+PH+2PLD	*At3g05630*
3	SNX5	PX	*At3g48195*
4	SNX4	PXA+PX	*At2g15900*
5	SNX3	PXA+PX	*At1g15240*
6	EREX	PX	*At3g15920*
7	EREX-like	PX	*At2g25350*
8	EREX-like 1	PX+SPEC	*At4g32160*
9	SNX1	PX	*At5g06140*
10	SNX2b	PX	*At5g07120*
11	SNX2a	PX	*At5g58440*

The PX domain acts as a wedge-shaped phosphoinositide-binding pocket. It homo- and hetero-dimerization facilitate cellular trafficking and proper membrane localization (Pourcher et al., 2010). PX domain-containing proteins (SNX group) are involved in endosomal and vacuolar sorting.

Three of these PX domain proteins are members of the sorting nexin-like (SNX) proteins. *AtSNX1* regulates the distribution of auxin by controlling the trafficking of the plasma membrane transporter *AtPIN2*. *AtSNX1* has a function in root growth and gravitropic response. Compared with WT, *snx1* mutants had shorter primary roots, produced fewer secondary roots and exhibited an altered root gravitropic response (Jaillais et al., 2006).

Another subcategory of PX-containing proteins consists of two PLD (PLDζ1 and PLDζ2) that will be detailed below. Other PX domain protein - ENDOSOMAL RAB EFFECTOR WITH PX DOMAIN (EREX, *At2g25350*) and its homologue EREX-LIKE1 (EREL, *At4g32160*) act together to help sorting and cargo delivery to protein storage vacuoles (Sakurai et al., 2016).

2.1.3.2.3 Epsin N-terminal homology and AP180 N-terminal homology domain

The ENTH and AP180 N-terminal homology (ANTH) domains are present in cytosolic proteins which are required in clathrin-mediated vesicle budding processes. Both bind to phospholipids and proteins. The ENTH domain is approximately 150 amino acids in length and is always found located at the N-terminus of proteins. The domain forms a compact globular structure, composed of nine alpha-helices connected by loops of varying length (**Fig. 8**) (De Camilli et al., 2002). ANTH domain is a globular structure consisting of 10 folded alpha helices and is similar to the smaller epsin N-terminal homology domain (Moshkanbaryans et al., 2014).

Fig. 8: Structure of ENTH domain: eight α helices connected by loops of varying lengths. Three helical hairpins (α1-2, α3-4, and α6-7) are stacked consecutively with a right-handed twist. Proteins containing this domain can bind to phospholipids including $PI(4,5)P_2$ and $PI(1,4,5)P_3$ (on image red molecule) (Ford et al., 2002).

The ENTH domain binds inositol phospholipids in the membrane, most notably $PI(4,5)P_2$, although the lipid binding specificity differs with individual members of the epsin family. The ENTH family consists of classical epsin proteins and the epsin-related (epsinR) proteins that play a role in clathrin-mediated endocytosis or Golgi-to-endosome protein trafficking, respectively. For example, mammalian epsin1 binds to $PI(4,5)P_2$, whereas mammalian epsinR and bacterial Ent3p bind to PI4P and $PI(3,5)P_2$, respectively (Itoh et al., 2001). The ENTH domain is essential for binding ENTH domain containing proteins to specific compartments and also creating curvature in the bound membranes for helping production of clathrin-coated vesicles (Blondeau et al., 2004).

Both ENTH and ANTH (E/ANTH) domains mediate the nucleation of clathrin coats on the plasma membrane or the TGN membrane due to connection with phospholipids and proteins (Holstein and Oliviusson, 2005). Epsin-related proteins can bind directly to clathrin through

their multiple clathrin binding motifs or could recruit clathrin to the plasma membrane or the TGN to generate clathrin-coated vesicles.

All plant ENTH proteins resemble mammalian epsins. Plant ENTH regions have high sequence identity (62.6%) and similarity (92.5%).

Sequence analysis of *A. thaliana* revealed three proteins containing the ENTH signature motif and eight proteins containing the ANTH signature motif. ANTH domain containing proteins can be clustered into two groups based on the presence or absence of NPF (asparagine-proline-phenylalanine) motifs (NPF-rich subfamily vs. NPF-less subfamily) (**Fig. 9**).

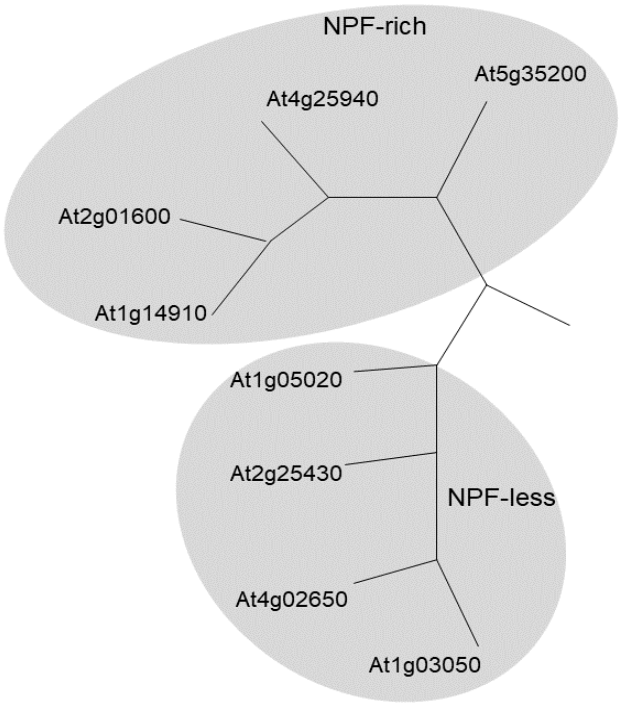

Fig. 9: Plant ANTH proteins. The eight members divide equally into two subgroups on the basis of the presence of the epsin-homology (EH)-interacting NPF motif (Holstein and Oliviusson, 2005).

The three *A. thaliana* proteins containing the ENTH domain are epsinR proteins, EPSIN1, EPSIN2, and EPSIN3 (Holstein and Oliviusson, 2005). *A. thaliana* EPSIN1 interacts with clathrin, adaptor proteins AP-1, vacuolar sorting receptor1 VSR1, and VTI11 (v-SNARE protein) and plays an important role in the vacuolar trafficking of a soluble protein from the Golgi complex to the central vacuole (Song et al., 2006). *A. thaliana* EpsinR2 plays an important role in protein trafficking through interactions with δ-adaptin, AtVTI12, clathrin, and PI3P. EpsinR2 may be recruited to a specific compartment rich in PI3P in plant cells.

2.1.3.2.4 C2 domain

The C2 domain (protein kinase C-conserved 2 domain) contains approximately 130 residues in length and can bind Ca^{2+} and other effectors, including phospholipids (such as phosphatidylserine, phosphatidylcholine and phosphatidylethanolamine), inositol phosphates, and proteins. The C2 domains have conserved three-dimensional structures. The Ca^{2+} binding is coordinated by four-five amino acid residues in bipartite loops inside the C2 domain.

The C2 domain is present in some PLDs. PLDγ and PLDβ contain Ca^{2+}-coordinating acidic amino acids, while PLDα has either positively charged or neutral amino acids. Consequently, Ca^{2+} affinity of PLDα could be lower than that of PLDβ and γ (Wang et al., 2000). These variations in the C2 domains form different biochemical properties that distinguish PLDα from PLDβ and γ (**Fig. 10**). The other PLDs have no C2 domain. There are 220 C2-domains containing proteins in the *A. thaliana* genome.

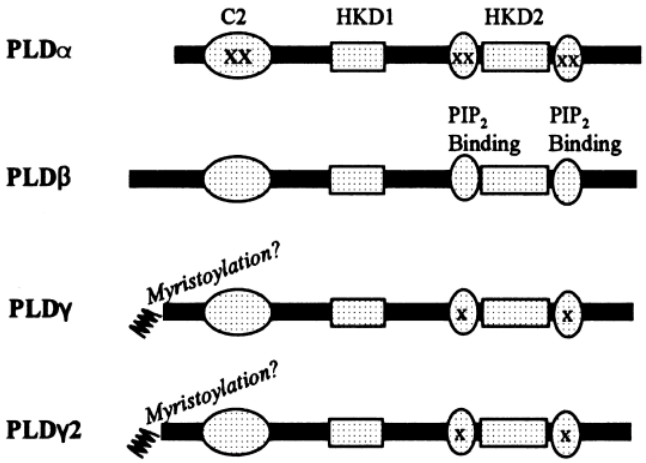

Fig. 10: Domain structures of PLDα, β, γ, and γ2 from *A. thaliana*. XX in the PLDα C2 marks the loss of two acidic residues potentially involved in Ca^{2+} binding. The number of Xs in the PPI-binding motifs marks the loss of the number of basic residues potentially required for PPI binding (Wang, 2000).

C2 domains have been shown to bind phospholipids via the Ca^{2+}-binding regions and phospholipids, phosphoinositides via a β3-β4 lysine-rich cluster. C2-domain proteins are involved in signal transduction, vesicle trafficking and other cellular processes. The *A. thaliana* BAP1 protein contains C2 domain; it negatively regulates defense responses and cell death. The loss of *BAP1* function confers an enhanced disease resistance to virulent bacterial and oomycete pathogens (Yang et al., 2006). One can distinguish two main roles of Ca^{2+} in the membrane targeting of C2 domains. The first is Ca^{2+} ions make a bridge between the C2 domain and anionic phospholipids. The second is Ca^{2+} ions induce intra- or inter-domain

conformational changes, which in turn trigger membrane–protein interactions (Cho, 2001). Ca^{2+}-dependent lipid-binding protein (*AtCLB*) containing a C2 domain binds specifically to the promoter of the *A. thaliana* thalianol synthase gene (*AtTHAS1*), whose expression is induced by gravity and light. AtCLB protein was capable of binding to the membrane lipid ceramide. The role of the *Atclb* gene in negatively regulating responses to abiotic stress in *A. thaliana* was identified. The loss of the *Atclb* gene function confers an enhanced drought and salt tolerance and a modified gravitropic response in T-DNA insertion knockout mutant lines (de Silva et al., 2011). All identified plant PI-PLCs contain a C2 domain (Pokotylo et al., 2014)

Inositol high polyphosphates and phosphoinositides have been described as targets for several C2 domains, including synaptotagmins, DOC2 and classical PKCs. The C2 domain preferentially binds to $PI(4,5)P_2$ and mammalian $PI(3,4,5)P_3$ (Chen et al., 2018). *A. thaliana* synaptotagmin 1 protein (SYT1) containing two C2 domains display phospholipid binding activities. Loss of function of *A. thaliana SYT1* causes a reduction in plasma membrane integrity, which leads to a decrease in cell viability (Schapire et al., 2008).

2.1.3.2.5 FYVE-domain

The FYVE domain got the name after the four proteins in which this zinc-finger domain was first identified in 1996: Fab1p, YOTB, Vac1p and EEA1 (Stenmark et al., 1996). The FYVE domain is essential for endocytosis and vesicular trafficking and it binds only PI3P. The *A. thaliana* genome consists of 16 proteins with FYVE domain (**Table 3**), that could be divided into three categories. One is the Fab family of PI5K. Another includes PRAF proteins (PH domain, Regulator of Chromosome Condensation (RCC) and FYVE), which contain both a PH and a FYVE domain. PRAF proteins seem to be plant specific, because no mammalian homologues are known.

Table 3. *A. thaliana* FYVE domain proteins. Domain structures of *A. thaliana* proteins containing FYVE domains.
Abbreviations: PH, pleckstrin homology; RCC, regulator of chromosome condensation; RING, really interesting new gene finger domain.

No	Name	Domains	AGI
1	Praf1	PH+6RCC1+FYVE	*At1g65920*
2	Praf2	PH+6RCC1+FYVE	*At3g47660*
3	Praf3	PH+6RCC1+FYVE	*At1g69710*

4	Praf4	PH+6RCC1+FYVE	*At1g76950*
5	Praf5	PH+6RCC1+FYVE	*At5g42140*
6	Praf6, RCC1	PH+6RCC1+FYVE	*At3g23270*
7	Praf7	PH+6RCC1+FYVE	*At4g14370*
8	Praf8	PH+6RCC1+FYVE	*At5g12350*
9	Praf9	PH+7RCC1+FYVE	*At5g19420*
10	FAB1B	FYVE+Chaperonin+PIP5K	*At3g14270*
11	FAB1A	FYVE+Chaperonin+PIP5K	*At4g33240*
12	Fyve1	FYVE	*At1g20110*
13	Fyve2	FYVE	*At3g43230*
14	Fyve3	FYVE	*At1g29800*
15	Fyve4	FYVE	*At1g61690*
16	Ring-Fyve, CSU1	RING+FYVE	*At1g61620*

2.1.3.3 PLDs as phosphoinositide-binding proteins

Connections between phosphoinositides and PLDs are crucial for PLDs catalytic activation and/or membrane binding. In the next part I will describe the most important point about PLD-phosphoinositide ability.

2.1.3.3.1 PLD diversity

$PI(4,5)P_2$ is a cofactor of some PLDs that produce PA, a key plant signaling lipid (Pokotylo et al., 2018). In *A. thaliana*, PLD is divided into two classes (**Fig. 11**), differing by the presence of distinct N-terminal phospholipid-binding domains (PX-PH vs. C2). Two of the twelve PLDs contain a PX domain and a PH domain (PLDζ1 and PLDζ2), whereas the remaining ten contain a C2 domain (PLDα (1–3), β (1, 2), γ (1–3), δ, ε) (Hong et al., 2016). The PLDζ1 and PLDζ2 are distinctively different from other PLDs; they have PX and PH domains. PLDε is distinctively different from the other 11 PLDs in *A. thaliana*. It has the C2 structural fold, but contains no acidic residues involved in Ca^{2+} binding in the C2 domain. PLDε is the one that is most closely related to the PX/PH PLDζs.

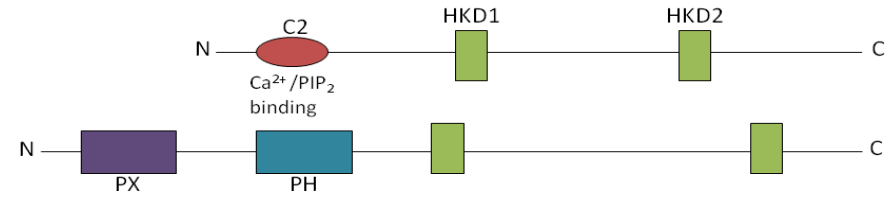

	C2	PX	PH
PLDα1	+	-	-
PLDα2	+	-	-
PLDα3	+	-	-
PLDβ1	+	-	-
PLDβ2	+	-	-
PLDγ1	+	-	-
PLDγ2	+	-	-
PLDγ3	+	-	-
PLDδ	+	-	-
PLDε	+	-	-
PLDζ1	-	+	+
PLDζ2	-	+	+

Fig. 11: *A. thaliana* PLD domain structures and distinguishable biochemical properties.
C2 domain (PLDα (1–3), β (1, 2), γ (1–3), δ, ε); PX domain and a PH domain (PLDζ1 and PLDζ2) (Qin and Wang, 2002).

2.1.3.3.2 PIP2 binding by PLD

$PI(4,5)P_2$ binding can enhance substrate affinity of the PLD enzymes. $PI(4,5)P_2$ is required for the activity of PLDβ, γ, and ζ. PLDαs and ε are active without $PI(4,5)P_2$ which correlates with the fact that some key residues are absent in the $PI(4,5)P_2$ binding domain (Wang, 2002). Although PLDδ is active without $PI(4,5)P_2$, application of $PI(4,5)P_2$ promotes PLDδ activity. PLDβ1 has a $PI(4,5)P_2$ binding region (PBR1) located after the first HKD domain, and PBR1 binds $PI(4,5)P_2$ and is essential for PLDβ1 activity (Wang, 2002). Moreover, PLDβ1 have two polybasic motifs (K/RxxxxK/RxK/RK/R) for $PI(4,5)P_2$ binding flanking the second HKD domain, while PLDαs, γs, δ and ε do not have some of the key residues in corresponding region (Qin and Wang, 2002).

2.1.3.3.3 Other features of PLDs

The C2 domain is needed for binding of Ca^{2+} and phospholipids, which is essential for enzyme activity (Song et al., 2006). PLDβs, γs and δ all have acidic residues for Ca^{2+} binding while PLDαs and PLDε lack some of the Ca^{2+} binding residues. The difference in acidic residues in the C2 domain of PLDs may explain different requirements of Ca^{2+} for enzyme activity. PLDα is the most common plant PLD, which does not require phosphoinositides for activity when tested at millimolar levels of Ca^{2+} (Pappan and Wang, 1999). In comparison,

PLDβ and γ1 are $PI(4,5)P_2$ dependent and have maximum activity at micromolar levels of Ca^{2+} (Qin et al., 1997). PLDβ1 is a plasma membrane localized and interacts with an actin which motif located after the second HKD motif (Kusner et al., 2002).

In *A. thaliana*, the PLDα class contains three members. PLDα1 and α2 are very similar, whereas PLDα3 is more distinct from other PLDs. PLDα1 localizes in the cytosol and membranes. It moved between them in response to stresses (Wang et al., 2000). PLDα3 is associated with the plasma membrane. PLDα1 has a motif between 562 and 586 amino acid residues with high similarity to the DRY motif in proteins interacting with the heterotrimeric G protein subunit Gα. PLDα1 interacts with Gα and stimulates its GTPase activity (Zhao and Wang, 2004, p. 1).

PLDδ is associated with the plasma membrane and binds to microtubule (Gardiner et al., 2001). PLDδ is activated in response to H_2O_2, dehydration, freezing and salinity stress. *AtPLDδ* is required for ABA-induced stomatal closure (Distéfano et al., 2012). In PLDδ, there is an oleate-binding motif located after the first HKD domain and this motif is responsible for oleate-stimulation of PLDδ. PLDα and δ classes have been linked to high salinity and water-deficit stress as well as to the ABA stress hormone (Bargmann et al., 2009). PLDζ2 is associated with the tonoplast membrane (Yamaryo et al., 2008). PLDγ was detected in the plasma membrane, intracellular membrane, nuclei and mitochondria (Fan et al., 1999). PLDε are primarily associated with the plasma membrane.

C2-PLDs used PC, PE and PG as substrates but with different preferences whereas PX/PH-PLDζ1 selectively uses PC as substrate (Qin and Wang, 2002). The different substrate preferences point that different PLDs may selectively hydrolyze different phospholipids and form PAs with different acyl composition. Different PLDs perform unique and important functions in specific plant growth, development or stress response processes.

2.1.3.3.4 PLD in plant response to development

Rigorously I should only discuss PLDs that are dependent on phosphoinositide. But for the clarity of the section, I will also discuss the involvement of all PLD in developmental processes.

The PLD-mediated lipid degradation has been proposed to play a role in membrane degradation in tissue senescence and seed aging. The first way through which PLD influence is exerted is involvement in phytohormone signaling. PLDα was involved in ABA signaling in *A. thaliana*. Suppression of PLDα gene leads to retarded senescence (Fan et al., 1997). It was shown by delayed yellowing, higher contents of chlorophyll and phospholipids, greater

photosynthetic activity, and lower ion leakage when compared with the leaves with normal PLD activity. This effect is obtained because PLDα is a key component contributing to membrane degradation in phytohormone-promoted senescence and PLDα is involved in ABA signaling (Kocourková et al., 2021). Suppression of PLDα in *A. thaliana* also led to enhanced seed quality and viability after storage and after accelerated aging (Devaiah et al., 2007).

PLD is also involved in signaling pathways of ET, another phytohormone involved in stress responses and senescence. Treated *A. thaliana* leaves with ET lead to increased PLDa gene expression, protein level, and activity (Fan et al., 1997).

It has been reported that level of PLD gene expression are controlled developmentally in *A. thaliana*. The PLDα promoter activity is higher in metabolically active tissues, such as, meristematic and elongation zones, than in mature and senescent ones (Novák et al., 2018). In young and rapidly growing tissues PLD provides the mitogenic signals and intermediates for membrane lipid synthesis and remodeling. A high level of PLD expression was noted at the junction regions between primary and lateral roots.

PLDζ1 gene function is implicated in mediating initiation and maintenance of root hairs (Ohashi et al., 2003). The root-hair pattern of *A. thaliana* is regulated by gene GLABRA2 (GL2). *AtPLDζ1* was identified as a direct target of GL2. Inducible expression of *AtPLDζ1* promoted ectopic root-hair initiation, through modulation of phospholipid signaling (Ohashi et al., 2003). In addition, the loss of PLDζ1 and PLDζ2 decreases primary root growth (Li et al., 2006). PA produced by PLD interacts with *AtPDK1*, stimulates a protein kinase cascade, and promotes root apical growth and initiation (Anthony et al., 2004).

It has been reported about the distinctive effect of PLDε on plant growth. Increased expression of other PLD genes, e.g. PLDα2, PLDα3 or PLDδ, does not result in overt growth enhancement while PLDε promotes root growth and biomass accumulation. However, the level of expression of PLDε in vegetative tissue is much lower than that of PLDα1 (Hong et al., 2008).

A. thaliana PLDδ negatively regulates pollen tube growth through F-actin dynamics. Loss of PLDδ function led to a significant increase in pollen tube growth, whereas PLDδ overexpression resulted in pollen tube growth inhibition (Jia et al., 2021).

2.1.3.3.5 PLD in plant response to stress

Here also I will discuss the involvement of all PLDs in stress response, and not only that of phosphoinositide dependent PLDs.

The differences described above in the mode of enzyme activation, subcellular localization indicates that PLDs can be activated differently and have different functions. PLD activity rises in response to various environmental stresses. PLDs are needed for plant growth, development, and response to abiotic and biotic stresses. In this part I will focus on different PLD responses to stress.

Osmotic stress is one of the most important limiting factors for plant growth and plants have some adaptation mechanisms to reduce the damage caused by stress. One of the defense components for that is PLDδ - the most abundant PLD in *A. thaliana* except PLDα1 and is the one of the major sources of endogenous PA (Qin and Wang, 2002). The α-subunit (Gα) of heterotrimeric G-protein interacts with *A. thaliana* PLDα1 (N. Yang et al., 2021). In addition, PLDδ is activated in *A. thaliana* during high salinity and rapid dehydration. Moreover, compared to WT plants, PLDδ knockout plants show decreasing tolerance to freezing injuries, while PLDδ overexpression - increasing tolerance (W. Li et al., 2004). Conversely, PLDα1 abrogation through antisense suppression in *A. thaliana* resulted in a significant increase in freezing tolerance of both non-acclimated and cold-acclimated plants (Rajashekar et al., 2006). Cold treatment activates PLD with forming PtdBut when cold treatment was performed in presence of 0.7% (v/v) butanol present in the medium. PLD triggering was also observed when the temperature of the treatment was set at 0°C or 10°C. PLD activation resulted in accumulation of PA (Munnik et al., 2000, p. 200; Ruelland et al., 2002). PLDα1 is required for high salinity and hyperosmotic stress tolerance in *A. thaliana* (Bargmann et al., 2009). Another role of PLDα1 in *A. thaliana* is regulation of stomatal closure. PLDα1 deficiency leads to ABA insensitive in the induction of stomatal closure. PLDα1-derived PA binds to ABI1, a negative regulator of ABA signaling, to regulate water loss through stomata (Mishra et al., 2006). One more member of PLDα that is involved in stress response is PLDα3. PLDα3 promotes root growth in response to osmotic stress. Under hyperosmotic stress, PLDα3-KO plants have shorter and fewer roots, whereas PLDα3-OE plants have longer and more roots (Devaiah et al., 2007).

Another type of stress which involves PLD is hypoxia. It causes metabolic disturbances at physiological, biochemical and genetic levels and results in decreased plant growth and development. It was reported about involvement of all 10 PLD types with C2 domains in Ca^{2+} signaling under hypoxia using 10 C2-*pld* mutants. Among them the PLDβ2, PLDδ and PLDε displayed less significant roles in Ca^{2+} signaling under hypoxia primarily due to their structural differences (Premkumar et al., 2019).

Important role of PLDβ1 and δ was shown in plant resistance to pathogens. *A. thaliana* deficient in PLDβ1 demonstrated increased resistance to *P. syringae* with an increased accumulation of ROS and SA. On the contrary, PLDβ1-deficient plants have a decreased level of JA (jasmonic acid) and PA production induced by *Botrytis cinerea* infection, as well as JA-inducible gene expression (Zhao et al., 2013, p. 1). PLDβ1 seems to act as a negative regulator of defense responses against biotrophic pathogens, by negatively affecting SA-mediated and positively regulating JA-mediated defense signaling pathways. PLDδ is involved in defense against non-host fungal attack. PLDδ together with PLDα1 mediates the symbiotic interaction and beneficial growth effects between endophytic fungus *P. indica* and *A. thaliana* (Camehl et al., 2011). PLDδ alone helps to avoid from penetration the nonadapted pathogen barley powdery mildew fungus *Bgh* and pea powdery mildew fungus *Erysiphe pisi* into the *A. thaliana* epidermal cell wall (Pinosa et al., 2013). PLDδ was localized in the plasma membrane at the site of fungal attack, where it surrounds the cell wall reinforcement. PA is essential for the resistance against the penetration of powdery mildew fungus, since a decrease in PA production by *n*-butanol increased the penetration rate of fungal spores on WT leaves (Pinosa et al., 2013). PLDδ knockout leads to the loss of ETI-induced and cell wall-based defense against the *P. syringae*, suggesting a role of PLD in plant–microbe interaction and defense responses (Johansson et al., 2014a).

I am now going to introduce the physiological mechanisms in which I am going to study the involvement of PI4Ks in root development and immunity.

2.2 PLANT IMMUNITY

2.2.1 Plant defense mechanisms

Plants meet a wide range of microorganisms during their life, and their interactions with these microorganisms can be either helpful or destructive. Plants have evolved a complex immune system to protect themselves against phytopathogens including viruses, bacteria, fungi, oomycetes, nematodes or herbivores. Plant pathogens are often clustered into three types predicated on nutrient acquisition and as a consequence - viability of host tissue (Kraepiel and Barny, 2016). Biotrophic pathogens establish a long-term feeding relationship with the living cells of plants. Viruses and viroids are biotrophs (Singh and Singh, 1988). They are fully dependent on plant metabolism. While viruses and viroids are intracellular parasites, some biotrophic fungi and oomycetes are able to form specific feeding structures named haustoria, which do not enter the cell but increase the pathogen-plant interface. A detailed

description of haustoria formation is in chapter 2.2.5. On the other hand, necrotrophs produce toxins and hydrolytic enzymes, which enable them to disrupt plant cells and utilize nutrients. Necrotrophic pathogens feed off killed cells. Hemibiotrophs share features with both biotrophs and necrotrophs and usually transit from biotrophic stage to necrotrophic (Shao et al., 2021).

Some chemicals belong to pre-formed defenses, other ones to the inducible. Constitutive defenses that are always "on" include mechanical barriers such as cell walls, cuticle and waxes protecting epidermal cells (Zaynab et al., 2019). It protects the plant from invasion and gives the plant strength and rigidity. In addition to the constitutively present barriers, plants are also equipped with an inducible defense system, which is activated by pathogen recognition. It consists *inter alia* in the production of chemicals toxic to the pathogens as phytoalexins, in pathogen-degrading enzymes, in programmed cell death necessary to circumvent the pathogen spreading and in the induction of enzymes that reinforce the cell wall (Bacete et al., 2018).

Plenty of pathogens can overcome different plant defense strategies and use various ways for penetration. Among them are direct penetration into epidermal and mesophyll cells (only some fungi and oomycetes), through natural openings (stomata, hydathodes, lenticels) or wounds (**Fig. 12**). Bacteria that are located in a water film over stomatal openings easily can get inside and reach the sub-stomatal cavity where they can multiply and start infection. Shortly after recognition of the PAMPs (pathogen associated molecular patterns), plants are capable of closing stomata to restrict the pathogen invasion. Fungal spores generally germinate on the plant surface and germ tubes may directly penetrate epidermal cells through natural openings. Hydathodes are more or less permanently open pores at the margins and tips of the leaves. They are associated with guttation, but not with defence. Lenticels are passive openings on the fruits, stems and tubers that are filled with loosely connected cells to allow passage of air and seem to offer little resistance to pathogen entry (Agrios, 2005).

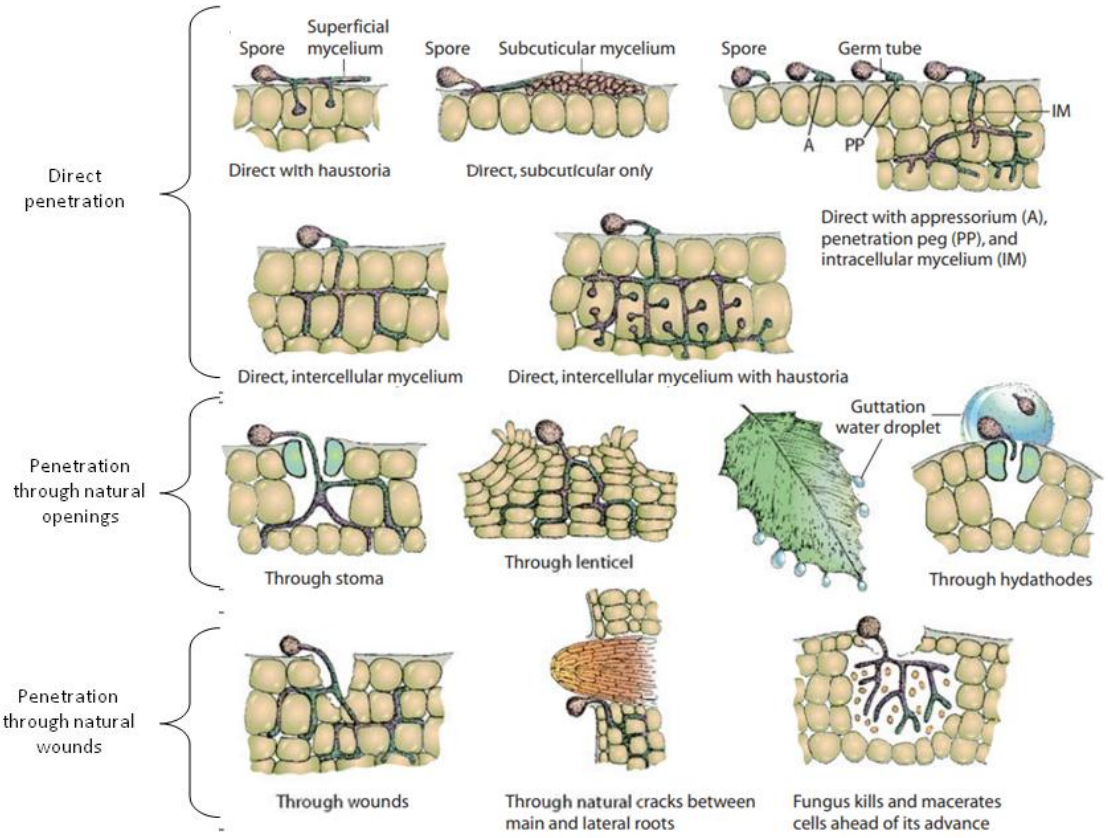

Fig. 12: Methods of penetration and invasion by fungi. There are three types: direct, through natural openings (stomata, hydathodes, lenticels), through wounds (Agrios, 2005).

2.2.1.1 Mechanical and chemical defenses

The first line of plant defense is cuticle and waxes. They form an intact and impenetrable barrier that offers protection against a variety of possible attacks. Epicuticular waxes have mixed functions as mechanical barriers and antifungal properties (accumulating antimicrobial β-lactones). The wax efficiently protects plants against environmental stress, mainly desiccation. The rough wax microstructure reduces the contact surface of the leaf to biotic stressors such as insects, herbivores, fungal infections or microbial spores. It prevents pathogen attaching and formation of water film, in which the spores can germinate. Another protective strategy is the use of trichomes and thorns. For example, trichomes are hair-like epidermal outgrowths. They protect the plant from heat and also from the formation of water film, which e.g. disables spore germination. In some cases filled with toxic compounds that are released upon wounding (Schilmiller et al., 2008).

Plant secondary metabolites have a role in defense against herbivores, pests and pathogens. For example, phytoalexins produced by plants act as protection against pests and pathogens. They may be present constitutively in an inactive storage form (e.g., a glycoside) from which

they are released upon pest or pathogen perception (Osbourn, 1996). Phytoalexins consist of diverse chemical families such as, for instance, phenolics, terpenoids, furanoacetylenes, steroid glycoalkaloids, sulfur-containing compounds and indoles (Jeandet, 2015). For example, camalexins are the main sulfur-containing tryptophan-derived alkaloids in *Brassicaceae* plants that accumulate in response to pathogenic infection (C. Pedras et al., 2011). In *A. thaliana*, camalexin can be induced after pathogen recognition (Gust et al., 2007). Not only biotic, but also abiotic stress (such as ultraviolets, chemicals and heavy metal ions) could induce camalexin in *A. thaliana* leaves (Tierens et al., 2002). Other group includes members that are constitutively present - phytoanticipins. Among phytoanticipins are saponins, glucosinolates, cyanogenic glucosides, benzoxazinone glucosides (mainly for grass family (Poaceae)). Saponins are glycosides which are mostly present in flowering plants (Faizal and Geelen, 2013). Glucosinolates are produced mainly by plants belonging to the order *Brassicales* (Halkier and Gershenzon, 2006). *A. thaliana* contains two groups of these compounds – methionine-derived aliphatic glucosinolates and tryptophan-derived indolic glucosinolates (Wittstock and Halkier, 2002).

2.2.1.2 Cell-surface and intracellular plant immunity

Plants have evolved an immune system that helps detect pathogens. Pathogens have molecular patterns on their surface and also secrete some molecules that activate an inducible part of immunity. There are two types of receptors that can recognize these patterns: cell surface-localized pattern recognition receptors (PRRs) and intracellular nucleotide-binding domain leucine-rich repeat receptors (NLRs).

PRRs recognize microbe-associated molecular patterns (MAMPs), PAMPs and danger associated molecular patterns (DAMPs). MAMPs and PAMPs are small molecules conserved within a class of microbes (Nürnberger and Brunner, 2002). MAMPs are a more general name including also non-pathogenic (e.g. symbiotic) microorganisms. DAMPs are plant-derived molecular patterns that are released from pathogen-infected cells or wounded tissue (Lotze et al., 2007). The recognition of MAMPs, PAMPs and DAMPs by plant cells triggers intracellular signaling events, such as protein phosphorylation, ROS production, calcium influx, extracellular alkalization, and defense gene expression (Song et al., 2021) (**Fig. 13**).

NLRs specifically recognize pathogen-secreted effectors, are activated through the oligomerization and mediate ETI. ETI activation leads to the programmed cell death.

Both PRR-triggered and NLR-triggered immunity (PTI and ETI) lead to the defense responses including the production of reactive oxygen species (ROS), an influx of

extracellular calcium, kinase activation and global transcriptional reprogramming (Bjornson and Zipfel, 2021).

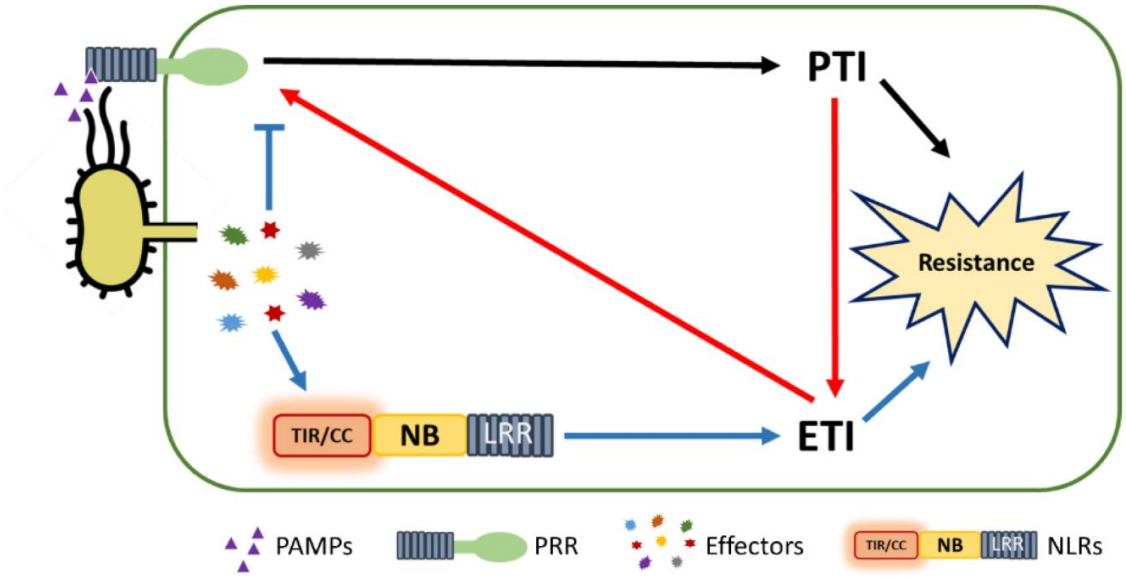

Fig. 13: Schematic diagram of the plant immune system. Plants contain two types of immune receptors for their immunity. Cell surface-localized pattern recognition receptors (PRR) perceive pathogen-associated molecular patterns (PAMPs) and initiate pattern-triggered immunity (PTI; indicated by black arrows). The intracellular NLR receptors sense the effector that is a molecule delivered by the pathogen into the plant cell with the goal to inhibit PTI. Direct or indirect effector binding activates NLR oligomerization resulting in NLR-dependent effector-triggered immunity (ETI, indicated by blue arrows). Red arrows indicate crosstalk between PTI and ETI (Nguyen et al., 2021).

2.2.1.3 Molecular patterns recognised by plants

MAMPs are the main components for the microbes and are conserved among pathogens, non-pathogenic and saprophytic microorganisms. MAMPs cover all microbes regardless of their pathogenicity. PAMPs are MAMPs specific for pathogenic microorganisms (Nürnberger and Brunner, 2002). Among them we can find lipooligosaccharides of gram-negative bacteria, bacterial flagellin, bacterial Elongation Factor-Tu (EF-Tu), glucans and glycoproteins from oomycetes, chitin from fungus cell wall etc (Zhang and Zhou, 2010) (**Table 4**). They are essential components of microbes bodies (except for EF-Tu, Elf) and have physiological function in their fitness and survival (Nürnberger and Brunner, 2002). Flagellin is contained in the flagellum, a locomotory organ of gram-negative bacteria. It has highly conserved N- and C-terminal domains (D1 and D2 domains) with an intervening hypervariable region (D3). The flagellar filament includes approximately 20,000 subunits of flagellin. EF-Tu is one of the most abundant and highly conserved proteins in bacteria. The primary function of EF-Tu

is to transport aminoacylated tRNAs to the ribosome (Berchtold et al., 1993). The N-acetylated 18-aa peptide, elf18, located at N-terminus of EF-Tu protein, serves as a core peptide to elicit plant immunity (Kunze et al., 2004). Lipopolysaccharides are bacterial glycoconjugates found on the outer membrane of gram-negative bacteria. Harpin is an acidic, heat-stable, glycine- and leucine-rich, water-soluble protein, secreted by bacteria with a type III secretion system such as *P. syringae* and *Erwinia amylovora* (Dong et al., 1999). However, secretion of harpin is common to many pathogenic bacteria, and harpin induces strong responses in both host as well as non-host plants (Alfano et al., 1996). Harpins impaire chloroplast function through modifications of the thylakoid membrane structure that increase photosynthetic rates (Garmier et al., 2007). Bacteria respond to a rapid temperature drop by small cold shock proteins (CSP) (Keto-Timonen et al., 2016). CSP acts as a highly active elicitor of defense responses in tobacco. Plant CSPs also exhibit nucleic acid binding and chaperone activity (Nakaminami et al., 2006). Peptidoglycan is a major component of the cell wall of gram-positive bacteria. Fungi cell-wall polysaccharide - chitin and the main fungal sterol - ergosterol, induce plant defense response (Wan et al., 2008).

Table 4. PAMPs perceived by plant cells.

PAMPs	Active motif	Pathogen	Reference
flagellin	flg 22 (amino terminal fragment of flagellin)	Gram negative bacteria	(Gómez-Gómez et al., 2001)
Elongation Factor-Tu	elf18 (N-acetylated amino terminal fragment of EF-Tu)	Gram negative bacteria	(Kawashima et al., 1996)
Lipopolysaccharide (LPS)	Lipid A/Inner core/Glucosamine backbone	Gram negative bacteria	(Erbs and Newman, 2012)
Harpin (HrpZ)	-	Gram negative bacteria	(Lee et al., 2001)
Cold-shock protein	RPN1-motif	Gram negative, Gram-positive bacteria	(Felix and Boller, 2003)
Peptidoglycan	Muramyl dipeptide	Gram-positive bacteria	(Jones and Takemoto, 2004)
Chitin/Chitosan	Chitin oligosaccharides	All fungi	(Wan et al., 2008)
Ergosterol	-	All fungi	(Granado et al., 1995)
Cerebrosides A and C	Sphingoid base	Fungi (Magnaporthe	(Umemura et al., 2004)

		spp.)	
Sulfated fucans	Fucan oligosaccharide	Brown algae	(Klarzynski et al., 2003)
Transglutaminase	Pep13 motif	Phytophthora spp.	(Brunner et al., 2002)
Arachidonic acid	-	Oomycetes	(Boller and Felix, 2009)

DAMPs can be peptides, polysaccharides, nucleotides or oligogalacturonides (**Table 5**). During biotic or abiotic stress, plant polypeptides can be proteolytically processed and released to the extracellular space to act as DAMP signals.

Table 5. DAMPs perceived by plant cells (Hou et al., 2019).

Category	DAMPs	Molecular structure or epitope	Source or precursor	Receptor or signaling regulator	Plant	Reference
Epidermis cuticle	Cutin monomers	C16, C18 hydroxy and epoxy fatty acids	Epidermis cuticle	-	*Arabidopsis thaliana, Solanum lycopersicum*	(Fauth et al., 1998)
Cell wall polysaccharide fragments or degrading products	Oligogalacturonides	Polymers of 10-15 a-1-4-linked GalAs	Cell wall pectin	WAK1 (A. thaliana)	*A. thaliana, Glycine max, Nicotiana tabacum*	(Galletti et al., 2011)
	Cell oligomers	Polymers of 2-7 ß-1,4-linked glucoses	Cell wall cellulose	-	*A. thaliana*	(Souza et al., 2017)
	Xyloglucan oligosaccharides	Polymers of ß-1,4-linked glucose with xylose, galactose, and fructose side chains				(Claverie et al., 2018)
	Methanol	Methanol	Cell wall pectin	-	*A. thaliana, N. tabacum*	(Dixit et al., 2013)
Apoplastic peptides and proteins	CAPE1	11-aa peptide	Apoplastic PR1	-	*A. thaliana, S. lycopersicum*	(Chen et al., 2014)
	GmSUBPEP	12-aa peptide	Apoplastic subtilase	-	*G. max*	(Pearce et al., 2010)
	GRIp	11-aa peptide	Cytosolic GRI	PRK5	*A. thaliana*	(Wrzaczek et al., 2015)
	Systemin	18-aa peptide	Cytosolic prosystemin	SYR1/2	*Some Solanaceae species*	(Wang et al., 2018)
	HypSys	15-, 18-, or 20-aa peptides	Apoplastic or cytoplasmic preproHypSys	-	*Some Solanaceae species*	(Pearce, 2011)
	Peps	23-36-aa peptides	Cytosolic and vacuolar	PEPR1/2	*A. thaliana, Zea mays, S.*	(Hander et al., 2019)

			PROPEPs		*lycopersicum, Oryza sativa*	
	PIP1/2	11-aa peptides	Apoplastic preproPIP1/2	RLK7	*A. thaliana*	(Hou et al., 2014) Shuguo Hou 2014
	GmPep914/890	8-aa peptide	Apoplastic or cytoplasmic GmproPep914/980	-	*G. max*	(Lee et al., 2018)
	Zip1	17-aa peptide	Apoplastic PROZIP1	-	*Z. mays*	(Ziemann et al., 2018)
	IDL6p	11-aa peptide	Apoplastic or cytoplasmic IDL6 precursors	HEA/HSL2	*A. thaliana*	(Wang et al., 2017)
	RALFs	~50-aa cysteine-rich peptides	Apoplastic or cytoplasmic RALF precursors	FER	*A. thaliana, N. tabacum, S.lycopersicum*	(Stegmann et al., 2017)
	PSKs	5-aa peptides	Apoplastic or cytoplasmic PSK precursors	PSKR1/2	*A. thaliana, N. tabacum, S.lycopersicum*	(Mosher and Kemmerling, 2013)
	HMGB3	HMGB3 protein	Cytosolic and nuclear HMGB3	-	*A. thaliana*	(Choi et al., 2016) Hyong Woo Choi 2016
	Inceptin	11-aa peptide	Chloroplastic ATP synthase y-subunit	-	*Vigna ungulculata*	(Schmelz et al., 2006)
Extracellular nucleotides	eATP	ATP	Cytosolic ATP	DoRN1/P2K1	*A. thaliana, N. tabacum*	(Chivasa et al., 2009)
	eNAD(P)	NAD(P)	Cytosolic NAD(P)	LecRK-1,8	*A. thaliana*	(Mou, 2017)
	eDNA	DNA fragments <700 bp in length	Cytosolic and nuclear DNA	-	*Phaseolus vulgaris, Phaseolus lunatus, Pisum sativum, Z. mays*	(Barbero et al., 2021)
Extracellular sugars	Extracellular sugars	Sucrose, glucose, fructose, maltose	Cytosolic sugars	RGS1	*A. thaliana, N. tabacum, Solanum tuberosum*	(Bolouri Moghaddam and Van den Ende, 2012)
Extracellular amino acids and glutathione	Proteinogenic amino acids	Glutamate, cysteine, histidine, aspartic acid	Cytosolic amino acids	GLR3.3/3.6 or others	*A. thaliana, S.lycopersicum, O. sativa*	(Kadotani et al., 2016)
	Glutathione	Glutathione	Cytosolic glutathione	GLR3.3/3.6	*A. thaliana*	(Li et al., 2013, p. 3)

2.2.1.3.1 Recognition of molecular patterns by pattern recognition receptors

PAMPs, MAMPs and DAMPS are detected by PRRs. PRRs are cell-membrane localized receptors. One distinguishes receptor-like kinases (RLKs) and receptor-like proteins (RLPs).

RLKs have an extracellular domain for ligand-binding, single transmembrane domain and an intracellular kinase domain that is important for signal transduction. RLPs have a similar structure, but without the intracellular kinase domain. There are different types of extracellular domains. Based on it, PRRs can be divided into the leucine-rich repeat (LRR)-, lysin motif (LysM)-, lectin-, wall-associated kinase (WAK) and other subfamilies (Couto and Zipfel, 2016) (**Fig. 14**). Some LRR-RLKs serve as a receptor for hormones. For example, BRASSINOSTEROID INSENSITIVE 1 (BRI1) binds brassinolide and is involved in brassinosteroid signaling (Sun et al., 2013a).

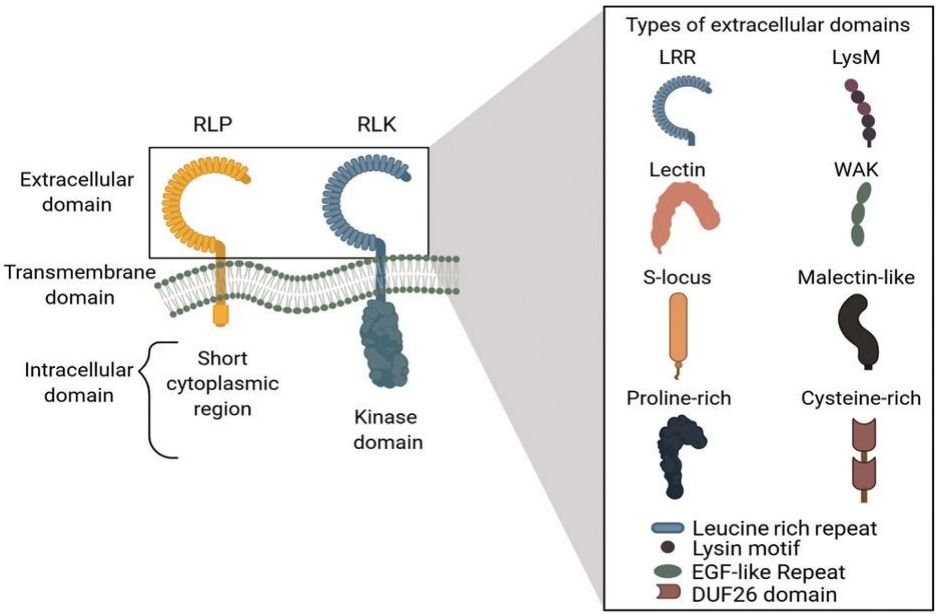

Fig. 14: Plant cell-surface receptors. RECEPTOR-LIKE KINASE (RLK) contains an extracellular domain, transmembrane domain and a kinase domain. RECEPTOR-LIKE PROTEIN (RLP) possesses an extracellular domain, transmembrane domain and a short cytoplasmic region, but lacks a cytoplasmic kinase domain. RLKs and RLPs are classified in several subgroups based on the diverse composition of the extracellular domains. These include: leucine-rich repeat (LRR) domain; LysM, constituted by lysin motifs; lectin; wall-associated kinases (WAK), comprised of epidermal growth factor-like repeat; S-locus domain; malectin-like; proline-rich; and cysteine-rich repeat, consisting of DUF26 domain (Escocard de Azevedo Manhães et al., 2021).

MAMPs, PAMPs and DAMPs are recognized by cell surface-localized PRRs, consequently activating PTI. Activation leads to the recruiting of co-receptors. Subsequently, receptor-like cytoplasmic kinases phosphorylate downstream components (e.g. RBOHD, CNGCs/OSCA1.3, MAPKKKs, and WRKYs) to trigger ROS burst, Ca^{2+} influx, MAPK activation, phytohormone production and transcriptional reprogramming.

2.2.2 Receptors used in the study

2.2.2.1 FLS2 receptors

The FLS2 receptor belongs to the LRR-RLKs family (Zipfel, 2014) (**Fig. 15**). It is essential for flagellin perception. FLS2 recognizes bacterial flagellin via the direct binding of 22 amino acids epitope (flg22), located close to the N terminus of flagellin.

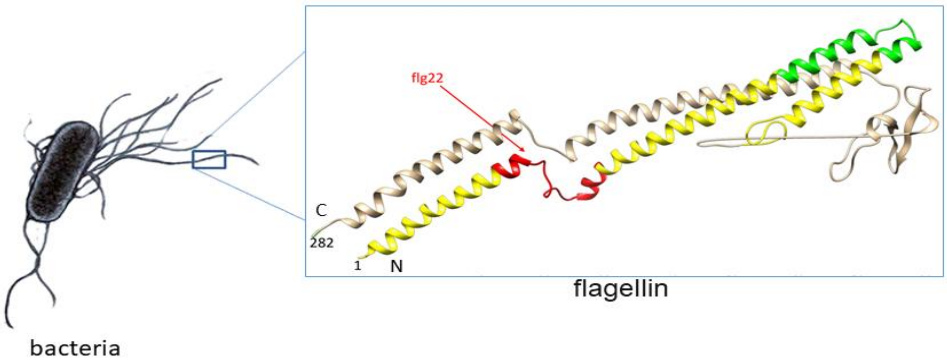

Fig. 15: 3D structure of bacterial flagellin. Epitope flg22 is highlighted in red (Ciarroni et al., 2018).

Flg22 binding to plant receptor kinase FLS2 leads to the recruitment of the LRR-RLK BAK1, which acts as a coreceptor for flg22 and is required for the full activation of FLS2 and flg22-triggered immune signaling (Zipfel et al., 2006)**.**

2.2.2.2 PEPR1/2 receptors

PEPR1 and PEPR2 receptors belong to the LRR-RLKs family. PEPR1 and PEPR2 are homologous proteins, containing extracellular LRR motifs (**Fig. 16**).

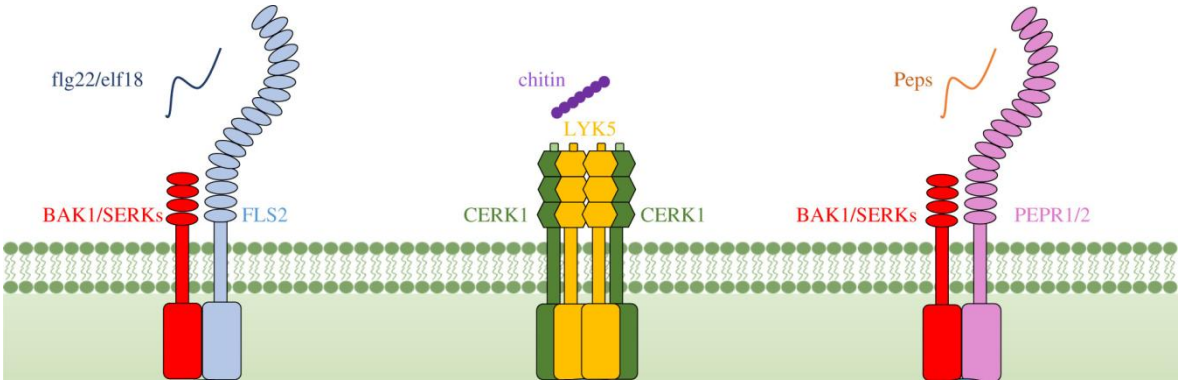

Fig. 16: Representative images of FLS2, CERK and PEPR receptors. Ovals - LRR domain (for FLS2, PEPR1/2 and BAK1), for CERK - LysM domain, small rectangle - transmembrane domain, big rectangle - kinase domain (Zhou et al., 2019).

Both kinases act as receptors for Peps (Tang et al., 2015). Plant elicitor peptide 1 (Pep1), a 23-amino acid endogenous peptide was initially identified as a DAMP in *A. thaliana* (Huffaker et al., 2006). It is derived from the carboxyl end of an approximately 100-aa long precursor protein, PROPEP1. *A. thaliana* encodes eight PROPEP paralogs (PROPEP1-PROPEP8) that contain conserved Pep epitopes in their C-terminus.

Individual PROPEPs have been shown to localize to the cytosol or to be associated with the tonoplast (Bartels et al., 2013), but it is perceived outside of cells, contributing to the assumption that Peps are released into the apoplast during cell damage. Each kinase interacts with different Pep resulting in different responses. PEPR1 recognizes all eight Peps, but PEPR2 detects Pep1 and Pep2. Pep1 binds to the PEPR1-LRR domain, induces heterodimerization between PEPR1 and its coreceptor BAK1, and BAK1-dependent PEPR activation (Tang et al., 2015). Pep-PEPR1 also activates SA, JA, and ET-mediated immune pathways (Ross et al., 2014).

2.2.2.3 CERK1 receptors

CERK1 (chitin elicitor receptor kinase1) receptors belong to the LysM-RLK family. They are responsible for the perception of chitin, the main component of fungal cell walls. Chitin is a polymer of N-acetyl-Dglucosamine (Boller, 1995). CERK1 contains three extracellular LysM-domains and an intracellular kinase domain (**Fig. 16**) (Wan et al., 2012). CERK1 can bind to chitin on its own, although this interaction is very weak, so it has been suggested that a second protein may be involved. Lysine motif receptor kinase (LYK) is very similar to CERK1, and is much better at attaching to chitin in *A. thaliana*. Chitin binds to the LysM domains on two monomers, resulting in homodimerization of CERK1 co-receptor and intracellular kinase domain activity (T. Liu et al., 2012). It was shown that CERK1 phosphorylates receptor-like cytoplasmic kinases BIK1 and PBL19/27 in *A. thaliana* (Yamaguchi et al., 2017). PBL19 and PBL27 phosphorylate MAPKKKs to activate mitogen-activated protein kinase (MAPK) cascades (Shinya et al., 2014). BIK1 regulates chitin-induced Ca^{2+} influx and ROS burst. Feronia, IOS1, and the ubiquitin E3 ligase PUB4 are positive regulators of chitin responses.

After chitin sensing, CERK1 recruits the CERK1-interacting protein phosphatase 1 that deactivates CERK1 by dephosphorylating its Tyr428 (Liu et al., 2018).

CERK1 may mediate the perception of a bacterial PAMP. *A. thaliana cerk1* mutants showed enhanced disease symptoms and higher bacterial growth when *Pto* DC3000 was sprayed onto

leaves (Gimenez-Ibanez et al., 2009). *A. thaliana* CERK1 mediates plant immunity in response to non-host resistance to *Fusarium oxysporum* (Huaping et al., 2017). CERK1 also involved in salt tolerance. It interacts with calcium channel protein ANNEXIN 1, which is responsible for salt-induced calcium inward flow (Espinoza et al., 2017). CERK1 has been suggested to cooperate with two LysM-RLPs, LYM1 and LYM3, to regulate bacterial peptidoglycan-triggered immunity in *A. thaliana* (Willmann et al., 2011). CERK1 has been characterized as a receptor or coreceptor for fungi derived molecules besides chitin. In *A. thaliana*, CERK1 has been shown to mediate immune responses to the fungal non branched β-1,3-glucan in an LYK5-independent manner (Mélida et al., 2018).

2.2.2.4 BAK1 receptors

BAK1 (BRI1-associated receptor kinase 1) is a co-receptor belonging to the LRR-RLK family. BAK1 is a member of the SERK family and mostly forms ligand-induced heteromers with other RKs for subsequent signaling. *A. thaliana* contains five members of the SERK family. BAK1 includes a small extracellular LRR domain with five repeats. The LRR domain is followed by a SPP motif, the serine and proline rich domain that defines the SERK protein family (Chinchilla et al., 2009), a single membrane-spanning domain, a cytoplasmic kinase domain and a short C-terminal tail (**Fig. 17**).

BAK1 forms a ligand-inducible complex with the LRR-RK brassinosteroid (BR) receptor BRI1 through the receptor transphosphorylation that increases kinase activity. BAK1 acts as a positive regulator of the BRI1 pathway, *bak1* mutants are hyposensitive to BR (Wang et al., 2008).

BAK1 establishes a ligand-dependent complex with several PRRs. It is needed for the perception of bacterial PAMPs elf18, LPSs, PGNs, HrpZ, csp22 (derived from cold shock protein), the oomycete PAMP - INF1, and the DAMP - Pep1. BAK1 forms a ligand-dependent complex with FLS2. This connection occurs within seconds of flg22 binding and leads to rapid phosphorylation of FLS2 and BAK1 (**Fig. 16**). Loss of BAK1 results in reduced flg22 responses (Chinchilla et al., 2007).

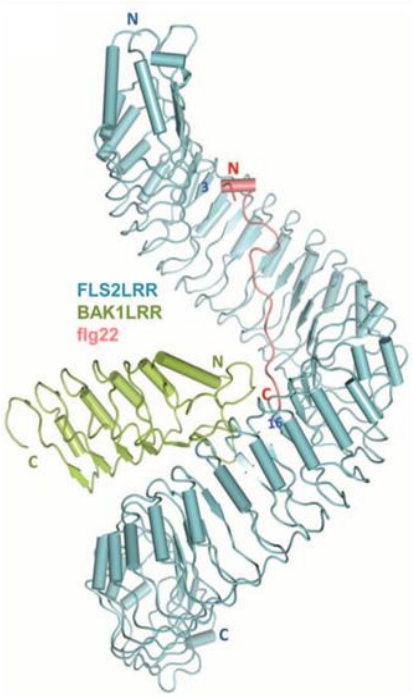

Fig. 17: Crystal structure overall structure of FLS2LRR-flg22-BAK1LRR. "N" and "C" represent the N and C terminus, respectively. FLG22 is in red, FLS2 in blue and BAK1 in green (Sun et al., 2013b).

2.2.2.5 NLR signaling

The second major class of immune receptors consists of proteins belonging to the NLR family. The main difference between NLR and PRRs is that NLR proteins detect pathogen-generated virulence molecules in the cytoplasm (Bonardi and Dangl, 2012). NLR receptors are encoded by resistance genes. Plant NLR proteins have a C-terminal leucine-rich repeat domain (highly polymorphic and variable in the number of the repeats, and typically confers recognition specificity) and a central NB-ARC domain (nucleotide-binding adaptor shared by Apaf-1, Resistance proteins, and CED-4) (modulates sensor NLR activation state through the essential catalytic P-loop motif) (van der Biezen and Jones, 1998). Plant NLRs are roughly divided into two groups, depending on their N-terminal structures. CNL type NLRs (CC-NB-LRR) have a N-terminal coiled-coil (CC) domain while TNL type NLRs (TIR-NB-LRR) have a N-terminal Toll/interleukin-1 receptor domain (TIR) (Meyers et al., 2003) (**Fig. 18A**). Both CC and TIR domains have been demonstrated to play key roles in the formation of dimers and oligomers. CC and TIR are signaling domains, the NBD and LRR domains perform regulatory and sensor functions. Recognition of the effector involves an intramolecular conformation change and ATP binding (**Fig. 18**). During direct or indirect

recognition of effector proteins, NLR could create oligomeric complexes - resistosomes. They activate defence responses usually associated with a cell death. *A. thaliana* has CNL type ZAR1, encoded by the resistance gene HOPZ-ACTIVATED RESISTANCE 1. ZAR1 induces defense mechanisms through an indirect recognition of several bacterial pathogen effectors. These bacterial effector proteins change various RLCKs by acetylation, ribosylation, or uridylylation to trigger virulence. ZAR1 recognizes these modifications and activates immune signaling (Burdett et al., 2019).

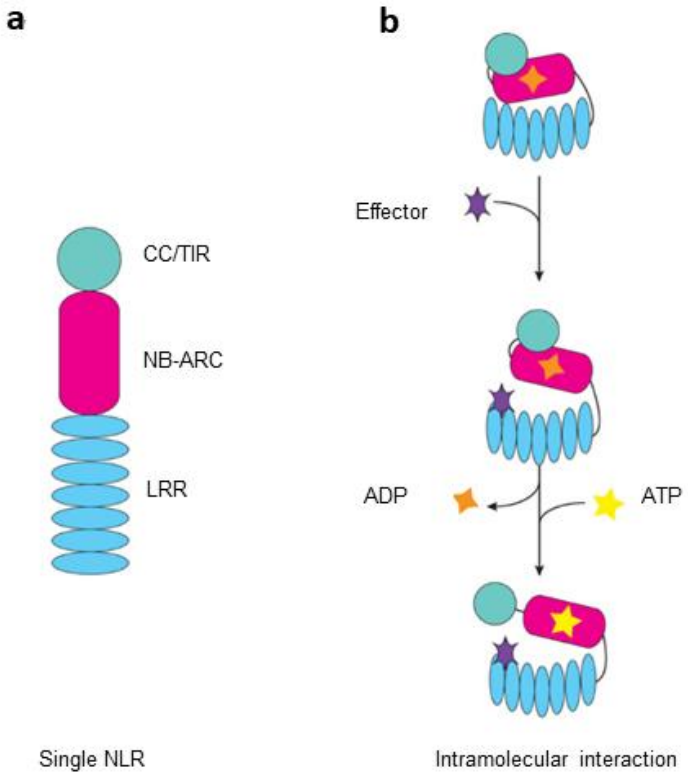

Fig. 18: Schematic representation of intramolecular interactions of plant NLRs. **a)** domain modularity of plant NLRs; **b)** intramolecular interactions maintain the NLR in an "off" state through the inhibitory function of the LRR domain (top). Effector recognition results in a conformational change that allows nucleotide cycling and NLR activation (middle). Catalytic activity of the NB domain triggers a second conformational change that exposes the N-terminal domain (bottom) (Bonardi and Dangl, 2012).

A TIR domain is α/β protein domain, typically comprises five parallel β-strands alternating with five α-helices (Toshchakov and Javmen, 2020). The CC domain contains compact four-helical bundles (Maruta et al., 2022) (**Fig. 19**).

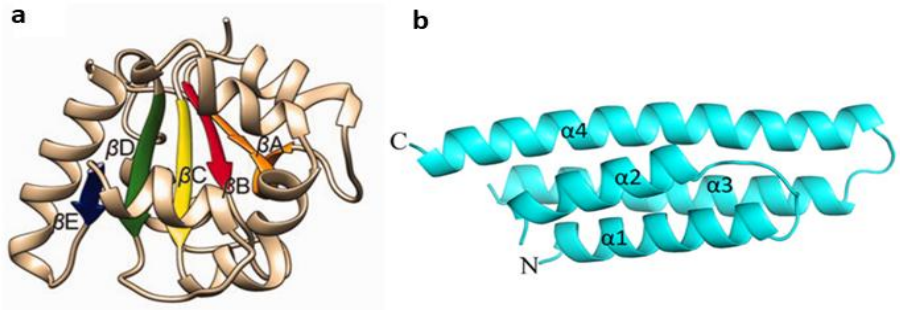

Fig. 19: a) structure of TIR domain. Five strands indicated by different colors (Toshchakov and Javmen, 2020); **b)** structure of CC domain. Four-helix bundle α1-α4. (Hao et al., 2013).

The activity of NLR is regulated by dimerization or oligomerization, self-inhibition, epigenetic and transcriptional regulation, alternative splicing and proteasome-mediated degradation. In the cell NLR can be in the inactive, intermediate and activated states. The example of NLR activation could be described with the microbial pathogen *Xanthomonas campestris*. ZAR1 indirectly recognizes the *Xanthomonas* effector AvrAC through effector-mediated uridylation of the plant kinase PBL2 (Li et al., 2015). Inactive ZAR1 self-associates through inter-domain interactions and interacts with the pseudokinase RKS1 through its LRR domain. Upon uridylation, PBL2 recruits and binds to RKS1 that modify conformation in ZAR1's NBS domain causing release of ADP and formation of a ZAR1–RSK1–PBL2 trimeric complex that corresponds to the intermediate state. ZAR1 dATP or ATP binding induces conformational changes in the NBS domain, which leads to oligomerization of the complex into a higher order wheel-like pentamer - resistosome (Xing et al., 2019). During oligomerization the N-terminal α-helices of the ZAR1 CC domains form a protruding funnel-like structure. The N-terminal α-helix is essential for enhanced membrane association and signaling upon ZAR1 activation. ATP binding, oligomerization and cell death induction are common features of NLR activation. Active CNLs form pores in the membranes and affect selective membrane permeability. Membrane disruption could also induce DAMP signaling and be perceived by PRRs to amplify immune responses (Couto and Zipfel, 2016).
SNC1 is one of the member NLR group receptors that was studied in the work.

2.2.2.5.1 SNC1

A. thaliana SNC1 encodes a TIR-NB-LRR-type R protein. Suppressor of *npr1-1*, constitutive 1 (SNC1) in *A. thaliana* localize in the nucleus, decrease nuclear resistance protein pool against avirulent pathogens and attenuates the activation of downstream defense responses

(Zhu et al., 2010). ABA deficiency promotes the activity and nuclear localization of SNC1. SNC1 is involved in the SA-dependent defense response pathway. A gain-of-function mutant in *SNC1* resulting from a point mutation *snc1*, shows enhanced stability of the SNC1 protein, constitutive activation of autoimmunity and reduced plant size (Cheng et al., 2011), suggesting a crucial role of SNC1 in plant immune responses. *snc1* plants are smaller than WT plants, accumulate high levels of SA, and often have curly leaves.The loss-of-function mutant of SNC1, *snc1-11,* abolished expression of full length SNC1 transcript (Yang and Hua, 2004). *snc1-11* mutant is morphologically normal and expresses normal levels of defense-related genes (Garner et al., 2021). As for the regulation of SNC1, MOS1 (MODIFIER OF snc1-1) factor is essential for the upregulation of SNC1 gene at the chromatin level (Li et al., 2010) and glycosyltransferase UGT73C7 mediates the redirection of phenylpropanoid metabolism to regulate the transcription of SNC1 (Chen et al., 2020).

2.2.3 Plant phytohormones

2.2.3.1 Salicylic acid

SA is one of the critical plant hormones that activates disease resistance in *A. thaliana*. SA is a phenolic molecule, synthesized by plants and increases both in PTI and ETI.

SA plays a major role in plant defense (Vlot et al., 2009). Pathogen infection induces SA biosynthesis and accumulation. Also it is involved in physiological processes, such as flowering and seed germination (Rajjou et al., 2006). SA is controlling the biochemical processes in plants, involving stomatal closure, production of chlorophyll and proteins, nutrient uptake, transpiration, and photosynthesis (Abbas, 2019).

SA could be modified by methylation, glycosylation or conjugation to amino acids, making it transportable (Ludwig-Müller et al., 2015) or inactive (Dean et al., 2003). SA glucose ester (SGE), SA 2-O-ß-D glucoside (SAG) and methyl salicylate (MeSA) serve for transportation; inactive derivatives are dihydroxyderivatives, 2,3- and 2,5-dihydroxybenzoic acid (2,3-DHBA and 2,5-DHBA, respectively). The SA glycosides could be actively transported from the cytosol to the vacuole as an inactive storage form that can later be converted back to SA (Dean et al., 2005). Membrane permeability and volatility of SA can be increased by methylation, which leads to effective long-distance transport of SA (Park et al., 2007).

External SA application changes expression of several genes (Krinke et al., 2007; Van Leeuwen et al., 2007). Transcription of the majority of SA-regulated genes is dependent on NONEXPRESSOR OF PR GENES1 (NPR1) (Ryu et al., 2006). Two subsets of resistance genes act via pathways that involve enhanced disease susceptibility1 (EDS1) or non-race-

specific disease resistance 1 (NDR1), proteins that regulate SA biosynthesis (Vlot et al., 2009). Nucleocytoplasmic lipase-like protein (EDS1) mediates recognition pathogen effectors by TIR-type NLRs that activate transcriptional reprogramming, resistance and host cell death (Xu et al., 2015). CC-type NLRs require NDR1 to activate the downstream signaling pathway (Aarts et al., 1998). SA is involved in plant responses to abiotic stresses, such as drought, chilling, heavy metal toxicity, heat, and osmotic stress (Rivas-San Vicente and Plasencia, 2011), regulates developmental and physiological processes such as seed germination (Rajjou et al., 2006), vegetative growth, senescence (Vogelmann et al., 2012) and stomatal closure (Khokon et al., 2011).

SA has two distinct biosynthetic pathways: the isochorismate (IC) pathway (Route 1) and the phenylalanine ammonia-lyase (PAL) pathway (Route 2) (**Fig. 20**). Both IC and PAL are derived from chorismate, the end product of the shikimate pathway (Wildermuth et al., 2001). The ICS (isochorismate synthase) pathway is well described in *A. thaliana*.

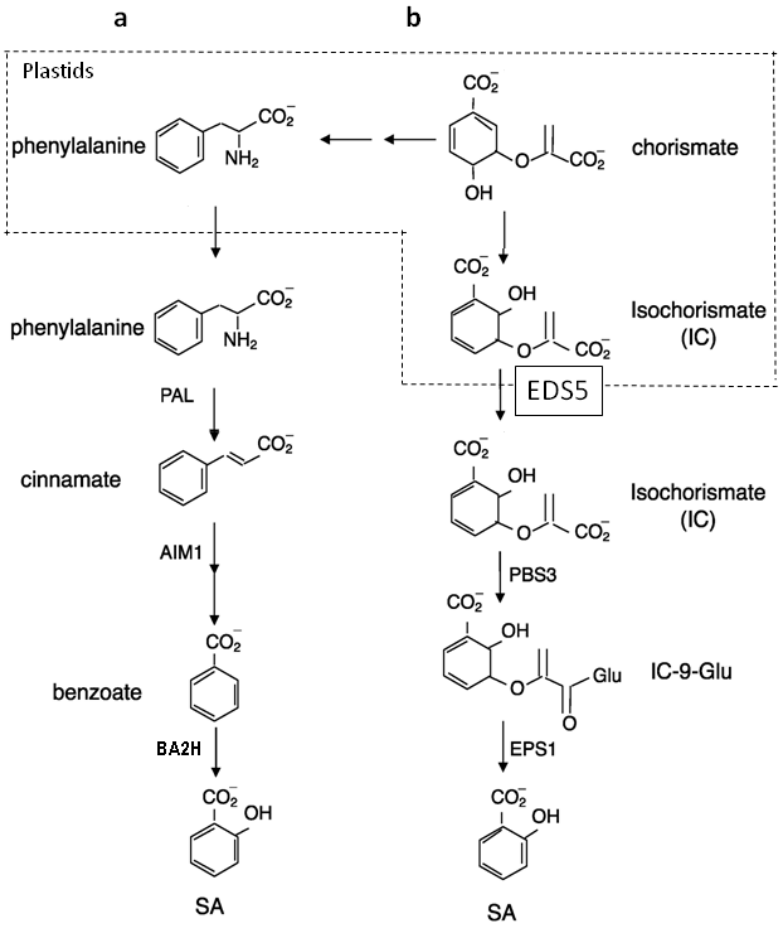

Fig. 20: Pathways for the salicylic acid biosynthesis in plants. **a)** the isochorismate synthase (ICS) pathway in *A. thaliana*. Chorismate is converted to isochorismate (IC) by ICS1/ICS2 in plastids. IC is transported to cytosol by the MATE transporter Enhanced Disease Susceptibility 5 (EDS5). AvrPphB

Susceptible 3 (PBS3) catalyzes the conjugation of IC to glutamate (Glu) to produce IC-9-Glu, which breaks down spontaneously to produce SA. Enhanced Pseudomonas Susceptibility 1 (EPS1) enhances the conversion of IC-9-Glu to SA. **b)** the proposed phenylalanine ammonia lyase (PAL) pathway. PALs convert phenylalanine (Phe) to trans-cinnamic acid (t-CA), which is oxidized to form benzoic acid (BA) by Abnormal Inflorescence Meristem 1 (AIM1). SA is then produced by hydroxylation of BA via a hypothetical BA-2-hydroxylase (BA2H) (Peng et al., 2021).

The first pathway for SA biosynthesis starts from chorismate, which is converted into IC by ICS (Gu et al., 2018). The *A. thaliana* genome contains two ICS homologs, *ICS1* and *ICS2* (Macaulay et al., 2017), *ICS1* is the main contributor. Both ICS1 and ICS2 are localized in the chloroplasts (Groszmann et al., 2015). EDS5 is a transporter for isochorismate from the plastids to the cytosol. Then an amidotransferase PBS3 catalyzes the conjugation of isochorismate to glutamate with isochorismate-9-glutamate (IC-9-Glu) formaton. IC-9-Glu can spontaneously decompose (Rekhter et al., 2019) into SA or be converted to SA by enhanced pseudomonas susceptibility 1 (Torrens-Spence et al., 2019).

The PAL pathway also contributes to SA biosynthesis. *A. thaliana* has four PAL homologs. The enzyme PAL converts phenylalanine into trans-cinnamic acid (tCA) and then converted to SA via benzoic acid (BA). The conversion of phenylalanine to t-CA by PAL is one of the rate-determining steps in SA biosynthesis. Another component of PAL pathway, abnormal inflorescence meristem1 (AIM1), has been identified in *A. thaliana* and rice and is a member of the multifunctional protein family (Arent et al., 2010). AIM1 is involved in the β-oxidation of fatty acids and is required for the conversion of tCA into benzoic acid in *A. thaliana* seeds (Wiszniewski et al., 2014). The last step, converting BA into SA, is catalyzed by a presumed benzoic acid hydroxylase. This enzyme has not yet been identified (Lefevere et al., 2020).

2.2.3.2 Jasmonic acid

Jasmonates (jasmonic acid, its precursors and derivatives), are endogenous growth-regulating polyunsaturated fatty acid-derived phytohormones. They are involved in a wide range of plant processes such as growth, development, senescence, and defense (Yan et al., 2014).

JA regulates plant growth and development, for example, axis elongation during embryogenesis, flower development, leaf senescence, root formation, and stomatal opening (Lakehal and Bellini, 2019). During abiotic stress, JA is involved in physiological responses such as activation of the antioxidant system, accumulation of amino acids and soluble sugars, regulation of stomatal opening and closing (Karpets et al., 2014).

JA is associated with SA, ET, IAA and other hormones to support plants adaptation to the environment. The effects of SA on the JA pathway can be antagonistic, synergistic, or

neutral. JA-responsive genes *PDF1.2* and *VSP2* are highly sensitive to suppression by SA. Several regulators of the interaction between the SA and JA pathways have been shown: the redox sensitive transcriptional coregulator NPR1, several WRKY and TGA transcription factors (TF) (Caarls, 2016).

It has been shown that some WRKY TF (*WRKY50*, *WRKY51*, *WRKY70*, and *WRKY62*) are regulated by the JA signaling pathway (J. Li et al., 2017). *WRKY70* overexpression leads to the constitutive expression of SA-responsive *PR* (pathogenesis-related) genes and enhanced resistance to the biotrophic pathogen *Erysiphe cichoracearum* but repressed the expression of JA-responsive marker gene *PDF1.2* and compromised resistance to the necrotrophic pathogen *Alternaria brassicicola* (J. Li et al., 2004).

Interestingly, JA signaling pathway is also triggered through the plasma membrane receptors PEPR1 that are activated by AtPEP1. AtPEP1 also activates plasma membrane phospholipase (DAD1, DGL, and PLD in *A. thaliana*) that releases linolenic acid (a precursor of JA synthesis) from the phospholipid (Hind et al., 2010).

JA could be transported both short- and long-distance (Sun and Zhang, 2021). In plants, JA could accumulate at the site of injury due to mechanical damage or insect feeding. Deposition leads to the defense genes expression. In the local defense response, exist two ways of short-distance transmission of the JA. First, AtPEP1 released by the wounding acts as a signaling molecule, transported to the adjacent site through the apoplast and phloem to activate the JA cascade reaction pathway. Second, JA and JA-Ile induced by AtPEP1 act as signals and are transported to adjacent sites for defensive responses (Truman et al., 2007). Also it is known about the long-distance transmission of JA signals via vascular bundle transmission and/or airborne transmission.

To activate JA responses at low JA concentrations plants used ABC transporter AtJAT1/AtABCG16 that localized on the nuclear and plasma membranes (Q. Li et al., 2017). When the concentration of JAs is high, JA transporters on the cytoplasmic membrane become dominant that allow to reduce intracellular JA and JA-Ile concentrations to desensitize the JA signal. The JAs signaling could be activated in other cells through JA transportation to the apoplast. During stress AtJAT1/AtABCG16 rapidly regulate the dynamics of JA/JA-Ile in cells, allowing quick transport of JA-Ile into the nucleus to avoid the inhibition of plant growth and development by the defense response (Ruan et al., 2019).

2.2.3.3 Ethylene

ET is multifunctional phytohormone that controls growth and senescence of plants, fruit ripening (Nazar et al., 2014). It is gaseous and has a simple C_2H_4 structure. ET receptors localized on the endoplasmic reticulum and Golgi apparatus which negatively regulate ethylene responses (Dong et al., 2008).

ET could have a positive and negative impact on plant immunity. In *A. thaliana*, ET activates SA-responsive *PR-1* expression (De Vos et al., 2006). Conversely, the ET-responsive transcription factors EIN3 and EIL1 were involved in the repression of PAMP-responsive genes in *A. thaliana*, including the SA biosynthesis gene *ICS/SID2*, resulting in reduced accumulation of SA (Chen et al., 2009). ET is produced in response to multiple environmental stresses both abiotic and biotic. The ET level is higher during the first stage of leaf formation and decreases until it reaches maturity when the leaf is completely expanded, then it increases again during the early step of the senescence initiation. Leaf senescence is activated at the mature stage of leaf development when leaves are fully expanded. The balance between ET and auxin is crucial for the regulation of leaf abscission. During leaf senescence, the auxin concentration declined and tissue sensitivity to ET increased as well as ethylene biosynthesis (Botton and Ruperti, 2019).

Five different types of ET receptors are present in *A. thaliana*: ETR1, ERS1, EIN4, ETR2, and ERS2 (Li et al., 2020). Each contains N-terminal transmembrane, GAF, and histidine (His) kinase domains, and ETR1, EIN4, and ETR2 also contain a receiver domain. In the absence of the hormone, ET receptors activate constitutive triple response 1 (CTR1). CTR1 phosphorylates ethylene insensitive (EIN)-2, an ER-bound, Nramp-like transmembrane protein, to repress its ability to induce ethylene responses (Wen et al., 2012). After the binding of ET to a receptor, CTR1 activity is repressed, and in the absence of CTR1 phosphorylation, EIN2 undergoes proteolytic processing to release its C-terminal domain, which migrates to the nucleus to activate a transcriptional cascade involving EIN3/EIN3-like and ethylene response factor (ERF) transcription factors (Wen et al., 2012).

ET levels vary throughout a circadian cycle. Low ET levels were observed at dawn, increasing during the first half of the day, peaking between midday and evening, and decreasing again during the evening, with the peak slightly shifting in time depending on the species (Thain et al., 2004)**.**

2.2.3.4 Auxins

Auxins play a major role in plant growth and development under different environmental conditions. Auxin is responsible for apical dominance and phototropism. Auxin promotes cell growth and elongation of the plant. In the elongation process, auxin alters the plant wall plasticity making it easier for the plant to grow upwards. Auxin also influences root formation (Abu-Zahra et al., 2013).

The natural auxins include indole-3-acetic acid, 4-chloroindole-3-acetic acid, phenylacetic acid (PAA), indole-3-propionic acid and inactive auxin precursors indole-3-butyric acid (**Fig. 21**). IAA is found to be present in much larger quantities than any other auxins.

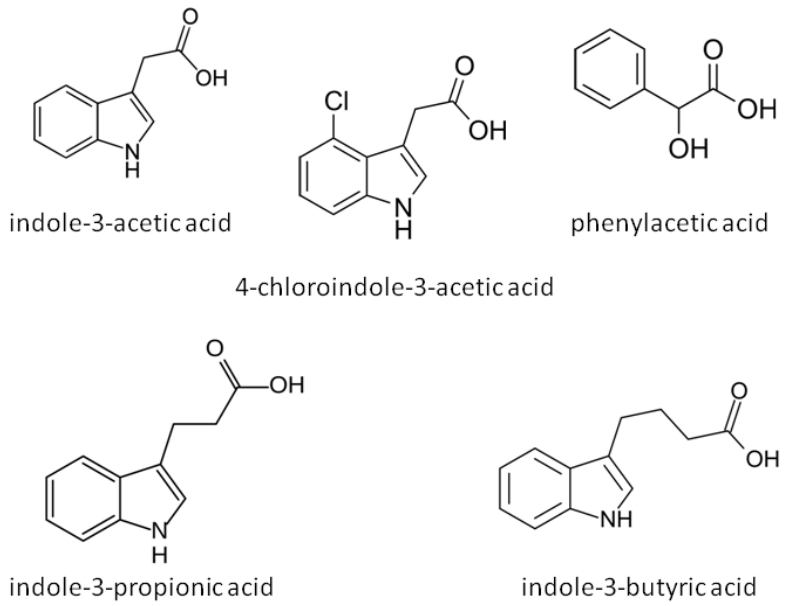

Fig. 21: Chemical structures of natural auxins in plants: indole-3-acetic acid, 4-chloroindole-3-acetic acid, phenylacetic acid (PAA), indole-3-propionic acid and inactive auxin precursors indole-3-butyric acid.

Communication between host plant and microorganisms can occur through secretion of proteins, metabolites and/or volatile organic compounds. Auxin as a signaling molecule could influence beneficial plant–microbe interactions. Plenty of microorganisms have been shown to produce auxin and influence host plant development (Spaepen and Vanderleyden, 2011). For example, *Trichoderma virens*, a plant-beneficial fungus, produces auxin related compounds and increases the aerial and root growth of *A. thaliana* (Kazan, 2013). Similarly, the plant-growth-promoting bacterium, *Pseudomonas fluorescens*, promotes lateral root formation in an auxin-dependent manner (Chu et al., 2020, p. 01). Auxins produced by bacteria and fungi could control root hair initiation and root tip growth in plants (Splivallo et

al., 2009). *A. tumefaciens* enhances biosynthesis of two distinct auxins in the formation of crown galls (Mashiguchi et al., 2019).

The aromatic amino acid L-tryptophan (Trp) is a main precursor for IAA biosynthesis in plants. Trp is synthesized in chloroplasts via the shikimate pathway. Trp-dependent auxin biosynthesis includes production of several intermediates such as indole-3-acetaldoxime, indole-3-acetamide and indole-3-pyruvic acid.

Also exists a Trp-independent pathway for auxin synthesis due to cytosolic indole synthase. It mediates Trp-independent IAA production via the conversion of indole-3-glycerolphosphate to indole (Normanly et al., 1993).

Auxins regulate various physiological processes in plant development, including the establishment of bilateral symmetry in the embryo, root formation and apical dominance, but also in environmental responses such as gravitropism and phototropism (Du et al., 2020). Gravitropism happens due to redistribution of auxin in the elongation zone. Roots bend in response to gravity due to a regulated auxin movement. Auxin accumulates in the lower parts of the root, inhibits cell elongation and causes the root to bend.

IAA levels must be precisely regulated during plant growth in response to external and internal cues. The IAA concentration within cells and tissues is controlled by directional transport, localized biosynthesis and inactivation of IAA (Casanova-Sáez et al., 2021). Two transport mechanisms exist in plants that enable auxin transport from the shoot to the root cap. First, a rapid type mechanism occurs in the phloem, carrying most of the IAA from apical tissues to the root. Second, a slower type mechanism provides protein-controlled cell-to-cell transport, called polar auxin transport (Petrášek and Friml, 2009). This cell-to-cell movement of auxin requires both influx and efflux carrier proteins in the plasma membrane and also in the intracellular spaces. This polar transport is essential for the short distance distribution of auxin, which is mediated by membrane auxin-carrying proteins, including the PIN-formed (PIN) proteins and the ATP-binding cassette subfamily B. The eight *A. thaliana* PIN proteins are divided into two subfamilies based on the presence or absence of a central hydrophilic domain (**Fig. 22**) (Zwiewka et al., 2019). The larger PIN1-type subfamily comprises PIN1, PIN2, PIN3, PIN4, PIN6 and PIN7, while the PIN5-type subfamily comprises PIN5 and PIN8 (Simon et al., 2016).

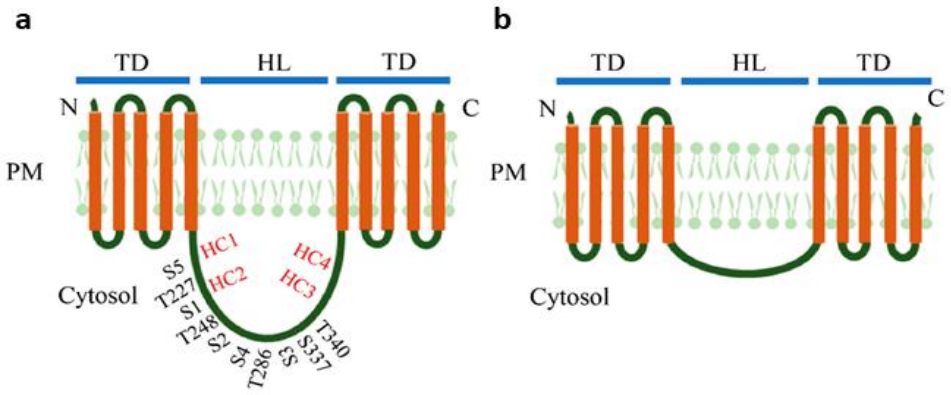

Fig. 22: Molecular structures of (**a**) long PIN proteins (PIN1–4, 6 and 7) and (**b**) short PIN proteins (PIN5 and 8). The PIN proteins harbor a typical central long hydrophilic loop (HL) between amino- and carboxy-terminal ends with five transmembrane domains (TD) spanning on the plasma membrane (PM). The phosphosites on the HL of long PINs are shown (Zhou and Luo, 2018).

2.2.3.5 Cytokinins

CK are involved in the regulation of many developmental and physiological processes including leaf senescence, activity of shoot and root meristems, chloroplast development, regulation of cell division, embryogenesis, vascular development (Argueso et al., 2010; Kieber and Schaller, 2014).

In *A. thaliana*, CKs produced by *Bacillus megaterium* stimulate growth (Ortíz-Castro et al., 2008). CKs synthesized by bacteria induce resistance in *A. thaliana* against bacterial pathogens (Großkinsky et al., 2016). CKs are a major factor in plant–microbe interactions during nodule organogenesis and pathogenesis. Plant cytokinins systemically induce resistance against pathogen infection. This resistance is regulated by endogenous cytokinin and salicylic acid signaling (Choi et al., 2011). Higher levels of CK in plants increased resistance to pathogens (Albrecht and Argueso, 2017).

The hormone is first perceived by dimerized transmembrane receptors belonging to the cyclase/histidine kinase associated sensory extracellular-4,5-domain-containing histidine kinase (HK) family. *A. thaliana* has AHK2, AHK3, and AHK4 receptors that work through a four-step phosphorelay signaling chain involving two other downstream effectors. Among them are histidine phosphotransfer proteins (HPt) and B-type response regulators (RR) which serve as transcription factors regulating CK response genes (Werner and Schmülling, 2009).

Several type of natural cytokinins were identified in plants: N 6-(Δ2-isopentenyl) adenine (iP), trans-zeatin (tZ), cis-zeatin (cZ), dihydrozeatin, and topolins (**Fig. 23**) (Sakakibara, 2006). iP and tZ are the major derivatives and also have higher affinity for the receptors. The biosynthesis of cytokinins happens in two ways: first is derived from tRNA degradation and

the second from the isopentenylation of free adenine nucleotides. In both ways a crucial enzyme is isopentenyl transferase. Meanwhile, the formation of cZ depends on the activity of two tRNA-IPTs. Substrates for free adenosine synthesis are dimethylallyl diphosphate and AMP of iP ribonucleoside and iP, respectively (Gu et al., 2018).

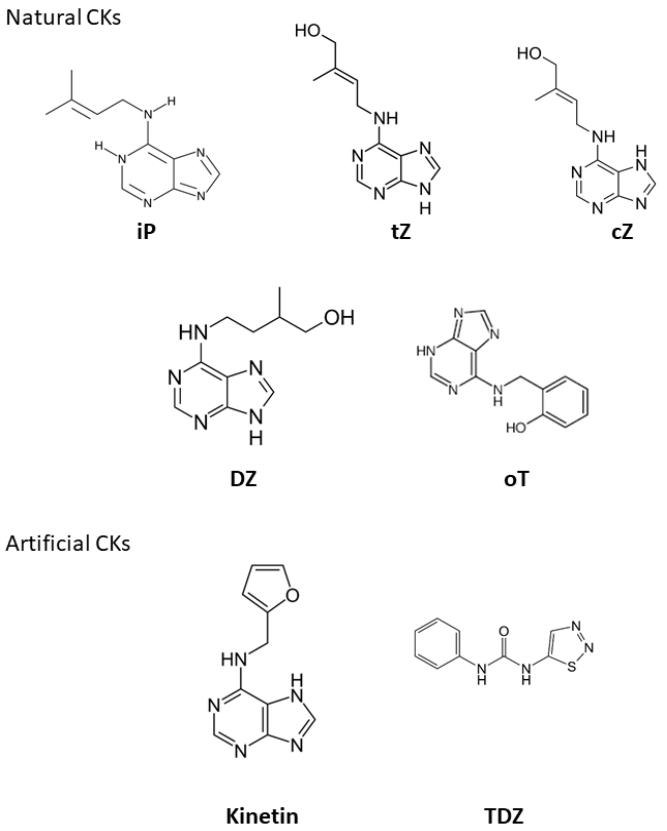

Fig. 23: Structure and composition of cytokinins. Structures of various cytokinins (*CKs*). *N* 6-(Δ2-isopentenyl) adenine (*iP*), *trans*-zeatin (*tZ*), *cis*-zeatin (*cZ*), dihydrozeatin (*DZ*), and *ortho*-topolin (*oT*) are shown as representative natural CKs. Kinetin and thidiazuron (*TDZ*) may activate cytokinin receptors when administered, but are not physiological regulators of plant growth (Osugi and Sakakibara, 2015).

Recent studies indicate that cytokinins were synthesized not only in roots and transported into shoots, but throughout the plant, including in aerial tissues (Kamada-Nobusada and Sakakibara, 2009).

Cytokinins are transported from roots to shoots via the xylem (primarily as tZ-ribosides) and from shoots to roots via the phloem (primarily as iP-type cytokinins) (Zürcher and Müller, 2016).

The levels of active cytokinins in a cell can decrease through either conjugation to glucose or through irreversible cleavage by cytokinin oxidases (Kieber and Schaller, 2014).

Cytokinin perception occurs due to a two-component signaling pathway, such as *A. thaliana* histidine-containing phosphotransfer proteins (AHPs) and *A. thaliana* response regulators (ARRs) (Hwang et al., 2012) (**Fig. 24**).

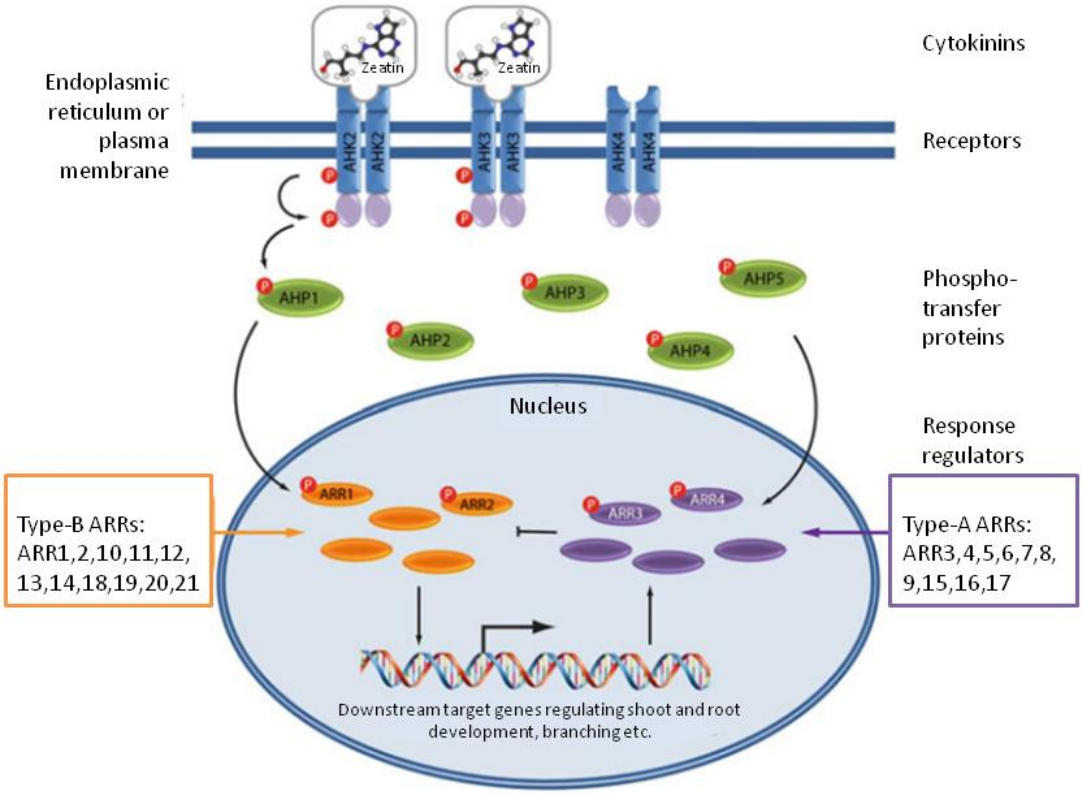

Fig. 24: Schematic representation of cytokinin signal transduction pathway. This is an example of the signaling intermediates of one of the phytohormones. *A. thaliana* Histidine Kinase 2, 3, 4 are cytokinin receptors on cell membranes. Dimers of the receptors bind cytokinins such as zeatin. AHP *A. thaliana* Histidine Phosphotransfer proteins serve as phosphate shuttle from the cytoplasm to the nucleus. ARR *A. thaliana* Response Regulator proteins are the response regulators that affect the transcription of downstream target genes that are activated by cytokinins (Ramamoorthy and Kumar, 2012).

2.2.3.6 Brassinosteroids

BRs are a class of steroid hormones in plants that regulate a wide range of physiological processes including plant growth, development and immunity. The most active BR, BL.

The most abundant BRs are BL and castasterone, produced in various plant organs and acting mostly in the neighboring cells and tissues (Clouse and Sasse, 1998). The physiological effects of brassinosteroids rely on specific recognition of the compound by a protein complex including LRR-RLKs BRI1 (Nam and Li, 2002) and BAK1, which in turn initiates an intracellular phosphorylation relay cascade (Russinova et al., 2004). BRI1 subsequently phosphorylates its inhibitor BKI1 and induces its dissociation from the plasma membrane

(Ma et al., 2016), thus enabling heterodimerization, reciprocal phosphorylation, and full activation of BRI1 and BAK1 kinases (Wang and Chory, 2006). BRI1 phosphorylates BR-signaling kinase1, constitutive differential growth1, and some of their homologs, leading to activation of BSU1 (BRI1 suppressor 1) and BSU1-Like1-3 (BSL 1-3) (Lin et al., 2013). BSU1/BSLs then inactivate BIN2 (Brassinosteroid-Insensitive 2). As a result, BIN2 substrates brassinazole-resistant 1 and bri1-EMS suppressor 1 get dephosphorylated and transported to the nucleus where they target promoters containing BR-response element CGTGC/TG and/or E-box (CANNTG) motif to regulate the expression of thousands of BRs-responsive genes that are crucial for plant growth and development (He et al., 2005). As a result, particular groups of genes are being induced or repressed, modifying cell metabolism and whole plant physiology. The effect of BRs on transcriptomes is not restricted to a few specific genetic targets but affects genes associated with other hormone signaling pathways, especially SA, ABA, JA and auxins (Aerts et al., 2021).

BRs have been implicated in plant interactions with all three trophic-type pathogens: biotrophs, hemibiotrophs and necrotrophs. BRs able to increase resistance and protect plants from the majority of biotrophs. In *A. thaliana* treatment with BR induce tolerance to cucumber mosaic virus (CMV) infection, thus BR signaling was necessary for CMV resistance (Zhang et al., 2015). BR-induced CMV tolerance was triggered with an antioxidant system. The effects of BRs on hemibiotrophic and necrotrophic pathogens are pleiotropic; they either promote resistance, increase susceptibility, or have no effect, depending on the pathogens and plant species involved. For example, external BR treatment induces resistance in barley plants to several fungal pathogens exhibiting different trophic lifestyles (Ali et al., 2013). However, the same application showed no effect on inducing the resistance on *A. thaliana* plants infected with the hemibiotrophic bacteria *P. syringae* or the necrotrophic fungus *Alternaria brassicicola* (Albrecht et al., 2012)**.**

2.2.3.7 Role of hormones in root development

Plants continuously grow and form new organs in response to developmental and environmental stimuli. *A. thaliana* is a multicellular organism, whose growth depends on cell division and cell expansion. In the *A. thaliana* root, primary growth processes are well-studied.

Permanent growth supported by the activity of stem cells, located in stem cell niches (SCN). SCN have derivatives, meristematic daughter cells, that form a meristem root zone (Heidstra and Sabatini, 2014). The root forms through root apical meristem that regulates axial primary

growth. Firstly SCN activates proliferation of daughter cells, generating the division zone (DZ). When cells stop dividing, they obtain an elongated morphology with forming the elongation zone (EZ). After that cells get tissue-specific features on the basis of their radial position, in the differentiation zone (DiffZ). Separation between dividing and differentiating cells form transition zone (TZ) (Dolan et al., 1993). Throughout the whole time root coordinate activity of the different zones (**Fig. 25**).

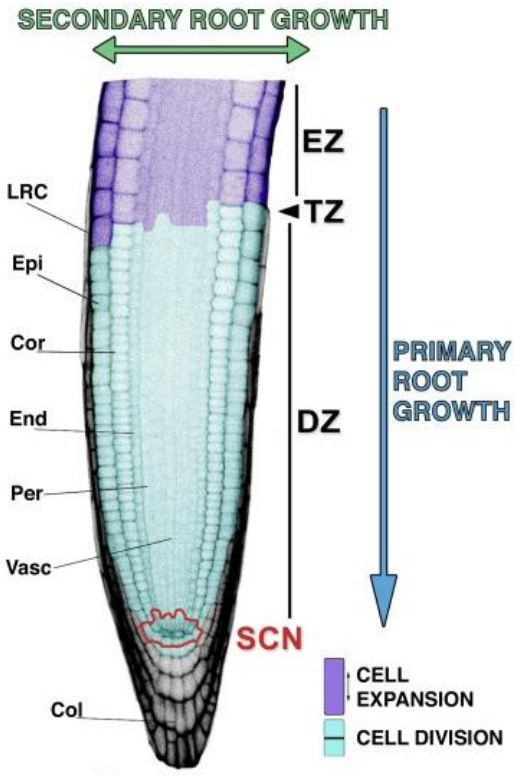

Fig. 25: Overview of the *A. thaliana* root apical meristem, its tissues and the main processes contributing to its primary and secondary growth. Representation of an *A. thaliana* root apex, with its tissue layers and its longitudinal zonation. The root apical meristem can be outlined as a series of concentric cylinders where each cylinder represents a tissue wrapping the inner ones: the vascular tissue (Vasc) as the inner tissue; then, the pericycle (Per); the endodermis (End); the cortex (Cor); the epidermis (Epi); the lateral root cap (LRC) as the outermost protective tissue. Basally and externally, the columella (Col) covers the tip of the meristem. The different root zones are false-colored to highlight the corresponding cell process occurring there. The SCN is composed by the organizing cells and a group of five sets of stem cells that divide asymmetrically and anticlinally, giving rise to meristematic daughter cells that generate all root tissues. In the DZ (in cyan), daughter cells undergo a finite number of stereotyped cell divisions. When the transit-amplifying cell population reaches the EZ (in purple) cells exit the cell cycle and start to acquire the tissue-specific morphological and genetic landmarks that lead to their terminal differentiation. Arrows indicate primary and secondary growth direction in the root (Svolacchia et al., 2020).

Secondary root growth includes continuous generation of vascular tissues due to the activity of the vascular cambium, a bifacial lateral meristem. The cambium forms both types of vascular tissue - water-transporting xylem and sugar-transporting phloem.

Plant hormones (auxin, gibberellin (GA), CK, BR, ABA, ET and JA) regulate plant growth and root development. Different hormones regulate root architecture differently. BR positively regulates lateral root whereas, ABA, GA, JA, ET, CK, inhibit lateral root development. Conversely, primary root development is positively regulated by BR, root hair development positively regulated by BR and ET (Saini et al., 2013).

In *A. thaliana*, CK stimulates cell differentiation, inhibiting both auxin transport and signaling. CK and auxin regulate root meristem size and ensure root growth. CK signaling is regulated by a negative feedback loop with *Short hypocotyl2* (*SHY2*) gene. *SHY2* is a member of the auxin repressor Aux/IAA gene family (Chapman and Estelle, 2009). CK directly activates *SHY2* gene transcription, which negatively regulates *PIN* genes that are responsible for auxin transport and distribution. In comparison, auxin triggers the degradation of SHY2 protein and activity of the *PIN* genes and root growth (Benjamins and Scheres, 2008). Auxin biosynthesis was increased in developing root and shoot tissues upon application or induced biosynthesis of CK.

Auxin and BR together regulate plant root growth and development (Choudhary et al., 2012). The *BRAVIS RADIX (BRX)* gene of *A. thaliana* maintains the threshold of BR level to permit optimum action for auxin. *BRX* expression induced by auxin and mildly repressed by BR (Mouchel et al., 2006). External treatment with BR leads to the expression of auxin responsive genes involved in root development (*AXR3/IAA17, AXR2/IAA7, SLR/IAA14*). BR also regulates polar auxin transport by the disruption of localization of auxin efflux carriers such as PIN3, PIN4 and influx carriers, AUX1/LAXs (Li et al., 2005).

Auxin and ET crosstalk regulates root gravitropism, root growth, lateral root development and differentiation and elongation of root hair (Pitts et al., 1998). ET stimulated auxin biosynthesis in root tips consequently inhibiting root elongation (Ruzicka et al., 2007). ET inhibits root growth by impairing auxin perception through TIR1 or auxin transport via influx/efflux carriers (Swarup et al., 2002).

JA inhibits primary and lateral root through an auxin independent pathway. Also JA could regulate auxin efflux carriers (Corti Monzón et al., 2012). Treatment by JA reduces PIN1 and PIN2 protein in the plasma membrane that leads to auxin accumulation in the root meristem (Sun et al., 2009).

2.2.4 'Pathogenesis-related' proteins and their role in defense against pathogens

PR proteins are induced during the response of plants to viruses, bacteria or fungi, oomycetes, nematodes, and phytophagous insects. The first four PR-protein families were isolated in tobacco (Van Loon and Van Kammen, 1970). PR genes have also been found to be induced under the treatment with phytohormones, chemicals, under osmotic stress, drought, salinity, wounding, heavy metals, and endogenous treatment. PR proteins are highly resistant to proteolytic degradation and to low pH values, have low molecular mass. They are localized in compartments such as the vacuole, the cell wall and/or the apoplast (Stintzi et al., 1993). *PR* genes are activated by the systemic acquired resistance (SAR) pathway, increasing at local infected sites as well as in non infected parts of the plant. PR proteins may be acidic or basic, depending on their isoelectric points. Most acidic PR proteins are secreted into the extracellular spaces, whereas basic PR proteins are predominantly found in the vacuole (Niki et al., 1998). PR proteins are localized in almost all plant organs including leaves, stems, roots, and flowers. Acidic PRs are upregulated by various signaling molecules like SA and ROS, while basic PRs are upregulated by ET and MeJa during pathogen attack (Sinha et al., 2014). They are divided into 17 families based on molecular mass, isoelectric point, localization, and biological activity (**Table 6**).

Table 6. Classification of pathogenesis-related proteins (Saboki, n.d.).

Families	Properties	Example
PR-1	Antifungal	Tobacco PR-1a
PR-2	β-1,3-Glucanase	Tobacco PR-2
PR-3	Chitinase type I, II, IV, V, VI, VII	Tobacco P, Q
PR-4	Chitinase type I, II	Tobacco "R"
PR-5	Thaumatin-like	Tobacco S
PR-6	Proteinase inhibitor	Tomato inhibitor I
PR-7	Endoproteinase	Tomato P69
PR-8	Chitinase type III	Cucumber chitinase
PR-9	Peroxidase	Tobacco "lignin-forming peroxidase"

PR-10	Ribonuclease-like	Parsley “PR1”
PR-11	Chitinase, type I	Tobacco “class V” chitinase
PR-12	Defensin	Radish Rs-AFP3
PR-13	Thionin	Arabidopsis THI2.1
PR-14	Lipid transfer protein	Barley LTP4
PR-15	Oxalate oxidase	Barley OxOa (germin)
PR-16	Oxalate oxidase-like	Barley OxOLP
PR-17	Unknown	Tobacco PRp27

PR1s are the most abundantly produced PR proteins upon pathogen attack. Members of the PR1 form a superfamily of secreted proteins named CAP (from cysteine rich secretory protein (CRISP), antigen 5, and PR1 proteins). *A. thaliana* has 22 types of *PR1*-type genes. Only one of them, *A. thaliana PR1* (*PR1*, *At2g14610*), is induced by pathogens, insects, or chemical treatments, whereas other *PR1*-type genes are constitutively expressed in roots and pollen (van Loon et al., 2006).

Among PR proteins PR2, PR3, PR4, PR5, PR12 have been rated as the potent antifungal proteins in plants (Ali et al., 2018).

Antibacterial properties were shown for the PR10 (ribonuclease-like proteins), PR12 (defensins), PR13 (thionins) and PR14 (lipid-transfer protein). Among them PR10 shows a broad spectrum of antibacterial activity against *P. syringae*, *Agrobacterium tumefaciens*, *A. radiobacter*, *P. aureofaciens* and *Serratia marcescens* (Jiang et al., 2015).

SA in response to pathogen attack could activate the expression of *PR1*, *PR2* and *PR5* genes. Increased expression of *PR3*, *PR4* and *PR12* is the indication of the activation of the JA pathway in *A. thaliana*. Abiotic stresses can also mediate expression of *PR* genes. Salt and drought stress significantly increases the expression of *PR* genes in *A. thaliana* plants (Singh et al., 2013). *PR2* and *PR3* protect cell damage due to cold stress and also possess antifreeze activity (Janská et al., 2010).

2.2.5 Plant resistance

Plants are also capable of inducing defence mechanisms and resistance to pathogens in tissues distant from the site of primary infection. SAR and induced systemic resistance (ISR) are two forms of induced resistance wherein plant defenses are preconditioned by prior

infection or treatment that results in the whole plant resistance against subsequent challenge by a pathogen or parasite. SAR acts nonspecifically throughout the plant. It has been suggested that SAR is most effective against biotrophic and hemibiotrophic pathogens and not against necrotrophic ones (Glazebrook, 2005). SAR requires the signal molecule SA and is associated with accumulation of PR proteins, which contribute to resistance. The roles of PR proteins will be described in chapter 2.3. ISR is a form of plant protection whose roots have been colonized by specific strains of non-pathogenic fluorescent *Pseudomonas* spp. (Pescador Azofra, 2021). SAR is SA-dependent plant defense, whereas ISR is dependent on JA and ET. Beneficial microorganisms secrete secondary metabolites that directly antagonize pathogenic bacteria and act as immune elicitors to raise ISR (Pršić and Ongena, 2020). Among them are phenazines, produced by beneficial *Pseudomonas* bacteria, cyclic lipopeptides surfactin and VOC 2,3-butanediol, produced by *Bacillus* spp. (Chowdhury et al., 2014). Another example is extracellular polysaccharides from *B. cereus* AR156 that could induce systemic resistance to *P. syringae* in *A. thaliana* (Jiang et al., 2016, p. 156). Plants can detect the presence of pathogens through membrane receptors. In the case when pathogens secrete proteins known as “effectors” inside the cell, they can interact with intracellular receptors.

2.2.5.1 *Blumeria graminis* f. sp *hordei* and its life cycle

Fungus *Bgh*, causes a serious disease of barley (*Hordeum vulgare*) called powdery mildew (**Fig. 26**). Usual symptoms include grey areas on the upper surface of the leaves (fluffy fungal mycelium). Leaves remain green and active for some time following infection, then gradually become chlorotic and die. During disease progression, the mycelium often becomes dotted with black points (cleistothecia), which are the sexual bodies of the fungus.

Fig. 26: *Blumeria graminis* f. sp. *hordei* infecting barley. Barley powdery mildew infected plants at 5–6 dpi, showing emergence of white pustules as disease symptoms. At this stage, the leaves are green and turgescent (Lambertucci et al., 2019).

Life cycle of *Bgh* includes germination of conidiospores on the plant leaf surface. This is followed by the formation of structures called appressoria and the development of infection hyphae called penetration pegs. Penetration pegs then develop into haustoria, a rootlike structure that invaginates, but doesn't go through the host plasma membrane (**Fig. 27**). Afterwards, fungus get all nutrients from the host (Hückelhoven, 2005). Haustorial body surrounded by the fungal haustorial plasma membrane and plant extrahaustorial membrane. The extrahaustorial matrix is located between the fungal plasma membrane and the extrahaustorial membrane. The haustorium contains water and nutrients from the host, single nucleus, numerous mitochondria, β-1,3-polyglucans (e.g. callose), xyloglucans, rhamnogalacturonans, and arabinogalactan proteins. Haustorial cytoplasm and extrahaustorial membrane contain a high number of vesicles. On the plant side, the endoplasmic reticulum and plant multi-vesicular bodies locate close to the extrahaustorial membrane (Micali et al., 2011). Some data suggest that PI(4,5)P2 is integrated into the plant extrahaustorial membrane, while PI4P appears to be absent from the extrahaustorial membrane (Qin et al., 2020).

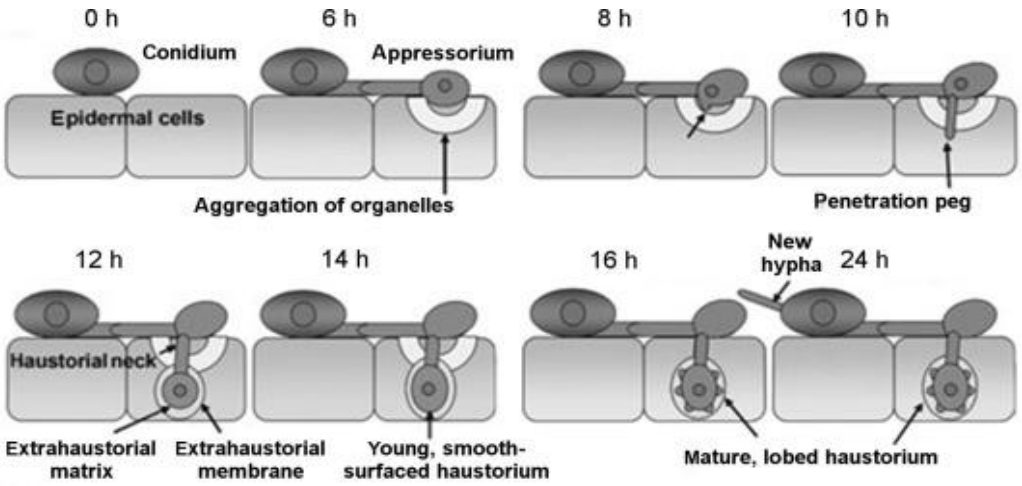

Fig. 27: The infection process of *Blumeria graminis* on barley (Money, 2016).

2.2.5.2 Non-host resistance of *Arabidopsis thaliana* to *Blumeria graminis* f. sp *hordei*

The terms 'non-host plant' and 'non-host pathogen' means that pathogens have a limited range of plants on which they cause disease. Often only plants of a single genus are hosts for a particular pathogen; this is the case for many powdery mildew, rust and bacterial pathogens. All other plants are by definition 'non-host plants', and the attacking microbes are 'non-host pathogens' (Thordal-Christensen, 2003). Barley is a host plant to *Bgh*, and therefore causes a serious disease, although *Bgh* forms nonhost interactions with other plant species. It is known that *A. thaliana* is non-host to *Bgh*. Non-host resistance means that all genotypes of a plant species provide resistance to all genotypes of a pathogen species; resistance means inability of a pathogen to complete its life cycle on that plant species (Ashburner et al., 2000).

2.2.5.2.1 The *Arabidopsis–Blumeria graminis* f. sp *hordei* interaction

The *A. thaliana–Bgh* interaction was extensively investigated (Collins et al., 2003). When conidiospores germinate leading to the formation of the appressoria on plant surface, papillae are produced by plant as a defence response (in the most cases 80-90%). Papillae acts as a barrier (Johansson et al., 2014b). It is supposed that haustoria failed to develop (**Fig. 28**) (Assaad et al., 2004a).

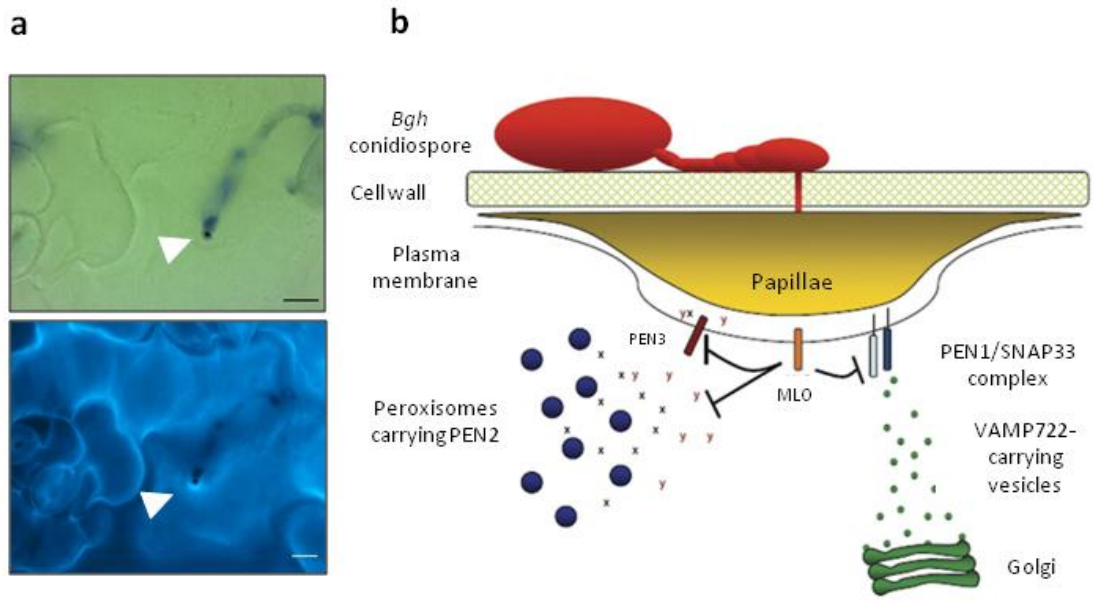

Fig. 28: Papillae formation in the case of penetration failure in *A. thaliana.* **a)** Representative images of papillae, formed after 24 h after inoculation with *Bgh* spores on the 4-weeks-old *A.thaliana* plants. Trypan blue staining and bright field imaging (upper panel), aniline blue staining and UV excitation (lower panel). White arrow indicates papillae structure; Scale bar: 5 µm; **b)** General structure of papillae (Underwood and Somerville, 2008).

2.2.5.2.2 Papillae composition

Papillae consist of callose, cellulose, phenolic compounds, lignin, hydrolases, reactive oxygen species, syntaxin and SNARE proteins (Chowdhury et al., 2014). Correlations were documented between penetration resistance and the presence of osmiophillic substances in papillae (Ebrahim-Nesbat et al., 1986). Osmium has affinity for phospholipids, unsaturated fatty acids, tannins, and phenolic polymers (**Fig. 29**).

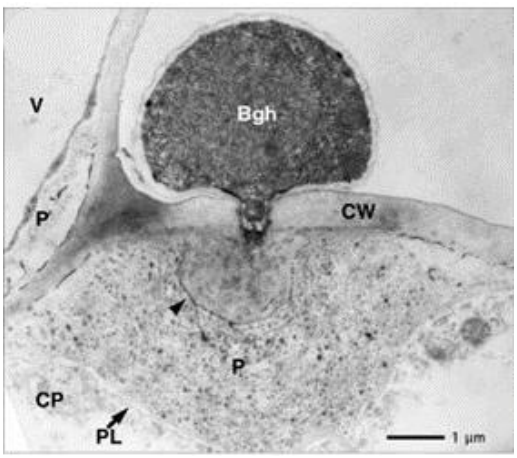

Fig. 29: Transmission electron micrographs of *Bgh* on *Arabidopsis*, 48 hpi. Osmiophillic (darkly stained) bodies in the papilla and the layering of osmiophillic substances (arrowhead). CP, cytoplasm;

CW, cell wall; P, papilla; PL, membrane continuous with plasma membrane; V, vacuole (Assaad et al., 2004b).

The PLD family of enzymes, which directly generate PA through the hydrolysis of structural phospholipids, plays a vital role in lipid-based signaling cascades in plants. In addition, PLD and its product PA have been involved in modulating plant immunity. Distinct from other PLDs, PLDδ is activated by oleic acid and serves as a direct link between the plasma membrane and the microtubule cytoskeleton (Pleskot et al., 2013).

PLDδ is involved in penetration resistance against *Bgh* in *A. thaliana*. PA generated by PLDδ accumulates in papillae and recruits effector proteins, such as protein kinases, phosphatases, and NADPH oxidases, thereby initiating PA-related plant defense signaling (Xing et al., 2021).

Recycling during the deposition of material in papilla is crucial for an efficient penetration resistance. Polarization of actin filaments toward the fungal penetration site in leaf epidermal cells involves precise spatiotemporal myosin regulation. Polarized actin filaments mediate trafficking of organelles and vesicles to the penetration site. Disruption of myosin activity prevents pathogen-triggered actin filaments reorganization and organelle movement leading to impaired accumulation of cell wall components in papillae (callose, lignin-like compounds, and PEN1) and reduced penetration resistance (Yang et al., 2014).

2.2.5.2.3 Role of PEN protein in penetration resistance

Besides, penetration resistance in *A. thaliana* depends on several *PENETRATION* (*PEN*) genes encoding a syntaxin (PEN1), a glycosyl hydrolase (PEN2), and an ABC transporter (PEN3). *PEN1* encodes *A. thaliana* syntaxin SYP121. Syntaxins are members of the superfamily of SNARE domain-containing proteins that are known to mediate resistance to nonadapted pathogens through vesicle trafficking.

Based on the conserved residues in the central layer of the SNARE complex, they can also be classified as Q (glutamine)- and R (arginine)- SNAREs (Fasshauer et al., 1998) (Fasshauer et al. 1998). Q-SNAREs can be further classified into four types, Qa-, Qb-, Qc-, and Qb + c-SNAREs. R-SNAREs are known as vesicle-associated membrane proteins (VAMPs). According to subcellular localization, SNAREs have been classified as t (target)- and v (vesicle)-SNAREs (**Fig. 30**).

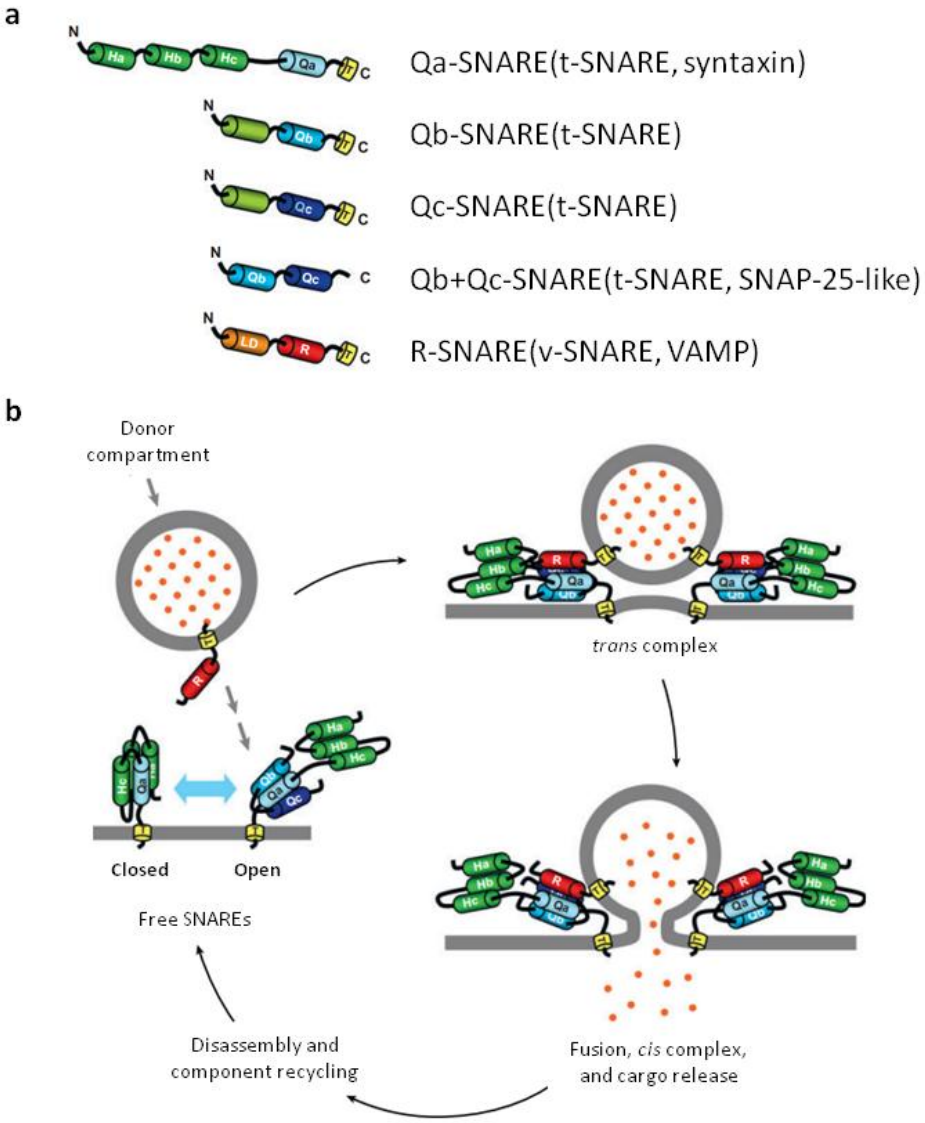

Fig. 30: Domain architecture of major plant SNARE subfamilies and molecular mechanics of SNARE complex formation and vesicle fusion. **a)** Scheme of the general domain organization of plant SNARE proteins; **b)** Scheme of the principle of binary and ternary SNARE complex formation (Lipka et al., 2007).

PEN1/SYP121, SNAP33 and VAMP72 form ternary SNARE complexes (Kwon et al., 2008). Structure function analysis of these complexes showed that phosphorylation of N-terminal PEN1/SYP121 syntaxins is required for full defense activity *in planta* (Pajonk et al., 2008). Loss of PEN1 function leads to almost 90% penetration success of *Bgh* spores (Collins et al., 2003). It was shown that PEN1/SYP121 continuously circulates between the plasma membrane and endosomes. Moreover, no *de novo* PEN1/SYP121 protein synthesis occurs during the accumulation in papillae (Nielsen and Thordal-Christensen, 2012). PEN1/SYP121 is located not only on the plasma membrane near the papillae, but also inside the papillae (Assaad et al., 2004b).

A. thaliana has PEN1/SYP121 homolog, SYP122 that is mostly located at the plasma membrane. It does not accumulate in papillae and *syp122* mutants show an altered cell wall composition but in contrast to *pen1* mutants there is no effect on the pre-invasive immunity towards *Bgh* (Pajonk et al., 2008). From functional analysis was revealed that PEN1/SYP121 proteins were involved predominantly in lipid metabolism, most notable being GDSL lipases (GDSL refers to the consensus amino acid sequence of Gly, Asp, Ser, and Leu around the active site Ser), and cargos associated with oxidative stress responses and protein folding. Several protease inhibitors were identified mainly as SYP122-specific cargo, alongside with cell wall-associated proteins and seed storage proteins (Waghmare et al., 2018).

Concerning the other PEN proteins, the PEN2/PEN3-dependent pathway is linked to metabolism and transport of tryptophan-derived secondary metabolites. PEN2 encodes a peroxisome-localized myrosinase involved in hydrolyzing indole glucosinolates and PEN3 encodes a plasma membrane-localized ABC transporter (Stein et al., 2006). The current model suggests that PEN2 produces an active compound which is excreted into the apoplast by PEN3 to stop fungal ingress (Bednarek et al., 2009).

3. AIMS OF THE PROJECT

The type III PI4Ks have been extensively investigated not only by the teams in which I performed my thesis research, but also by other research groups over the years. To explore the role of type III PI4Ks, the use of mutants is an approach of choice. However, no homozygous mutant in PI4KIIIα1 is viable. Therefore, the mutant approach has been used to study the role of PI4KIIIβ1 and PI4KIIIβ2. The *A. thaliana* mutant line *pi4kIIIβ1β2* (SALK_040479/SALK_09069) carries T-DNA insertions in both *PI4KIIIβ1* and *PI4KIIIβ2* (**Fig. 31**).

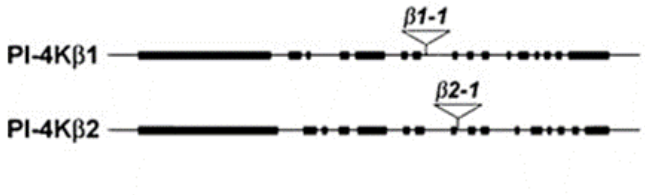

Fig. 31: Sequencing of β1-1 and β2-1 T-DNA insertion sites confirmed the positions of the T-DNA inserts within PI-4Kβ1 (intron 7) and -4Kβ2 (intron 8) in these two lines (Preuss et al., 2006).

My work could be divided into three parts. The aim of the first part was to elucidate whether *pi4kIIIβ1β2* phenotype could be related to the problem with hormone related processes, and more specifically to IAA related responses. Among them was IAA treatment with subsequent measurements of root, cortical cell, and meristem length. Employing DR5-GUS reporter and DII-VENUS construct helped me check auxin transcriptional response. In addition, responses of selected genes to auxin were tested.

PI4K is interesting in studying not only in terms of phenotype features, but also in plant-microbe interaction. That's why I decided to expand the topic. The aim of the second part was to elucidate the reason for higher *pi4kIIIβ1β2* susceptibility to non-adapted fungal pathogen *Blumeria graminis* pv. *hordei.* For that I investigated the involvement of PI4Ks in non-host resistance, especially in papillae formation. Using different biosensors, I checked the localization and the accumulation level of phospholipids like PA, PI4P, PI(4,5)P2 and protein PEN1/SYP121.

In the third part, I wanted to understand what activates the EDS1/PAD4 signaling that promotes ICS1 expression and SA accumulation in *pi4kβ1β2* mutants. The *pi4kβ1β2* double mutant constitutively accumulated a high SA level via EDS1/PAD4 pathway. To elucidate

that, I used mutant approach methodology to see if receptors were involved in some of the phenotypes of the *pi4kβ1β2* mutant. Rosette size and callose measurements, evaluating resistance to *P. syringae*, *PR1* expression, were used as a proxy of SA accumulation.

4. MATERIAL AND METHODS

4.1 CHEMICALS

SILWET L-77	Agro Bio Opava
Sucrose	Lach-Ner, Ltd.
$MgCl_2$	Fluka AG
Kanamycin	Sigma Aldrich, USA
TWEEN20	Sigma Aldrich, USA
Murashige–Skoog basal salt medium	Duchefa, Haarlem, Netherlands
Plant agar	Duchefa, Haarlem, Netherlands
IAA	Duchefa, Haarlem, Netherlands
BAP	Sigma Aldrich, USA
SA	Sigma Aldrich, USA
NaOH	Lach-Ner, Ltd.
Substrate tablets Jiffy	Kristiansand, Norway
Tris-HCl	Sigma Aldrich, USA
NaCl	Lach-Ner, Ltd.
EDTA	Serva Feinbiochemica
SDS	Sigma Aldrich, USA
Isopropanol	Erba Lachema
Master Mix Dream TaqTM Green PCR 2x	Thermo Fisher Scientific
Agarose	SeaKem® LE Agarose Lonza
GelRed	Biotium
TAE (Tris-acetate-EDTA)	Thermo Fisher Scientific
DNA Ladder	GeneON
DNA-free kit	Ambion, USA
Spectrum Plant Total RNA kit	Sigma Aldrich, USA
M-MLV RNase H− Point Mutant reverse transcriptase	Promega Corp., USA
Oligo dT21 primer	Metabion, Germany
X-Gluc	Thermo Fisher Scientific
NaH_2PO_4	Erba Lachema
Triton-X	Duchefa, Haarlem, Netherlands
FM 4-64	Molecular Probes
Paraformaldehyde	Sigma Aldrich, USA

Pectolyase Y-23	Duchefa, Haarlem, Netherlands
Dimethyl sulfoxide	Sigma Aldrich, USA
anti-PIN2 rabbit antibody	(kindly provided by Prof. C. Luschnig, dilution 1:500)
anti-rabbit Alexa Fluor 546 antibody	Thermo Fisher Scientific, dilution 1:1000
Glycerol	Sigma Aldrich, USA
Aniline blue	Sigma Aldrich, USA
K_2HPO_4	Erba Lachema

4.2 PLANT MATERIAL

A. thaliana ecotype Columbia-0 was used as WT.

The following single mutant lines were obtained from The Nottingham Arabidopsis Stock Centre (NASC): *sid2-3* (salk_042603 (Nawrath and Métraux, 1999)), *pepr1* (salk_059281), *pepr2* (salk_098161), *snc1-11* (salk_047058), *bak1-4* (salk_116202), *wrky70* (salk_025198), *fls2* (salk_026801C) (**Fig. 32**).

The *cerk1-2* (GABI_096F09) from Frédéric Brunner, ZMBP, University of Tübingen (**Fig. 32**).

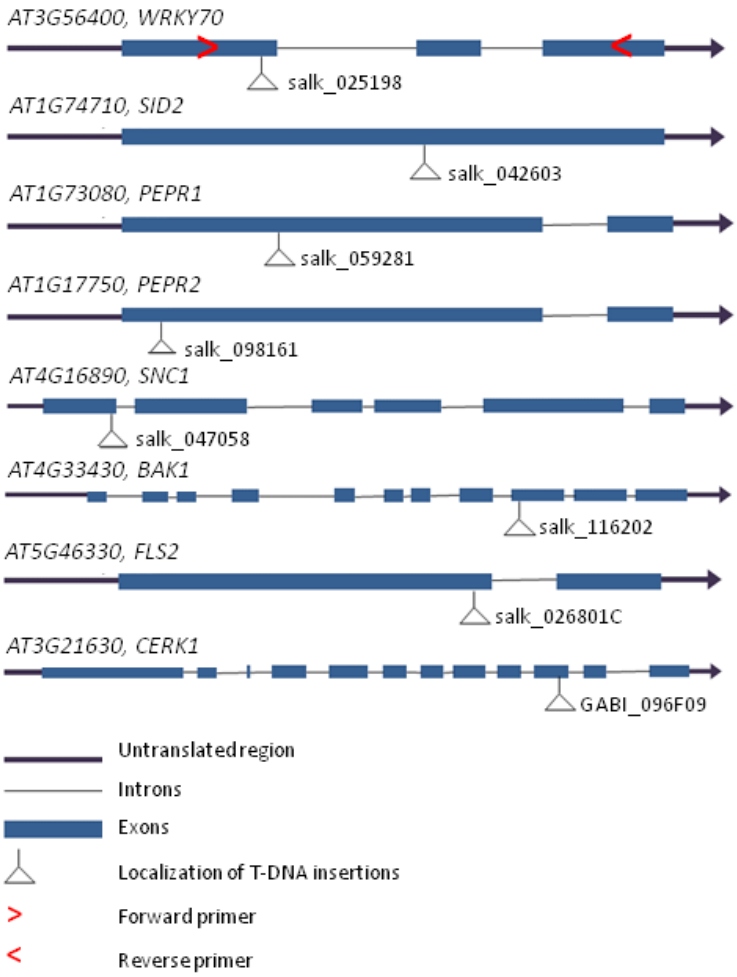

Fig. 32: Schematic representation of gene structure indicating the location of T-DNA insertions. For *WRKY70* indicates primer positions.

Lipid sensor lines (PI4P sensor, 2xFAPP1-mCherry (Lin et al., 2019); PA sensor mCitrine-1xPASS (NASC #2107781); PI(4,5)P_2 sensor 2xmCHERRY-2xPH (PLC) (NASC #2105622) originated from Yvon Jallais laboratory (Laboratoire Reproduction et Développement des Plantes, Université de Lyon, France) (Gomez et al., 2022). They were obtained through the NASC.

The *pi4kβ1β2* (SALK_040479/SALK_09069 (Preuss et al., 2004)) and the *sid2/pi4kβ1β2* (SALK_042603/SALK_040479/SALK_09069) were already in the laboratory, and obtained through crosses (Šašek et al., 2014).

Some *A. thaliana* lines with specific constructs were obtained through colleagues. The CycB1::GUS (Colón-Carmona et al., 1999) and DR5::GUS (Ulmasov et al., 1995) were given by Anne Guivarc'h (iEES-Paris). The *pUBC*::Lifeact-GFP line was obtained from Fatima Cvrčková (Cvrčková and Oulehlová, 2017); the 35S::GFP-SYP121 was obtained

from Mads Nielsen (Department of Plant and Environmental Sciences, Copenhagen Plant Science Center, University of Copenhagen) (Nielsen et al., 2012).

PIN2::PIN2-GFP (Ischebeck et al., 2013) and PIN2::PIN2-GFP in a *pi4kβ1β2* background (Lin et al., 2019), were obtained from Department of cellular biochemistry (Ingo Heilman group), Institute of Biochemistry and Biotechnology, Martin-Luther-University Halle-Wittenberg, Halle (Saale), Germany (Lin et al., 2019).

4.2.1 Mutant creation by crosses

The CycB1::GUS (Colón-Carmona et al., 1999) and DR5::GUS (Ulmasov et al., 1995), 35S::GFP-SYP121 and *pUBC*::Lifeact-GFP constructs were introduced into the *pi4kβ1β2* background by crossing, and homozygous F2 or later seeds were used. For CycB1::GUS and DR5::GUS selection was made by PCR specific to GUS until a homozygous line was obtained. For 35S::GFP-SYP121 and *pUBC*::Lifeact-GFP selection was made by microscopy until all plants had GFP shining.

The following double, triple and quadruple mutants: *pepr1/pepr2, pepr1/pi4kß1ß2, pepr2/pi4kß1ß2, pepr1/pepr2/pi4kß1ß2, cerk1-2/pi4kß1ß2, bak1-4/pi4kß1ß2, snc1-11/pi4kβ1β2, wrky70/pi4kβ1β2, sid2/wrky70/pi4kβ1β2* mutants were generated by crossing. Homozygous plants were identified in the F2 or further generations, using PCR.

Genotyping primers are listed in **Table 1**.

4.2.2 Mutant creation by plant transformation

The DII-VENUS construct in *Agrobacterium* was created in the Laboratoire de Reproduction et Développement des Plantes, Université de Lyon, France (Brunoud et al., 2012). The DII-VENUS construct was introduced into *pi4kβ1β2* by floral dip transformation. This method is based on loading unopened plant flowers in a solution of *Agrobacterium tumefaciens* in the presence of a surfactant (0.02% Silwet L-77). Healthy non-transformed *A. thaliana* plants were grown in soil pots until they contain as many unopened flowers as possible. A culture of *Agrobacterium tumefaciens* which carries the desired gene on a binary vector was grown overnight in 5 ml of LB medium (28°C at the rotary shaker, 200 rpm). The culture was then transferred to 500 ml of LB medium and re-cultured overnight (28°C, 200 rpm). Both cultures were performed in the presence of the antibiotic kanamycin (50 μg/ml). Cell density is not critical for successful transformation (OD_{600} can range from 0.1-2). Composition of LB medium: NaCl - 10 g/l, yeast extract - 10 g/l, tryptone - 5 g/l, pH=7. The medium was autoclaved for 20 min. at 120˚C. The *Agrobacterium* culture was spun at the bottom of the

cuvette (6000 rpm for 10 min) and the pellet is resuspended in 5% sucrose solution - 500 ml. Before inoculating the plants, Silwet L-77 detergent (final concentration in solution 0.02%) was added to the solution, which must be mixed well. The aboveground part of the plant was immersed in the *Agrobacterium* solution for 20 seconds. The plants were then drained. The plants were covered for 16-24 h with a transparent plastic cover to maintain high humidity (plants should not be exposed to strong sunlight). The next day, the cover was removed.The plants were watered regularly. It stops as soon as the seeds were ripe. Dry pods with seeds were harvested. Three independent lines were selected and the T4 generation was studied.

4.3 METHODS RELATED TO PLANT CULTIVATION

4.3.1 Experiments with seedlings

Seeds were surface sterilized with 1.6% sodium hypochlorite solution containing 0.02% (v/v) TWEEN20. Seeds were stratified for 2 days at 4°C in the dark. Seeds were germinated for 3 days in Petri dishes containing half-strength Murashige–Skoog basal salt medium, pH=5.7, supplemented with 1% (w/v) sucrose and 0.8% (w/v) plant agar at 22 °C under a 16 h light/8 h dark regime in a vertical position.

For selection of DII-VENUS transformed seedlings, they were selected on half-strength Murashige and Skoog plates supplemented with 20 g/L^{-1} sucrose and 50 $\mu g/mL^{-1}$ kanamycin. Plants that passed the antibiotic test were further examined under a microscope.

For the primary root length analysis, 4 days after germination, seedlings were transferred to square Petri plates containing the same medium supplemented or not with hormones (IAA at 0.05, 0.1 or 1 μM final concentration; BAP at 0.1, 0.5, 1 or 5 μM; SA at 2, 10 or 20 μM). Stock solutions at 200 mM were prepared in distilled water and a few drops of 1 N NaOH. After 7 days of cultivation in vertical position Petri dishes were scanned for the primary root length measurement.

For DII-Venus assay 7-day-old seedlings were used. Seedlings were transferred to the plates with media supplemented 0.01 μM IAA for 1 h and subjected to microscopy.

For 4-64 staining 5-day-old *A. thaliana* seedlings expressing PIN2::PIN2:GFP were incubated with 2 μM FM 4-64 in half-strength Murashige and Skoog liquid medium in multi-well plates for 5 min and then rinsed 3 times in liquid medium.

For actin structure evaluation 7-days-old seedlings were used. Seedlings expressing *pUBC*::Lifeact-GFP were sprayed with 10 μM latB (latrunculin B) for different time incubations (30, 90 and 150 min) and were used for confocal microscopy.

4.3.2 Experiments with 4-week-old plants

For experiments with 4-week-old plant stratification for 2 days at 4°C in dark conditions was applied to break dormancy. Seeds were transferred to pots with substrate tablets and grown in cultivation chambers (Snijders, Drogenbos, Belgium at 22°C day temperature, 65–70% humidity and 16 h light/8 h dark (LD) or 12 h light/12 h dark (SD)). After 1 week, the seedlings were replanted to one plant per pot. Four week old plants were used for analysis.
Rosette size of soil-grown plants were measured by FiJi (area tool). Rosette weight was determined using analytical scales.

4.4 METHODS CONCERNING NUCLEIC ACIDS

4.4.1 Genomic DNA extraction

For DNA extraction, 1-2 leaves from each plant were collected in tubes with 1 g of 1.3 mm silica beads. Leaves were homogenized in tubes using a FastPrep-24 instrument (MP Biomedicals, USA) (6 m/sec, 25 sec). After that, 400 µL of extraction buffer (200 mM Tris-HCL pH=8.0, 250 mM NaCL, 25 mM EDTA, 0.5% (w/v) SDS) were added. Leaves were homogenized a second time with the same condition. Subsequently, samples were centrifuged for 1 min at 13000 rpm. Then, 300 µL were transferred to a new Eppendorf tube with 300 µL isopropanol. After a quick vortex the tube was centrifuged for 5 min at 13000 rpm. The pellet was left for drying and then resuspended in 100 µL of 10 mM Tris-HCL, pH=7.6, 1 mM EDTA.

4.4.2 PCR analyses for genotyping

For genotyping PCR analyses were performed with subsequent primers from **Table 7**. The PCR was done in 20 µL in presence of 10 µL Master Mix, 0.5 µM of each primer, and 2 µL extracted DNA. For T-DNA mutants, two PCRs were made: LBb1.3 primer aligning to the left border of the insertion with reverse primer (LB+RP) and forward primer with reverse primer (LP+RP). Amplification product from a heterozygous individual should give bands from both LP+RP and LB+RP primer combinations as it contains a single T-DNA insert in either of the alleles. Amplification from a homozygous individual is expected only from LB+RP primer combination as it has T-DNA inserted in both copies of the gene, and WT plants would give a higher size band with LP+RP (**Fig. 33**).

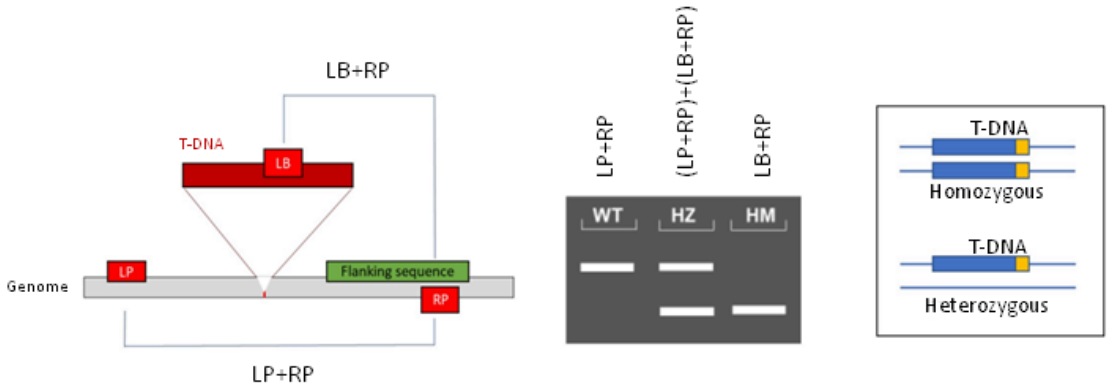

Fig. 33: PCR genotyping for analysis of T-DNA insertion mutant plants.
LP: Left primer; RP: Right primer and LB: Left border primer, HZ: Heterozygous, HM: Homozygous (Batth et al., 2020).

The PCR program consisted of a 15 min initial denaturation step at 95°C followed by 30 min annealing at 55°C, and 30 min primer extension at 72°C, 40 number of cycles.

The specific sizes of the genes PCR product and a control band were assessed after horizontal electrophoresis on a 1% agarose gel containing 0.01% GelRed in 0.1X TAE (Tris-acetate-EDTA) buffer (40 mM Tris (pH=7.6), 20 mM acetic acid, 1 mM EDTA). For size determination, DNA Ladder was loaded in the gel. The bands were observed with the Biorad Universal Hood II Gel Doc System.

Table 7. List of primers used for genotyping.

Name	**FP**	**RP**
GUS	GGCCAGCGTATCGTGCTGCG	GGTCGTGCACCATCAGCACG
pi4kb1	AGGACGTAACCAGAGGGGTAG	CGTTGTGACCCGTCATTAATC
pi4kb2	AAACCTCCTTATCTTCCGCTG	ATGAACGAAATTGGGTTCTCC
LBb1.3	ATTTTGCCGATTTCGGAAC	
sid2-3	ACCCTAATTTGGATTTGGTGC	AGCTCTAGGCCTAGTTGCAGC
pepr1	CAACAACAATGTGGAGGATA	AACGAGATTACCGAACTGAA
pepr2	AAGAAGATGGCTTAATGCTG	CAGTTGTGCCAGTAACAGTG
snc1-11	TCGGCATAACATCGTAAGAGC	CAAGCTTTCGTGGAGAAGATG
cerk1-2	ATGCTGATATCGGAGACGTTG	AGCACACGGTTCCAGTTTATG
bak1-4	CATGACATCATCATCATTCGC	ATTTTGCAGTTTTGCCAACAC

fls2	TCCTGATCTGCCTGCAATAAG	GTTGGAGCAAGCAACAGATTC
wrky70	TGATCTTCGGAATCCATGAAG	CAAACCACACCAAGAGGAAAG

4.4.3 Total RNA extraction

RNA were isolated from 7-day-old seedling roots and shoots (total fresh weight 100-200 mg), leaves of 4-week-old plant. Samples were homogenized in tubes with 1 g of 1.3 mm silica beads using a FastPrep-24 instrument (MP Biomedicals, USA). Total RNA was isolated using a Spectrum Plant Total RNA kit (Sigma-Aldrich, USA) and treated with a DNA-free kit (Ambion, USA). The quantity of extracted RNA was measured using NanoDrop.

4.4.4 RNA-Sequencing

Sequencing was carried out using an Illumina NexSeq500 by the IPS2 POPS platform. RNA-seq libraries were made using the TruSeq Stranded mRNA kit (Illumina®, California, USA). The RNA-seq samples were Single End (SE) sequenced, stranded with a sizing of 260 bp and a read length of 75 bases, lane repartition and barcoding gave approximately 45 million SE reads per sample.

4.4.5 Bioinformatic analyses and statistical treatments for RNA-seq

To facilitate comparisons, each sample followed the same steps from trimming to counts. RNA-Seq preprocessing included trimming library adapters and performing quality controls. The raw data (fastq) were trimmed using the Trimmomatic (Bolger et al., 2014) tool for a Phred Quality Score Qscore >20, read length >30 bases, and ribosome sequences were removed with the sortMeRNA tool (Kopylova et al., 2012). The genomic mapper STAR (version 2.7. 3a (Dobin et al., 2013)) was used to align reads against the *A. thaliana* genome (from TAIRv10), with options--outSAMprimaryFlag AllBestScore --outFilterMultimapScoreRange 0 to keep the bests results. Transcript abundance of each gene was calculated with STAR and counts only single reads for which reads map unambiguously one gene, thus removing multi-hits. According to these rules, around 97% of SE reads were associated with a gene, 1-2% of SE reads were unmapped and 1.22-1.66% of SE reads with multi-hits were removed. Differential analyses followed the procedure previously described (Rigaill et al., 2018). Briefly, genes with less than 1 read after a counts-per-million (CPM) normalization in at least one half of the samples were discarded. Library size was normalized using the trimmed mean of M-value (TMM) method and count distribution was modeled with

a negative binomial generalized linear model. Dispersion was estimated by the edgeR method (McCarthy et al., 2012) in the statistical software 'R'(2018)) (Version 3.2.5 R Development Core Team (2005). Expression differences compared 2 samples using likelihood ratio tests and *p*-values were adjusted with the Benjamini-Hochberg procedure to control False Discovery Rate (FDR). A gene was declared differentially expressed if the adjusted *p*-value < 0.05.

Genes were classified using the Classification SuperViewer Tool developed by (Zhu, 2003) as described previously (Kalachova et al., 2016). The classification source was set to Gene Ontology categories as defined by (Ashburner et al., 2000). The frequency of each category was normalized to the whole Arabidopsis set. The mean and standard deviation for 100 boot-straps of our input set were calculated to provide some idea as to over- or under-representation reliability. Similarity analyses were performed using tools developed by Genevestigator (Zimmermann et al., 2004). The "Hierarchical clustering" tool works on the expression matrix defined by a microarray experiment selection and a gene selection. The "Biclustering" tool identifies groups of genes that are expressed above or under a set threshold ratio in a subset of conditions rather than in all conditions.

4.4.6 Transcript abundance evaluation by qPCR

Gene transcription measurement was conducted as described previously (Kalachova et al., 2019). In general, 1 μg of RNA was converted into cDNA with M-MLV RNase H− Point Mutant reverse transcriptase and an anchored oligo dT21 primer. Gene expression was quantified by qRT-PCR using a LightCycler 480 SYBR Green I Master kit and LightCycler 480 (Roche, Switzerland). The PCR conditions were 95°C for 10 min followed by 45 cycles of 95°C for 10 s, 55°C for 20 s, and 72°C for 20 s. Melting curve analysis was then conducted. CT values of target genes were normalized to the housekeeping gene *TIP41*. The list of the primers used is given in **Table 8**.

Table 8. List of primers used for qPCR.

Gene ID	Name	FP	RP
AT1G04240	*SHY2*	GCTCTAGAATGGATGAGTTTGTTAACC	TCGCCCGGGTACACCACAGCCTAAACC
AT5G23060	*CaS*	GGCTCAAACGCTTGACCTTC	CACGCGGTTCTTAGCATTCG
AT1G44575	*NPQ4*	CATTGGAGCTCTCGGAGACAGAGGAA	CTCGTTCGCCTTCGTGAACCCAAACAAT

AT1G75690	*LQY1*	ATGCCAGTTTCAGCTCCATC	TTAGTCATCGTCCTTGAACTC
AT1G72610	*GER1*	CATTACCGCTGGGTTTGTCT	CATGACCTGTCCTGGTTTGA
AT2G40340	*DREB2C*	CAAGTTCAGGTTTTGGTCAGGTG	GCAATCTCCATAGGGTTGAGGC
AT1G64590		GAGTTTCCTGATGCGGAGAT	TGAGGATGTTGAGTGGGAGA
AT4G15290	*CSLB05*	CATTCAACTATTGTTAAGGTGGT	CTCCAGTTTTGTAATGATGAAGG
AT5G44130	*FLA13*	ACCAACAGACAACGCTTTCC	GAGCAGCCGCTTTCTTAGAG
AT1G19900	*RUBY*	CGAATCTTCGTCCCAAGATTATATCTCC	ACTTTACCCAAACACCTTCGC
AT4G36110	*SAUR9*	CAACGACGTGCCAAAAGGT	CACATAGCGACTTCGGTGTTGA
AT3G45700	*NPF2.4*	CAGAAGCTAATCCGCAAACC	AGGAACCAGCCATAGCACTG
AT4G37390	*BRU6*	TAGCGGTGGATTACCGATGGC	TCTAATGATGCTTCTGCTGCTCC
7011691	*GFP*	AGGATCGAGCTTAAGGGAAT	AGTTGAACGCTTCCATCTTC
AT3G11820	*PEN1*	ATGTCACGAGCAGACCAAGA	GAGGAAGAACCA GGTCCACA
AT2G44490	*PEN2*	TAACATGCTTCTAGCGCACGCAG	CATCTG GATCACTCGGATCATATG
AT1G59870	*PEN3*	GGTGTTAAGAACAGTCTCGTC AC	TCTTCTGACCTCCAGATATACC
AT2G14610	*PR1*	AGTTGTTTGGAGAAAGTCAG	GTTCACATAATTCCCACGA
AT3G57260	*PR2*	CGATCCAGGGTACTCATACCA	CTCCGACACCACGATTTCCA
AT3G28390	*SAND*	CTGTCTTCTCATCTCTTGTC	TCTTGCAATATGGTTCCTG
AT3G54000	*TIP41*	GTGAAAACTGTTGGAGAGAAGCAA	TCAACTGGATACCCTTTCGCA
AT3G52400	*SYP122*	CTCTCCGGCTCGTTTAAAACC	GCACATTCTCCCAACCGTCT
AT1G49240	*ACT8*	TTCATCGGCCGTTGCATTTC	AATGTCATCAGCATCGGCCA
	EGFP	CCGGGGTGGTGCCCATCC	TGTGGCTGTTGTAGTTGT
AT3G56400	*WRKY70*	TAAGATACCACTCACCAAAAACTTCCTC AA	CTCATGGTCTTAGTCCTAATGTA GTGGT

4.5 METHODS RELATED TO PLANT PHYSIOLOGY

4.5.1 Root length measurement

After 7 days of cultivation in vertical position Petri dishes were scanned for the primary root length measurement. Images were imported into FiJi software and root hair length was

measured manually using a segmented line tool. At least 60 root hairs from 10 seedlings were analyzed for each variant.

4.5.2 Gravitropic test

Gravitropic response test was performed as previously described (Retzer et al., 2019). Five-day-old seedlings were transferred onto fresh Petri Dishes containing half-strength Murashige–Skoog basal salt medium, pH=5.7, supplemented with 1% (w/v) sucrose and 0.8% (w/v) plant agar and aligned in a horizontal orientation. Plants were scanned at indicated time points using a Horizontal LSM880 with Airyscan module for 12 h and images were used to determine root reorientation. The root turning angle and length were calculated for each time point. Ten roots were imaged for each genotype.

4.5.3 GUS staining

GUS staining was performed as previously described (Figueroa-Balderas et al., 2006). Briefly, 4 or 8-day-old seedlings were incubated in 2 mM X-Gluc, 50 mM NaH_2PO_4, pH=7, 0.5% (v/v) Triton-X, 0.5 mM K-ferricyanide, for 16 h at 37°C. Chlorophyll was removed by repeated washing with 80% (v/v) ethanol. Imaging was performed using an ApoTome Zeiss microscope with a 5x objective at bright field settings.

4.5.4 Hormone measurements

Whole roots (50-100 mg) were harvested from 7-day-old vertical grown seedlings. At least 6 samples were analyzed for WT and *pi4kβ1β2*. Hormone analysis was performed at Laboratory of Hormonal Regulations in Plants laboratory of Institute of Experimental Botany of the Czech Academy of Sciences by Petre I. Dobrev with a LC/MS system consisting of UHPLC 1290 Infinity II (Agilent, Santa Clara, CA, USA) coupled to 6495 Triple Quadrupole Mass Spectrometer (Agilent, Santa Clara, CA, USA), operating in MRM mode, with quantification by the isotope dilution method. The detailed methodology was described previously (Figueroa-Balderas et al., 2006).

4.5.5 Root growth assay with pep1

Seeds were sown on solid half-strength Murashige–Skoog basal salt medium, stratified for 2 days at 4°C in the dark, and placed vertically in the light. At 10 day after germination, seedlings were transferred to square transparent Petri dishes with solid half-strength Murashige–Skoog basal salt medium supplemented with or without the 50 nM of peptides

and incubated for another 4 days, after which the plates were scanned and root growth was measured using FiJi.

4.6 METHODS CONCERNING PATHOGEN INOCULATION

4.6.1 Treatment with *Blumeria graminis*

Blumeria graminis f. sp. *hordei (Bgh)* was cultivated continuously on winter barley (cv. Stupický staročeský) grown under short day conditions (19°C, 10/14 h, 50% humidity, at a light intensity of 70 μmol m^{-2} s^{-1}). Plants, approximately 4-weeks-old, were inoculated by spreading spores from infected barley onto the adaxial side of their leaves (from leaf to leaf). To obtain a uniform distribution of conidia, inoculation was performed using an inoculation tower to spray 150-200 conidia per square mm.

4.6.2 *Pseudomonas syringae* pv. *tomato* DC3000 infection assay

Inoculation with *P. syringae* pv. *tomato* DC3000 was performed according to Katagiri et al. (2002) with modifications. Bacteria were cultivated overnight on LB medium plates containing rifampicin (50 μg μL^{-1}). *P. syringae* pv. *tomato* DC3000 were taken from the plate and resuspended in 10 mM $MgCl_2$ (OD_{600} = 0.001). Four-week-old plants were infiltrated with this suspension.

One disc (6 mm) from one leaf, three leaves at the same developmental stage from one plant and three plants were collected as one sample of one genotype at 0 and 3 dpi. Leaf discs were ground in 10 mM $MgCl_2$ and decimal dilutions were made. Quantification of bacteria was based on colony forming units counting.

4.7 METHODS CONCERNING MICROSCOPY

4.7.1 Root morphology microscopy

After 7 days of cultivation in vertical position, Petri dishes seedlings scanned for the primary root length measurement (Epson Perfection V700 Photo, Suwa, Japan, at 600 dpi resolution). For the measurement of the lengths of meristem, elongation zone and cortical cells, roots were observed under an ApoTome Zeiss microscope with a 5x objective at bright field settings. Images were analyzed with FiJi software (Schindelin et al., 2012). At least 12 seedlings were analyzed for each variant. For the measurement of root hair length and

density, 5-day-old seedlings were photographed under a stereo microscope (SteREO Discovery V8, Carl Zeiss GmbH, Jena, Germany) equipped with an AxioCam HRc camera.

4.7.2 Confocal microscopy

A Zeiss LSM 880 inverted confocal laser scanning microscope (Carl Zeiss AG, Germany) was used with a 40x C-Apochromat objective (NA=1.2 W). Fluorescence signals were processed with Zen Blue software (Zeiss) where PIN2 distribution was evaluated as a ratio of mean fluorescence intensity at the apical plasma membrane to mean intracellular fluorescence intensity of individual cells. Fluorescence associated with LifeAct-GFP, PEN1-GFP or DII-VENUS was acquired by excitation at 488 nm and emission at 490–540 nm for GFP. Fluorescence associated with 2xFAPP1-mCherry or 2xmCHERRY-2xPH(PLC) was acquired by excitation 552 nm and emission at 610-650 nm. Fluorescence associated with mCitrine-1xPASS was acquired by excitation 488-515 nm and emission at 525-550 nm. Images were acquired in z-stacks (step size 0.43 μm, 10-20 sections per stack). LifeAct-GFP signal density, DII-VENUS signal intensity or signal intensity associated with lipid sensors were calculated by FiJi software as the percent occupancy of GFP signal in each maximum intensity projection. For each variant, fluorescent intensity of at least 5 roots were analyzed with 1-5 ROI (region of interest) per 1 root (ROI corresponding to one entire cell for actin; ROI corresponding to meristematic zone for DII-VENUS). For analyzing the skewness, all z-stack images were skeletonized and projected using a plugin moment calculator; the skewness of the actin filaments, indicating the degree of actin bundling, was measured (Lu and Day, 2017).

For tracking PIN2:GFP distribution in WT and *pi4kβ1β2* over time, ten frames were continuously obtained by confocal microscopy to track the movement of PIN2:GFP in root epidermis cells in the transition zone and compiled to a movie. PIN2:GFP subcellular distribution and cell properties were monitored on a Zeiss LSM880 microscope (AxioObserver, objective C-Apochromat 40x/1.2 W Korr FCS M27, Filter 493-598, Laser 488 nM, using zoom factor 6. Original picture size was 35,42 μm x 35,42 μm, scale bar is 10 μm.

For root hair video showing cytoplasmic streaming, maximum intensity projections of a Z-stack of a root hair were taken over time. Fluorescent and bright-field channelsare presented together. Fluorescent channel: visualization of cytoplasmic streaming in root hair cell outgrowing a root hair, based on differential movement of fluorescent intracellular structures in the line PIN2::PIN2:GFP compared to the mutant expressing PIN2:GFP. The movie was

reconstructed from confocal pictures captured in 20 frames (time-lapse) and in 18 (WT background)/19 slices (mutant background) through the root hair along the z-axis. Original picture size is 106.27 µm x 106.27 µm, pictures were captured with EC Plan-Neofluar 20x/0.50 (WD=2.0 mm) objective, using zoom factor 4. Scale bar is 10 µm. Brightfield channel: visualization of cytoplasmic streaming in a movie reconstructed from confocal pictures captured in 20 frames (time-lapse) and in 18 (WT background)/19 slices (mutant background) along the root hair in the z-axis. Original picture size is 106.27 µm x 106.27 µm, pictures were captured with EC Plan-Neofluar 20x/0.50 (WD=2.0mm) objective, using zoom factor 4. Scale bar is 10 µm.

For 4-64 staining seedlings were observed using a confocal scanning microscope Zeiss LSM 880 equipped with C-Apochromat 40x/1.2 W objective.

4.7.3 PIN2 immunolocalization

For whole mount immunolocalization of 5-day-old seedlings, the protocol was adapted to the InSituPro VS liquid-handling robot (Intavis AG, Germany). Prior to immunolocalization, seedlings were fixed 1 h with 4% (w/v) paraformaldehyde dissolved in MTSB (Modified Tryptone Soy Broth) (50 mM PIPES, 5 mM EGTA, 5 mM $MgSO_4 \cdot 7H_2O$ pH=7, adjusted with KOH), at room temperature, with no vacuum. In the robot, the procedure started with several washes with MTSB-T (MTSB+0.01% (v/v) TritonX-100) then cell walls were digested with 0.05% (w/v) Pectolyase Y-23 in MTSB-T and membranes were permeated with DMSO/Igepal in MTSB-T. Samples were blocked with BSA (blocking solution: 2% (w/v) BSA in MTSB-T) and incubated first with anti-PIN2 rabbit antibody (dilution 1:500) and then a secondary anti-rabbit Alexa Fluor 546 antibody (dilution 1:1000). Both antibodies were diluted in BSA. Between the described steps, washes with MTSB-T were provided and at the end MTSB-T was exchanged for deionized water. Seedlings were then transferred from the robot to 50% (v.v) glycerol in deionized water and the fluorescence signal was measured using a confocal scanning microscope Zeiss LSM 880 with Airyscan module.

4.7.4 Callose staining and microscopy

Four-week-old *A. thaliana* plants were treated for 24 h with *P. syringae*. Distilled water infiltration was used as a control (mock) treatment. Infiltrated leaves were discolored in ethanol/glacial acetic acid (3:1, v/v). The leaves were then rehydrated in successive baths of 70% (v/v) ethanol (at least 1 h), 50% (v/v) ethanol (at least 1 h), 30% (v/v) ethanol (at least 1

h) and water (at least 2 h). Leaves were stained for 4 h with 0.01% (w/v) aniline blue in 150 mM K_2HPO_4, pH=9.5. Callose deposition was observed by fluorescence microscopy using a Zeiss AxioImager ApoTome2 (objective 10x). Callose accumulation was calculated using FiJi software (Schindelin et al., 2012) as the percent occupancy of aniline blue signal (spots). At least 15 independent leaves were analyzed per variant.

4.7.5 Penetration success and imaging

For penetration rate estimation and callose visualization, 24 hpi each leaf segment was stained in 250 mg/ml trypan blue for 10 min and bleached in a 1:3 (v/v) acetic-acid/ethanol solution for 24 h. The leaves were then rehydrated in successive baths of 70% (v/v) ethanol (at least 1 h), 50% (v/v) ethanol (at least 1 h), 30% (v/v) ethanol (at least 1 h) and water (at least 2 h) and stained for 4 h with 0.01% (w/v) aniline blue in 150 mM K_2HPO_4, pH=9.5.
Stained leaves were observed by classical epifluorescence microscopy and bright-field microscopy using a Zeiss AxioImager ApoTome2 (objective 100x). For each genotype, three biological replicates were performed, considering at least 100 infection sites per variant.

4.8 DATA ANALYSIS AND STATISTICS

Student's *t*-test and one-way ANOVA with Tukey's HSD post-hoc test were applied; the exact number of values and statistical procedures are stated in the figure legends.

4.8.1 Data deposition

Experimental steps, from growth conditions to bioinformatic analyses, have been deposited in the CATdb database (Gagnot et al., 2008)) as ProjectID NGS2020_14_pi4kb1b2 and further submitted to the international repository GEO (Edgar et al., 2002) as ProjetID=GSE179635.

5. RESULTS

5.1 PART I. Auxin-related responses in roots

5.1.1 The *pi4kβ1β2* mutant is impaired in root growth

The PI4Kß1ß2 deficiency in *pi4kβ1β2* seedlings led to a decreased primary root length of up to 4-fold compared to the WT control (**Fig. 34a, b**). The shorter primary root of the mutant appeared to be due to shorter meristem and elongation zones (**Fig. 34c**). The shorter meristem of *pi4kβ1β2* was due to fewer cells (**Fig. 34d**), some of which showed unfinished cytokinesis. Interestingly, the CycB1::GUS associated signal occupied a smaller percentage area of the meristem in *pi4kβ1β2* roots when compared to the WT (**Fig. 34e, f**). The elongation zone was almost missing. In the differentiation zone, the *pi4kβ1β2* mutant had smaller cortical cells (**Fig. 35**) and either similar or very small root hair lengths when compared to the WT. This created apparent bare zones (**Fig. 34g, h**), while the overall total root hair density in *pi4kβ1β2* plants did not differ from WT (**Fig. 34i**). An analysis of the epidermal cell lines (Singh et al., 2008) showed that the regularity of trichoblasts/atrichoblasts formation was not affected in the mutant (**Fig. 36**). This confirmed that the apparent bare zones were not due to an absence of hairs but to shorter root hairs.

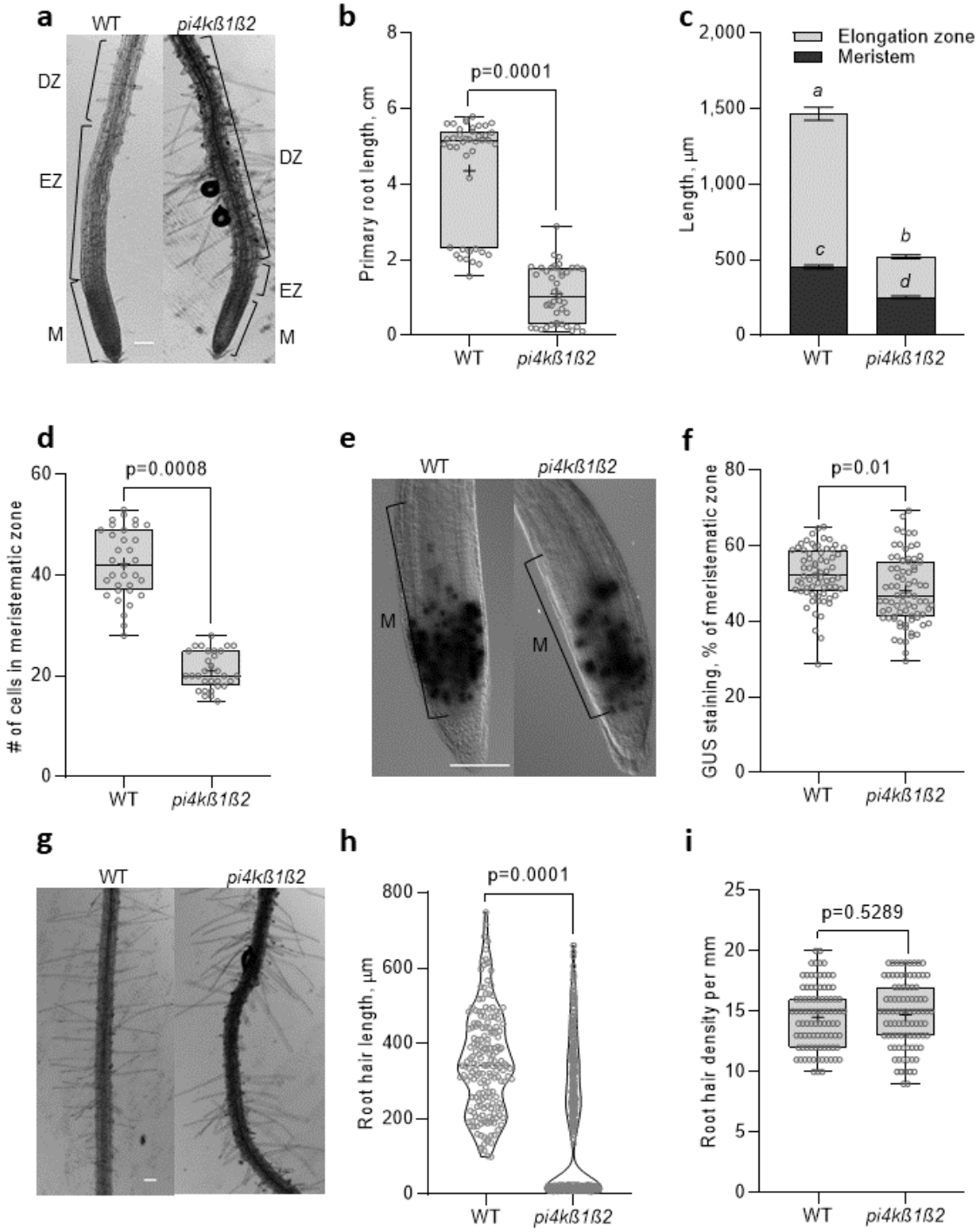

Fig. 34: Impaired root growth and morphological characteristics of the *pi4kβ1β2* mutant. a) representative pictures of the apical root parts of 11-day-old seedlings of *A. thaliana* WT and the

pi4kβ1β2 mutant: meristem (M), elongation zone (EZ) and differentiation zone (DZ) are marked, scale bar: 100 μm; **b)** primary root length, n=40; **c)** length of the meristematic and elongation zones, n=12, error bars represent mean ± SEM; different letters indicate statistically significant groups, one-way ANOVA with Tukey-HSD post-hoc test (p>0.05).; **d)** number of separated cells in the meristem, n=36; **e)** representative images of GUS staining in the root meristem of 4-day-old plants expressing CycB1::GUS, scale bar: 100 μm; **f)** relative area of CycB1::GUS expression, % of the meristematic zone; n=72; **g)** representative images of root hair distribution in the DZ of roots, scale bar: 100 μm; **h)** root hair length, n=180; **i**, root hair density, n=90. Central line of the boxplots represents the median, plus represents the mean, circles represent individual values from three biological repeats. *p*-value was calculated by Student t-test.

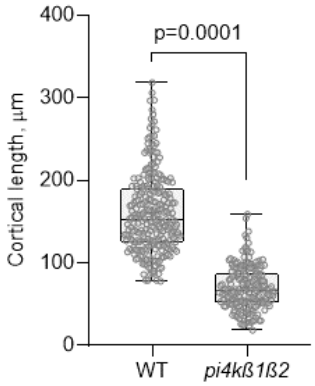

Fig. 35: Cortical cell length of 11-day-old seedlings of *A. thaliana* WT and *pi4kβ1β2* mutant; Student t-test, n=200.

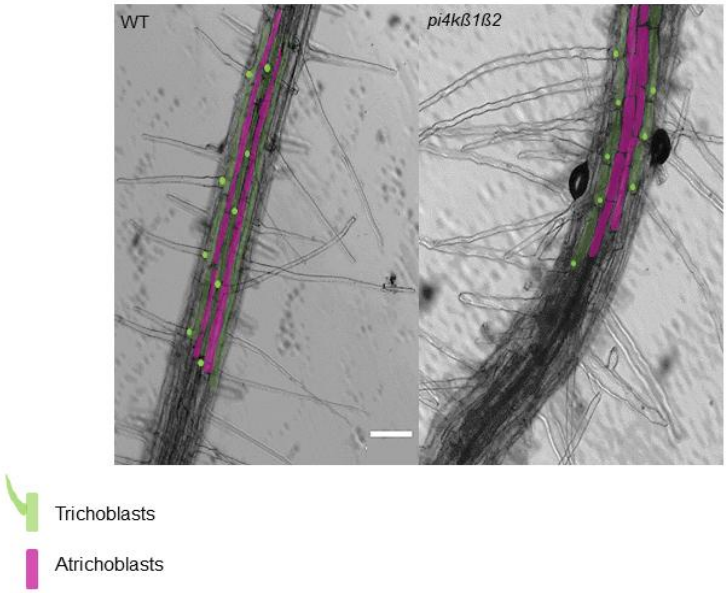

Fig. 36: Regularity of trichoblast (green) and atrichoblast (magenta) cell lines of 7-day-old seedlings of *A. thaliana* WT and *pi4kβ1β2* mutant, scale bar: 100 μm.

5.1.2 Responses to IAA and to gravistimulation are impaired in *pi4kβ1β2*

Mutant and WT 5-day-old seedlings were transferred to a cultivation medium containing various phytohormones. Seven days later, the lengths of the primary root, of the meristem and of the cortical cells were measured. The presence of IAA led to a decrease in the root length of WT plants; the decrease was more than 60% at 100 nM IAA. The *pi4kβ1β2* mutant was less sensitive to the auxin treatment, the decrease being only 20% at the concentrations tested (**Fig. 37a, Fig. 38**). A lower sensitivity to exogenous auxin was also detected at the cellular and/or tissue levels. At 50 nM IAA, the length of WT cortical cells showed a 30% decrease compared to the control, while the mutant was insensitive. At 1 µM IAA, the decrease in length of WT cortical cells was 50%, compared to the control, while the mutant remained insensitive (**Fig. 39a**). Concerning meristem size, 100 nM IAA caused a 20% shortening of its length in WT seedlings but no response was observed for the *pi4kβ1β2* mutant; this difference in IAA sensitivity was still apparent even at 1 µM (**Fig. 39b**). Interestingly, the sensitivity of primary root length to a cytokinin (BAP) or to SA did not differ between *pi4kβ1β2* and WT seedlings (**Fig. 39c, d**), thus indicating a specific response to auxins.

We then focused on another auxin-related process, the response to gravistimulation. Interestingly, both root elongation (i.e. the distance that the root tip grew since the 0' time point) and root orientation (i.e. the angle between the root tip at current and 0' time-point) were affected in the double mutant in due course of 12 h experiment (**Fig. 37b, c; Fig. 40**)

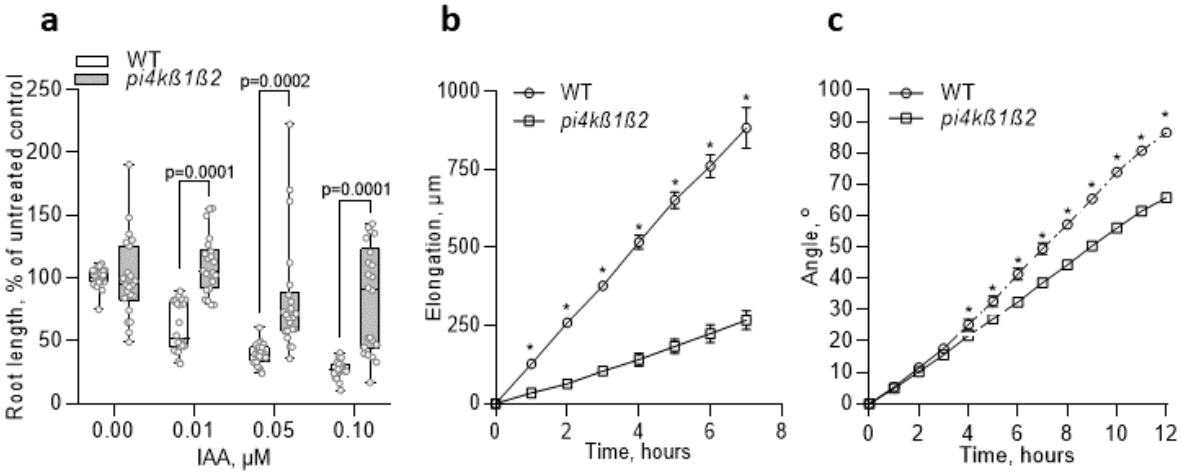

Fig. 37: Auxin-related phenotypes of the *pi4kβ1β2* mutant. **a)** primary root length of 11-day-old seedlings in response to different IAA concentrations, n=22. Central line of the boxplots represents the median, circles represent individual values; *p*-value is indicated for significantly different groups; *t*-test with correction for multiple comparisons; **b)** Elongation rate of primary root under gravistimulation, n=10; **c**, root tip orientation angle, n=10; **c)** gravitropic assay, 5-day-old seedlings were rotated to 90° on a horizontal microscope, images were taken every hour. Asterisks indicate

statistically significant differences between genotypes, p<0.05, paired *t*-test with correction for unequal variances. Experiments were repeated three times; data from a representative repeat are shown.

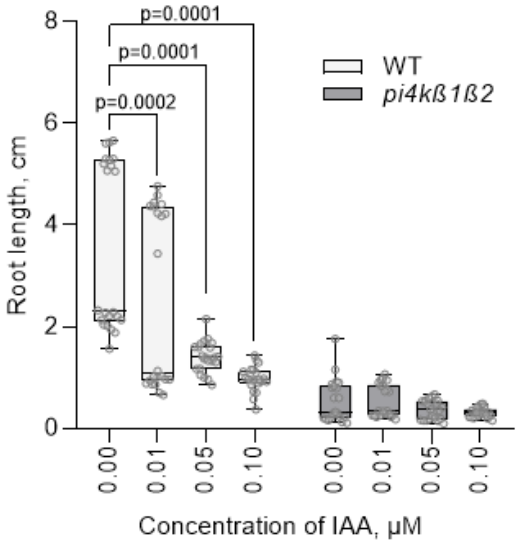

Fig. 38: Auxin-related phenotypes of the *pi4kβ1β2* mutant. Primary root length (absolute value) of 11-day-old seedlings in response to different IAA concentrations, n=22. P-value is indicated for variants significantly different from control with no IAA within each genotype, *t*-test with correction for multiple comparisons.

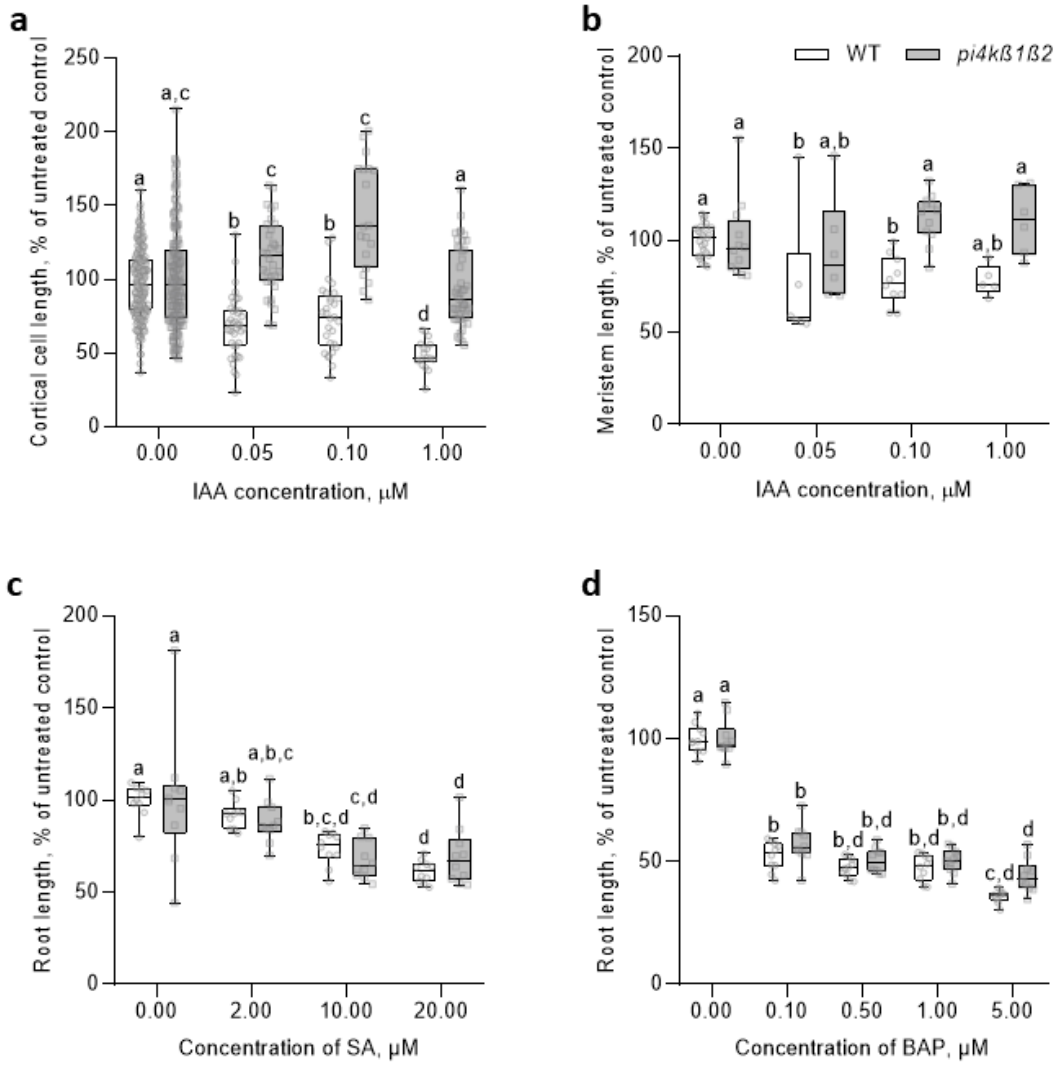

Fig. 39: Response to phytohormones of 11-day-old *A. thaliana* WT and *pi4kβ1β2* mutant seedlings, 7 days after their transfer to square Petri plates containing the same medium supplemented or not with hormones. **a)** IAA, cortical cell length, n=22; **b)** IAA, meristem length, n=22; **c)** SA, primary root length, n=10; **d)** BAP, primary root length, n=10. Central line of the boxplot represents the median; circles represent individual values from three biological repeats. Different letters indicate variants significantly different in every growing condition; one-way ANOVA with Tukey-HSD post-hoc test.

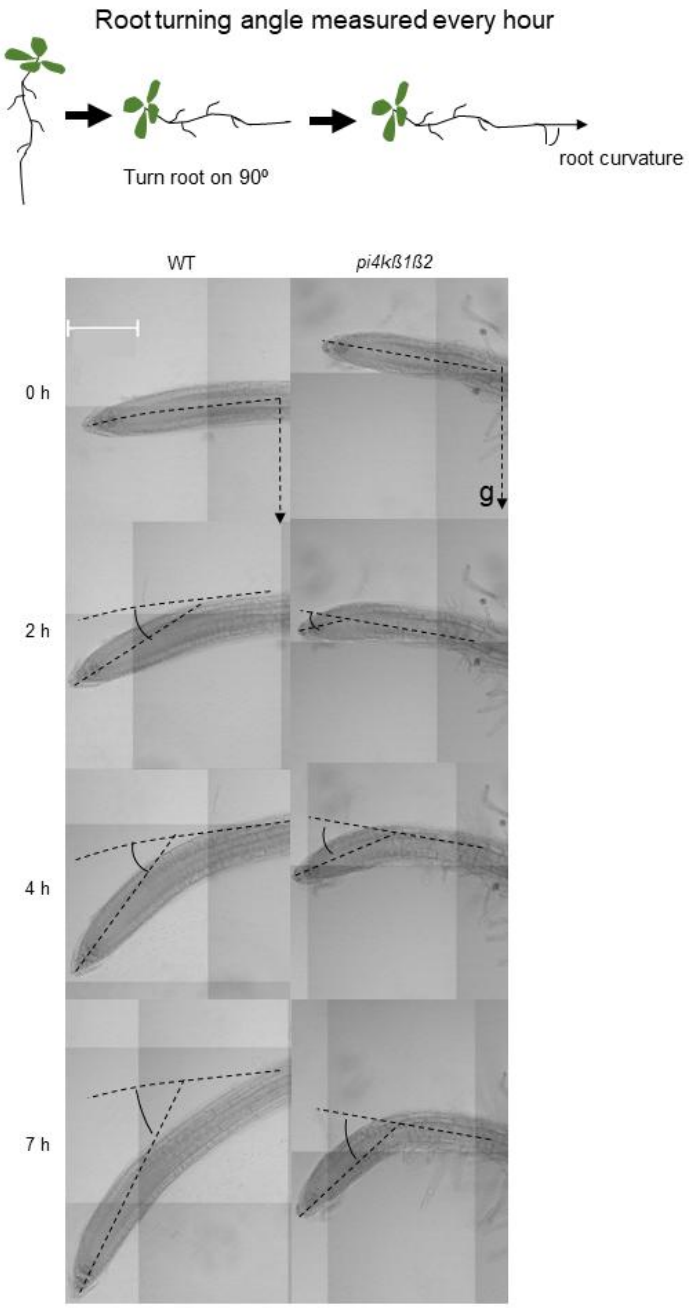

Fig. 40: Representative images of the gravitropic assay of 5-day-old seedlings of WT and *pi4kβ1β2* mutant. Seedlings cultivated vertically were rotated at 90° and imaged on a horizontal microscope for 7 h (one image per h), scale bar: 200 µm.

5.1.3 The transcriptome of *pi4kβ1β2* roots shows partial similarities to IAA-treated WT roots

In order to better detail the *pi4kβ1β2* root phenotypes, an RNAseq transcriptomic analysis of roots was performed. It was found that 2517 and 3418 genes were either up- or down-

regulated, respectively, in *pi4kβ1β2* roots compared to WT roots. To be more stringent, we then only considered the genes passing a threshold of log2 fold change of 1.5. On these genes we performed a Gene Ontology classification (**Fig. 41**).

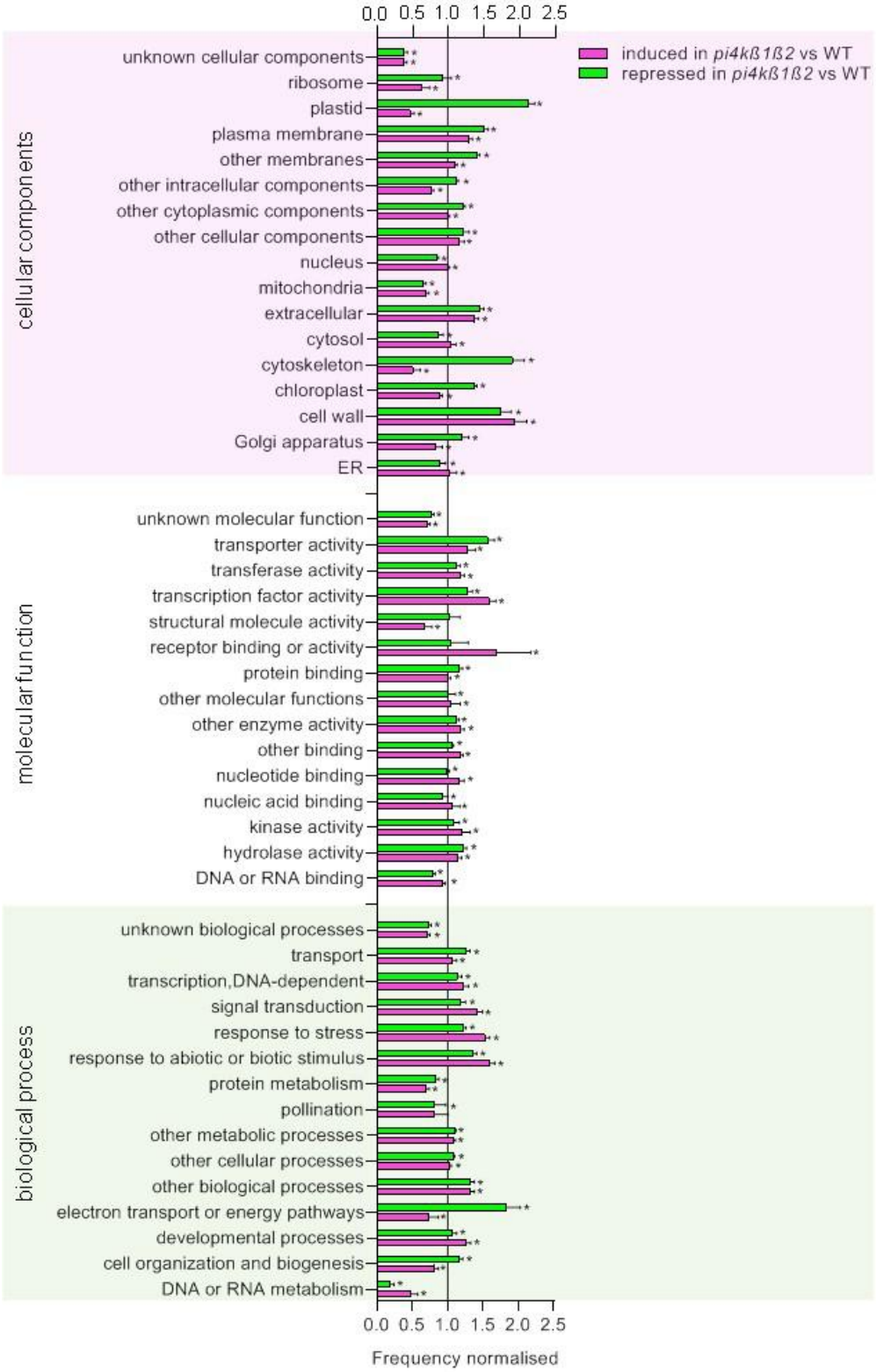

Fig. 41: Enrichment in GO categories in the sets of genes induced (230 genes) or repressed (264 genes) in *pi4kβ1β2* versus WT (Biological processes, molecular functions, cellular components). To focus on the most significant changes, we applied a log2 fold change filter. Genes with the differential expression higher or lower than 1.5 were classified using the Classification SuperViewer Tool developed by (Provart and Zhu, 2003). The classification source was set to Gene Ontology

categories as defined by (Ashburner et al., 2000). The frequency of a category, normalized to that in the whole Arabidopsis set. The mean and standard deviation for 100 bootstraps of our input set were calculated to provide some idea about over- or under-representation reliability.

Among the genes induced in *pi4kβ1β2* roots compared to WT, we found enrichment in genes encoding extracellular, plasma membrane, or cell wall localized proteins, and underrepresentation of genes encoding cytoskeleton or mitochondria-associated proteins. Interestingly, among the repressed genes, the cell wall-associated proteins were also enriched, while cytoskeleton-localized proteins were overrepresented. As for biological processes, we found enrichment in the categories of "response to stress", "signal transduction"and "development" for both groups of genes. Results of the RNAseq analysis were confirmed by qPCR on a selection of genes (**Fig. 42**).

a

id	Annotation	log2FoldChange	adjusted.PValue
AT1G04240 *(SHY2)*	AUX/IAA transcriptional regulator family protein	-1.45	2.47E-26
AT5G23060 *(CAS)*	calcium sensing receptor	-1.24	9.13E-13
AT1G44575 *(NPQ)*	Chlorophyll A-B binding family protein	-1.15	4.40E-16
AT1G75690 *(LQY)*	DnaJ/Hsp40 cysteine-rich domain superfamily protein	-1.71	1.47E-14
AT1G72610 *(GER)*	germin-like protein 1	-1.84	2.10E-13
AT2G40340 *(DREB2C)*	Integrase-type DNA-binding superfamily protein	0.75	1.48E-02

b

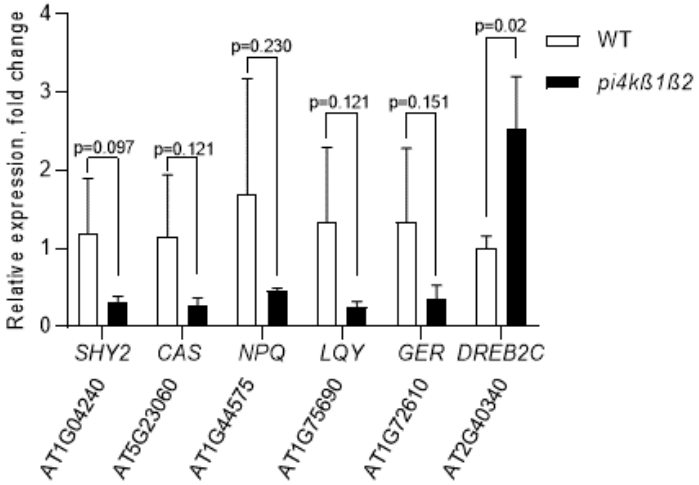

Fig. 42: Transcript levels of selected up- and down-regulated genes in *pi4kβ1β2* plants versus the WT. **a)** selected genes, with the log2 fold change as detected in the NGS experiment; **b)** transcript levels of the selected genes as measured by qPCR; Root samples were collected from 11-day-old seedlings of *A. thaliana* WT and the *pi4kβ1β2* mutant. Values were normalized to the WT. *TIP41* was

used as a reference gene. Data represents mean + SEM, one-way ANOVA with Tukey-HSD post-hoc test, n=3.

Among the genes most induced in *pi4kβ1β2* roots, we found several that were involved in response to hypoxia, oxidative stress and induced systemic resistance (**Fig. 43, 44**).

a

id	Annotation	log2FoldChange	adjusted.PValue
AT5G19880	Peroxidase superfamily protein	3.63	2.20E-37
AT2G29350	senescence-associated gene 13	5.43	9.30E-40
AT1G26390	FAD-binding Berberine family protein	4.89	1.54E-40
AT1G26410	FAD-binding Berberine family protein	4.84	3.69E-51
AT2G30660	ATP-dependent caseinolytic (Clp) protease/crotonase family protein	4.66	1.22E-12
AT4G28420	Tyrosine transaminase family protein	4.46	6.99E-20
AT2G30770	cytochrome P450, family 71, subfamily A, polypeptide 13	4.45	3.51E-25
AT2G30750	cytochrome P450, family 71, subfamily A, polypeptide 12	4.39	4.24E-28
AT4G31970	cytochrome P450, family 82, subfamily C, polypeptide 2	4.27	1.45E-11
AT1G52120	Mannose-binding lectin superfamily protein	4.23	8.68E-17
AT5G13320	Auxin-responsive GH3 family protein	4.13	3.80E-46
AT1G08080	alpha carbonic anhydrase 7	4.12	3.04E-11
AT1G52130	Mannose-binding lectin superfamily protein	4.11	1.22E-21
AT1G26240	Proline-rich extensin-like family protein	4.11	9.37E-32
AT1G01680	plant U-box 54	4.07	7.85E-11
AT3G47480	Calcium-binding EF-hand family protein	4.03	6.13E-31
AT4G15370	baruol synthase 1	3.92	4.60E-30
AT5G05340	Peroxidase superfamily protein	3.85	3.25E-57
AT3G60470	Plant protein of unknown function (DUF247)	3.68	1.57E-19
AT4G15100	serine carboxypeptidase-like 30	3.67	3.10E-25

b

id	Annotation	log2FoldChange	adjusted.PValue
AT1G61130	serine carboxypeptidase-like 32	-3.34	9.02E-26
AT3G08900	reversibly glycosylated polypeptide 3	-3.41	1.08E-06
AT3G13784	cell wall invertase 5	-3.47	4.88E-13
AT3G46400	Leucine-rich repeat protein kinase family protein	-3.57	2.00E-16
AT4G23496	SPIRAL1-like5	-3.58	2.70E-51
AT1G78440	Arabidopsis thaliana gibberellin 2-oxidase 1	-3.64	1.03E-14
AT2G42250	cytochrome P450, family 712, subfamily A, polypeptide 1	-3.68	2.63E-75
AT5G06900	cytochrome P450, family 93, subfamily D, polypeptide 1	-3.76	2.63E-12
AT1G78450	SOUL heme-binding family protein	-3.78	2.83E-12
AT1G52820	2-oxoglutarate (2OG) and Fe(II)-dependent oxygenase superfamily protein	-4.03	8.65E-168
AT3G62740	beta glucosidase 7	-4.25	9.48E-33
AT4G01890	Pectin lyase-like superfamily protein	-4.35	1.02E-26
AT5G06905	cytochrome P450, family 712, subfamily A, polypeptide 2	-4.38	2.51E-13
AT2G33810	squamosa promoter binding protein-like 3	-4.48	3.93E-13
AT3G30260	AGAMOUS-like 79	-4.70	8.13E-20
AT1G52790	2-oxoglutarate (2OG) and Fe(II)-dependent oxygenase superfamily protein	-5.03	2.50E-10
AT2G01280	Cyclin/Brf1-like TBP-binding protein	-5.16	3.63E-11
AT3G52970	cytochrome P450, family 76, subfamily G, polypeptide 1	-5.81	8.86E-26
AT1G53480	mto 1 responding down 1	-5.96	4.04E-47
AT2G24000	serine carboxypeptidase-like 22	-7.38	7.40E-16

Fig. 43: The 20 most induced (**a**) and 20 most repressed (**b**) genes for *pi4kβ1β2* mutant roots versus WT roots.

Next, the list of the 200 most up-regulated and 200 most down-regulated genes in *pi4kβ1β2* mutant roots versus WT roots was used as a signature to interrogate public transcriptomic data using the Genevestigator similarity search program (Preuss et al., 2006). This was performed against curated root experiments dealing with root samples and classified as "Hormone", "Temperature" or "Stress". Out of the 10 most similar experiments, 7 concerned treatments with auxin (**Fig. 44a**). Within this set of curated root experiments (**Fig. 44a**), we then only selected the experiments dealing with response to auxins. According to the responses in these experiments of the 200 most repressed genes in our *pi4kβ1β2* versus WT root comparison, the experiments and the genes were clustered (**Fig. 44b**). This allowed the identification of clusters of genes, down-regulated in *pi4kβ1β2* mutant roots compared to WT ones and down-regulated in some experiments dealing with the response to auxin (**Fig. 44b, clusters A, B, C; list of genes of these clusters in table 9**).

Table 9. Clusters of genes, down-regulated in *pi4kβ1β2* mutant roots compared to WT ones and down-regulated in curated public transcriptomics experiments dealing with the response to auxin (clusters A, B, C); genes that are down-regulated in *pi4kβ1β2* roots, but were shown to be upregulated by auxin in curated public transcriptomics experiments dealing with the response to auxin (cluster D); genes upregulated both in *pi4kβ1β2* mutant roots versus WT and up-regulated in curated experiments dealing with response to auxin in roots (cluster E); genes upregulated in *pi4kβ1β2* mutant roots versus WT but down-regulated in some curated experiments dealing with response to auxin in roots (F).

A		B	C	D	E	F
At1g19900	*AGP13*	*NPF6.4*	*At4g02850*	*ACT4*	*At3g46810*	*At1g26420*
ACSS	*AGP22*	*At1g22290*	*PUP4*	*At1g58120*	*At4g12490*	*UGT74E2*
FAR3	*At4g01140*	*At1g78990*	*TPPH*	*At3g26490*	*CDEF1*	*GSTF3*
CSLB5	*At4g22460*	*NPF2.3*	*ATT16*	*At5g22430*	*JAL4*	*NDB4*
PIP2-4	*MLP43*	*At1g03660*	*At1g64590*	*AIR1B*	*GH3.3*	*ORG3*
At3g19320	*ANNAT7*	*At5g37990*	*ERFO34*	*At3g06390*	*YDK1*	*PMAT1*
PME16	*SCPL31*		*XTH32*	*At1g11740*	*ZPF2*	*BGLU28*
At4g38690	*At1g33100*			*At2g19060*	*ACS9*	*PME60*
At4g12510	*At3g26460*			*At1g76800*	*CML12*	*At4g10500*
TIP2-3	*IPSP*			*ATLP-3*	*MRS2-8*	*MSRB8*
BGAL4	*At5g62330*				*DIR11*	*PER10*
At5g46900	*At4g01890*				*EXP12*	
	MRN1					

We did the same with the 200 most up-regulated genes in the *pi4kβ1β2* double mutant compared to WT roots and thus identified genes upregulated both in *pi4kβ1β2* mutant roots versus WT and up-regulated in curated experiments dealing with response to auxin in roots (**Fig. 44c, cluster E**). These clusters represent genes for which the effect of the *pi4kβ1β2* double mutation in the root compared to WT is similar to a treatment with auxin. Yet other clusters exist, consisting of genes that are down-regulated in *pi4kβ1β2* roots, but were shown to be upregulated by auxins in public transcriptomics data (**Fig. 44b, cluster D; table 1**), or genes that are up-regulated in *pi4kβ1β2* roots, but were shown to be upregulated by auxins in public transcriptomics data (**Fig. 44c, cluster F; table 1**). The transcript levels of selected auxin responsive genes representing different clusters were monitored by qPCR in mutant and WT plants, treated or not with 10 nM IAA for 24 h (**Fig. 44d)**. The transcript level of *AT1G64590, CSLB5, SAUR9, NPF2.4* and *BRU6* in the untreated roots of *pi4kβ1β2* mutant was similar to that in WT roots treated with auxins. On the other hand, the transcription of *CSLB5, FLA13* and *BRU6* did not change in response to auxin in the *pi4kβ1β2* mutant, showing another evidence of affected auxin response.

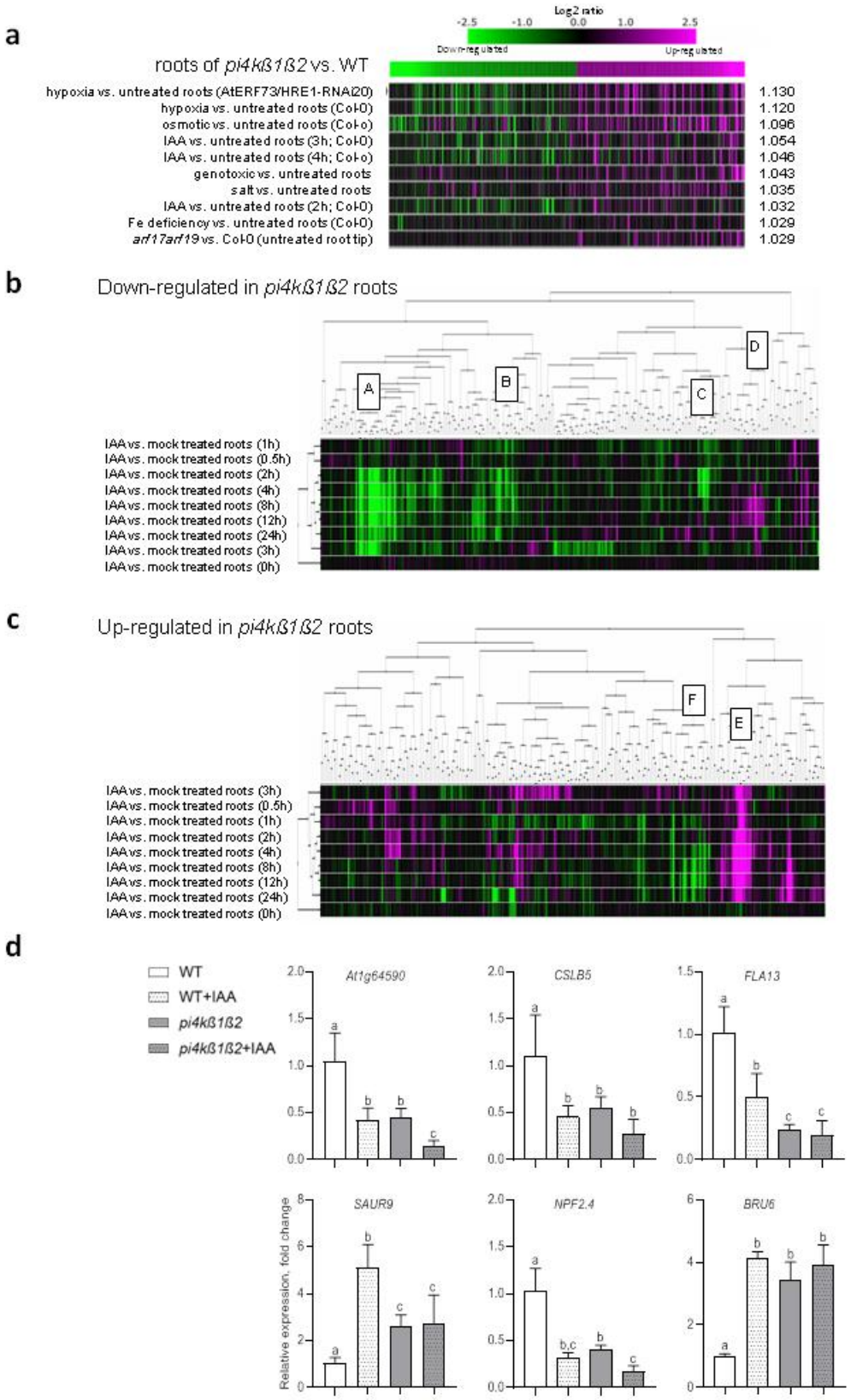

Fig. 44: Transcriptomic analysis of *pi4kβ1β2* roots. **a)** similarity between the *pi4kβ1β2* roots transcriptome (compared to WT) and the stress-, hormone- or temperature- responsive transcriptomes. The 200 genes most up-regulated in *pi4kβ1β2* roots compared to the WT and the

200 genes most down-regulated in *pi4kβ1β2* roots compared to the WT were used as a signature to search for transcriptome experiments with the highest similarity. The similarity search was performed against the 550 experiments classified as "stress", "temperature" or "hormone" by Genevestigator (Hruz et al., 2008). Experiments were sorted according to Euclidean distance. Expression of the signature genes in the 10 most similar experiments are shown in color-scale; **b, c)** hierarchical clustering of curated root experiments dealing with the response to auxins. The 9 curated root experiments dealing with auxins in Genevestigator were retrieved. According to the expression in these experiments of the 200 most down-regulated (b) genes in our *pi4kβ1β2 vs. WT* root comparison, the genes and experiments were clustered with the Biclustering tool in Genvestigator. The same was done using the 200 most up-regulated (c) genes in our *pi4kβ1β2 vs.* WT root comparison. Similarities between expression profiles were determined using Pearson correlation. For each experiment, the duration of hormone treatment is indicated. Separated gene clusters with highest levels of induction/repression are labeled and genes are specified on the right panel; **d)** response of selected genes to auxin. Five-day-old seedlings were transferred to a medium containing 10 nM IAA, and roots for RNA extraction were harvested after 24 h. The data are presented in means ± SE, n=9, with a Tukey honestly significant difference (HSD) multiple mean comparison post hoc test. Different letters indicate a significant difference (one-way ANOVA, Tukey HSD, p-value < 0.05).

5.1.4 Assessing auxin sensitivity of *pi4kβ1β2* roots

We next checked auxin transcriptional response by a reporter system, introducing by crossing the auxin sensitive synthetic promoter DR5 (Ulmasov et al., 1995) fused to a GUS reporter gene into *pi4kβ1β2* background. Surprisingly, the basal level of DR5 promoter activity was lower in root and leaf meristem of the *pi4kβ1β2* plants (**Fig. 45a, b**). After exposure to 10 nM IAA, an important increase of DR5-GUS signal was detected in WT meristems, but not in the *pi4kβ1β2* mutant (**Fig. 45a, b**), confirming that the sensitivity to IAA is impaired in the mutant line.

The DII-VENUS (Brunoud et al., 2012) construct was introduced into the *pi4kβ1β2* mutant by floral-dip agrobacterium transformation. DII-VENUS is a fast maturing form of a yellow fluorescent protein fused in-frame to the Aux/IAA-interaction domain (termed domain II;) and it is rapidly degraded in response to auxin (Brunoud et al., 2012). It is used as a reporter of auxin level. As the DII-Venus reporter was introduced by agrobacterium transformation, the potential positional effect of the insert cannot be excluded, so the basal fluorescent signal cannot be compared between the lines but signals can be compared within one line. After exposure to 10 nM IAA, a significant decrease of DII-VENUS fluorescence signal was detected in WT plants, but not in the *pi4kβ1β2* mutant (**Fig. 45c, d**). To check whether the mutant insensitivity to IAA might be a consequence of an elevated IAA level in control conditions, we extracted hormones from the total root system and measured the content of IAA metabolites and conjugates. No difference in the measured free IAA content was

detected between genotypes, while IAA-Glu, CamX, I3A and IAN concentrations were higher in the *pi4kβ1β2* mutant than in the wild type roots (**Fig. 45e**). In shoots comparison, an increased level of IAM and I3A (**Fig. 46**).

Based on our RNAseq data, the auxin efflux transporter *PIN2* gene was up-regulated, *PIN4* and *PIN5* - down-regulated in *pi4kβ1β2* roots, some of them were not changed (*PIN1*, *PIN3*). As for influx transporters *LAX1* and *LAX3* were down-regulated. Most of the genes involved in IAA conjugation belong to IAA–amido synthetases GH3 family proteins. The most induced in my data - GH3.12. The expression of GH3.12 is induced by SA (Dempsey et al., 2011). Moreover, *gh3.12* mutants displayed SA-related phenotypes (Okrent et al., 2009). Recently, GH3.12 (PBS3) was discovered to conjugate isochorismate with glutamate to produce isochorismate-glutamate, which is non-enzymatically and spontaneously converted into SA (Rekhter et al., 2019). Relying on data, auxin transport is impaired (**Fig. 47**).

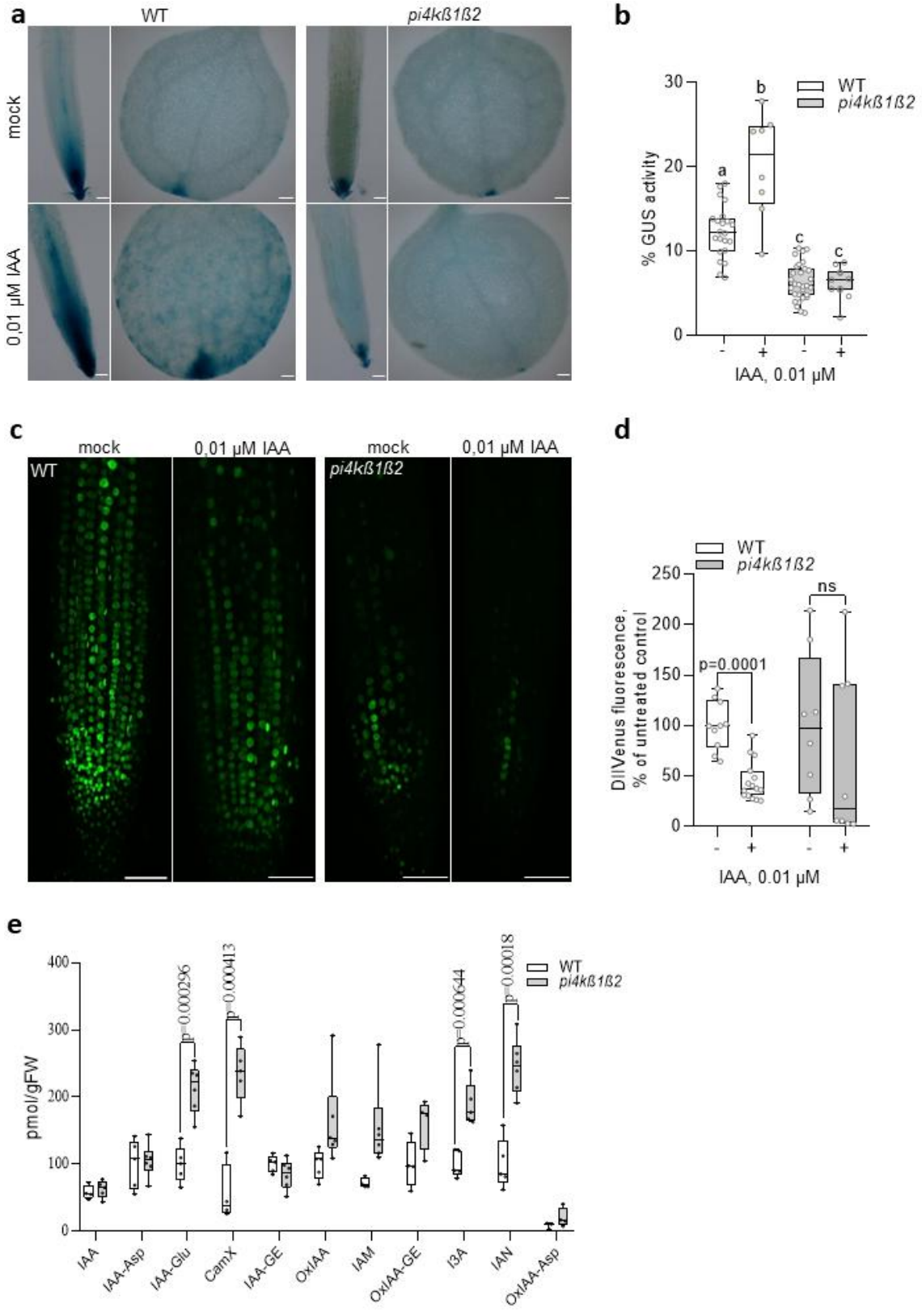

Fig. 45: Auxin sensitivity of the *pi4kβ1β2* mutant. **a)** representative images of DR5-GUS activity in 5-day-old roots and cotyledons in the presence or not of 0.01 µM IAA for 12 h, scale bar: 100 µm. **b)** DR5-GUS quantification, % of GUS-stained area in root meristem, n=10; **c)** representative

images of DII-VENUS fluorescence in root tip of 7-day-old seedlings in the presence or not of 0.01 µM IAA for 1 h, maximum intensity Z-projections of 10 nm stacks, scale bar: 50 µm; **d)** DII-VENUS fluorescence quantification, % of meristematic zone; n=10; **e)** quantitation of IAA metabolites and conjugates in 7-day-old roots, n=6; Central line of the boxplots represents the median, circles represent individual values; *p*-value is indicated for significantly different groups, ns – non significant; unpaired *t*-test (**d, e**); the data are presented in means ± SD, n=10, with a Tukey honestly significant difference (HSD) multiple mean comparison *post hoc* test. Different letters indicate a significant difference (one-way ANOVA, Tukey HSD, $P < 0.05$) (**b**); experiments were repeated three times; data from a representative repeat are shown. IAA - indole-3-acetic acid, IAA-Asp - IAA-aspartate, IAA-Glu - IAA-glutamate, CamX - camalexin, IAA-GE - IAA-glucose ester, OxIAA - oxo-IAA, IAM - Indole-3-acetamide (IAA precursor), OxIAA-GE - oxo-IAA-glucose ester, I3A - indole-3-aldehyde, IAN - Indole-3-acetonitrile (IAA precursor), OxIAA-Asp - oxo-IAA-aspartate.

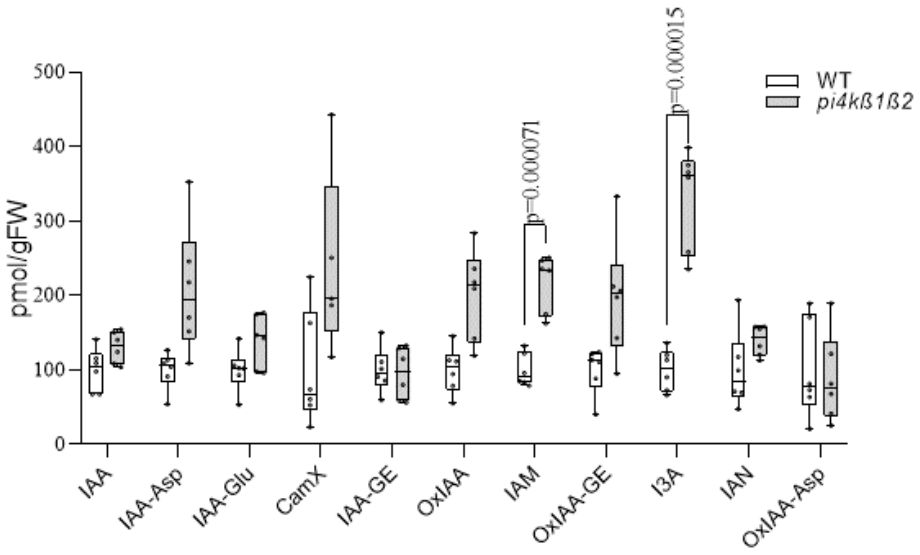

Fig. 46: Quantitation of IAA metabolites and conjugates in 7-day-old shoots, n=6; Central line of the boxplots represents the median, circles represent individual values; *p*-value is indicated for significantly different groups, ns – non significant; unpaired *t*-test.

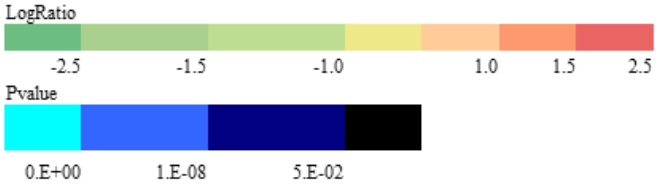

Auxin trasporter genes

id	Annotation		*pi4kβ1β2*	WT	log2FoldChange	adjusted.P Value
AT5G16530	Auxin efflux carrier family protein	PIN5	40,25	204,58	-2,39	6,80E-10
AT2G17500	Auxin efflux carrier family protein	PILS5	7238,79	12512,82	-0,80	1,46E-14
AT2G01420	Auxin efflux carrier family protein	PIN4	1585,18	2232,00	-0,49	3,54E-04
AT1G76520	Auxin efflux carrier family protein	PILS3	1986,16	1476,15	0,43	9,61E-05
AT5G57090	Auxin efflux carrier family protein	EIR1, PIN2	7825,96	5271,56	0,57	7,19E-16
AT4G25960	P-glycoprotein 2	ABCB2	290,49	137,76	1,07	2,21E-14
AT5G01240	like AUXIN RESISTANT 1	LAX1	297,82	765,49	-1,36	1,57E-40
AT1G77690	like AUX1 3	LAX3	3092,47	4671,07	-0,60	5,75E-10
AT1G73590	Auxin efflux carrier family protein	PIN1	2572,05	2395,06	0,09	
AT1G70940	Auxin efflux carrier family protein	PIN3	2659,96	2693,76	-0,03	
AT2G38120	Transmembrane amino acid transporter family protein	AUX1	6151,44	6104,81	0,01	

Auxin metabolism genes

id	Annotation		*pi4kβ1β2*	WT	log2FoldChange	adjusted.P Value
AT1G07780	phosphoribosylanthranilate isomerase 1	PAI1	643,09	530,70	0,28	1,47E-03
AT2G04400	Aldolase-type TIM barrel family protein	IGPS	3653,01	3211,51	0,19	4,17E-03
AT1G52410	TSK-associating protein 1	TSA1	479,45	1120,18	-1,22	3,97E-21
AT2G27150	abscisic aldehyde oxidase 3	AAO3	1018,47	819,36	0,32	1,84E-03
AT4G37550	Acetamidase/Formamidase family protein	AMH1	291,58	615,99	-1,08	6,29E-22
AT4G37560	Acetamidase/Formamidase family protein	AMH2	22,40	11,38	0,99	1,85E-03
AT5G17990	tryptophan biosynthesis 1	TRP1	2959,48	2405,64	0,30	8,72E-03
AT5G38530	tryptophan synthase beta type 2	TSBtype2	3918,79	3349,83	0,23	5,34E-03
AT1G04610	YUCCA 3	YUC3	491,20	647,89	-0,41	4,59E-03
AT2G33230	YUCCA 7	YUC7	26,78	14,70	0,86	1,71E-02
AT4G31500	cytochrome P450, family 83, subfamily B, polypeptide 1	CYP83B1	14766,74	19360,47	-0,39	2,41E-03
AT2G22330	cytochrome P450, family 79, subfamily B, polypeptide 3	CYP79B3	2776,94	7534,71	-1,43	2,28E-23
AT2G30770	cytochrome P450, family 71, subfamily A, polypeptide 13	CYP71A13	332,21	14,27	4,45	3,51E-25
AT3G44300	nitrilase 2	NIT2	8123,62	3498,14	1,22	1,34E-34
AT5G22300	nitrilase 4	NIT4	312,92	58,96	2,42	4,42E-36

Enzymes involved in auxin conjugation

id	Annotation		*pi4kβ1β2*	WT	log2FoldChange	adjusted.P Value
AT3G02875	Peptidase M20/M25/M40 family protein	ILR1	1098,16	925,59	0,25	1,21E-02
AT1G48690	Auxin-responsive GH3 family protein		518,01	775,26	-0,58	9,72E-04
AT5G13360	Auxin-responsive GH3 family protein		1331,43	1105,13	0,27	2,07E-03
AT5G51470	Auxin-responsive GH3 family protein		454,18	351,92	0,36	8,22E-03
AT1G23160	Auxin-responsive GH3 family protein	GH3.7	733,21	546,30	0,42	5,04E-05
AT2G14960	Auxin-responsive GH3 family protein	GH3.1	309,28	209,55	0,57	2,24E-02
AT5G54510	Auxin-responsive GH3 family protein	DFL1	2352,18	1461,33	0,67	3,42E-03
AT5G13370	Auxin-responsive GH3 family protein	GH3.15	667,04	211,69	1,65	3,71E-44
AT4G37390	Auxin-responsive GH3 family protein	BRU6	1370,92	404,44	1,78	4,29E-06
AT2G23170	Auxin-responsive GH3 family protein	GH3.3	1170,73	182,81	2,70	1,10E-07
AT5G13320	Auxin-responsive GH3 family protein	GH3.12	195,88	10,56	4,13	3,80E-48

Fig. 47: List of auxin transporter and metabolism genes differentially expressed in roots of *pi4kβ1β2* versus WT.

5.1.5 Localization of auxin efflux transporter PIN2 is altered in the *pi4kβ1β2* mutant

As auxin signaling is relying on the correct auxin transport between and within the cells, we investigated the localization and dynamics of auxin transporter PIN2. We analyzed plants expressing PIN2::PIN2-GFP by immunostaining (**Fig. 48a-e**) and confocal microscopy of PIN2-GFP in both WT and *pi4kβ1β2* backgrounds (**Fig. 48f-k**). Overall, PIN2 was distributed on the PM in the same cell types and with a similar polar distribution in mutant roots compared to WT roots. However, in the *pi4kβ1β2* mutant, several "black holes" in the signal were detected along the PM (**Fig. 48b, c, d, e, 49**). When counterstained with FM 4-64, a dye that labels the PM, it was seen that the unstained parts in the *pi4kβ1β2* roots corresponded to tunnels between adjacent cells (**Fig. 48c, d, e**). Confocal microscopy color-coded projections of pictures were taken over time to track PIN2 intracellular movement in the meristematic zone. The chaotic distribution of vesicles in *pi4kβ1β2* compared to the vesicles aligned in WT showed not only differences in the amount of GFP-marked intracellular vesicles, but also that their movement was less rectilinear and very fast in *pi4kβ1β2* (compare **Fig. 48f, g, h**, where vesicles are indicated by white arrows, and the corresponding). Differences in vacuolar morphology were also observed in *pi4kβ1β2* (**Fig. 48i, j; 50**), with bigger and less fragmented vacuoles than the WT. When focused on growing root hair cells, altered movement of fluorescent marked vesicles in mature root hair cells and elongating root hairs in *pi4kβ1β2 PIN2::PIN2-GFP* was observed. Bright field imaging also revealed differences in the flow of cytoplasmic streaming. Circulation of the cytoplasmic stream occurred close to the PM and in a straight path in the WT, whereas in the mutant stream flowed in less coordinated lanes (data not shown). We then studied the response to a dark shift of whole seedlings, a treatment known to enhance PIN2 delivery to the lytic vacuole (Singh et al., 2008). A 1 h dark shift caused the translocation of PIN2 to lytic vacuoles in WT roots but not in the double mutant (**Fig. 48k, l**). All these results point to altered intracellular trafficking dynamics in the roots of *pi4kβ1β2* seedlings.

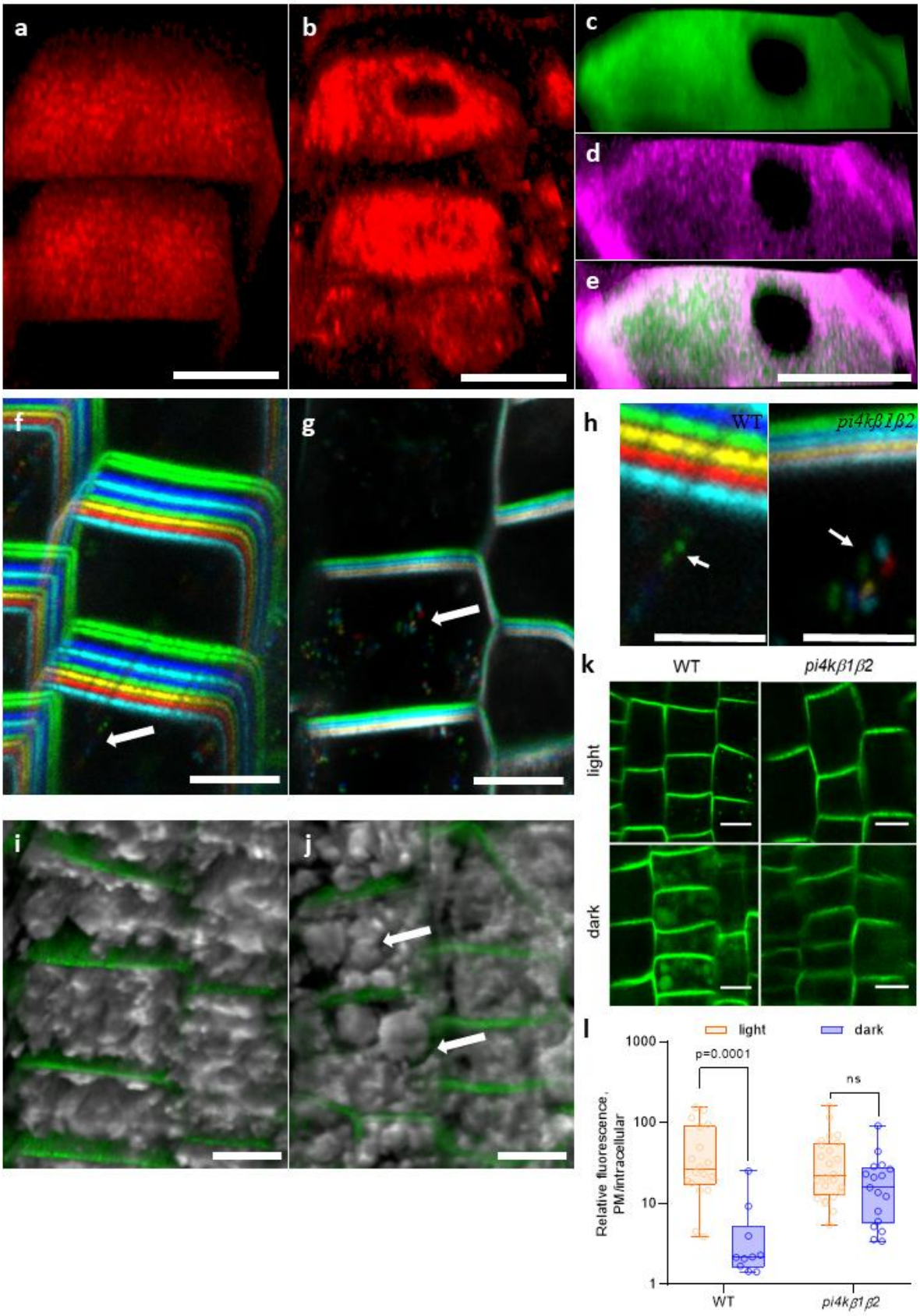

Fig. 48: Visualization of PIN2 subcellular distribution by confocal microscopy. **a)** distribution of PIN2 along the PM in WT roots, immunostaining; **b)** distribution of PIN2 along the PM in *pi4kβ1β2* roots, immunostaining; **c, d, e)** show PIN2 signal overlapping with FM4-64 dye, (**c**, FM4-

64; **d**, PIN2; **e**, merged signals); **f, g)** color-coded projection of PIN2 distribution and intracellular movement over time in **f**, WT and **g**, *pi4kβ1β2* backgrounds; arrows point to vesicles moving in time; h, zoomed part of f and g, scale bars 5 μm, arrows point to vesicles moving in time; **i, j)** merged 3D reconstruction of pictures taken along the z-axis of the bright field and fluorescent channel of PIN2 distribution along the PM and vacuole morphology in **i**, WT and **j**, *pi4kβ1β2* backgrounds; arrows point to enlarged vacuoles in *pi4kβ1β2*; **k)** visualization of PIN2 movement towards the lytic vacuole upon a dark shift of whole seedlings. After 1 h, the GFP signal was visible in the WT background, but not in *pi4kβ1β2*; **l)** quantification of the GFP signal intensity in the lytic vacuole, each circle represents the PM/intracellular ratio for a single cell; *p*-value is indicated for significantly different groups, ns – non significant; unpaired *t*-test with correction for multiple comparisons; n=25; scale bars: 10 μm.

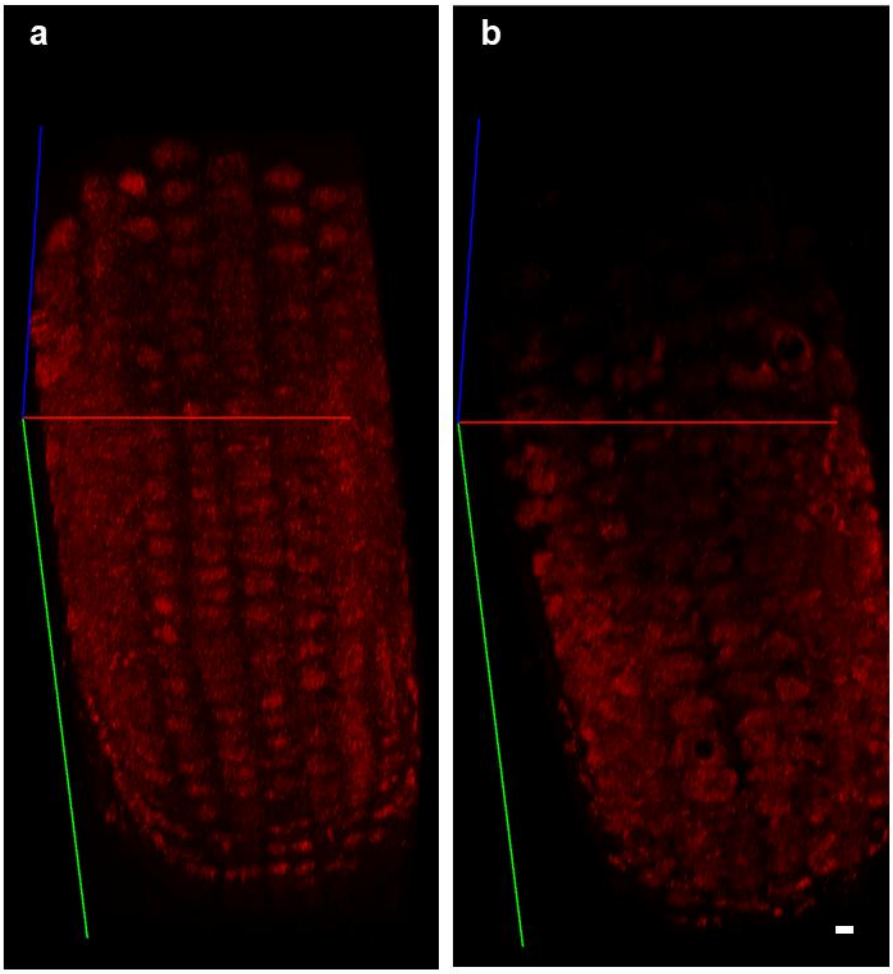

Fig. 49: 3D reconstruction root immunostaining against PIN2. Merged 3D reconstruction of pictures taken along the z-axis of the fluorescent channel to track distribution of PIN2 along the plasma membrane in **a**, WT and **b**, *pi4kβ1β2* background. Scale bar: 10 mm. Color lines represent axes in 3D reconstruction (X-red, Y-green, Z-Blue).

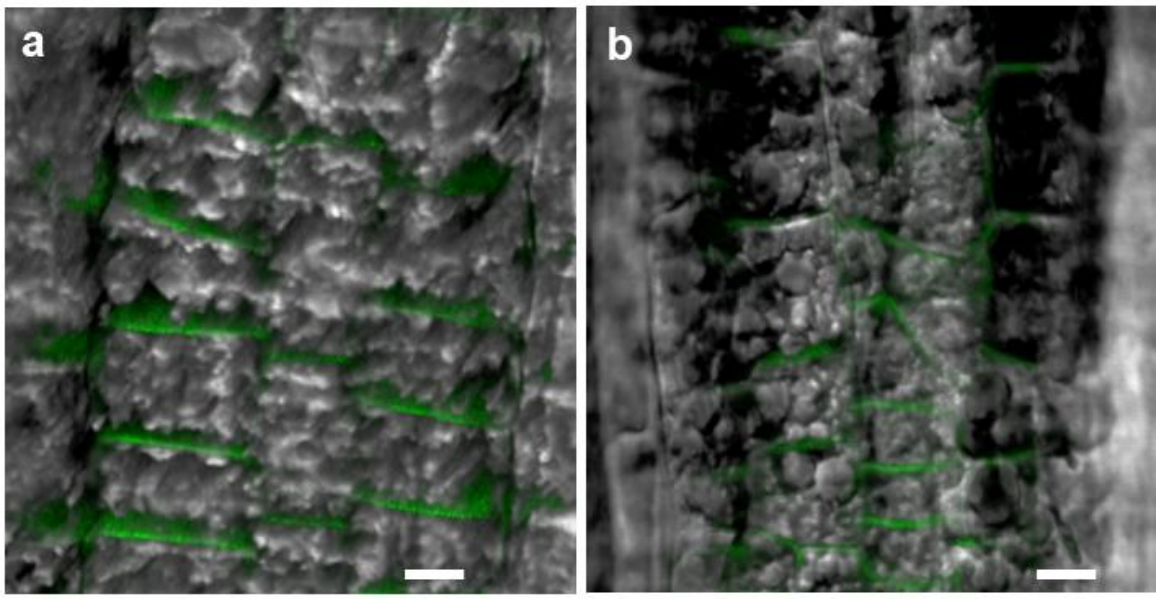

Fig. 50: 3D reconstruction root epidermis cell transition zone. Merged 3D reconstruction of pictures taken along the z-axis of the brightfield and fluorescent channel of PIN2:GFP distribution along the plasma membrane and vacuole morphology in **a**, WT and **b**, *pi4kβ1β2* background. Scale bar: 10 mm.

5.1.6 Actin stability and remodeling are affected in the *pi4kβ1β2* mutant

Five-day-old *pi4kβ1β2* seedlings expressing *pUBC*::Lifeact-GFP were sprayed with 10 µM latB, a drug that inhibits actin polymerization. Treated seedlings were then observed under a confocal microscope (**Fig. 51a**). Without a latB treatment, the fluorescence signal occupancy was lower in *pi4kβ1β2* compared to WT seedlings. After a 90 min exposure to latB, the fluorescence signal occupancy in *pi4kβ1β2* decreased 40%, while no change was detected in WT plants (**Fig. 51b**). After a 150 min of exposure to latB, the signal occupancy in WT showed a 35% decrease compared to the control, while the occupancy decreased to 54% for the *pi4kβ1β2* mutant compared to control conditions. Interestingly, while WT roots showed a gradual decrease in actin filament bundling (**Fig. 51c**) in due course of latB treatment, no significant changes were observed in the *pi4kβ1β2* double mutant.

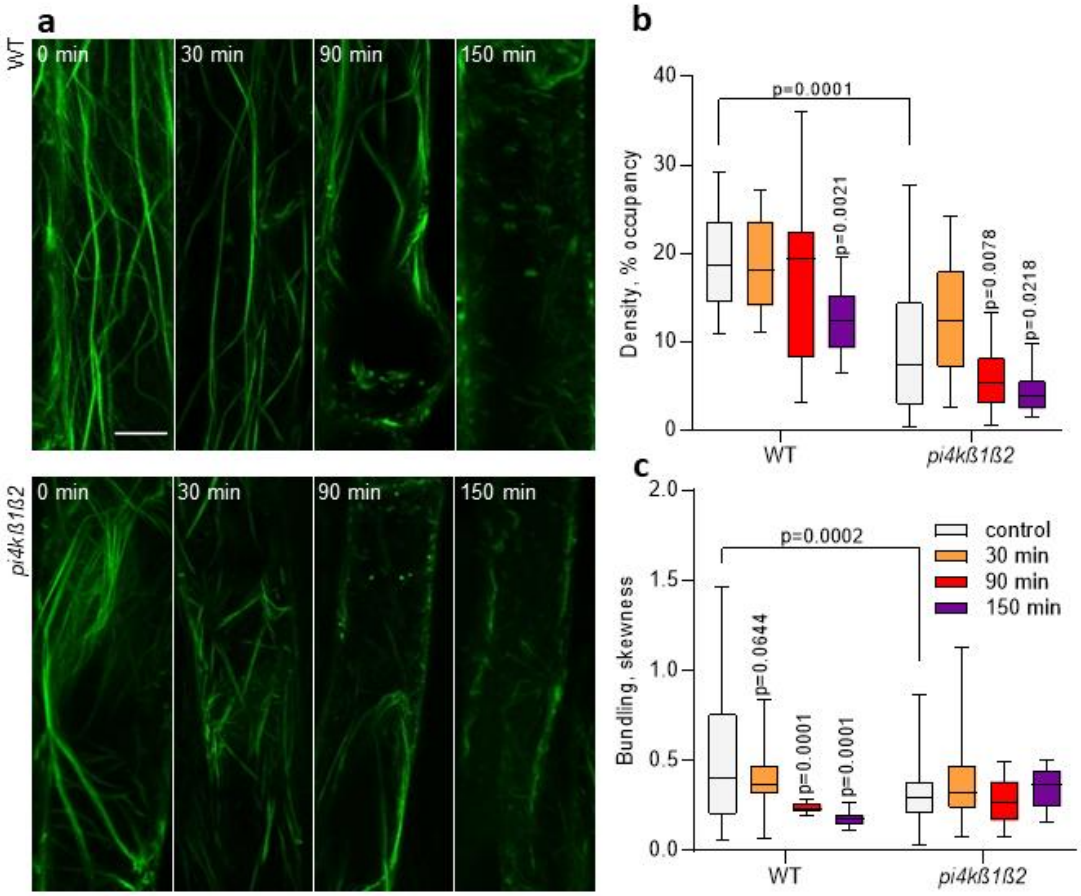

Fig. 51: Actin reorganization in the *pi4kβ1β2* mutant in response to latrunculin B. Five-day-old seedlings expressing *pUBC*::Lifeact-GFP were sprayed with 10 µM latB. **a)** representative maximum intensity projections of root epidermis of WT and *pi4kβ1β2* plants; confocal microscopy, scale bar: 10 µm.; **b)** quantitative analysis of the density (expressed as percentage of occupancy) of actin filament arrays in epidermal cells; **c)** quantitative analysis of the extent of filament bundling (expressed as skewness) in epidermal cells. Central line of the boxplots represents the median, plus represents the mean; circles represent individual values; *p*-value is indicated for significantly different time points within each genotype and for the comparison of genotypes immediately after treatment; one-way ANOVA with Tukey HSD *post-hoc* test; n=10.

5.1.7 Conclusion and discussion

In the first part, I showed that PI4Kß1ß2 deficiency led to up to a 4-fold decrease of primary root length compared to WT seedlings. A dwarf phenotype, both in the roots and aerial parts, has already been reported for the *pi4kβ1β2* mutant. Notably, the small rosette size of 4-week-old *pi4kβ1β2* mutant plants has been linked to an increased constitutive SA level (Šašek et al., 2014). Indeed, a *pi4kβ1β2/sid2* triple mutant did not accumulate SA and it did not display the stunted rosette phenotype. However, *pi4kβ1β2/sid2* seedlings still exhibited shorter roots than WT plants, thus showing that this root phenotype was a SA-independent process (Pluhařová et al., 2019; Šašek et al., 2014). Furthermore, SA accumulation did not occur in

young *pi4kβ1β2* seedlings (Pluhařová et al., 2019; Šašek et al., 2014), thereby confirming that the root length phenotype was not due to high SA levels. Similar SA levels in *pi4kβ1β2* and WT roots were found in this work (**Fig. 52**), thus confirming that the observed root phenotype was not related to altered SA levels and therefore it was an SA-independent process.

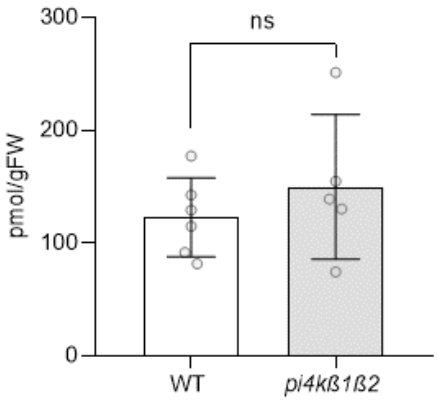

Fig. 52: Salicylic acid content of WT and *pi4kβ1β2* roots. Whole root systems (50-100 mg FW per sample) were harvested from 7-day-old vertical grown seedlings, n=6; Student t-test.

So what causes the short root phenotype of *pi4kβ1β2* seedlings? To answer this question, a detailed analysis of root morphology was undertaken (**Fig. 34**). The shorter primary roots of the double mutant appeared to be due to a reduced meristematic zone due to a lower number of cells. The CycB1::GUS associated signal occupied a significantly smaller (about 10%) area of the meristematic zone in *pi4kβ1β2* seedling roots when compared to the WT. This might explain in part why there were fewer cells in the meristematic zone of the mutant. An absent or a very short transition zone might also result from elevated auxin levels or an enhanced response to auxin. Indeed, the transition zone in a root begins where auxin levels attain a minimum (Brunoud et al., 2012). The shorter primary root length in the *pi4kβ1β2* double mutant was also associated with smaller cortical cells measured in the differentiation zone.

Due to the observed root phenotypes, an obvious next step was to assess the sensitivity of the double mutant to different hormones known to alter root growth. Root sensitivity to BAP or SA did not differ between *pi4kβ1β2* and WT seedlings. On the contrary, a loss of sensitivity in the double mutant to exogenous IAA was observed with respect to inhibition of primary root length, inhibition of cortical cell elongation, and elongation of the meristematic zone

(**Fig. 37, 39a, b**). This was in agreement with the experiments of Löfke et al., 2015 (Löfke et al., 2015), showing that altered vesicular trafficking due to inhibited PI4Kβ1β2 activity resulted in lower sensitivity to auxin NAA, altered vacuolar morphology and cell elongation (Preuss et al., 2004). Interestingly, *pi4kβ1β2* double mutant was less efficient in response to gravistimulation, another auxin-related process. Notably, not only the root elongation, but also the root tip orientation towards gravity vector were impaired in the mutant, suggesting gravity sensing defects.

The *pi4kβ1β2* mutant also showed an altered subcellular trafficking behavior of PIN2, including trapping of the PIN2-GFP fusion protein in rapidly moving vesicles and a reduced transport towards the lytic vacuole upon a dark shift of *pi4kβ1β2* seedlings. Differences in *pi4kβ1β2* vacuolar morphology were also observed, with bigger and less fragmented vacuoles compared to the WT. This phenotype corresponds to that observed when WT *A. thaliana* were treated with WM, an inhibitor of PI4K activity (Löfke et al., 2015). In *pi4kβ1β2* roots, PIN2 localization by immunostaining and staining with FM64 evidenced “black holes” or stubs corresponding to tunnels between adjacent cells also referred to as “cell wall stubs”. This can be linked with unfinished cytokinesis (Kang et al., 2003, p. 0; Lin et al., 2019).

Based on our observations, a working model is proposed that assembles multiple causes leading to the short root phenotype of the *pi4kβ1β2* mutant that arises from several root developmental defects, including reduced cell number and length (**Fig. 53**). Many correlate with altered dynamics of intracellular delivery processes. Plasma membrane establishment remains incomplete, cell architecture is misshaped, and PIN2 turnover is altered in the root elongation zone. This can be associated with a lower stability of the actin filaments network. Based on DII-VENUS degradation and gene expression, there appears to be a lack of response to auxin, endogenous or exogenous, in the *pi4kβ1β2* mutant. A link between altered trafficking/cytoskeleton integrity and this lack of gene expression response will require further investigations. These data on PI4Kβ mutants and the sensitivity to auxin were published in an article (Starodubtseva et al., 2022).

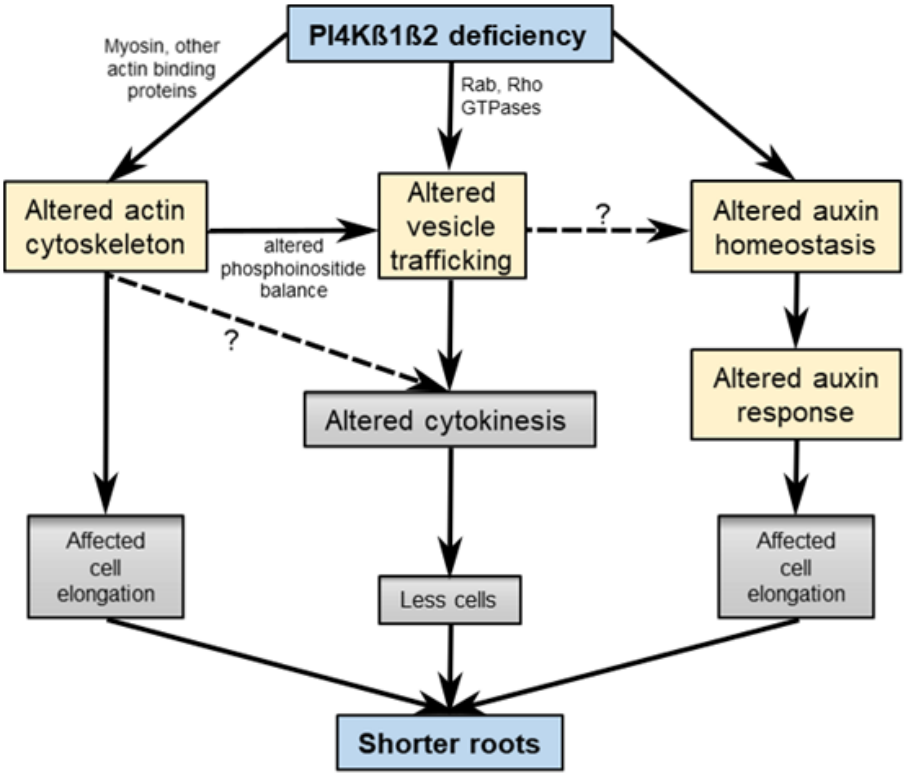

Fig. 53: Working model for the impact of *pi4kβ1β2* mutations on root length. The *pi4kβ1β2* mutations lead to an altered actin cytoskeleton, an altered vesicle trafficking and an altered sensitivity to auxin including ate the gene expression level. Altered trafficking can be linked to PI4K interacting with small G proteins like Rab or Rho proteins; it could also be a consequence of the weakened cytoskeleton. It is hypothesized that both altered cytoskeleton and trafficking prevent a correct cytokinesis. Finally, we propose that the short root phenotype results from multiple causes: altered actin cytoskeleton, altered cytokinesis, altered trafficking, and altered auxin responses.

In 2020, our team firstly identified that *pi4kβ1β2* has altered SA-independent non-host resistance to the non-host pathogen *Blumeria graminis* f. sp. *hordei* (Kalachova et al., 2020). In this work, the *pi4kβ1β2* double mutant showed an enhanced successful penetration of *Bgh* 24 hpi, as seen by the enhanced number of haustoria and dead cells. A similar defect in penetration resistance was seen in *pi4kβ1β2/sid2*, indicating the SA-independent character of this phenomenon. Higher penetration correlated with greater callose accumulation in the plant tissue. These results seemed to me very promising and interesting. Therefore, I decided to continue research in this direction. The second part is mainly aimed at studying the altered resistance of *pi4kβ1β2* double mutant to *Blumeria graminis* f. sp. *hordei.*

5.2 PART II. Non-host resistance in *pi4kβ1β2* mutant

In 2020, the teams with whom I performed my thesis research found that *A.thaliana pi4kβ1β2* mutants, deficient in phosphatidylinositol-4-kinases β1 and β2, were susceptible to the non-adapted fungal pathogen *Blumeria graminis* pv. *hordei* (*Bgh*) (Kalachova et al., 2020). However, the mechanisms underlying such susceptibility have not been described. The aim of this part of my thesis is to investigate the involvement of PI4Ks in non-host resistance, especially in papilla formation. The papillae is a unique formation at the penetration site of the fungus that consists of polysaccharides (i.e. callose) and vesicular bodies filled with antimicrobial compounds. One of the key components of the papilla is the protein SYP121, which is recruited to the forming papilla and has lipid-binding properties.

5.2.1 Interaction with non-adapted pathogen results in changes in phospholipid composition of plasma membrane

To study phosphoinositide accumulation during the *A. thaliana* - *Bgh* interaction, I used plants that possessed different biosensor constructs. I used a 2xFAPP1-mCherry biosensor for evaluating accumulation of PI4P (**Fig. 54a**), a mCitrine-1xPASS biosensor for PA (**Fig. 54b**) and a 2xmCHERRY-2xPH biosensor for PI(4,5)P_2 (**Fig. 54c**) in 4-week-old *A. thaliana* WT leaves in response to the fungus. The brightness of the signal is directly related to the accumulation level (Gomez et al., 2022; Lin et al., 2019). In **Figure 54**, the left column corresponds to biosensor fluorescence, the central column corresponds to the biosensor fluorescence merged with the brightfield channel, and the right column is a focus of the middle image centered on the forming papillae (**Fig. 54**). For a better understanding of the images, the fungal spores and appressoria were delimited with white dashed lines. The accumulation of the different phospholipids is seen by the shining of their respective biosensors. We can observe that the accumulation of phospholipids (PI4P, PA, PI(4,5)P_2) was detected in the papillae structure 24 h after inoculation. PI4P is a direct product of the action of PI4Ks. Since the PI4K is the main subject of my work, the next step was to test the *pi4kβ1β2* mutant for resistance to the *Bgh* pathogen.

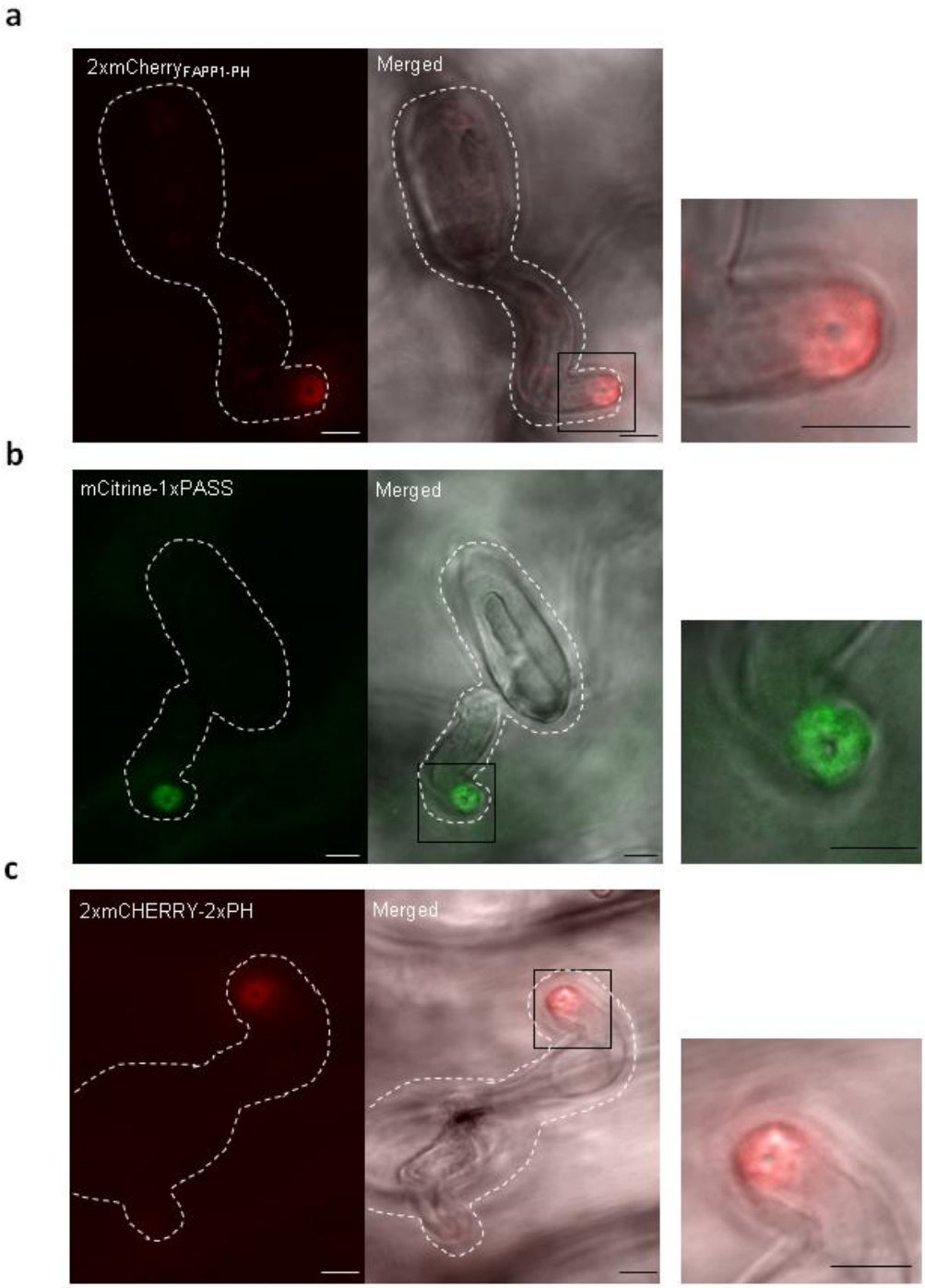

Fig. 54: Phospholipid sensors in WT. Four-week-plants were inoculated with *Bgh* and the microscopy was done after 24 h. **a)** representative images of PI4P signal in papillae, sensor 2xFAPP1-mCherry; **b)** representative images of PA, sensor mCitrine-1xPASS; **c)** representative images of PI(4,5)P_2, sensor 2xmCHERRY-2xPH(PLC). Scale bars: 5 µm

5.2.2 The *pi4kβ1β2* mutant displays less resistance to *Blumeria* infection

To test the resistance ability of the *pi4kβ1β2* mutant plants, I assessed penetration success in response to the non-host pathogen *Bgh*.

Four-week-old plants were inoculated with *Bgh* spores for 24 h, were stained with trypan blue and the penetration level was assessed visually under Apotome microscope. Penetration output could be divided into either penetration failure or penetration success. Penetration failure correlates with the formation of an efficient resistance plant structure, the papillae. As for penetration success, we can distinguish several subcategories depending on the developmental stage of *Bgh*, such as the formation of a haustorium and the response of the plant, such as a hypersensitive response (HR), deviated papillae and granulated cytoplasm (**Fig. 55a**).

In the WT plants, penetration failure represented approximately 80% of the output, whereas for *pi4kβ1β2* mutants it was for 35% (**Fig. 55b, c**). Notably, the *pi4kβ1β2* double mutant showed increased rate of haustoria-formation stage and plant dead-cell stage. This is consistent with what has already been published by the team I worked in (Leontovyčová et al., 2019).

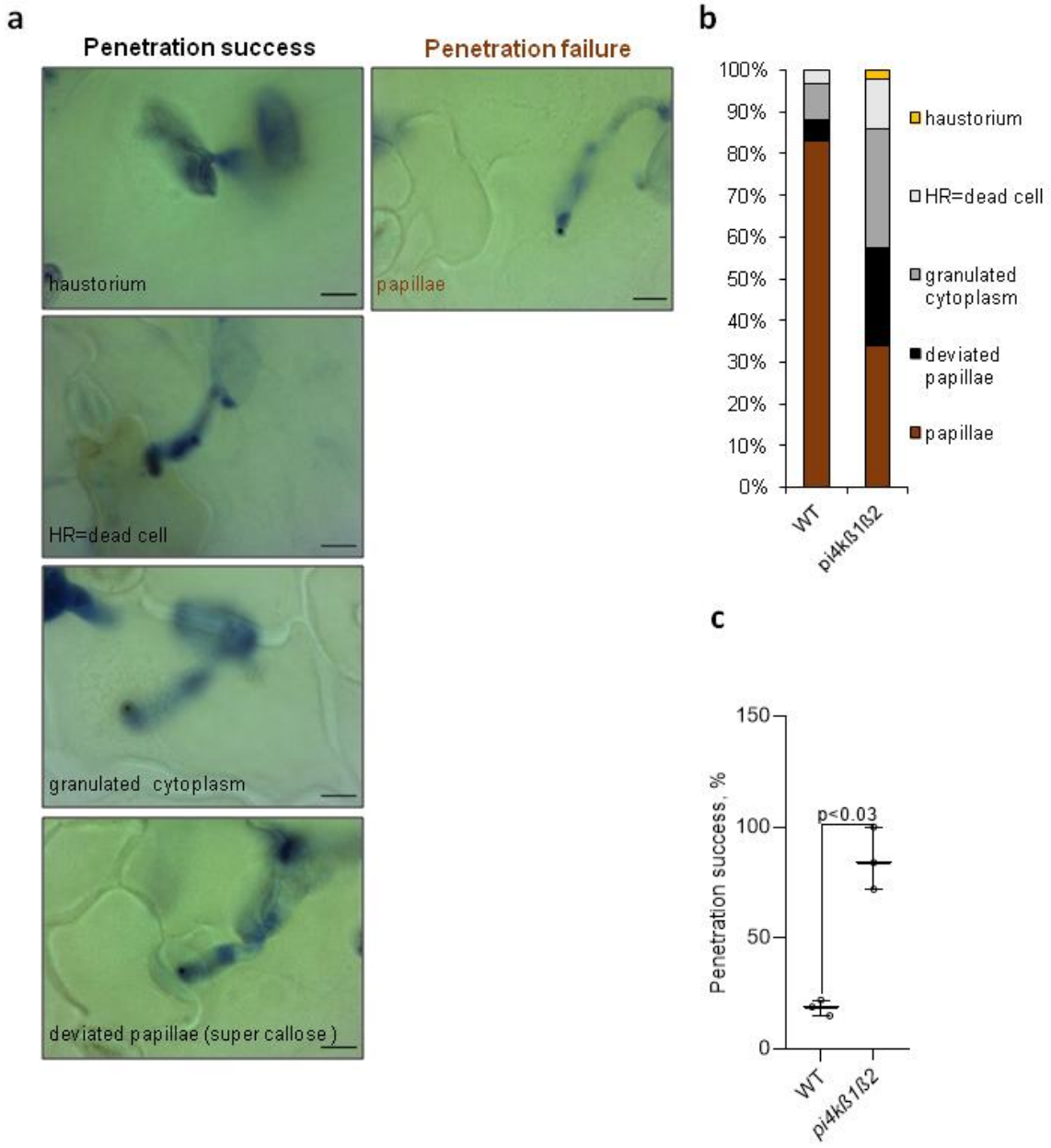

Fig. 55: a) representative images of five types of interactions counted in the penetration success analysis after trypan blue staining; Scale bars: 5 µm. **b)** data showing penetration success category of *Bgh* 24 hpi in each genotype: the mean number of cells with either haustoria or dead cells, respectively; (3 repetitions together, n=300 spores for each genotype); **c)** penetration success in WT and *pi4kβ1β2* mutant; Student t-test, n=3.

The *pi4kβ1β2* mutants showed altered resistance to *Bgh* fungi, with higher levels of penetration and dead cells. My hypothesis was that the susceptibility effect was related to the impaired formation of plant defense structure - papillae. Deficient mutants showed a high number of deviated papillae formation during pathogen attack compared to WT (25% in *pi4kβ1β2* versus 5% in WT) (**Fig. 55b**).

5.2.3 The *pi4kβ1β2* mutant accumulates less PI4P during infection

During papillae formation, plants accumulate plenty of molecules near the pathogen entry site, including PI4P. The *pi4kβ1β2* double mutant plants lack PI4Kβ enzymes that produce PI4P. To visualize PI4P level and localization in the mutant plants, I used the 2xFAPP1-mCherry biosensor in *pi4kβ1β2* plants, obtained by crossing. After 24 h of inoculation with *Bgh* spores, PI4P accumulation in the papillae was observed by confocal microscopy (**Fig. 56**). Fluorescence intensity was measured in WT and *pi4kβ1β2* mutant plants. The left column corresponds to the biosensor fluorescence, the central column is the biosensor fluorescence merged with the brightfield channel, and the right column is a crop of the middle image centered on the forming papilla (**Fig. 57**). For a better understanding of the images, the fungal spores and appressoria were delineated with white dashed lines. Like in WT plants, PI4P was localized in plant papillae structure in the *pi4kβ1β2* mutant plants (**Fig. 56a**). The intensity of the shining was proportional to the level of accumulation (Simon et al., 2014). PI4P content was much lower in *pi4kβ1β2* plants compared to that in WT (**Fig. 56b**).

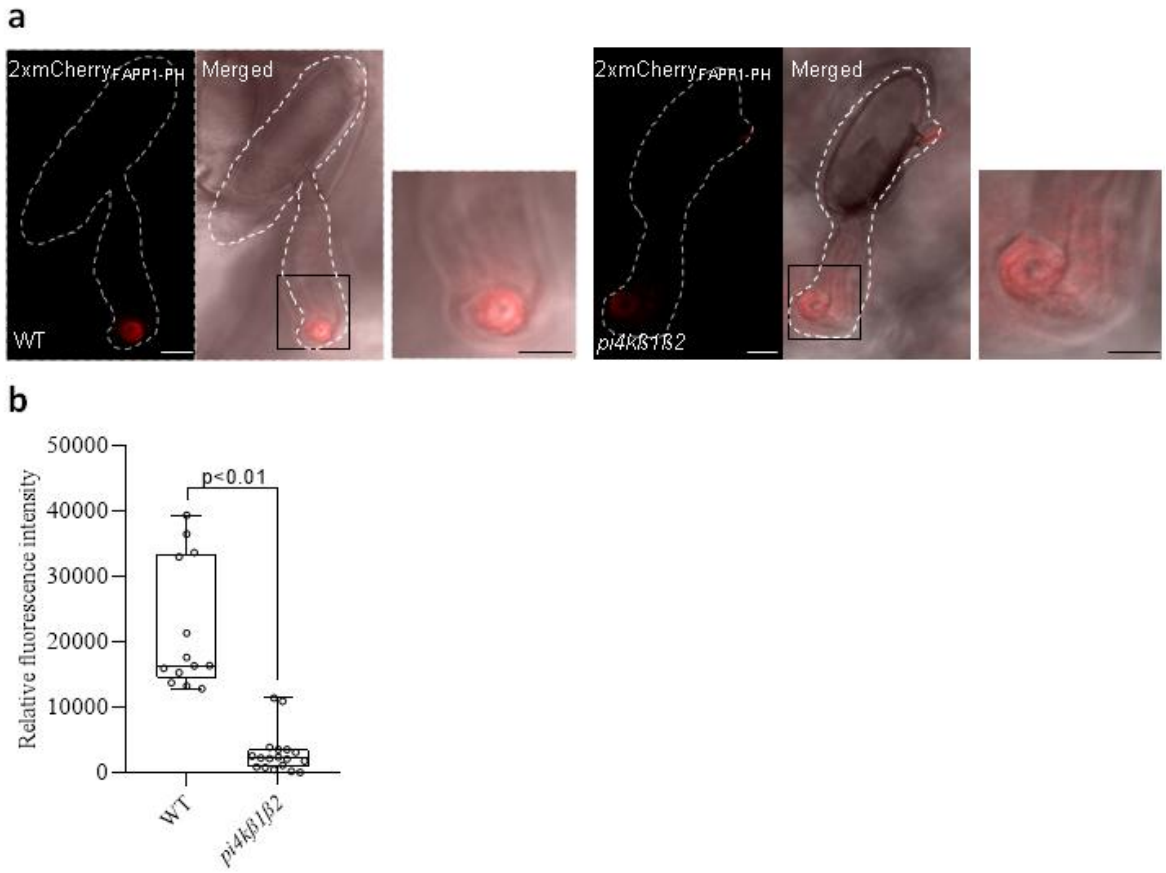

Fig. 56: PI4P accumulation in papillae, sensor 2xFAPP1-mCherry. Four-week-old plants were inoculated with *Bgh* for 24 h and observed by confocal microscopy. **a)** representative images of PI4P

signal in papillae in WT and *pi4kβ1β2*, sensor 2xFAPP1-mCherry; **b)** PI4P fluorescence quantification; Student t-test; n=13; Scale bars: 5 µm.

Consequently, the susceptibility of the *pi4kβ1β2* mutant plants to *Bgh* could be related to the altered papillae formation, which correlates with less PI4P. The lack of PI4K led to a lack of PI4P accumulation, which is one of the essential components of successful papillae. Papillae accumulate not only phospholipids but also other molecules. One of the most important proteins for successful papillae is a member of the SNARE protein - SYP121 (PEN1).

5.2.4 SYP121 (PEN1) protein localization in *pi4kβ1β2* mutant

The protein syntaxin (SYP121, PEN1) is a member of the SNARE family involved in the formation of papillae. PEN1/SYP121 is not only found on the plasma membrane near the papillae, but also inside the papillae. PEN1/SYP121 constantly circulates between the plasma membrane and the endosomes (Nielsen and Thordal-Christensen, 2012). Investigating PEN1/SYP121 localization seemed very promising to me, because the normal transport of the protein requires a well-established trafficking system, which is lacking in the *pi4kβ1β2* mutant plants. Therefore, I decided to check the localization and accumulation of PEN1/SYP121 in my mutant plants. For this purpose, I crossed 35S::GFP-SYP121 construct into *pi4kβ1β2*. Then plants were inoculated with *Bgh* for 6, 24 and 48 h and observed under a confocal microscope (**Fig. 57a, b**). After 6 h, no spore germination was observed. After 24 and 48 h, the spores germinated and started to form appressorium formation. As for the plant structures, papillae was detectable. GFP-SYP121 signals in the *pi4kβ1β2* mutant and WT were well detected in the papillae, indicating that the localization of the PEN1/SYP121 protein was not altered in the mutants (**Fig. 57b**).

To compare the level of signal intensity between WT and *pi4kβ1β2*, I checked GFP expression by qPCR. Unfortunately, silencing was observed in the *pi4kβ1β2* mutants, which made it impossible to compare the intensity signals between the two genotypes (**Fig. 57c**). The presence of several T-DNA inserts in the *pi4kβ1β2* mutant might have led to the silencing effect and the failure of 35S::GFP-SYP121 expression (Daxinger et al., 2008).

Since I could not compare the intensity of the GFP signal, I decided to check the expression of PEN1/SYP121 by qPCR. The expression of PEN1/SYP121 was increased after *Bgh* inoculation in WT plants, whereas this was not the case in *pi4kβ1β2* mutants (**Fig. 57d**). A deficiency of PEN1/SYP121 protein could lead to *pi4kβ1β2* susceptibility independently of

the correct localization of the protein in the papillae. Most likely, the PEN1 protein was not expressed after inoculation with the pathogen as it should be in WT.

To clarify the cause of the susceptibility of the mutants, other constructs should be used and other molecules measured. This will be discussed in the Perspectives part.

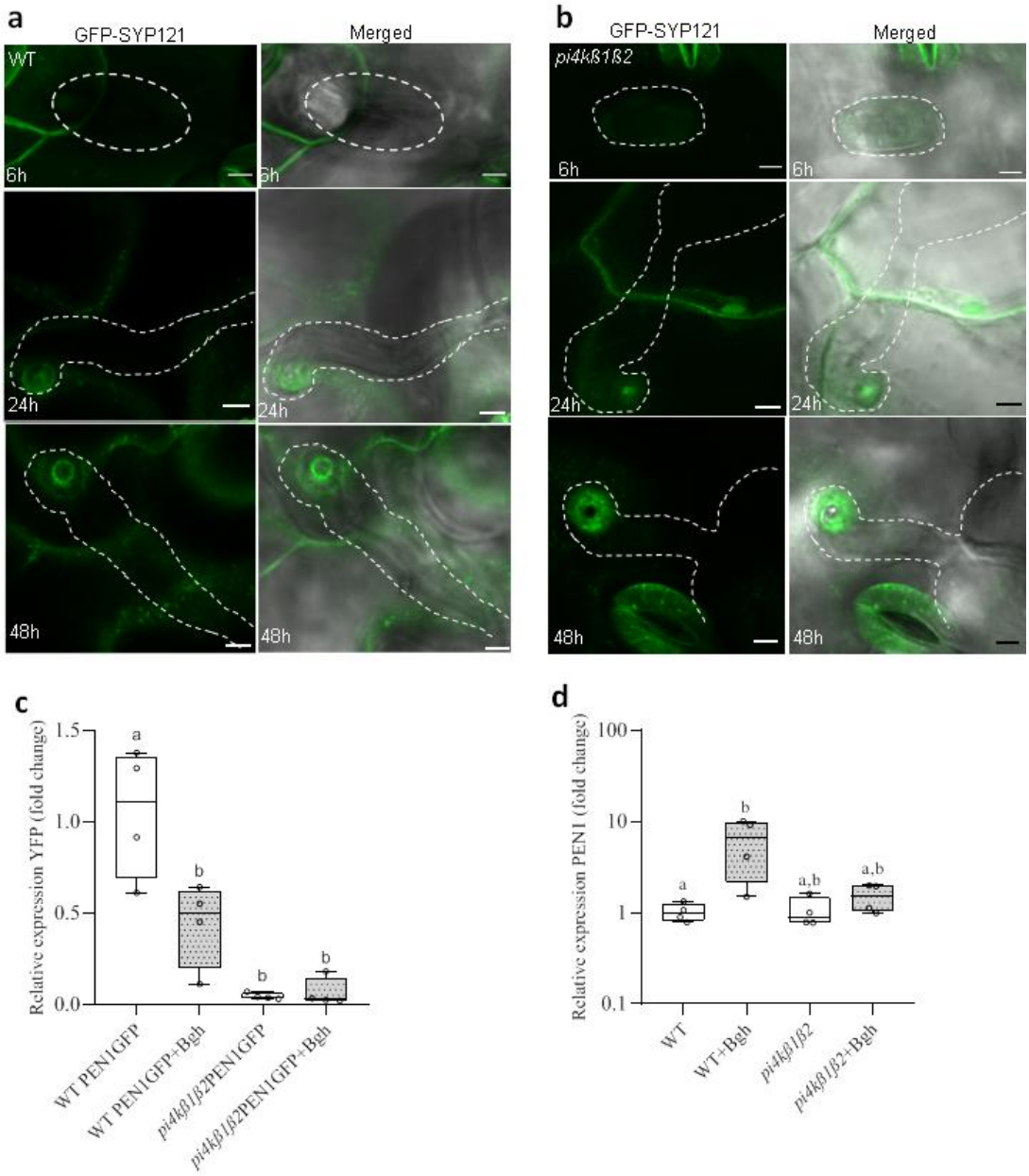

Fig. 57: GFP-SYP121 accumulation in papillae, under 35S::GFP-SYP121 promoter. Four-week-old plants were inoculated with *Bgh* for 6, 24 and 48 h and noted by confocal microscopy. **a)** GFP-SYP121 in papilla for WT, Scale bars: 5 µm; **b)** GFP-SYP121 in papillae for *pi4kβ1β2* mutant (increased intensity), Scale bars: 5 µm; **c)** transcript levels of *YFP* in WT and *pi4kβ1β2* mutant with or without *Bgh*; **d)** transcript levels of *PEN1* in WT and *pi4kβ1β2* mutant with or without *Bgh*; one-way ANOVA with Tukey HSD *post-hoc* test.

5.2.5 Conclusion

Despite the fact that much work has already been done to investigate the role of PI4Ks, many aspects are still unclear and need to be explored. In 2020, the teams where I did my thesis found that *A. thaliana pi4kβ1β2* mutants lacking the phosphatidylinositol-4-kinases β1 and β2 were susceptible to *Bgh*. However, the mechanisms underlying this had not been described (Kalachova et al., 2020). The aim of the second part of my thesis was to investigate and better describe the involvement of PI4Ks in non-host resistance, especially in papillae formation.

I demonstrated the accumulation of phospholipids in papillae during *Bgh* attack. Using biosensors, I saw intensive fluorescent signals of PA, PI(4,5)P and PI4P in WT plants. As for the *pi4kβ1β2* mutant, the localization of PI4P in the papillae was the same in the *pi4kβ1β2* mutants compared to the WT plants after *Bgh* inoculation. The same conclusion could not be said about the intensity of the PI4P signal. The shining level was much lower in the *pi4kβ1β2* mutants compared to the WT plants.

Not only phospholipids, but also proteins accumulate in the papillae. I studied the accumulation of the protein PEN1/SYP121 during *Bgh* treatment. PEN1/SYP121 is one of the most important proteins for the effective formation of papillae. The localization of PEN1/SYP121 in the papillae was the same in the *pi4kβ1β2* mutants compared to the WT plants. The intensity signal could not be evaluated due to the presence of several T-DNA inserts in the *pi4kβ1β2* mutant, which led to the silencing effect and failure of the 35S::GFP-SYP121 construct. Nevertheless, I was able to measure the level of *PEN1* transcript expression and surprisingly it was repressed in the *pi4kβ1β2* mutant. I could assume that a PI4K mutation caused a reduced PEN1 protein content and led to a deformed papillae and susceptibility to *Bgh* (**Fig. 58**).

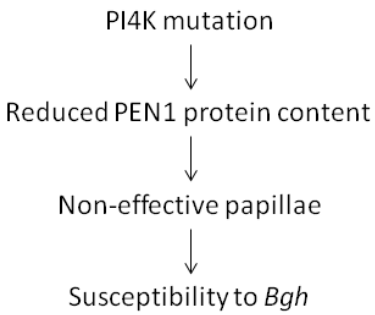

Fig. 58: Hypothesis concerning *pi4kβ1β2* susceptibility. PI4K mutation leads to reduced levels of PEN1 protein that results in the forming non-effective papillae and causes susceptibility to *Bgh.*

A previously published paper has shown that *pen1-1* mutants have a 40% higher penetration rate compared to WT (Takemoto et al., 2006). Therefore, my results showed an accumulation of phospholipids in the papillae and a lower PI4P intensity signal in the *pi4kβ1β2* mutants. This could be one of the reasons for the formation of non-effective papillae and increased sensitivity of the *pi4kβ1β2* mutants to *Bgh*.

5.2.6 Discussion and Perspectives

My work on understanding the role of PI4Kβ1β2 in *A. thaliana* resistance to *Bgh* is only beginning. There is still a lot of work to be done. In fact, my results are very preliminary. Consequently, discussing my data corresponds also to presenting the perspectives to the work.

The establishment of non-host resistance is based on several mechanisms, including membrane trafficking, which is necessary to rapidly transport defense-associated molecules to specific subcellular compartments (Wang et al., 2016). Such molecules are, for example, phenols, callose, cell wall proteins and cell wall polymers.

To investigate the involvement of PI4Ks in non-host resistance, especially in papillae formation, it is important to understand the lipid composition of the papillae in the *pi4kβ1β2* mutant. Since the PI4K product PI4P is the precursor for $PI(4,5)P_2$, it would be interesting to determine the $PI(4,5)P_2$ level in the *pi4kβ1β2* mutant in our biological system. Indeed I have shown that $PI(4,5)P_2$ was accumulated in WT papillae. I would expect a decrease of $PI(4,5)P_2$ accumulation in *pi4kβ1β2* papillae. For this purpose, I will need to cross 2x-mCHERRY-2xPH with *pi4kβ1β2* in the future.

Note that not only the papillae but also the structure of haustoria can be studied (Koh et al., 2005; Qin et al., 2020). Haustoria, a structure originating from the fungus, form when papillae are not formed effectively or when papillae are absent. In the *pi4kβ1β2* mutant, haustoria also form due to the lack of papillae formation. It would therefore be interesting to monitor PI4P and $PI(4,5)P_2$ in the haustoria formed in *pi4kβ1β2* mutants infected by *Bgh*. Qin et al., 2020 checked penetration of *A. thaliana* with the powdery mildew fungus *Erysiphe cichoracearum*. In contrast to the non-adapted pathogen I used in my work (*Bgh*), *Erysiphe cichoracearum* is an adapted powdery mildew fungus able to complete its life cycle on *A. thaliana* host plants. *A. thaliana* supports the normal growth of *E. cichoracearum* including the development of the haustorium. They showed that $PI(4,5)P_2$ pools were dynamically upregulated at the pathogen infection sites and further integrated into the extrahaustorial

membrane. On the contrary, PI4P showed consistent levels at the plasma membrane and was absent in the extrahaustorial membrane when inoculated with the *Erysiphe cichoracearum* **(Fig. 59)**.

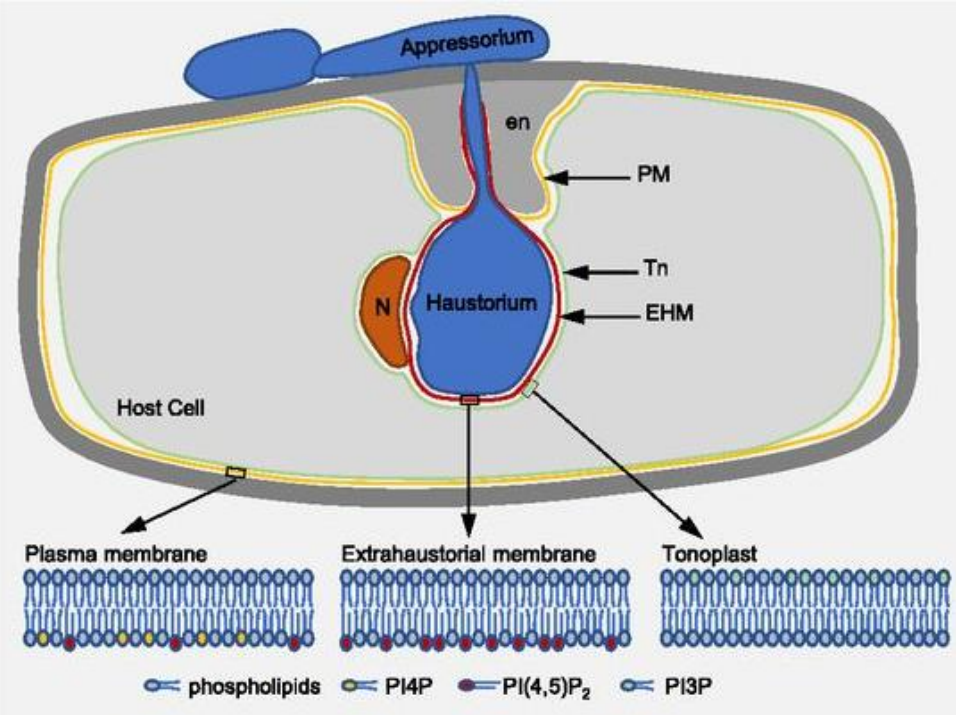

Fig. 59: Diagram illustrating the distribution of host phosphoinositide species in different membrane compartments associated with an *E. cichoracearum* haustorium in infected epidermal cells; ha, haustorium; Tn, tonoplast; PM, plasma membrane; en, encasement (Qin et al., 2020).

Checking the PI4P and PI(4,5)P_2 in papillae would be great in WT and *pi4kβ1β2* plants; but it can also be of interest to check these phosphoinositides in the haustorium of *pi4kβ1β2* plants submitted to *Bgh*, to check if a similar profile than the one found for compatible interaction (*E. cichoracearum*) is found.

PI4P5-kinases (PIP5K) convert PI4P to PI(4,5)P_2 in eukaryotes (Choi et al., 2015). It would be interesting to test *pip5k1/pip5k2* mutants resistance to the *Bgh* inoculation. It should allow us to see whether the *pi4kβ1β2* phenotypes (less resistance) are due to PIP or to PIP2. Ideally, monitoring lipids with the sensor in the *pip5k1/pip5k2* mutants could be considered. The *pip5k1/pip5k2* mutant was used in the study of *A. thaliana* - *E. cichoracearum* interaction (Qin et al., 2020).

PI4P can have an action of its own. As we have just mentioned, it can also act as a precursor PI(4,5)P_2. PI4P and PI(4,5)P_2 can be substrates to PI-PLC, leading to DAG that can be phosphorylated into PA. Besides, PI(4,5)P_2 can be a cofactors to some PLDs the product of

which is also PA. For all these reasons it would be interesting to determine the level of PA. In WT, using the mCitrine-1xPASS, I have seen PA accumulation in papillae during the *Bgh* infection. It is likely that the accumulation is reduced in *pi4kβ1β2* mutant. To check that, I will need to cross *A. thaliana* containing the mCitrine-1xPASS construct with *pi4kβ1β2*.

Concerning the localization of PI4P and PI(4,5)P_2 in papillae, the question is whether these lipids are produced there, both of them, or if they are recruited to this structure. Interestingly, cellular trafficking pathways were shown to be important for the redistribution and recruitment of PI(4,5)P_2 to the extrahaustorial membrane in the *A. thaliana* - *E. cichoracearum* system. This was shown by the use of latrunculin A, oryzalin, BFA, or wortmannin (Qin et al., 2020). Oryzalin (which depolymerizes microtubules) and BFA (inhibits vesicle-mediated trafficking) showed no effect on PI(4,5)P_2 accumulation at the extrahaustorial membrane. Latrunculin A, which sequesters G-actin and prevents F-actin assembly, led to a significant depletion of PI(4,5)P_2 from the extrahaustorial membrane. Treatment with a high concentration of wortmannin (30 µM) caused a significant depletion of PI(4,5)P_2 at the extrahaustorial membrane. It is known that wortmannin at high concentration inhibits the function of type III PI 4-kinases and thereby reduces the PI4P content. The results suggest that PI(4,5)P_2 accumulation at the extrahaustorial membrane is contingent on actin cytoskeleton formation and is less sensitive to GNOM-mediated vesicular transport. The PI(4,5)P_2 is probably derived from *de novo* synthesis from the precursor PI4P via the type III PI 4-kinases. What about in papillae, in our system? I think the wortmannin treatment needs to be done with *Bgh* inoculation for WT *A. thaliana*. This would be indeed interesting to assess if the *pi4kβ1β2* double mutation does mimic the effects of wortmannin. I am reminded that another PI4K, α1, exists and is also sensitive to wortmannin. The polarization of actin filament bundles towards fungal *Bgh* invasion has been published previously (Yang et al., 2014). Fine-tuned cytoskeleton systems provide correct movement of cytoplasm, proteins, secretory vesicles and organelles toward the penetration sites. According to the first part of my results - *pi4kβ1β2* mutants have altered actin cytoskeleton. The *pUBC*::Lifeact-GFP construct could be used to monitor the actin cytoskeleton in the WT and the *pi4kβ1β2* mutant near penetration sites, during *Bgh* interaction. Altered actin cytoskeleton of the *pi4kβ1β2* mutant could also be the reason for forming non-effective papillae (**Fig. 60**).

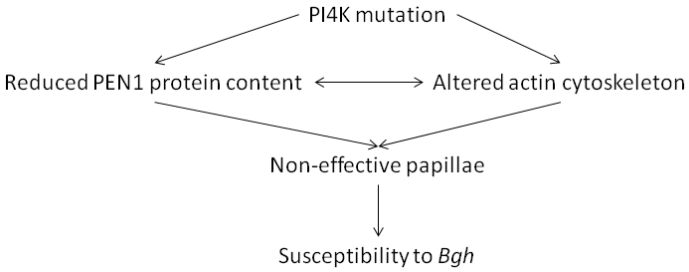

Fig. 60: Hypothesis concerning *pi4kβ1β2* susceptibility. PI4K mutation leads to reduced levels of PEN1 protein and altered actin cytoskeleton. Both would result in the forming non-effective papillae and cause susceptibility to *Bgh.*

Concerning vesicular trafficking, Qin et al., (2020) used FM4-64, a lipophilic styryl dye commonly used as a fluorescent probe to detect plasma membrane internalization during endocytosis and membrane trafficking (Jelínková et al., 2010). In epidermal cells harboring haustoria, enhanced $PI(4,5)P_2$ signals formed amorphous assemblies that colocalized with FM4-64-labeled aggregates. These results suggest that induced $PI(4,5)P_2$ pools in haustorium-forming cells are likely associated with enhanced trafficking from plasma membrane (Qin et al., 2020). I think it would be useful to perform confocal imaging colocalization of $PI(4,5)P_2$ signals with the FM4-64-labeling in the *pi4kβ1β2* mutant plant with and without *Bgh* inoculation. Considering that the mutant has a trafficking disorder, $PI(4,5)P_2$ signals in *Bgh*-infected and noninfected cells will be coupled with less or no $PI(4,5)P_2$ signals, associated with reduced PM trafficking. Altered PM trafficking could be the reason for decreased content of crucial papillae components.

Finally, visualizing the PI4K (*β1, β2* and also *a1* forms) and PI4P5K1 and PI4P5K2 enzymes should be done during fungal inoculation. It might be interesting to see the exact localization of the enzyme at the time of papilla formation.

Besides, since I detected PA in papillae during *A. thaliana* - *Bgh* interaction, it would be necessary to investigate where it comes from. A pharmacological approach can help have ideas. Adding *n*-butanol during the interaction would reduce the production of PA by PLD (due to the transphosphatidylation that produces phosphatidyl-butanol detrimentally to PA). I would first check PA level with the mCitrine-1xPASS sensor in WT in presence of *n*-butanol. If PLD is responsible for PA accumulation during *Bgh* interaction, I expect to detect less PA in papillae. Similarly, I should check penetration success in the presence of *n*-butanol. If the PA is necessary for papillae formation, I would see it with microcopy.

If the *n*-butanol data are encouraging, then in a second time I would try to check penetration success during *Bgh* interaction in different PLD mutants. As mentioned in the introduction PLDs are encoded in a multigenic family comprising 12 members. Amongst the PLDs, some are PI(4,5)P_2-dependent, some are not. The PI(4,5)P_2 dependent ones are of particular interest, but I think it wiser to check all the mutants. To deal with possible redundancy, the use of multiple mutants might be necessary. The teams of my thesis, that are experts in lipid signaling, already possess different *pld* mutants, by T-DNA insertion. Yet, the use of the cas9/crispr system for genome editing might be suitable to mutate different genes of the same subtype (like PLDβs or PLDγs). Yet, this work has already been done, in 2013 Francesco Pinosa (Pinosa et al., 2013) already showed that 0.6% *n*-butanol led to higher *Bgh* penetration rates in *A. thaliana*. Using *pldδ* mutant they showed it was less resistant to penetration. They also checked other *pld* mutants, such as *pldβ1-2 pldβ2* and *pldζ1 pldζ2*. Of the assessed mutants only *pldδ* had an altered penetration rate. Using *pldδ* in presence or not of *n*-butanol, they could conclude that is the sole PLD isoform involved in penetration resistance. PLDδ was targeted to the membranes of papillae in the extracellular space during infection by *Bgh* (Xing et al., 2019). So it seems that PLDδ is the PLD involved in the resistance. PLDδ is active without PI(4,5)P_2 but can be activated by it (Wang and Wang, 2001). Yet, it would be interesting to see if PLDδ is dependent on PI4Ks. More particularly, is its localization affected in the *pi4kβ1β2* mutant? And how is the PA level affected in the *pldδ*. In all cases, to check the effect of *n*-butanol on PA as seen with the biosensor remains interesting.

Yet, PA can also be produced by DGKs. Here, again we can start by a pharmacological approach, with R59022 the inhibitor (Cacas et al., 2017; Kalachova et al., 2022). The inhibitor should be used in WT plants possessing the mCitrine-1xPASS construct in interaction with *Bgh*. The effects of R59022 on papillae formation (and penetration success) is also to be checked. Then, according to the obtained data, checking penetration success in different *dgk* mutants should be done. DGKs are encoded by 7 genes in *A. thaliana*. My French team has a collection of different single and multiple mutants that can be used to that effect.

Then, according to the results obtained with either *pld* or *dgk* mutants, the localization of the enzymes of interest (a specific PLD or a specific DGK) during the *A. thaliana* - *Bgh* interaction should be investigated, most likely by fusion with a fluorescent protein.

Moreover, it would be interesting to make a transcriptome analysis of *A. thaliana* inoculated with *Bgh*. Especially the level of PI4K, PI4P5K PLDs or DGKS encoding genes.

Finally, in addition to lipids, other important components of the effective papilla in the *pi4kβ1β2* mutant should be checked. The effective papillae consist of two layers; the first inner layer contains callose and arabinoxylan and the second outer layer contains cellulose and arabinoxylan (Chowdhury et al., 2014).

Therefore, I propose as perspective to this work:

1. Cross mCitrine-1xPASS and 2xmCHERRY-2xPH with *pi4kβ1β2* to assess the accumulation of PI(4,5)P_2 and the level of PA.
2. Examine the haustorium structure of *pi4kβ1β2* mutants: check PI4P, PI(4,5)P_2 and PA localization; check if a similar profile than the one found for compatible interaction (*E. cichoracearum*) is found.
3. Test *pip5k1/pip5k2* mutants resistance to the *Bgh* inoculation.
4. Monitoring lipids with the sensor in the *pip5k1/pip5k2* mutants could be considered.
5. Wortmannin treatment needs to be done with *Bgh* inoculation for WT *A. thaliana.*
6. The pUBC::Lifeact-GFP construct could be used to monitor the actin cytoskeleton in the WT and the *pi4kβ1β2* mutant near penetration sites.
7. Check vesicular trafficking in *pi4kβ1β2* mutants infected cells with *Bgh*, using FM4-64 with colocalization of PI(4,5)P_2.
8. Visualize the PI4K (β1, β2 and also a1 forms) and PI4P5K1, PI4P5K2 enzymes during *Bgh* inoculation.
9. Check PA level with the mCitrine-1xPASS sensor in WT in presence of *n*-butanol.
10. Check penetration success in the presence of *n*-butanol.
11. The R59022 inhibitor should be used in WT plants possessing the mCitrine-1xPASS construct in interaction with *Bgh*.
12. Transcriptome analysis of *A. thaliana* inoculated with *Bgh.*
13. Arabinoxylan could be measured by immunolocalization technique of (Hervé et al., 2011) using antibodies (LM11 antibody (specific for unsubstituted xylan and arabinoxylan)).
14. The cellulose could be labeled with a solution of Pontamine Fast Scarlet 4B (Chowdhury et al., 2014).
15. Camalexin content could be determined using a previously described fluorometric method (Glazebrook and Ausubel, 1994).
16. ROS could be measured by fluorescent dyes (such as H2DCFDA, DHE or Amplex red or spectrophotometric methods (Ortega-Villasante et al., 2016).
17. The callose deposition could be measured by aniline blue staining.

5.3 PART III. Understanding why *pi4kβ1β2* mutant accumulates SA: a mutant approach

The last part of my work was also related to immunity. PI4Kβ1β2 deficiency in the *pi4kβ1β2* mutants resulted in a high level of SA accumulation. The mechanism for this is still unknown. We hypothesized that the reason for permanently activated immunity might be due to a misprocessing of immunity-related receptors that would be constitutively activated.

Microbe-associated molecular patterns are perceived by cell surface-localized PRRs. All well-characterized PRRs are RLKs or RLPs (Monaghan and Zipfel, 2012). Both types of PRRs contain a ligand-binding ectodomain and a transmembrane domain, but only RLKs have an intracellular kinase domain (Macho and Zipfel, 2014). My aim was to check whether the mutation of some receptors could have an impact on the SA accumulation of *pi4kβ1β2* mutants. To identify the relationship between the *pi4kβ1β2* phenotype (constitutive immunity) and immunity-related receptors, we generated several multiple mutants. I decided to work with receptors from different groups. They were receptors from different groups - RLKs class (FLS2, PEPR1/2, BAK1 - leucine-rich repeat-receptor kinases; CERK - lysin motif receptor-like kinase); TIR-NBS-LRR type of R protein (ETI pathway) - SNC and transcription factor - WRKY70.

I therefore generated the following multiple mutants: *fls2/pi4kβ1β2, pepr1/pepr2, pepr1/pi4kβ1β2, pepr2/pi4kβ1β2, pepr1/pepr2/pi4kβ1β2, snc1-11/pi4kβ1β2, cerk1-2/pi4kβ1β2.*

The mutant approach methodology was used to see if receptors were involved in some of the phenotypes of the *pi4kβ1β2* mutant. Rosette size and callose measurements, evaluating resistance to *P. syringae*, *PR1* expression, were used as a proxy of SA accumulation.

In addition, I also wanted to see the localization of the receptors and test if they were mislocated or misprocessed. For the PEPR1/2 receptors, I took confocal images to check their localization.

5.3.1 Are immunity related receptors involved in *pi4kβ1β2* phenotypes?

5.3.1.1 Effect of a *fls2* mutation

The *A. thaliana* well-studied PRR is the FLS2 receptor, which specifically binds to the bacterial peptide PAMP flagellin. In terms of rosette size, the *fls2/pi4kβ1β2* rosettes were statistically larger than those of the *pi4kβ1β2* double mutants, which could indicate partial

reversion (**Fig. 61a**). Nevertheless, *PR1* expression and resistance to *P. syringae* were the same between *fls2/pi4kβ1β2* and *pi4kβ1β2* plants (**Fig. 61b, c**). As for callose content, the *fls2/pi4kβ1β2* triple mutant showed reversion, as the percentage area of callose depositions was not statistically different from that of the WT plants (**Fig. 61d**).

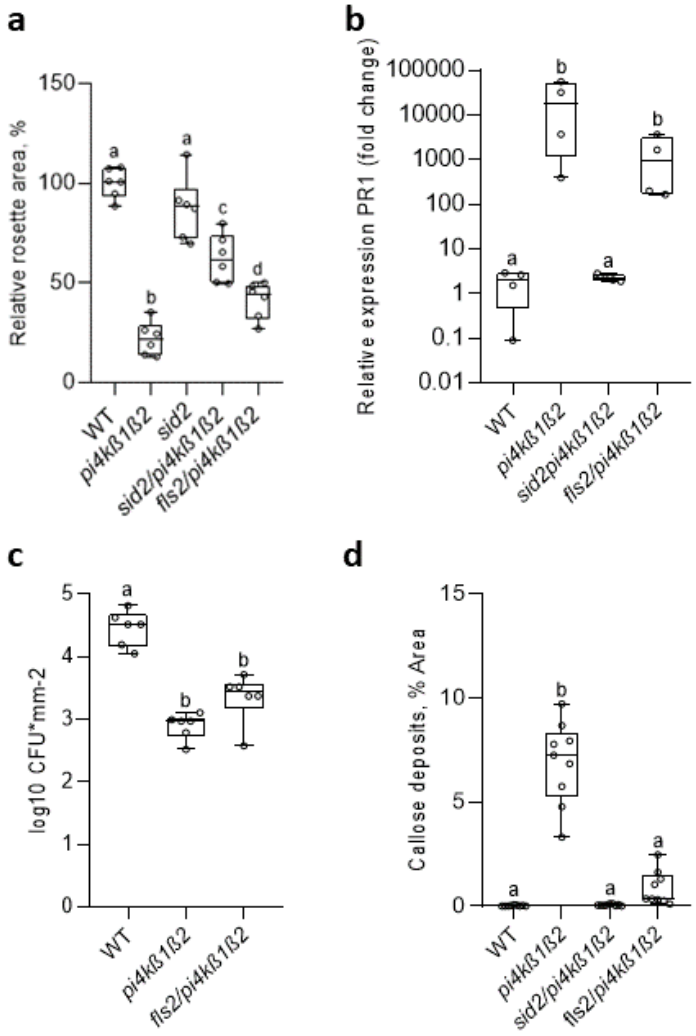

Fig. 61: Effect of a *fls2* mutation on SA-related phenotypes. **a)** relative rosette size, n=6; **b)** PR1 expression, n=4; **c)** *P. syringae* proliferation, n=6; **d)** callose deposition, n=9. Central line of the boxplot represents the median; circles represent individual values from three biological repeats. Different letters indicate variants significantly different in every genotype (one-way ANOVA, Tukey HSD, $P < 0.05$).

This reversion of callose accumulation was not consistent with the lack of reversion of *PR1* expression, resistance to *P. syringae* and the partial reversion of the rosette size. Repetition of the measurement of callose deposition is required, as well as measurement of rosette size. Besides, SA quantitation is necessary.

5.3.1.2 Localization of PEPR1 and PEPR2 receptors

The *A. thaliana* endogenous elicitor peptides (Peps) are released into the apoplast after cell damage and induce immunity by direct binding to the membrane-localized leucine-rich repeat receptor kinases, PEP RECEPTOR1 (PEPR1) and PEPR2 (Ortiz-Morea et al., 2016). By sensing Peps, PEPR1 and PEPR2 contribute to the defense response in *A. thaliana*. Both PEPR1 and PEPR2 are receptor kinases. First, I wanted to check the localization of PEPR1 and PEPR2 receptors in 7-day-old *pi4kβ1β2* seedlings and compare it to that in WT plants. Originally, it was suspected that the *pi4kβ1β2* mutants might have a disturbed localisation and/or dynamics of the PEPR1 and/or PEPR2 receptors.

To visualize the receptors, I used PEPR1:YFP and PEPR2:YFP under native promoter lines for confocal imaging. According to preliminary data, PEPR1 and PEPR2 receptors were located in the differentiation zone in both WT and *pi4kβ1β2* plants (**Fig. 62a, b**). PEPR1 receptor localization was shown in **Fig. 62a** (left panel for WT plants; right panel for *pi4kβ1β2* plants); PEPR2 receptor localization was shown in **Fig. 62b** (left panel for WT plants; right panel for *pi4kβ1β2* plants). It was also interesting to see the localization of the receptors inside the cell. The signal was visible on the plasma membrane and in the vesicles in both WT and *pi4kβ1β2* plants. Thus, the arrangement of the proteins was identical between the WT and the *pi4kβ1β2* mutant. No specific localisation was identified for the mutant.

To test the functionality of *pi4kβ1β2* PEPR receptors, I performed a treatment with pep1. My hypothesis was that *pi4kβ1β2* mutants might be insensitive to pep1. I checked sensitivity to pep1 by assessing root length.

Ten-day-old seedlings were transferred to plates containing 50 nM pep1 and roots were scanned after 4 days. The biologically active concentration was chosen according to (Ortiz-Morea et al., 2016). Incubation with pep1 resulted in root inhibition in WT and the *pi4kβ1β2* mutant (**Fig. 62d**). The mutant plants were thus able to perceive pep1, indicating the functionality of the receptor.

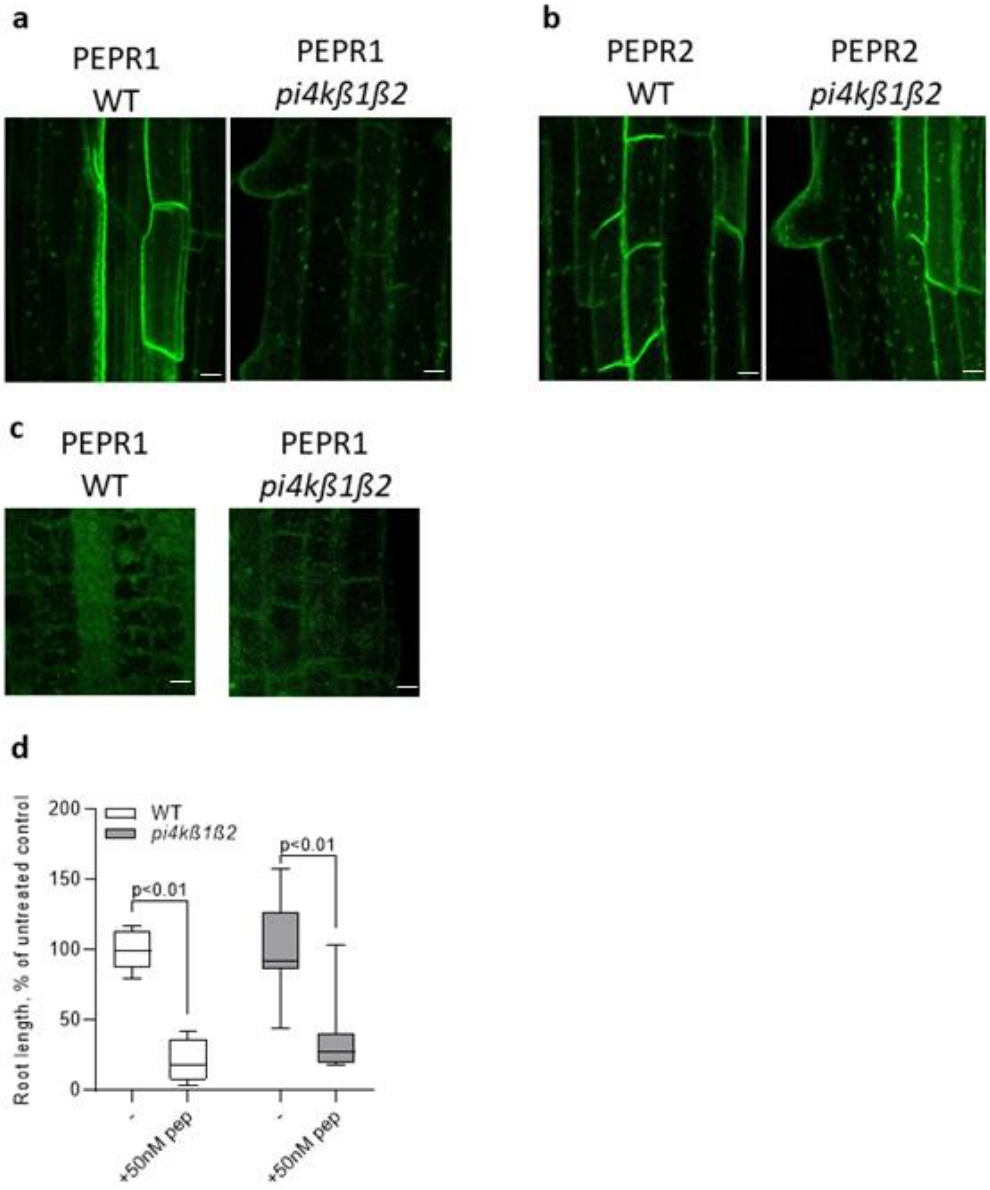

Fig. 62: a) PEPR1 receptor localization in WT (left panel) and *pi4kβ1β2* (right panel) in the differentiation zone, Scale bar: 10 µm; **b)** PEPR2 receptor localization in WT (left panel) and *pi4kβ1β2* (right panel) in the differentiation zone, Scale bar: 10 µm; **c)** PEPR1 receptor localization in WT (left panel) and *pi4kβ1β2* (right panel) in the meristem zone, Scale bar: 10 µm; **d)** root growth inhibition of WT and *pi4kβ1β2* plants in the presence of 50 nM pep1, n=10 (one-way ANOVA, Tukey HSD, $P < 0.05$).

5.3.1.3 Effect of a *pepr1* and *pepr2* mutations

To check the influence of PEPR1 and PEPR2 receptors on the SA-related phenotypes of *pi4kβ1β2* plants, I used double, triple and quadruple mutants, obtained by crossing: *pepr1/pepr2, sid2/pi4kβ1β2, pepr1/pi4kβ1β2, pepr2/pi4kβ1β2, pepr1/pepr2/pi4kβ1β2*. All experiments were made on 4-week-old plants. If the PEPR1 or PEPR2 receptors were

upstream to SA accumulation, I should then obtain reverted phenotypes, that with WT features.

First, I measured the rosette size. Triple and quadruple mutants (*pepr1/pi4kβ1β2*, *pepr2/pi4kβ1β2* and *pepr1/pepr2/pi4kβ1β2*) showed a partially reverted phenotype, but with a shorter rosette size compared to that of WT plants. The single *pepr2* and double *pepr1/pepr2* mutants had the same rosette size as the WT plants (**Fig. 63a**). The *pepr1* single mutants might have a smaller rosette size. The *sid2/pi4kβ1β2* triple mutant was used as a control for rosette size reversion.

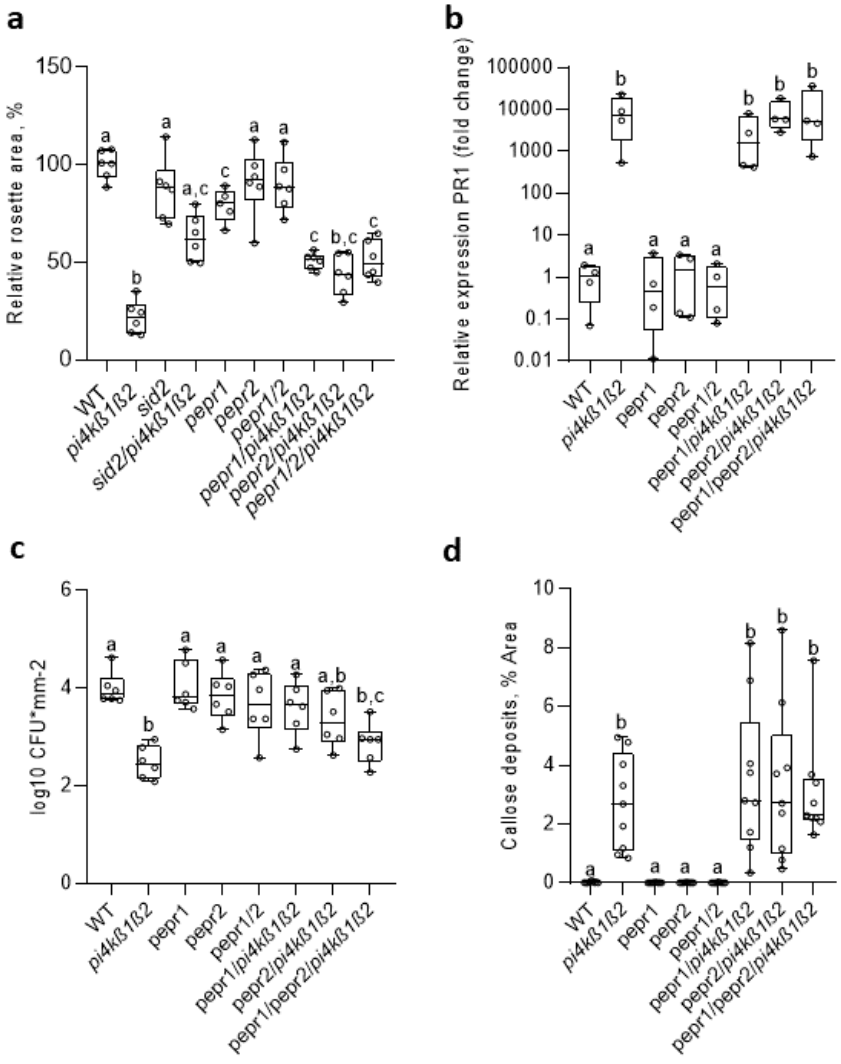

Fig. 63: Effect of *pepr1* and *pepr2* mutations on SA-related phenotypes. **a)** relative rosette size of WT, single mutant *sid2*, *pepr1*, *pepr2*, double mutant *pi4kβ1β2,* triple mutant *sid2/pi4kβ1β2, pepr1/pi4kβ1β2, pepr2/pi4kβ1β2* and quadruple mutant *pepr1/pepr2/pi4kβ1β2*, n=6*;* **b)** PR1 expression, n=4; **c)** *P. syringae* proliferation, n=6; **d)** callose deposition, n=9. Central line of the boxplot represents the median; circles represent individual values from three biological repeats. Different letters indicate variants significantly different in every genotype; one-way ANOVA with

Tukey-HSD post-hoc test, $P < 0.05$.

Subsequently, the expression of *PR1* was checked. In the *pi4kβ1β2* plants, there was a constitutively high *PR1* expression. No reversion was observed in this test: *PR1* expression was at the same level in the *pi4kβ1β2* and *pepr1/pi4kβ1β2*, *pepr2/pi4kβ1β2*, *pepr1/pepr2/pi4kβ1β2* mutant seedlings. The single and double mutants *pepr1*, *pepr2* and *pepr1/pepr2* had the same *PR1* transcript level as WT (**Fig. 63b**).

The PI4Kβ1β2 deficiency in the *pi4kβ1β2* mutants resulted in resistance to the hemibiotroph *P. syringae*. To evaluate the resistance to the pathogen, 4-week-old plants were infiltrated with the pathogen. The *pepr1*, *pepr2* and *pepr1/pepr2* mutants showed the same pathogen development as observed in the WT. Surprisingly, the *pepr1/pi4kβ1β2* triple mutant had also the same resistance as the WT plants. The *pepr2/pi4kβ1β2* and *pepr1/pepr2/pi4kβ1β2* mutants were not statistically different from *pi4kβ1β2*. In conclusion, a reversion concerning sensitivity to *P. syringae* was seen for *pepr1/pi4kβ1β2* mutants but was not found in the *pepr1/pepr2/pi4kβ1β2* mutants (**Fig. 63c**). This appears contradictory.

Callose evaluation was chosen for the final test. It was found that *pi4kβ1β2* mutants constitutively accumulated a high callose level. This accumulation was mainly SA dependent (Pluhařová et al., 2019). Callose deposition was the same for the plants with the *pi4kβ1β2* mutation, regardless of the presence of *pepr1* and/or *pepr2* mutations. This suggests that there is no reversion.

Therefore, mutations in PEPR1 or PEPR2 receptors could partially reverse the size phenotype of the *pi4kβ1β2* mutants. However, no reversion was observed in the other phenotypes studied (apart from a single doubtful reversion in the resistance to *P. syringae* tests). I suggested repeating the rosette size measurements and quantifying the SA level in the different mutants in future studies.

5.3.1.4 Effect of a *snc1* mutation

SNC1 is a TIR-NBS-LRR type of R protein. SNC1 plays a crucial role in the ETI pathway. I used the loss-of-function mutant of SNC1, *snc1-11*.

For the rosette size there was no reversion: *pi4kβ1β2* and *snc1-11*/*pi4kβ1β2* were not statistically different (**Fig. 64a**).

However, the high expression level of *PR1* was only found in the *pi4kβ1β2* mutants, while WT and *snc1-11*/*pi4kβ1β2* had the same level (**Fig. 64b**). It could therefore mean that the

snc1-11 mutation reverted the phenotype. However, resistance to *P. syringae* and callose accumulation revealed no reversion (**Fig. 64c, d)**. Again, my results were not consistent.

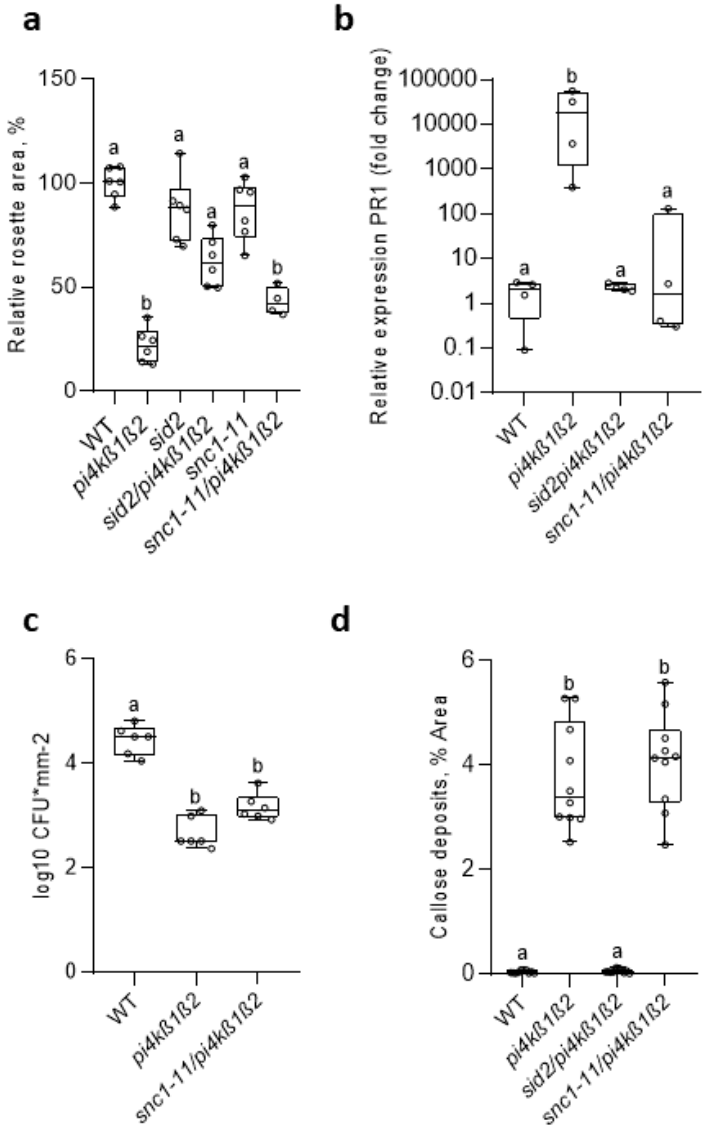

Fig. 64: Effect of a *snc1-11* mutation on SA-related phenotypes. **a)** relative rosette size, n=6; **b)** PR1 expression, n=4; **c)** *P. syringae* proliferation, n=6; **d)** callose deposition, n=10. Central line of the boxplot represents the median; circles represent individual values from three biological repeats. Different letters indicate variants significantly different in every genotype; one-way ANOVA with Tukey-HSD post-hoc test, $P < 0.05$.

5.3.1.5 Effect of a *cerk1* mutation

The last member of cell surface-localized pattern recognition receptors that I tested in my thesis was the CERK1 receptor. For the rosette size and callose accumulation, no reversion was observed (**Fig. 65a, c**). The values between *pi4kβ1β2* and *cerk1*/*pi4kβ1β2* mutants were not statistically different. For the resistance to *P. syringae*, the *cerk1*/*pi4kβ1β2* triple mutants could show partial reversion (**Fig. 65b**). Here again, the results are not consistent.

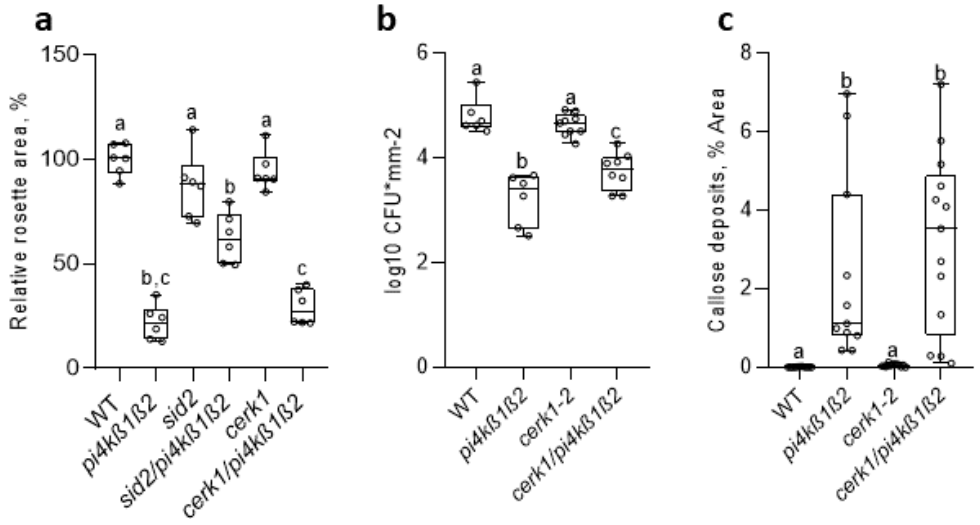

Fig. 65: Effect of a *cerk1* mutation on SA-related phenotypes. **a)** relative rosette size, n=6; **b)** *P. syringae* proliferation, n=6; **c)** callose deposition, n=10. Central line of the boxplot represents the median; circles represent individual values from three biological repeats. Different letters indicate variants significantly different in every genotype; one-way ANOVA with Tukey-HSD post-hoc test, $P < 0.05$.

5.3.1.6 Effect of a *bak1* mutation

Thus, although more research is needed, no clear reversals of all phenotypes associated with high SA could be detected by introducing mutations in one or more of the immunity-related receptors. The fact is that even though our working model is right, that is if the SA is accumulated in the *pi4kβ1β2* because the homeostasis of the immunity related receptors are is altered, then mutating only one or two receptors is not likely to be enough to revert the phenotype. The other receptors, not mutated, are numerous and might still cause the phenotype to express. Consequently, I decided to investigate the BAK1 receptor where the effects should be more obvious. BAK1 was originally identified as a BRI1-associated receptor kinase that mediates brassinosteroid signaling (Lu et al., 2010). It is a co-receptor for many PRRs. I generated the following multiple mutants: *bak1-4/pi4kβ1β2, bak1-*

4/pi4kβ1β2/sid2. The same age of the plants and the same test set-up as for the PEPR receptors were used for the evaluation.

The first rosette size test, it was noticeable that the single *bak1-4* mutants themselves were smaller than the WT plants (**Fig. 66a**). In addition, the size of the *bak1-4/pi4kβ1β2* rosette was similar to that of *pi4kβ1β2* and lower to that of *bak1-4*. The phenotype was not reverted. Surprisingly, the quadruple *bak1-4/pi4kβ1β2/sid2* mutant did not differ from the *bak1-4/pi4kβ1β2* triple mutant, but was smaller than the *sid2/pi4kβ1β2* mutant. If the small size of the plants with *pi4kβ1β2* mutations were only due to high SA, size reversion, at least partial, should be found in the *bak1-4/pi4kβ1β2/sid2* mutant, which was not the case (**Fig. 66a**).

The evaluation of *PR1* expression revealed interesting data. This expression in the *bak1-4/pi4kβ1β2* triple mutant was intermediate between that in the *bak1-4* mutant and that in the *pi4kβ1β2* mutant (**Fig. 66b**).

In the resistance test, the *bak1-4/pi4kβ1β2* mutants were surprisingly even more resistant than the *pi4kβ1β2* plants (**Fig. 66c**). The *bak1-4* single mutant had the same resistance as the WT plants. Callose accumulation was also higher in *bak1-4/pi4kβ1β2* plants than in *pi4kβ1β2* plants (**Fig. 66d**).

Therefore, the *bak1-4* mutation introduces an enhancement of the *pi4kβ1β2* phenotypes concerning resistance and callose levels, but leads to a partial reversion for *PR1* expression.

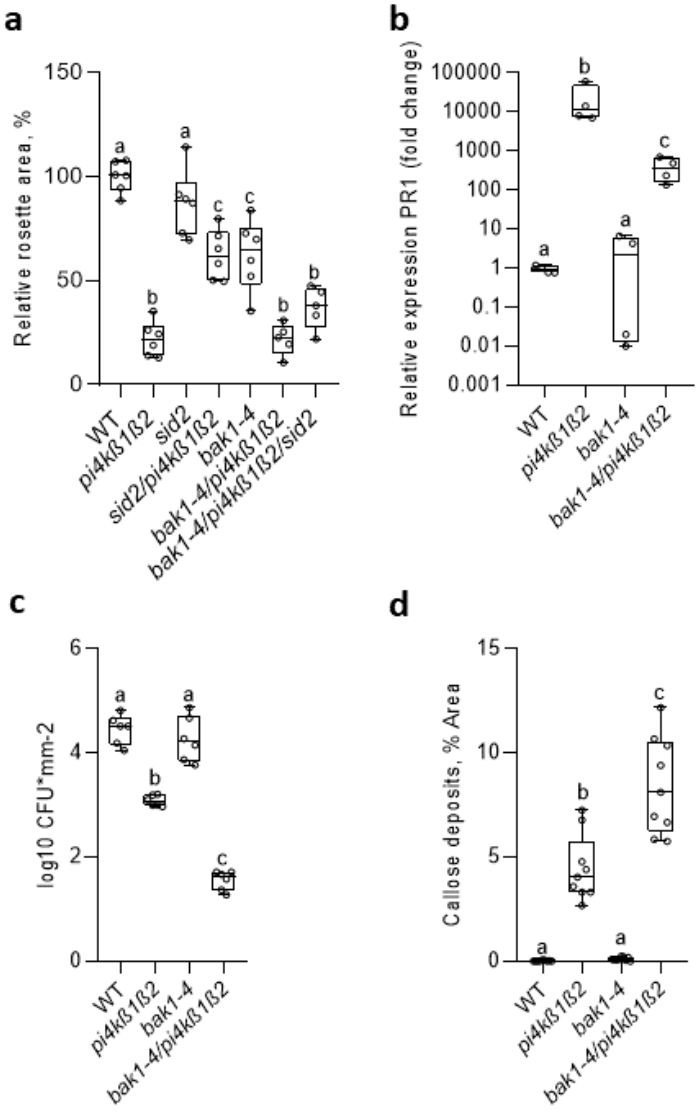

Fig. 66: Effect of a *bak1* mutation on SA-related phenotypes. **a)** relative rosette size, n=6; **b)** PR1 expression, n=4; **c)** *P. syringae* proliferation, n=6; **d)** callose deposition, n=9. Central line of the boxplot represents the median; circles represent individual values from three biological repeats. Different letters indicate variants significantly different in every genotype; one-way ANOVA with Tukey-HSD post-hoc test, $P < 0.05$.

5.3.2 Role of WRKY70 transcription factor in the SA related phenotypes of *pi4kβ1β2* double mutant

5.3.2.1 Effect of a *wrky70* mutation

In a transcriptomic analysis (unpublished) carried out before I arrived at the lab, the French and Czech teams compared the transcriptomes of *sid2/pi4kβ1β2*, *pi4kβ1β2* and *sid2* plants. The samples were obtained from 15-day-old seedlings. Not surprisingly, the comparison of

pi4kβ1β2 and WT showed that the double mutant expressed many genes associated with SA. Many of these genes were also expressed in the *pi4kβ1β2* versus *sid2/pi4kβ1β2* comparison, confirming their expression is due to the high SA level of *pi4kβ1β2.* This transcriptome analysis was not part of my PhD thesis and I will not elaborate on it. However, the transcriptome of *sid2/pi4kβ1β2* was also compared with that of *sid2* plants. This comparison was interesting because it was possible to see processes dependent on the *pi4kβ1β2* directly, independently of the increase of SA. Amongst the genes differentially expressed in this comparison (*sid2/pi4kβ1β2* versus *sid2),* if we focus on the genes related to biotic stress response, we might be able to identify processes related to biotic stress that could be the reason why the SA signaling pathway is triggered. In this context, the attention of my French supervisor was drawn to the transcriptional factor WRKY70. This gene was found to be more highly expressed in *sid2/pi4kβ1β2* compared to *sid2*, implying that it was induced in *pi4kβ1β2* independently of SA. Interestingly WRKY70 was shown to be involved in SA signaling and in the SA/JA crosstalk (J. Li et al., 2017). Its expression was not altered in the *pi4kβ1β2* versus WT comparison nor in the *pi4kβ1β2* versus *sid2/pi4kβ1β2*, which might be due to the fact that in high SA conditions its expression might be shut down.

In this context, my project was to investigate the role of WRKY70 in the SA-related phenotypes of *pi4kβ1β2.* I used *wrky70/pi4kβ1β2* and *sid2/wrky70/pi4kβ1β2* mutants. Phenotyping tests were performed as previously described. Interestingly, I obtained a reversion effect in all the tests. Indeed, quite a good reversion was obtained for rosette size and weight (**Fig. 67a, b**). The *wrky70/pi4kβ1β2* and *sid2/wrky70/pi4kβ1β2* mutants had the same rosette size as the *sid2*/*pi4kβ1β2* control (**Fig. 67a**). Accordingly, rosette weights were the same in *wrky70/pi4kβ1β2* versus *sid2/pi4kβ1β2* and *sid2/wrky70/pi4kβ1β2* versus WT (**Fig. 67b**).

PR1 expression was equal between WT and *wrky70/pi4kβ1β2, sid2/wrky70/pi4kβ1β2* mutants (**Fig. 67c**). A similar profile was found for the level of callose accumulation (**Fig. 67e**).

The resistance assay with *P. syringae* showed a lower level of resistance for *wrky70/pi4kβ1β2* and *sid2/wrky70/pi4kβ1β2* than *pi4kβ1β2* (**Fig. 67d**). The resistance of these mutants appeared to be even lower than that of WT. Nevertheless, the sensitivity of WT appeared to be underestimated in this experiment.

WRKY70 expression was assessed by qPCR (**Fig. 67f**). As expected, the level was decreased in the *sid2/wrky70/pi4kβ1β2* and *wrky70/pi4kβ1β2* mutants. *WRKY70* expression in *pi4kβ1β2* was higher than in WT and *sid2/pi4kβ1β2* plants (**Fig. 67f**).

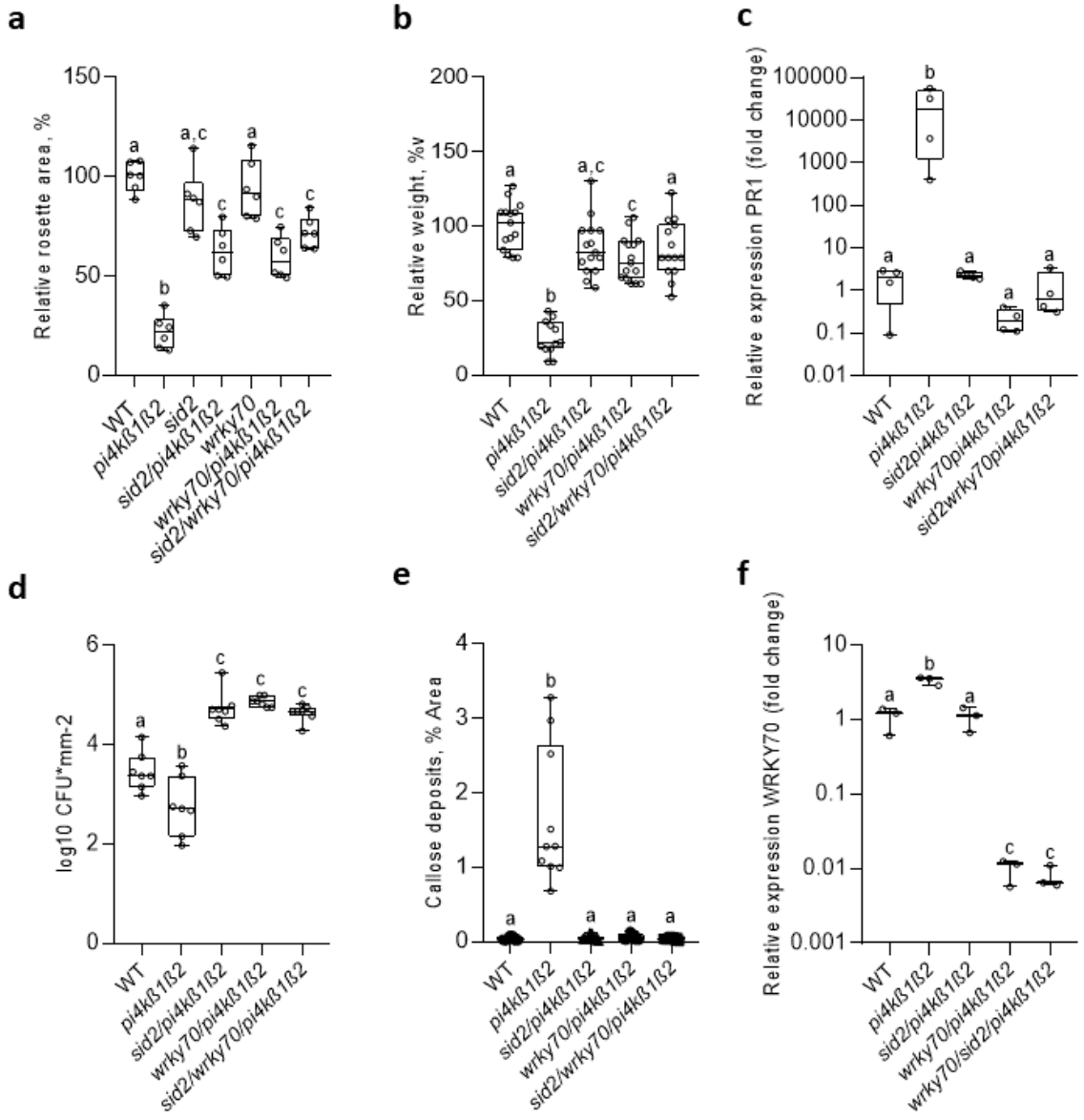

Fig. 67: Effect of a *wrky70* mutation on SA-related phenotypes. **a)** relative rosette size area, n=6; **b)** rosette weight, n=12; **c)** relative expression PR1, n=4; **d)** resistance to the *P. syringae*. Infiltration treatment of 4-week-old plants, n=7; **e)** quantification of callose deposition, n=10; **f)** relative expression WRKY70, n=3. Central line of the boxplot represents the median; circles represent individual values from three biological repeats. Different letters indicate variants significantly different in every genotype; one-way ANOVA with Tukey-HSD post-hoc test, $P < 0.05$.

5.3.3 Conclusion

In order to draw a conclusion on *pi4kβ1β2* phenotype features, further experiments are necessary, which was not possible in the frame of my PhD thesis. PI4Kβ1β2 deficiency in the *pi4kβ1β2* mutants resulted in impaired development: reduced primary root length and rosette size, callose accumulation, resistance to the hemibiotroph *P. syringae*, increased expression

of *PR1*. The *pi4kβ1β2* mutant has persistently active immunity and a high level of SA accumulation. The mechanism behind this is still unknown. The constitutive activation of immunity involves constantly active receptors. I suspected that the *pi4kβ1β2* mutants might have non-functioning or mislocalized receptors.

My aim was to check whether the mutation of some receptors could have an impact on the phenotype features of the triple mutants. In addition, I also wanted to investigate the localization of the receptors and test whether they were mislocated or misprocessed. To determine the relationship between the *pi4kβ1β2* phenotype and active immunity, I generated several receptor mutants. They were receptors from different groups - RLKs class (FLS2, PEPR1/2, BAK1 - leucine-rich repeat-receptor kinases; CERK - lysin motif receptor-like kinase); TIR-NBS-LRR type of R protein (ETI pathway) - SNC and transcription factor - WRKY70. There were triple mutants (*fls2/pi4kβ1β2, pepr1/pi4kβ1β2, pepr2/pi4kβ1β2, cerk1-2/pi4kβ1β2, snc1-11/pi4kβ1β2, bak1-4/pi4kβ1β2, wrky70/pi4kβ1β2*); quadruple mutant (*pepr1/pepr2/pi4kβ1β2*); double mutant (*pi4kβ1β2* and *pepr1/pepr2*) and single mutant (*pepr1, pepr2, cerk1-2, bak1-4*). The next methodology was used to see if receptors were involved in the SA phenotype of the *pi4kβ1β2* mutant: rosette size and callose measurements, assessment of resistance to *P. syringae*, *PR1* expression. For the PEPR1/2 receptors, I took confocal images to check their localization and functionality. I hoped to obtain a reverted plant phenotype with WT features, meaning that these receptors/regulators are upstream of SA accumulation. For each receptor I have a different reversion result, so I will discuss it separately.

For the FLS2 receptor, in terms of rosette size, the *fls2/pi4kβ1β2* rosettes are statistically larger than those of the *pi4kβ1β2* double mutants, which could indicate a partial reversion. Nevertheless *PR1* expression and resistance to *P. syringae* were the same between *fls2/pi4kβ1β2* and *pi4kβ1β2* plants. As for callose content, the *fls2/pi4kβ1β2* triple mutant showed reversion, as the percentage area of callose deposition was not statistically different from that of the WT plants. This reversion for callose accumulation is not consistent with the lack of reversion for *PR1* expression and resistance to *P. syringae*. Repeat measurement of callose accumulation is required, as well as measurement of rosette size.

The part with PEPR1 and PEPR2 receptors showed partial reversion only when rosette size was measured. No reversion was observed in other tests. It was surprising to see the normal localization of the PEPR receptor in *pi4kβ1β2* mutants and its functionality in sensing pep1. In both WT and *pi4kβ1β2* mutants, PEPR1 and PEPR2 receptors are localized on the membrane and in the vesicles; in the differentiation zone. PEPR1 signal was also observed in

the meristem zone. Several papers have been published on the localization patterns of PEPR1 and PEPR2 receptors. To clarify localization patterns, Ortiz-Morea et al., (2016) expressed the genomic sequences of PEPR1 and PEPR2 fused with GFP under their native promoters. The PEPR1-GFP signal was detected in root cells of the differentiation zone and also in the root meristem. Consistent with Bartels et al., (2013) data, the activity of the *PEPR2* promoter was more restricted to the central cylinder of the root, while GUS expression of the *PEPR1* promoter was present in most root tissues. From my data I saw that the signal was distributed throughout the root. In the meristem zone signal was observed only for the PEPR1 receptor, both in WT (**left panel Fig. 62c**) and in the mutant plants (**right panel Fig. 62c**). The signal was visible on the plasma membrane and inside the cell in the vesicles. These preliminary data are a good start, but they should be repeated and further developed.

The last representative of the cell surface localized pattern recognition receptors that I tested in my work was the CERK1 receptor. No reversion was observed in rosette size and callose accumulation. The levels between *pi4kβ1β2* and *cerk1*/*pi4kβ1β2* mutants were not statistically different. For resistance to *P. syringae*, the *cerk1*/*pi4kβ1β2* triple mutants could show partial reversion. Again, the results are not consistent.

Then I decided to test the BAK1 mutation. BAK1 was originally identified as a BRI1-associated receptor kinase that mediates brassinosteroid signaling (Lu et al., 2010). It is a co-receptor for many PRRs. For the BAK1 receptor, I obtained a rather interesting result. Reversion effect was found in *PR1* expression, resistance assay and callose measurements. Surprisingly *bak1-4/pi4kβ1β2* was even more resistant to *P. syringae* and contained more callose than *pi4kβ1β2* mutants.

Concerning the generated multiple mutant, the ones involving *wrky70* mutant were the most promising. The *wrky70/pi4kβ1β2* and *sid2/wrky70/pi4kβ1β2* mutants had the same phenotype as WT plants. For example, the *wrky70/pi4kβ1β2* and *sid2/wrky70/pi4kβ1β2* had the same rosette size as the control *sid2/pi4kβ1β2*. The same trend was observed for rosette weight, *PR1* expression, resistance to *P. syringae* and callose content. The expression level for *wrky70* was higher in *pi4kβ1β2* than in WT plants. The reversions were consistent in all assays and quite strong.

5.3.4 Discussion and Perspectives

Concerning the idea of understanding why in the *pi4kβ1β2* mutant there is more SA, it has been shown that PUB12 and PUB13, U-box E3 ubiquitin ligases, polyubiquitinated FLS2 and promoted flagellin-induced FLS2 degradation. FLS2-BAK1 complexes localize

predominantly at the plasma membrane and continuously cycle between plasma membranes and internal TGN/early endosome compartments. TGN/early endosome compartments are enriched for PI-4P through the recruitment of PI4Kβ1β2 by active RabA4B. The presence of RabA4B and PI-4P recruits PUB13. Upon flg22, flg22-FLS2-BAK1 complexes are rapidly internalized and ubiquitinated by PUB13 in TGN/early endosome compartments containing RabA4B and RabA4B-recruited PI4Kβ1β2. Loss of PI-4P and/or PUB13 on RabA4B-associated TGN/EE compartments interferes with the recycling of FLS2-BAK1 to the plasma membrane (non elicited cells) or the sorting and turnover of flg22-FLS2-BAK1 complexes in multivesicular body/vacuole compartments (elicited cells) (**Fig. 68**).

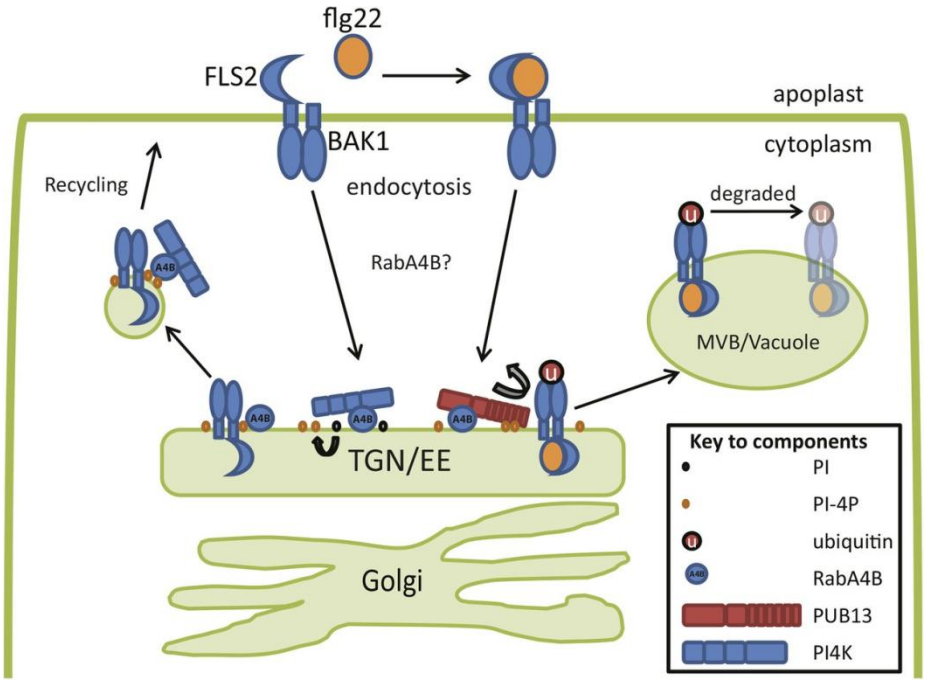

Fig. 68: Model for the RabA4B-mediated recruitment of PUB13 and PI4Kβ1/β2 to regulate the plant defense response (Antignani et al., 2015, p. 13).

Besides, we know that PUB13 interacts with PI4P (Antignani et al., 2015, p. 13). Interactions between PUB13 and PI4P from the one hand and between PUB13 and FLS2 from the other hand creates a link between PI4Kβ1β2 and FLS2 (**Fig. 69a**). Is it possible that PI4Kβ enzymes are necessary for PUB13 action on FLS2 that is the direct ubiquitination of FLS2? In that case, in absence of PI4Kβ1β2 (*pi4kβ1β2* mutant), there would be less ubiquitination of FLS2 and therefore a constitutive immunity (**Fig. 69b**). Such an action on immunity receptors of PI4Kβ1β2 via PUB13 could concern receptors other than FLS2. Indeed, PUB13 has also been shown to ubiquitinate LYSIN MOTIF RECEPTOR KINASE 5 (LYK5), an RLK

perceiving the fungal cell wall component chitin, and leads to LYK5 degradation and down-regulation of chitin-triggered immune responses (Liao et al., 2017). *A. thaliana* BRI1 endocytosis and protein abundance are also regulated by PUB12- and PUB13-mediated ubiquitination. Brassinolide perception promotes BRI1 association with PUB12 and PUB13 and its ubiquitination. Loss of PUB12 and PUB13 results in reduced BRI1 ubiquitination and internalization together with BRI1 accumulation in the plasma membrane (J. Zhou et al., 2018). A similar mechanism could be expected for immunity related receptors, i.e. loss of PUB13 would lead to more receptors. Interestingly, the SA content in *pub13* mutants was 63% higher than in WT of *A. thaliana* (Li et al., 2012). The *pub12* and *pub13* mutants displayed elevated immune responses to flagellin treatment (Lu et al., 2011) (**Fig. 69c**). Overall growth defects observed in *pub13* mutants were largely restored to the wild type in the *pub13/fls2* double mutant background (Antignani et al., 2015).

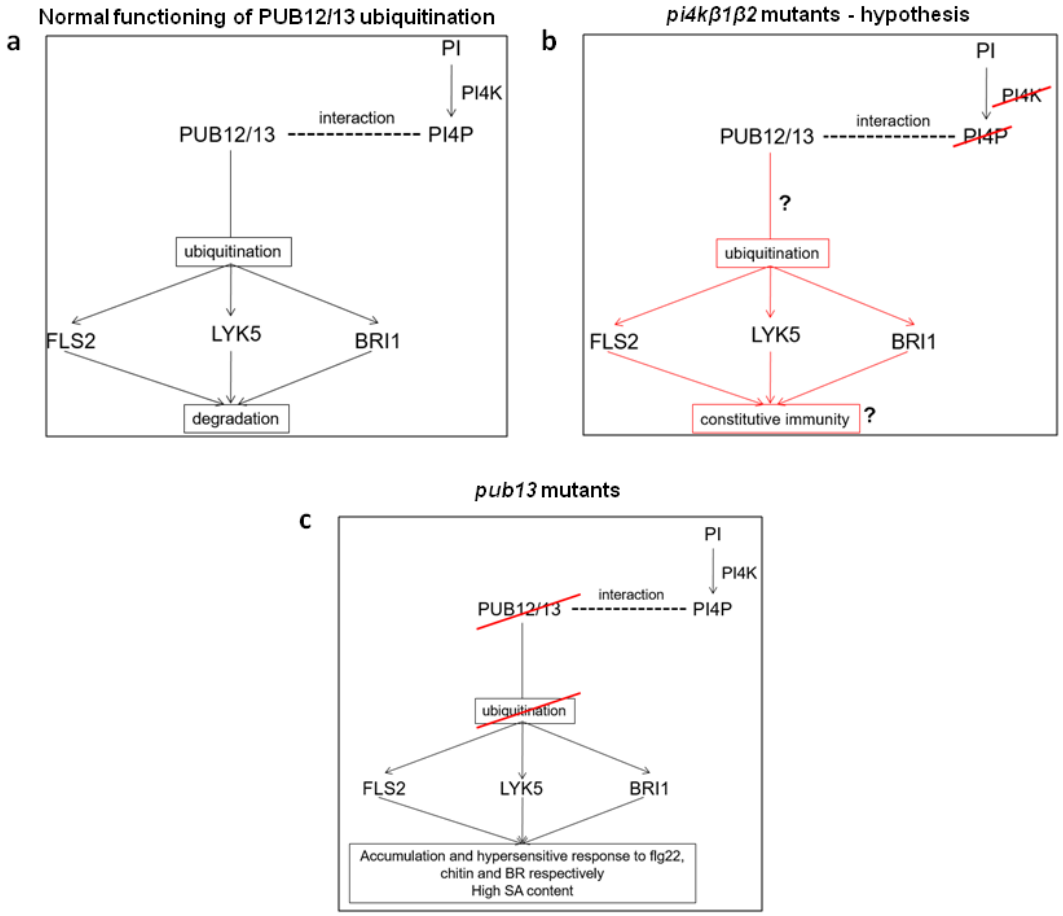

Fig. 69: Comparing the PUB12/13 functioning in the WT plants, *pub13* mutants and *pi4kβ1β2* mutants. **a)** normal functioning of PUB12/13 in WT plants; **b)** *pi4kβ1β2* mutants hypothesized altered PUB12/13 activity that leads to constitutive immunity; **c)** in *pub13* mutants accumulation of receptors in the plasma membrane.

In the future, I need to check the FLS2 ubiquitination level in the *pi4kβ1β2* mutant to be sure that PI4K deficiency leads to altered PUB12/13 ubiquitination. It is possible to do with *in vivo* ubiquitination assay of FLS2 (Göhre et al., 2008, p. 2). They used immunoprecipitation method with anti-FLS2 antibody bound to protein G-coupled magnetic beads after which immunoblot analysis with anti-FLS2 and anti-ubiquitin antibodies.

We also need to check FLS2 protein level in the *pi4kβ1β2* mutant. It could be done by western blot analyses with FLS2-specific antibodies (Chinchilla et al., 2006).

Also it would be nice to make the dynamics of FLS2 internalization with FLS2::GFP construct. I have FLS2::GFP construct in WT seeds, so I will need to make a crossing with *pi4kβ1β2* mutant to be able see the differences between the genotypes.

Interestingly, my Czech team made a proteome analysis of plasma membrane enriched fraction of *pi4kβ1β2* mutant. Some immunity related receptors were shown to be more present in the mutant versus in the WT. One of the receptors is CERK1 (Junková et al., 2021). CERK1 and LYK5 form a receptor complex for the perception of chitin. Junková et al., (2021) suggested that the protein level of CERK1 may be regulated indirectly by PUB12, because PUB12 interacted with the intracellular domain of CERK1, but PUB12 did not ubiquitinate CERK1 (Yamaguchi et al., 2017). It would be interesting to make a Western blot analysis of CERK1 protein levels in the double mutant versus wild-type plants.

Concerning other receptors, the localization of PEPR1/2 receptors and the perception of pep1 peptide were checked. Both in WT and *pi4kβ1β2* mutants, PEPR1 and PEPR2 receptors are localized on the membrane and in the vesicles, in the differentiation zone. The PEPR1 signal was also observed in the meristem zone. Mutant plants were able to perceive pep1 that indicate receptor functionality. I think it would be great to examine the localization of PEPR1 and PEPR2 receptors dynamically, like I did for PIN2 protein (described in result section part 1). This approach could show if there are trafficking problems in *pi4kβ1β2* mutants concerning these receptors. As shown earlier, there were altered intracellular trafficking dynamics in the roots of *pi4kβ1β2* seedlings. Consistently, I could expect differences in the dynamics of PEPR1 and PEPR2 receptors in *pi4kβ1β2* compared to WT. Besides, as explained above for PUB12/13 action, the protein level of PEPR receptors should be checked in *pi4kβ1β2* and *sid2/pi4kβ1β2* mutants. This could be done either by a dedicated antibody or by the use of a construct made of PEPR1 fused to a tag, under the control of PEPR1 native promoter. Concerning the phenotypes, rosette size showed partial reversion, which can not be said about the other tests. Faced to such a contradiction, we clearly need to assess SA level in

these mutants. In fact, priority is to check SA level in all generated triple and quadruple mutants.

Concerning the BAK1 receptor, I got interesting results. As published earlier, *A. thaliana* mutants impaired in brassinosteroid perception or signaling, including the *bak1-4* mutant, display an altered rosette morphology and smaller size (Schwessinger et al., 2011). Thus, it was not surprising that the rosette size of *bak1-4/pi4kβ1β2* was the same as *pi4kβ1β2.* Because even though we switched off the immune response by *bak1-4* mutation, and maybe this switched off the SA overaccumulation, there would still be a brassinolide effect. In the *bak1-4/pi4kβ1β2/sid2* mutant, the *sid2* mutation is likely to inhibit the accumulation of SA. This confirms that the short size of *bak1-4/pi4kβ1β2/sid2* is probably due to alteration in the brassinosteroid signaling. The fact that the triple mutant *bak1-4/pi4kβ1β2* was smaller than the quadruple *bak1-4/pi4kβ1β2/sid2* mutant could be due to both SA and brassinosteroid alteration in the triple mutant (as compared to "only" brassinosteroid in the quadruple mutant). Definitely SA content should be measured for the full set of plants. The partial reversions of *bak1-4/pi4kβ1β2* mutants in *PR1* expression could mean less SA level in the mutant compared to *pi4kβ1β2* double mutant. The single mutant *bak1-4* have normal SA level (Yang Gao 2017). It would be also interesting to see the *PR1* expression also for quadruple mutant *bak1-4/pi4kβ1β2/sid2*. It could have full reversion. Concerning the test with *P. syringae*, it was unexpected to see the higher resistance of *bak1-4/pi4kβ1β2* mutants compared to *pi4kβ1β2* plants. It would be nice to confirm with other pathogens, like *Botrytis cinerea* and other pathogens. The same trend was with callose measurements that also need to be checked in response to other pathogens. Single mutant *bak1-4*, as expected, have the same resistance as WT plants (BirgitKemmerling 2007). These phenotypes I saw might result from two things: effects on SA and effect on brassinosteroid signaling. BAK1 has a dual role: from brassinolide (as an interactor of the LRR-RK Brassinosteroid (BR)-Insensitive 1 (BRI1), which binds brassinolide) to immunity effect (it associates with FLS2 receptor) (Wang et al., 2008). To split these roles, Benjamin Schwessinger identified a *bak1* mutant that is impaired in the immunity aspect, but not in the brassinosteroid signaling. The *bak1-5* is a single-amino-acid-substitution mutant of BAK1 that results in hypoactive kinase activity and has been reported to show defects in positive regulation of immune response pathways but appears not to affect brassinolide signaling or cell death regulation pathways (Wierzba and Tax, 2016). On the contrary, the *bak1-4* mutant is a null allele that displays defects in brassinolide signaling, immune response activation, pathogen-induced cell death, and general loss of cell death regulation. The *bak1-4* might also be disturbed in brassinolide signaling so

what I saw might be a cross talk between brassinolide and *pi4kβ1β2.* In the future, I need to use the *bak1-5* mutant that is only disturbed in co-receptor function and not in brassinolide signaling.

Of my results, the most promising data concern the WRKY70 receptor. Reversion occurred in all phenotyping tests. Either *WRKY70* controls SA level in the *pi4kβ1β2* plants or it could mean that *WRKY70* is downstream of SA: introducing *wrky70* mutation would lead to no more SA signaling. Indeed, *WRKY70* is considered to be a transcription factor acting downstream SA. In fact it is a node of convergence for JA-mediated and SA-mediated signals in plant defense. *WRKY70* is a common component in SA- and JA-mediated signal pathways. More precisely, the expression of *WRKY70* is activated by SA and repressed by JA (J. Li et al., 2004) (**Fig. 70**).

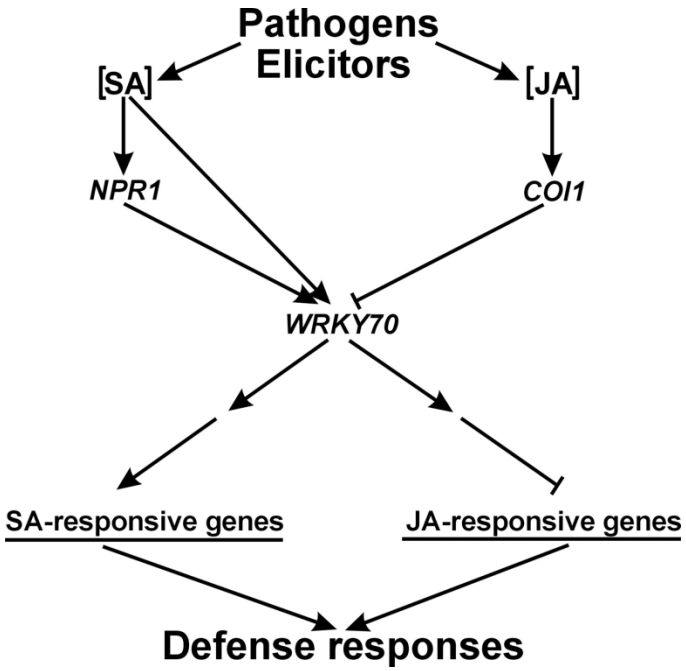

Fig. 70: Working model showing WRKY70-mediated cross talk between SA- and JA-dependent defense signaling.
Recognition of a particular pathogen or pathogen-derived elicitor may trigger the synthesis of SA or JA (or both) and lead to subsequent activation of the corresponding signal pathways. The balance between the two pathways determines the level of *WRKY70* expression. As a consequence, *WRKY70* level determines which type of response is favored. High *WRKY70* levels activate expression of SAR-related genes while repressing JA-responsive gene expression. Conversely, low *WRKY70* levels favor JA-responses over SAR. Thus, *WRKY70* acts directly or indirectly by integrating signals from both pathways, the outcome being dependent on the initial signal strength (J. Li et al., 2004).

The overexpression of *WRKY70* was shown to promote up-regulation of SAR-related defense genes and resistance to the hemibiotroph *P. syringae* and the biotroph *E. cichoracearum* while enhancing susceptibility to the necrotroph *Alternaria brassicicola* (J. Li et al., 2004).
The basal levels of free SA, ethylene and JA were not significantly different between the WT plant and *WRKY70*-overexpressing or *WRKY70*-silenced lines (J. Li et al., 2004). This pleads for *WRKY70* being downstream SA, in the pathway leading from SA to *PR* gene expression. More specifically, it would act downstream NPR1. In my work, the reversion phenotype of *wrky70/pi4kβ1β2* mutant could be caused by normal SA level compared with increased level of *pi4kβ1β2*. As mentioned earlier, the *WRKY70* signaling is a very complex issue and would certainly require further study.
However, the role of *WRKY70* in immunity appears to be more complex. It has been shown that not only *WRKY70* acts downstream SA, but it also participates in controlling SA level. *WRKY70* and its closest homolog *WRKY54* have been identified as negative regulators of SA biosynthesis, acting through a negative feedback loop. A *wrky54/wrky70* double mutant is characterized by an elevated SA level (Wang et al., 2006). This shows that *WRKY70* can participate in a loop that diminishes SA level. In a similar way, it is also well documented that *npr1* mutants have increased SA levels (Dong, 2004). The way *WRKY70* could control SA level might be by repressing *SARD1* by binding the motif GACTTTT in the absence of pathogens (M. Zhou et al., 2018). *SARD1*, together with its close homolog *CBP60g*, functions as a transcription factor that directly binds to the promoters of genes that control SA synthesis, such as *Isochorismate Synthase 1* (Sun et al., 2015). The *wrky54/wrky70* double mutant has more *SARD1* and *CBP60g* expression level than the WT (Chen et al., PSB, 2021), confirming *WRKY70* inhibits the basal level of *SARD1* and *CBP60g*. So these data pleads for *WRKY70* negatively regulating SA level, at least in basal conditions.
Interestingly, *snc2-1D* is an *A. thaliana* mutant that carries a gain-of-function mutation in a receptor-like protein that constitutively activates plant immune response that closely resembles *pi4kβ1β2* mutant. When a suppressor screen was performed, it appeared that mutations in *WRKY70* suppressed the constitutive defense response in *snc2-1D* (Zhang et al., 2010). However, in the *snc2-1D* mutant WRKY70 would positively regulate SA. The *snc2-1D* mutant has a higher *ICS1* expression level than the WT. Yet, *ICS1* expression is lower in *snc2-1D/wrky70* and back to WT level in *snc2-1D/wrky70/wrky54* (Chen et al., PSB, 2021). The same pattern is seen concerning *SARD1* and *CBP60g* expression levels. This implies that *WRKY70* positively regulates SA level, and it might do so by controlling *SARD1/CBP60*. Therefore, the situation might be similar to that in *pi4kβ1β2.*

Mechanistically, the fact that *WRKY70* can either activate or inhibit *SARD1* expression depends on its phosphorylation status. Upon infection *WRKY70* phosphorylated forms were increased; they activated *SARD1* expression through binding to a WT box (a cis element in *SARD1* promoter). Non-phosphorylated *WRKY70* repressed *SARD1* expression by binding to both W and WT cis-elements (Liu et am. 2021).

So, what does it suggest for our subject? It means that *WRKY70* can act upstream or downstream of SA. We definitely need to check whether *WRKY70* acts upstream SA, acting on *SARD1/CBP60g* and *ICS1* expression, or downstream SA. SA level needs to be checked in *wrky70*/*pi4kβ1β2* triple mutant. The expression levels of *SARD1*, *CBP60g* and *ICS1* also need to be assessed. Note that in root seedlings *SARD1* and *CBP60g* genes were up-regulated in *pi4kβ1β2* mutants, according to my transcriptome analysis (**Fig. 71**). It could be the reason for the high SA level and SA-related phenotype of *pi4kβ1β2* mutants. To check this hypothesis, I need to create a *sard1/pi4kβ1β2* and *cbp60g/pi4kβ1β2* triple mutants. Yet, the transcriptome concerns seedling in which the accumulation of SA has not yet occurred. qPCR data on older plants, where SA accumulation occurs, need to be done.

id	Annotation	log2FoldChange	adjusted.PValue
AT1G73805 (SARD1)	Calmodulin binding protein-like	1.14	0,000000134
AT5G26920 (CBP60g)	Cam-binding protein 60-like G	2.45	1,07E-51

Fig. 71: Transcript levels of *SARD1* and *CBP60g* genes in *pi4kß1ß2* seedlings versus the WT with the log2 fold change as detected in the NGS experiment (root data).

Therefore, I propose as perspective to this work:

1. Check SA level in all generated triple and quadruple mutants.
2. For FLS2 group mutants: repeat measurement of callose accumulation and rosette size. For the last one use of the platform at Amiens University.
3. Check the FLS2 ubiquitination level by *in vivo* ubiquitination of FLS2 assay for *pi4kβ1β2*.
4. Make the dynamics of FLS2 internalization with FLS2::GFP construct.
5. Visualize the PEPR1 and PEPR2 receptors and measure trafficking rate.

6. Measure the protein level of PEPR receptors in *pi4kβ1β2* and *sid2/pi4kβ1β2* mutants. This could be done either by a dedicated antibody or by the use of a construct made of PEPR1 fused to a tag, under the control of PEPR1 native promoter.
7. Check the pep1 perception on *pepr1*, *pepr2*, *pepr1/pepr2* and *pepr1/pepr2/pi4kß1ß2* mutants to show the dependence of the presence of receptors on the possibility of perception. It is a control for the assay of *pi4kβ1β2* sensitivity to pep1.
8. For *bak* group mutants: we need to generate the mutants based on *pi4kβ1β2* crossed with the *bak1-5* mutant. In the set of obtained mutants, the phenotyping needs to be done.
9. Check *PR1* expression for all members, including quadruple mutant *bak1-4/pi4kβ1β2/sid2*.
10. Make a resistance test with other pathogens, like *Botrytis cinerea.*
11. Test callose level in response to other pathogens.
12. Generate *cbp60g/pi4kβ1β2* and *sard1/pi4kβ1β2* triple mutants.
13. Make the same list of experiments with *cbp60g/pi4kβ1β2* and *sard1/pi4kβ1β2* to see the phenotype.
14. Check the *WRKY70* expression.
15. Measure the protein level of the WRKY70.

6. CONCLUSIONS

This thesis focuses on the study role of type III PI4Ks. The mutant approach has been used. I have worked with a double mutant *pi4kβ1β2* defective plant in both the *PI4Kβ* genes. The main findings presented in the **Fig. 72**. I will now describe the main conclusions based on the main known facts about the mutant and the intermediate tests carried out to understand the relationship between the cause of the absence of the kinase and the corresponding consequences.

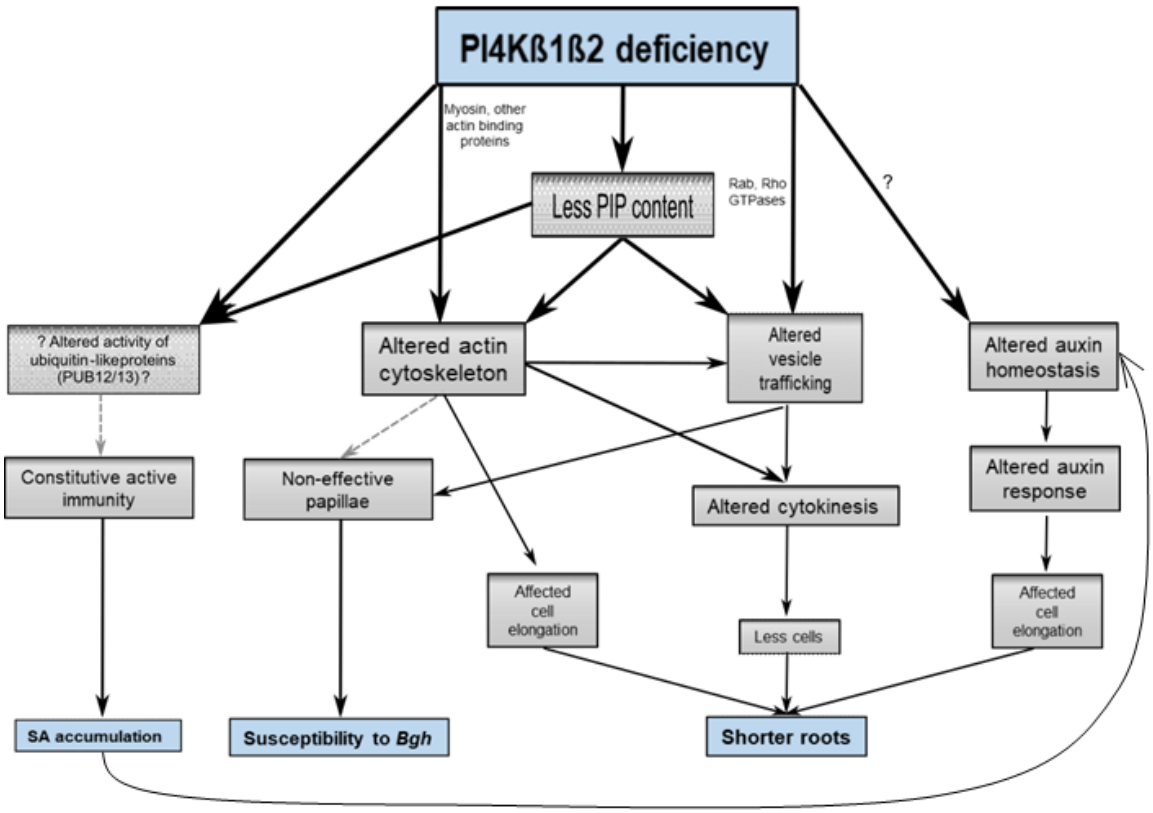

Fig. 72: General working model of PI4K deficiency. The bigger blue box represents the main aim of the study - role of type III PI4Ks. Three smaller blue boxes are the main consequences of PI4K deficiency. Grey boxes are facts that were investigated in this work or are not confirmed yet (hypothesis). Hypothesis boxes contain question marks inside.
Short roots were studied in seedlings; where no SA accumulation occurs. But SA accumulation, when it occurs, can impact auxin homeostasis. Dashed lines are not confirmed links. Black lines are confirmed links.

Not only the characterisation of the developmental phenotypes and the functioning of immunity, but also the *A. thaliana* - *Bgh* interaction were investigated in the *pi4kβ1β2* mutant plants.

The main known consequences of PI4K deficiencies are: impaired root growth in seedlings, SA accumulation and higher susceptibility to the non-adapted fungal pathogen *Blumeria graminis* pv. *hordei* (small blue boxes in **Fig. 72)**.

Some of the known mutant features cause the various defects. For example, an altered actin skeleton leads to altered vesicle transport, which could be the reason for the formation of non-effective papillae and disturbed cytokinesis (dashed arrows from the box "Altered actin cytoskeleton").

In the double mutant, a loss of sensitivity to exogenous IAA was observed in terms of inhibition of primary root length, inhibition of cortical cell elongation and elongation of the meristematic zone. No difference in the measured content of free IAA was observed between WT and the mutant plants, while the concentrations of some conjugates such as IAA-Glu, CamX, I3A and IAN were higher in the *pi4kβ1β2* mutant than in the WT roots. Based on DII-VENUS degradation and gene expression, the *pi4kβ1β2* mutant does not appear to respond to endogenous or exogenous auxin. The low response to auxin could be due to this higher conjugation activity. Whether there is a link between altered trafficking/cytoskeleton integrity and the conjugation activity requires further investigations. These data on PI4Kβ mutants and the sensitivity to auxin were published in an article (Starodubtseva et al., 2022).

A major consequence of PI4K deficiency is lower PI4P content. PI4P is an important signaling molecule that can serve as a substrate for phospholipases C (PLCs), leading to diacylglycerol and the corresponding phosphorylated inositol. PI4P also interacts directly with membrane proteins or cytosolic proteins, which it can recruit to membranes. Given the broad spectrum of PI4P involvement in different processes, it is logical to assume that its absence in the mutant will result in corresponding consequences in different areas (dashed arrows from the box "Less PI4P content"). One of the consequences is a lower PI4P accumulation in the papillae, leading to a higher penetration rate under *Bgh*, because of the non-effective papillae forming. The question for the future is to study the link between PI4K mutation, PI4P deficiency and non-effective papillae formation. Since some ubiquitin-like proteins require PI4P for their activity, I might also expect their substrates - plasma membrane receptors - to not function properly. My hypothesis was that faulty cycling of the receptors leads to SA accumulation and constitutive active immunity. This idea should be explored further in the future.

While many questions about the role of PI4K remain to be explored, my work opens up new aspects that were previously unknown. My work shows that the absence of the PI4K not only

leads to a significant disturbance in the developmental phenotypes of the mutant, but also to a dysfunction in the immune response as well as to a disturbed interaction with *Blumeria*.

7. REFERENCES

Aarts, N., Metz, M., Holub, E., Staskawicz, B.J., Daniels, M.J., Parker, J.E., 1998. Different requirements for EDS1 and NDR1 by disease resistance genes define at least two R gene-mediated signaling pathways in Arabidopsis. Proc Natl Acad Sci U S A 95, 10306–10311. https://doi.org/10.1073/pnas.95.17.10306

Abbas, S.M., 2019. Exogenous application of salicylic acid at different plant growth stages improves physiological processes in marigold (Tagetes erecta L.). PAKJAS 56, 541–548. https://doi.org/10.21162/PAKJAS/19.7276

Abu-Zahra, T., Shadiadeh, A., Abubaker, S.M., Qrunfleh, I., 2013. Influence of Auxin Concentrations on Different Ornamental Plants Rooting. International Journal of Botany 9, 96–99. https://doi.org/10.3923/ijb.2013.96.99

Aerts, N., Mendes, M.P., Wees, S.C.M.V., 2021. Multiple levels of crosstalk in hormone networks regulating plant defense. The Plant Journal 105, 489–504. https://doi.org/10.1111/tpj.15124

Aggarwal, C., Łabuz, J., Gabryś, H., 2013. Phosphoinositides Play Differential Roles in Regulating Phototropin1- and Phototropin2-Mediated Chloroplast Movements in Arabidopsis. PLOS ONE 8, e55393. https://doi.org/10.1371/journal.pone.0055393

Agorio, A., Giraudat, J., Bianchi, M.W., Marion, J., Espagne, C., Castaings, L., Lelièvre, F., Curie, C., Thomine, S., Merlot, S., 2017. Phosphatidylinositol 3-phosphate–binding protein AtPH1 controls the localization of the metal transporter NRAMP1 in Arabidopsis. Proceedings of the National Academy of Sciences 114, E3354–E3363. https://doi.org/10.1073/pnas.1702975114

Agrios, G.N., 2005. chapter two - Parasitism and disease development, in: Agrios, G.N. (Ed.), Plant Pathology (Fifth Edition). Academic Press, San Diego, pp. 77–104. https://doi.org/10.1016/B978-0-08-047378-9.50008-7

Akhter, S., Uddin, M.N., Jeong, I.S., Kim, D.W., Liu, X.-M., Bahk, J.D., 2016. Role of Arabidopsis AtPI4Kγ3, a type II phosphoinositide 4-kinase, in abiotic stress responses and floral transition. Plant Biotechnology Journal 14, 215–230. https://doi.org/10.1111/pbi.12376

Albrecht, C., Boutrot, F., Segonzac, C., Schwessinger, B., Gimenez-Ibanez, S., Chinchilla, D., Rathjen, J.P., de Vries, S.C., Zipfel, C., 2012. Brassinosteroids inhibit pathogen-associated molecular pattern–triggered immune signaling independent of the receptor kinase BAK1. Proceedings of the National Academy of Sciences 109, 303–308. https://doi.org/10.1073/pnas.1109921108

Albrecht, T., Argueso, C.T., 2017. Should I fight or should I grow now? The role of cytokinins in plant growth and immunity and in the growth-defence trade-off. Ann Bot 119, 725–735. https://doi.org/10.1093/aob/mcw211

Alfano, J.R., Bauer, D.W., Milos, T.M., Collmer, A., 1996. Analysis of the role of the Pseudomonas syringae pv. syringae HrpZ harpin in elicitation of the hypersensitive response in tobacco using functionally non-polar hrpZ deletion mutations, truncated HrpZ fragments, and hrmA mutations. Molecular Microbiology 19, 715–728. https://doi.org/10.1046/j.1365-2958.1996.415946.x

Ali, S., Ganai, B.A., Kamili, A.N., Bhat, A.A., Mir, Z.A., Bhat, J.A., Tyagi, A., Islam, S.T., Mushtaq, M., Yadav, P., Rawat, S., Grover, A., 2018. Pathogenesis-related proteins and peptides as promising tools for engineering plants with multiple stress tolerance. Microbiological Research 212–213, 29–37. https://doi.org/10.1016/j.micres.2018.04.008

Ali, S.S., Kumar, G.B.S., Khan, M., Doohan, F.M., 2013. Brassinosteroid enhances resistance to fusarium diseases of barley. Phytopathology 103, 1260–1267. https://doi.org/10.1094/PHYTO-05-13-0111-R

Allen, J.R., Wilkinson, E.G., Strader, L.C., 2022. Creativity comes from interactions: modules of protein interactions in plants. The FEBS Journal 289, 1492–1514. https://doi.org/10.1111/febs.15847

Anthony, R.G., Henriques, R., Helfer, A., Mészáros, T., Rios, G., Testerink, C., Munnik, T., Deák, M., Koncz, C., Bögre, L., 2004. A protein kinase target of a PDK1 signalling pathway is involved in root hair growth in Arabidopsis. EMBO J 23, 572–581. https://doi.org/10.1038/sj.emboj.7600068

Antignani, V., Klocko, A.L., Bak, G., Chandrasekaran, S.D., Dunivin, T., Nielsen, E., 2015. Recruitment of PLANT U-BOX13 and the PI4Kβ1/β2 Phosphatidylinositol-4 Kinases by the Small GTPase RabA4B Plays Important Roles during Salicylic Acid-Mediated Plant Defense Signaling in Arabidopsis. The Plant Cell 27, 243–261. https://doi.org/10.1105/tpc.114.134262

Apone, F., Alyeshmerni, N., Wiens, K., Chalmers, D., Chrispeels, M.J., Colucci, G., 2003. The G-Protein-Coupled Receptor GCR1 Regulates DNA Synthesis through Activation of Phosphatidylinositol-Specific Phospholipase C. Plant Physiology 133, 571–579. https://doi.org/10.1104/pp.103.026005

Apostolakos, P., Panteris, E., Galatis, B., 2008. The involvement of phospholipases C and D in the asymmetric division of subsidiary cell mother cells of Zea mays. Cell Motility 65, 863–875. https://doi.org/10.1002/cm.20308

Arent, S., Christensen, C.E., Pye, V.E., Nørgaard, A., Henriksen, A., 2010. The Multifunctional Protein in Peroxisomal β-Oxidation: Structure and substrate specificity of the Arabidopsis thaliana protein MFP2 *. Journal of Biological Chemistry 285, 24066–24077. https://doi.org/10.1074/jbc.M110.106005

Argueso, C.T., Raines, T., Kieber, J.J., 2010. Cytokinin signaling and transcriptional networks. Current Opinion in Plant Biology 13, 533–539. https://doi.org/10.1016/j.pbi.2010.08.006

Arisz, S.A., Testerink, C., Munnik, T., 2009. Plant PA signaling via diacylglycerol kinase. Biochimica et Biophysica Acta (BBA) - Molecular and Cell Biology of Lipids, Phospholipase D 1791, 869–875. https://doi.org/10.1016/j.bbalip.2009.04.006

Ashburner, M., Ball, C.A., Blake, J.A., Botstein, D., Butler, H., Cherry, J.M., Davis, A.P., Dolinski, K., Dwight, S.S., Eppig, J.T., Harris, M.A., Hill, D.P., Issel-Tarver, L., Kasarskis, A., Lewis, S., Matese, J.C., Richardson, J.E., Ringwald, M., Rubin, G.M., Sherlock, G., 2000. Gene Ontology: tool for the unification of biology. Nat Genet 25, 25–29. https://doi.org/10.1038/75556

Assaad, F.F., Qiu, J.-L., Youngs, H., Ehrhardt, D., Zimmerli, L., Kalde, M., Wanner, G., Peck, S.C., Edwards, H., Ramonell, K., Somerville, C.R., Thordal-Christensen, H., 2004a. The PEN1 syntaxin defines a novel cellular compartment upon fungal attack and is required for the timely assembly of papillae. Mol Biol Cell 15, 5118–5129. https://doi.org/10.1091/mbc.e04-02-0140

Assaad, F.F., Qiu, J.-L., Youngs, H., Ehrhardt, D., Zimmerli, L., Kalde, M., Wanner, G., Peck, S.C., Edwards, H., Ramonell, K., Somerville, C.R., Thordal-Christensen, H., 2004b. The PEN1 Syntaxin Defines a Novel Cellular Compartment upon Fungal Attack and Is Required for the Timely Assembly of Papillae. Mol Biol Cell 15, 5118–5129. https://doi.org/10.1091/mbc.E04-02-0140

Bacete, L., Mélida, H., Miedes, E., Molina, A., 2018. Plant cell wall-mediated immunity: cell wall changes trigger disease resistance responses. The Plant Journal 93, 614–636. https://doi.org/10.1111/tpj.13807

Balla, A., Tuymetova, G., Tsiomenko, A., Várnai, P., Balla, T., 2005. A plasma membrane pool of phosphatidylinositol 4-phosphate is generated by phosphatidylinositol 4-kinase type-III alpha: studies with the PH domains of the oxysterol binding protein and FAPP1. Mol Biol Cell 16, 1282–1295. https://doi.org/10.1091/mbc.e04-07-0578

Balla, T., 1998. Phosphatidylinositol 4-kinases. Biochim Biophys Acta 1436, 69–85. https://doi.org/10.1016/s0005-2760(98)00134-9

Barbero, F., Guglielmotto, M., Islam, M., Maffei, M.E., 2021. Extracellular Fragmented Self-DNA Is Involved in Plant Responses to Biotic Stress. Frontiers in Plant Science 12.

Bargmann, B.O.R., Laxalt, A.M., Riet, B. ter, van Schooten, B., Merquiol, E., Testerink, C., Haring, M.A., Bartels, D., Munnik, T., 2009. Multiple PLDs Required for High Salinity and Water Deficit Tolerance in Plants. Plant and Cell Physiology 50, 78–89. https://doi.org/10.1093/pcp/pcn173

Bartels, S., Lori, M., Mbengue, M., van Verk, M., Klauser, D., Hander, T., Böni, R., Robatzek, S., Boller, T., 2013. The family of Peps and their precursors in Arabidopsis: differential expression and localization but similar induction of pattern-triggered immune responses. Journal of Experimental Botany 64, 5309–5321. https://doi.org/10.1093/jxb/ert330

Barylko, B., Gerber, S.H., Binns, D.D., Grichine, N., Khvotchev, M., Südhof, T.C., Albanesi, J.P., 2001. A Novel Family of Phosphatidylinositol 4-Kinases Conserved from Yeast to Humans *. Journal of Biological Chemistry 276, 7705–7708. https://doi.org/10.1074/jbc.C000861200

Barylko, B., Mao, Y.S., Wlodarski, P., Jung, G., Binns, D.D., Sun, H.-Q., Yin, H.L., Albanesi, J.P., 2009. Palmitoylation Controls the Catalytic Activity and Subcellular Distribution of Phosphatidylinositol 4-Kinase IIα. J Biol Chem 284, 9994–10003. https://doi.org/10.1074/jbc.M900724200

Batth, R., Jain, M., Kumar, A., Nagar, P., Kumari, S., Mustafiz, A., 2020. Zn2+ dependent glyoxalase I plays the major role in methylglyoxal detoxification and salinity stress tolerance in plants. PLOS ONE 15, e0233493. https://doi.org/10.1371/journal.pone.0233493

Bednarek, P., Pislewska-Bednarek, M., Svatos, A., Schneider, B., Doubsky, J., Mansurova, M., Humphry, M., Consonni, C., Panstruga, R., Sanchez-Vallet, A., Molina, A., Schulze-Lefert, P., 2009. A glucosinolate metabolism pathway in living plant cells mediates broad-spectrum antifungal defense. Science 323, 101–106. https://doi.org/10.1126/science.1163732

Benjamins, R., Scheres, B., 2008. Auxin: The Looping Star in Plant Development. Annual Review of Plant Biology 59, 443–465. https://doi.org/10.1146/annurev.arplant.58.032806.103805

Berchtold, H., Reshetnikova, L., Reiser, C.O.A., Schirmer, N.K., Sprinzl, M., Hilgenfeld, R., 1993. Crystal structure of active elongation factor Tu reveals major domain rearrangements. Nature 365, 126–132. https://doi.org/10.1038/365126a0

Bethoney, K.A., King, M.C., Hinshaw, J.E., Ostap, E.M., Lemmon, M.A., 2009. A possible effector role for the pleckstrin homology (PH) domain of dynamin. Proceedings of the National Academy of Sciences 106, 13359–13364. https://doi.org/10.1073/pnas.0906945106

Bjornson, M., Zipfel, C., 2021. Plant immunity: Crosstalk between plant immune receptors. Current Biology 31, R796–R798. https://doi.org/10.1016/j.cub.2021.04.080

Blondeau, F., Ritter, B., Allaire, P.D., Wasiak, S., Girard, M., Hussain, N.K., Angers, A., Legendre-Guillemin, V., Roy, L., Boismenu, D., Kearney, R.E., Bell, A.W., Bergeron, J.J.M., McPherson, P.S., 2004. Tandem MS analysis of brain clathrin-coated vesicles reveals their critical involvement in synaptic vesicle recycling.

Proceedings of the National Academy of Sciences 101, 3833–3838. https://doi.org/10.1073/pnas.0308186101
Bolger, A.M., Lohse, M., Usadel, B., 2014. Trimmomatic: a flexible trimmer for Illumina sequence data. Bioinformatics 30, 2114–2120. https://doi.org/10.1093/bioinformatics/btu170
Boller, T., 1995. Chemoperception of microbial signals in plant cells. Annual review of plant physiology and plant molecular biology (USA).
Boller, T., Felix, G., 2009. A Renaissance of Elicitors: Perception of Microbe-Associated Molecular Patterns and Danger Signals by Pattern-Recognition Receptors. Annual review of plant biology 60, 379–406. https://doi.org/10.1146/annurev.arplant.57.032905.105346
Bolouri Moghaddam, M.R., Van den Ende, W., 2012. Sugars and plant innate immunity. Journal of Experimental Botany 63, 3989–3998. https://doi.org/10.1093/jxb/ers129
Bonardi, V., Dangl, J., 2012. How complex are intracellular immune receptor signaling complexes? Frontiers in Plant Science 3.
Botton, A., Ruperti, B., 2019. The Yes and No of the Ethylene Involvement in Abscission. Plants 8, 187. https://doi.org/10.3390/plants8060187
Brunner, F., Rosahl, S., Lee, J., Rudd, J.J., Geiler, C., Kauppinen, S., Rasmussen, G., Scheel, D., Nürnberger, T., 2002. Pep-13, a plant defense-inducing pathogen-associated pattern from Phytophthora transglutaminases. EMBO J 21, 6681–6688. https://doi.org/10.1093/emboj/cdf667
Brunoud, G., Wells, D.M., Oliva, M., Larrieu, A., Mirabet, V., Burrow, A.H., Beeckman, T., Kepinski, S., Traas, J., Bennett, M.J., Vernoux, T., 2012. A novel sensor to map auxin response and distribution at high spatio-temporal resolution. Nature 482, 103–106. https://doi.org/10.1038/nature10791
Burdett, H., Bentham, A.R., Williams, S.J., Dodds, P.N., Anderson, P.A., Banfield, M.J., Kobe, B., 2019. The Plant "Resistosome": Structural Insights into Immune Signaling. Cell Host & Microbe 26, 193–201. https://doi.org/10.1016/j.chom.2019.07.020
Caarls, L., 2016. Hormonal signaling in plant immunity [WWW Document]. URL https://dspace.library.uu.nl/handle/1874/340536 (accessed 8.12.22).
Cacas, J.-L., Buré, C., Grosjean, K., Gerbeau-Pissot, P., Lherminier, J., Rombouts, Y., Maes, E., Bossard, C., Gronnier, J., Furt, F., Fouillen, L., Germain, V., Bayer, E., Cluzet, S., Robert, F., Schmitter, J.-M., Deleu, M., Lins, L., Simon-Plas, F., Mongrand, S., 2016. Revisiting Plant Plasma Membrane Lipids in Tobacco: A Focus on Sphingolipids. Plant Physiol 170, 367–384. https://doi.org/10.1104/pp.15.00564
Cacas, J.-L., Gerbeau-Pissot, P., Fromentin, J., Cantrel, C., Thomas, D., Jeannette, E., Kalachova, T., Mongrand, S., Simon-Plas, F., Ruelland, E., 2017. Diacylglycerol kinases activate tobacco NADPH oxidase-dependent oxidative burst in response to cryptogein. Plant, Cell & Environment 40, 585–598. https://doi.org/10.1111/pce.12771
Cacas, J.-L., Vailleau, F., Davoine, C., Ennar, N., Agnel, J.-P., Tronchet, M., Ponchet, M., Blein, J.-P., Roby, D., Triantaphylides, C., Montillet, J.-L., 2005. The combined action of 9 lipoxygenase and galactolipase is sufficient to bring about programmed cell death during tobacco hypersensitive response. Plant, Cell & Environment 28, 1367–1378. https://doi.org/10.1111/j.1365-3040.2005.01369.x
Camehl, I., Drzewiecki, C., Vadassery, J., Shahollari, B., Sherameti, I., Forzani, C., Munnik, T., Hirt, H., Oelmüller, R., 2011. The OXI1 Kinase Pathway Mediates Piriformospora indica-Induced Growth Promotion in Arabidopsis. PLOS Pathogens 7, e1002051. https://doi.org/10.1371/journal.ppat.1002051

Casanova-Sáez, R., Mateo-Bonmatí, E., Ljung, K., 2021. Auxin Metabolism in Plants. Cold Spring Harb Perspect Biol 13, a039867. https://doi.org/10.1101/cshperspect.a039867

Cessna, S.G., Matsumoto, T.K., Lamb, G.N., Rice, S.J., Hochstedler, W.W., 2007. The externally derived portion of the hyperosmotic shock-activated cytosolic calcium pulse mediates adaptation to ionic stress in suspension-cultured tobacco cells. Journal of Plant Physiology 164, 815–823. https://doi.org/10.1016/j.jplph.2006.11.002

Chapman, E.J., Estelle, M., 2009. Cytokinin and auxin intersection in root meristems. Genome Biology 10, 210. https://doi.org/10.1186/gb-2009-10-2-210

Chen, H., Xue, L., Chintamanani, S., Germain, H., Lin, H., Cui, H., Cai, R., Zuo, J., Tang, X., Li, X., Guo, H., Zhou, J.-M., 2009. ETHYLENE INSENSITIVE3 and ETHYLENE INSENSITIVE3-LIKE1 repress SALICYLIC ACID INDUCTION DEFICIENT2 expression to negatively regulate plant innate immunity in Arabidopsis. Plant Cell 21, 2527–2540. https://doi.org/10.1105/tpc.108.065193

Chen, K.-E., Tillu, V.A., Chandra, M., Collins, B.M., 2018. Molecular Basis for Membrane Recruitment by the PX and C2 Domains of Class II Phosphoinositide 3-Kinase-C2α. Structure 26, 1612-1625.e4. https://doi.org/10.1016/j.str.2018.08.010

Chen, L., Huang, X.-X., Zhao, S.-M., Xiao, D.-W., Xiao, L.-T., Tong, J.-H., Wang, W.-S., Li, Y.-J., Ding, Z., Hou, B.-K., 2020. IPyA glucosylation mediates light and temperature signaling to regulate auxin-dependent hypocotyl elongation in Arabidopsis. Proceedings of the National Academy of Sciences 117, 6910–6917. https://doi.org/10.1073/pnas.2000172117

Chen, S., Ding, Y., Tian, H., Wang, S., Zhang, Y., n.d. WRKY54 and WRKY70 positively regulate SARD1 and CBP60g expression in plant immunity. Plant Signal Behav 16, 1932142. https://doi.org/10.1080/15592324.2021.1932142

Chen, X., Li, L., Xu, B., Zhao, S., Lu, P., He, Y., Ye, T., Feng, Y.-Q., Wu, Y., 2019. Phosphatidylinositol-specific phospholipase C2 functions in auxin-modulated root development. Plant, Cell & Environment 42, 1441–1457. https://doi.org/10.1111/pce.13492

Chen, Y.-L., Lee, C.-Y., Cheng, K.-T., Chang, W.-H., Huang, R.-N., Nam, H.G., Chen, Y.-R., 2014. Quantitative Peptidomics Study Reveals That a Wound-Induced Peptide from PR-1 Regulates Immune Signaling in Tomato. The Plant Cell 26, 4135–4148. https://doi.org/10.1105/tpc.114.131185

Cheng, Y., Li, Y., Huang, S., Huang, Y., Dong, X., Zhang, Y., Li, X., 2011. Stability of plant immune-receptor resistance proteins is controlled by SKP1-CULLIN1-F-box (SCF)-mediated protein degradation. Proceedings of the National Academy of Sciences of the United States of America 108, 14694–9. https://doi.org/10.1073/pnas.1105685108

Chinchilla, D., Bauer, Z., Regenass, M., Boller, T., Felix, G., 2006. The Arabidopsis Receptor Kinase FLS2 Binds flg22 and Determines the Specificity of Flagellin Perception. The Plant Cell 18, 465–476. https://doi.org/10.1105/tpc.105.036574

Chinchilla, D., Shan, L., He, P., de Vries, S., Kemmerling, B., 2009. One for all: the receptor-associated kinase BAK1. Trends Plant Sci 14, 535–541. https://doi.org/10.1016/j.tplants.2009.08.002

Chinchilla, D., Zipfel, C., Robatzek, S., Kemmerling, B., Nürnberger, T., Jones, J.D.G., Felix, G., Boller, T., 2007. A flagellin-induced complex of the receptor FLS2 and BAK1 initiates plant defence. Nature 448, 497–500. https://doi.org/10.1038/nature05999

Chivasa, S., Murphy, A.M., Hamilton, J.M., Lindsey, K., Carr, J.P., Slabas, A.R., 2009. Extracellular ATP is a regulator of pathogen defence in plants. The Plant Journal 60, 436–448. https://doi.org/10.1111/j.1365-313X.2009.03968.x

Cho, W., 2001. Membrane Targeting by C1 and C2 Domains *. Journal of Biological Chemistry 276, 32407–32410. https://doi.org/10.1074/jbc.R100007200

Choi, H.W., Manohar, M., Manosalva, P., Tian, M., Moreau, M., Klessig, D.F., 2016. Activation of Plant Innate Immunity by Extracellular High Mobility Group Box 3 and Its Inhibition by Salicylic Acid. PLOS Pathogens 12, e1005518. https://doi.org/10.1371/journal.ppat.1005518

Choi, J., Choi, D., Lee, S., Ryu, C.-M., Hwang, I., 2011. Cytokinins and plant immunity: old foes or new friends? Trends in Plant Science 16, 388–394. https://doi.org/10.1016/j.tplants.2011.03.003

Choi, S., Thapa, N., Tan, X., Hedman, A.C., Anderson, R.A., 2015. PIP kinases define PI4,5P2 signaling specificity by association with effectors. Biochimica et Biophysica Acta (BBA) - Molecular and Cell Biology of Lipids, Phosphoinositides 1851, 711–723. https://doi.org/10.1016/j.bbalip.2015.01.009

Choudhary, S.P., Yu, J.-Q., Yamaguchi-Shinozaki, K., Shinozaki, K., Tran, L.-S.P., 2012. Benefits of brassinosteroid crosstalk. Trends in Plant Science 17, 594–605. https://doi.org/10.1016/j.tplants.2012.05.012

Chowdhury, J., Henderson, M., Schweizer, P., Burton, R.A., Fincher, G.B., Little, A., 2014. Differential accumulation of callose, arabinoxylan and cellulose in nonpenetrated versus penetrated papillae on leaves of barley infected with Blumeria graminis f. sp. hordei. New Phytologist 204, 650–660. https://doi.org/10.1111/nph.12974

Chu, T.N., Bui, L.V., Hoang, M.T.T., 2020. Pseudomonas PS01 Isolated from Maize Rhizosphere Alters Root System Architecture and Promotes Plant Growth. Microorganisms 8, 471. https://doi.org/10.3390/microorganisms8040471

Ciarroni, S., Clarke, C.R., Liu, H., Eckshtain-Levi, N., Mazzaglia, A., Balestra, G.M., Vinatzer, B.A., 2018. A recombinant flagellin fragment, which includes the epitopes flg22 and flgII-28, provides a useful tool to study flagellin-triggered immunity. J Gen Plant Pathol 84, 169–175. https://doi.org/10.1007/s10327-018-0779-2

Claverie, J., Balacey, S., Lemaître-Guillier, C., Brulé, D., Chiltz, A., Granet, L., Noirot, E., Daire, X., Darblade, B., Héloir, M.-C., Poinssot, B., 2018. The Cell Wall-Derived Xyloglucan Is a New DAMP Triggering Plant Immunity in Vitis vinifera and Arabidopsis thaliana. Frontiers in Plant Science 9.

Clouse, S.D., Sasse, J.M., 1998. BRASSINOSTEROIDS: Essential Regulators of Plant Growth and Development. Annual Review of Plant Physiology and Plant Molecular Biology 49, 427–451. https://doi.org/10.1146/annurev.arplant.49.1.427

Cole, R.A., Fowler, J.E., 2006. Polarized growth: maintaining focus on the tip. Curr Opin Plant Biol 9, 579–588. https://doi.org/10.1016/j.pbi.2006.09.014

Collins, N.C., Thordal-Christensen, H., Lipka, V., Bau, S., Kombrink, E., Qiu, J.-L., Hückelhoven, R., Stein, M., Freialdenhoven, A., Somerville, S.C., Schulze-Lefert, P., 2003. SNARE-protein-mediated disease resistance at the plant cell wall. Nature 425, 973–977. https://doi.org/10.1038/nature02076

Colón-Carmona, A., You, R., Haimovitch-Gal, T., Doerner, P., 1999. Spatio-temporal analysis of mitotic activity with a labile cyclin–GUS fusion protein. The Plant Journal 20, 503–508. https://doi.org/10.1046/j.1365-313x.1999.00620.x

Corti Monzón, G., Pinedo, M., Lamattina, L., de la Canal, L., 2012. Sunflower root growth regulation: the role of jasmonic acid and its relation with auxins. Plant Growth Regul 66, 129–136. https://doi.org/10.1007/s10725-011-9636-4

Cousson, A., 2011. Arabidopsis Ca2+-dependent protein kinase CPK3 mediates relationship of putative inositol triphosphate receptor with slow-type anion channel. Biol Plant 55, 507–521. https://doi.org/10.1007/s10535-011-0117-4

Couto, D., Zipfel, C., 2016. Regulation of pattern recognition receptor signalling in plants. Nat Rev Immunol 16, 537–552. https://doi.org/10.1038/nri.2016.77

C. Pedras, M.S., E. Yaya, E., Glawischnig, E., 2011. The phytoalexins from cultivated and wild crucifers: Chemistry and biology. Natural Product Reports 28, 1381–1405. https://doi.org/10.1039/C1NP00020A

Cutler, S.R., Rodriguez, P.L., Finkelstein, R.R., Abrams, S.R., 2010. Abscisic Acid: Emergence of a Core Signaling Network. Annual Review of Plant Biology 61, 651–679. https://doi.org/10.1146/annurev-arplant-042809-112122

Cvrčková, F., Oulehlová, D., 2017. A new kymogram-based method reveals unexpected effects of marker protein expression and spatial anisotropy of cytoskeletal dynamics in plant cell cortex. Plant Methods 13, 19. https://doi.org/10.1186/s13007-017-0171-9

Daxinger, L., Hunter, B., Sheikh, M., Jauvion, V., Gasciolli, V., Vaucheret, H., Matzke, M., Furner, I., 2008. Unexpected silencing effects from T-DNA tags in Arabidopsis. Trends in Plant Science 13, 4–6. https://doi.org/10.1016/j.tplants.2007.10.007

De Camilli, P., Chen, H., Hyman, J., Panepucci, E., Bateman, A., Brunger, A.T., 2002. The ENTH domain. FEBS Letters 513, 11–18. https://doi.org/10.1016/S0014-5793(01)03306-3

De Matteis, M.A., Wilson, C., D'Angelo, G., 2013. Phosphatidylinositol-4-phosphate: The Golgi and beyond. BioEssays 35, 612–622. https://doi.org/10.1002/bies.201200180

de Silva, K., Laska, B., Brown, C., Sederoff, H.W., Khodakovskaya, M., 2011. Arabidopsis thaliana calcium-dependent lipid-binding protein (AtCLB): a novel repressor of abiotic stress response. Journal of Experimental Botany 62, 2679–2689. https://doi.org/10.1093/jxb/erq468

De Vos, M., Van Zaanen, W., Koornneef, A., Korzelius, J.P., Dicke, M., Van Loon, L.C., Pieterse, C.M.J., 2006. Herbivore-Induced Resistance against Microbial Pathogens in Arabidopsis. Plant Physiology 142, 352–363. https://doi.org/10.1104/pp.106.083907

Deak, M., Casamayor, A., Currie, R.A., Peter Downes, C., Alessi, D.R., 1999. Characterisation of a plant 3-phosphoinositide-dependent protein kinase-1 homologue which contains a pleckstrin homology domain. FEBS Letters 451, 220–226. https://doi.org/10.1016/S0014-5793(99)00556-6

Dean, J.V., Mohammed, L.A., Fitzpatrick, T., 2005. The formation, vacuolar localization, and tonoplast transport of salicylic acid glucose conjugates in tobacco cell suspension cultures. Planta 221, 287–296.

Dean, J.V., Shah, R.P., Mohammed, L.A., 2003. Formation and vacuolar localization of salicylic acid glucose conjugates in soybean cell suspension cultures. Physiologia Plantarum 118, 328–336. https://doi.org/10.1034/j.1399-3054.2003.00117.x

Delage, E., Ruelland, E., Guillas, I., Zachowski, A., Puyaubert, J., 2012. Arabidopsis Type-III Phosphatidylinositol 4-Kinases β1 and β2 are Upstream of the Phospholipase C Pathway Triggered by Cold Exposure. Plant and Cell Physiology 53, 565–576. https://doi.org/10.1093/pcp/pcs011

Dempsey, D.A., Vlot, A.C., Wildermuth, M.C., Klessig, D.F., 2011. Salicylic Acid Biosynthesis and Metabolism. Arabidopsis Book 9, e0156. https://doi.org/10.1199/tab.0156

Devaiah, S.P., Pan, X., Hong, Y., Roth, M., Welti, R., Wang, X., 2007. Enhancing seed quality and viability by suppressing phospholipase D in Arabidopsis. The Plant Journal 50, 950–957. https://doi.org/10.1111/j.1365-313X.2007.03103.x

DeWald, D.B., Torabinejad, J., Jones, C.A., Shope, J.C., Cangelosi, A.R., Thompson, J.E., Prestwich, G.D., Hama, H., 2001. Rapid accumulation of phosphatidylinositol 4,5-bisphosphate and inositol 1,4,5-trisphosphate correlates with calcium mobilization in

salt-stressed arabidopsis1. Plant Physiology 126, 759–769. https://doi.org/10.1104/pp.126.2.759
Di Fino, L.M., D'Ambrosio, J.M., Tejos, R., van Wijk, R., Lamattina, L., Munnik, T., Pagnussat, G.C., Laxalt, A.M., 2017. Arabidopsis phosphatidylinositol-phospholipase C2 (PLC2) is required for female gametogenesis and embryo development. Planta 245, 717–728. https://doi.org/10.1007/s00425-016-2634-z
Dieck, C., Boss, W., Perera, I., 2012. A Role for Phosphoinositides in Regulating Plant Nuclear Functions. Frontiers in Plant Science 3.
Distéfano, A.M., Scuffi, D., García-Mata, C., Lamattina, L., Laxalt, A.M., 2012. Phospholipase Dδ is involved in nitric oxide-induced stomatal closure. Planta 236, 1899–1907. https://doi.org/10.1007/s00425-012-1745-4
Dixit, S., Upadhyay, S.K., Singh, H., Sidhu, O.P., Verma, P.C., K, C., 2013. Enhanced Methanol Production in Plants Provides Broad Spectrum Insect Resistance. PLOS ONE 8, e79664. https://doi.org/10.1371/journal.pone.0079664
Djafi, N., Vergnolle, C., Cantrel, C., Wietrzyński, W., Delage, E., Cochet, F., Puyaubert, J., Soubigou-Taconnat, L., Gey, D., Collin, S., Balzergue, S., Zachowski, A., Ruelland, E., 2013. The Arabidopsis DREB2 genetic pathway is constitutively repressed by basal phosphoinositide-dependent phospholipase C coupled to diacylglycerol kinase. Frontiers in Plant Science 4, 307. https://doi.org/10.3389/fpls.2013.00307
Dobin, A., Davis, C.A., Schlesinger, F., Drenkow, J., Zaleski, C., Jha, S., Batut, P., Chaisson, M., Gingeras, T.R., 2013. STAR: ultrafast universal RNA-seq aligner. Bioinformatics 29, 15–21. https://doi.org/10.1093/bioinformatics/bts635
Dolan, L., Janmaat, K., Willemsen, V., Linstead, P., Poethig, S., Roberts, K., Scheres, B., 1993. Cellular organisation of the Arabidopsis thaliana root. Development 119, 71–84. https://doi.org/10.1242/dev.119.1.71
Dong, C.-H., Rivarola, M., Resnick, J.S., Maggin, B.D., Chang, C., 2008. Subcellular co-localization of Arabidopsis RTE1 and ETR1 supports a regulatory role for RTE1 in ETR1 ethylene signaling. The Plant Journal 53, 275–286. https://doi.org/10.1111/j.1365-313X.2007.03339.x
Dong, H., Delaney, T.P., Bauer, D.W., Beer, S.V., 1999. Harpin induces disease resistance in Arabidopsis through the systemic acquired resistance pathway mediated by salicylic acid and the NIM1 gene. The Plant Journal 20, 207–215. https://doi.org/10.1046/j.1365-313x.1999.00595.x
Dong, W., Lv, H., Xia, G., Wang, M., 2012. Does diacylglycerol serve as a signaling molecule in plants? Plant Signaling & Behavior 7, 472–475. https://doi.org/10.4161/psb.19644
Dong, X., 2004. NPR1, all things considered. Current Opinion in Plant Biology 7, 547–552. https://doi.org/10.1016/j.pbi.2004.07.005
Dove, S.K., Lloyd, C.W., Drøbak, B.K., 1994. Identification of a phosphatidylinositol 3-hydroxy kinase in plant cells: association with the cytoskeleton. Biochem J 303 (Pt 2), 347–350. https://doi.org/10.1042/bj3030347
Dowd, P.E., Coursol, S., Skirpan, A.L., Kao, T., Gilroy, S., 2006. Petunia Phospholipase C1 Is Involved in Pollen Tube Growth. The Plant Cell 18, 1438–1453. https://doi.org/10.1105/tpc.106.041582
Du, M., Spalding, E.P., Gray, W.M., 2020. Rapid Auxin-Mediated Cell Expansion. Annu Rev Plant Biol 71, 379–402. https://doi.org/10.1146/annurev-arplant-073019-025907
Ebrahim-Nesbat, F., Heitefuss, R., Rohringer, R., 1986. Ultrastructural and Histochemical Studies on Mildew of Barley (Erysiphe graminis DC. f. sp. hordei Marchal). Journal of Phytopathology 117, 289–300. https://doi.org/10.1111/j.1439-0434.1986.tb04367.x

Edgar, R., Domrachev, M., Lash, A.E., 2002. Gene Expression Omnibus: NCBI gene expression and hybridization array data repository. Nucleic Acids Res 30, 207–210. https://doi.org/10.1093/nar/30.1.207

Erbs, G., Newman, M.-A., 2012. The role of lipopolysaccharide and peptidoglycan, two glycosylated bacterial microbe-associated molecular patterns (MAMPs), in plant innate immunity. Mol Plant Pathol 13, 95–104. https://doi.org/10.1111/j.1364-3703.2011.00730.x

Escocard de Azevedo Manhães, A.M., Ortiz-Morea, F.A., He, P., Shan, L., 2021. Plant plasma membrane-resident receptors: Surveillance for infections and coordination for growth and development. Journal of Integrative Plant Biology 63, 79–101. https://doi.org/10.1111/jipb.13051

Espinoza, C., Liang, Y., Stacey, G., 2017. Chitin receptor CERK1 links salt stress and chitin-triggered innate immunity in Arabidopsis. The Plant Journal 89, 984–995. https://doi.org/10.1111/tpj.13437

Faizal, A., Geelen, D., 2013. Saponins and their role in biological processes in plants. Phytochem Rev 12, 877–893. https://doi.org/10.1007/s11101-013-9322-4

Fan, L., Zheng, S., Cui, D., Wang, X., 1999. Subcellular distribution and tissue expression of phospholipase Dalpha, Dbeta, and Dgamma in Arabidopsis. Plant Physiol 119, 1371–1378. https://doi.org/10.1104/pp.119.4.1371

Fan, L., Zheng, S., Wang, X., 1997. Antisense suppression of phospholipase D alpha retards abscisic acid- and ethylene-promoted senescence of postharvest Arabidopsis leaves. The Plant Cell 9, 2183–2196. https://doi.org/10.1105/tpc.9.12.2183

Fasshauer, D., Sutton, R.B., Brunger, A.T., Jahn, R., 1998. Conserved structural features of the synaptic fusion complex: SNARE proteins reclassified as Q- and R-SNAREs. Proc Natl Acad Sci U S A 95, 15781–15786.

Fauth, M., Schweizer, P., Buchala, A., Markstädter, C., Riederer, M., Kato, T., Kauss, H., 1998. Cutin Monomers and Surface Wax Constituents Elicit H2O2 in Conditioned Cucumber Hypocotyl Segments and Enhance the Activity of Other H2O2Elicitors1. Plant Physiology 117, 1373–1380. https://doi.org/10.1104/pp.117.4.1373

Felix, G., Boller, T., 2003. Molecular sensing of bacteria in plants. The highly conserved RNA-binding motif RNP-1 of bacterial cold shock proteins is recognized as an elicitor signal in tobacco. J Biol Chem 278, 6201–6208. https://doi.org/10.1074/jbc.M209880200

Figueroa-Balderas, R.E., García-Ponce, B., Rocha-Sosa, M., 2006. Hormonal and stress induction of the gene encoding common bean acetyl-coenzyme A carboxylase. Plant Physiol 142, 609–619. https://doi.org/10.1104/pp.106.085597

Ford, M.G.J., Mills, I.G., Peter, B.J., Vallis, Y., Praefcke, G.J.K., Evans, P.R., McMahon, H.T., 2002. Curvature of clathrin-coated pits driven by epsin. Nature 419, 361–366. https://doi.org/10.1038/nature01020

Fujii, S., Kobayashi, K., Lin, Y.-C., Liu, Y., Nakamura, Y., Wada, H., 2021. Phosphatidylglycerol synthesis facilitates plastid gene expression and light induction of nuclear photosynthetic genes. https://doi.org/10.1101/2021.09.08.459525

Fujimoto, M., Suda, Y., Vernhettes, S., Nakano, A., Ueda, T., 2015. Phosphatidylinositol 3-Kinase and 4-Kinase Have Distinct Roles in Intracellular Trafficking of Cellulose Synthase Complexes in Arabidopsis thaliana. Plant and Cell Physiology 56, 287–298. https://doi.org/10.1093/pcp/pcu195

Gagnot, S., Tamby, J.-P., Martin-Magniette, M.-L., Bitton, F., Taconnat, L., Balzergue, S., Aubourg, S., Renou, J.-P., Lecharny, A., Brunaud, V., 2008. CATdb: a public access to Arabidopsis transcriptome data from the URGV-CATMA platform. Nucleic Acids Res 36, D986-990. https://doi.org/10.1093/nar/gkm757

Galletti, R., Ferrari, S., De Lorenzo, G., 2011. Arabidopsis MPK3 and MPK6 Play Different Roles in Basal and Oligogalacturonide- or Flagellin-Induced Resistance against Botrytis cinerea. Plant Physiology 157, 804–814. https://doi.org/10.1104/pp.111.174003

Galvan-Ampudia, C.S., Cerutti, G., Legrand, J., Brunoud, G., Martin-Arevalillo, R., Azais, R., Bayle, V., Moussu, S., Wenzl, C., Jaillais, Y., Lohmann, J.U., Godin, C., Vernoux, T., 2020. Temporal integration of auxin information for the regulation of patterning. eLife 9, e55832. https://doi.org/10.7554/eLife.55832

Galvão, R.M., Kota, U., Soderblom, E.J., Goshe, M.B., Boss, W.F., 2008. Characterization of a new family of protein kinases from Arabidopsis containing phosphoinositide 3/4-kinase and ubiquitin-like domains. Biochem J 409, 117–127. https://doi.org/10.1042/BJ20070959

Gao, K., Liu, Y.-L., Li, B., Zhou, R.-G., Sun, D.-Y., Zheng, S.-Z., 2014. Arabidopsis thaliana Phosphoinositide-Specific Phospholipase C Isoform 3 (AtPLC3) and AtPLC9 have an Additive Effect on Thermotolerance. Plant and Cell Physiology 55, 1873–1883. https://doi.org/10.1093/pcp/pcu116

Gardiner, J., Harper, J., Weerakoon, N., Collings, D., Ritchie, S., Gilroy, S., Cyr, R., Marc, J., 2001. A 90-kD Phospholipase D from Tobacco Binds to Microtubules and the Plasma Membrane. The Plant cell 13, 2143–58. https://doi.org/10.2307/3871433

Garmier, M., Priault, P., Vidal, G., Driscoll, S., Djebbar, R., Boccara, M., Mathieu, C., Foyer, C.H., Paepe, R.D., 2007. Light and Oxygen Are Not Required for Harpin-induced Cell Death *. Journal of Biological Chemistry 282, 37556–37566. https://doi.org/10.1074/jbc.M707226200

Garner, C.M., Spears, B.J., Su, J., Cseke, L.J., Smith, S.N., Rogan, C.J., Gassmann, W., 2021. Opposing functions of the plant TOPLESS gene family during SNC1-mediated autoimmunity. PLOS Genetics 17, e1009026. https://doi.org/10.1371/journal.pgen.1009026

Gimenez-Ibanez, S., Hann, D.R., Ntoukakis, V., Petutschnig, E., Lipka, V., Rathjen, J.P., 2009. AvrPtoB Targets the LysM Receptor Kinase CERK1 to Promote Bacterial Virulence on Plants. Current Biology 19, 423–429. https://doi.org/10.1016/j.cub.2009.01.054

Glazebrook, J., 2005. Contrasting Mechanisms of Defense Against Biotrophic and Necrotrophic Pathogens. Annual Review of Phytopathology 43, 205–27.

Glazebrook, J., Ausubel, F.M., 1994. Isolation of phytoalexin-deficient mutants of Arabidopsis thaliana and characterization of their interactions with bacterial pathogens. Proceedings of the National Academy of Sciences 91, 8955–8959. https://doi.org/10.1073/pnas.91.19.8955

Göhre, V., Spallek, T., Häweker, H., Mersmann, S., Mentzel, T., Boller, T., de Torres, M., Mansfield, J.W., Robatzek, S., 2008. Plant Pattern-Recognition Receptor FLS2 Is Directed for Degradation by the Bacterial Ubiquitin Ligase AvrPtoB. Current Biology 18, 1824–1832. https://doi.org/10.1016/j.cub.2008.10.063

Gomez, R.E., Chambaud, C., Lupette, J., Castets, J., Pascal, S., Brocard, L., Noack, L., Jaillais, Y., Joubès, J., Bernard, A., 2022. Phosphatidylinositol-4-phosphate controls autophagosome formation in Arabidopsis thaliana. Nat Commun 13, 4385. https://doi.org/10.1038/s41467-022-32109-2

Gómez-Gómez, L., Bauer, Z., Boller, T., 2001. Both the extracellular leucine-rich repeat domain and the kinase activity of FSL2 are required for flagellin binding and signaling in Arabidopsis. Plant Cell 13, 1155–1163.

Granado, J., Felix, G., Boller, T., 1995. Perception of Fungal Sterols in Plants (Subnanomolar Concentrations of Ergosterol Elicit Extracellular Alkalinization in Tomato Cells). Plant Physiol 107, 485–490. https://doi.org/10.1104/pp.107.2.485

Gronnier, J., Crowet, J.-M., Habenstein, B., Nasir, M.N., Bayle, V., Hosy, E., Platre, M.P., Gouguet, P., Raffaele, S., Martinez, D., Grelard, A., Loquet, A., Simon-Plas, F., Gerbeau-Pissot, P., Der, C., Bayer, E.M., Jaillais, Y., Deleu, M., Germain, V., Lins, L., Mongrand, S., 2017. Structural basis for plant plasma membrane protein dynamics and organization into functional nanodomains. eLife 6, e26404. https://doi.org/10.7554/eLife.26404

Großkinsky, D.K., Tafner, R., Moreno, M.V., Stenglein, S.A., García de Salamone, I.E., Nelson, L.M., Novák, O., Strnad, M., van der Graaff, E., Roitsch, T., 2016. Cytokinin production by Pseudomonas fluorescens G20-18 determines biocontrol activity against Pseudomonas syringae in Arabidopsis. Sci Rep 6, 23310. https://doi.org/10.1038/srep23310

Groszmann, M., Gonzalez-Bayon, R., Lyons, R.L., Greaves, I.K., Kazan, K., Peacock, W.J., Dennis, E.S., 2015. Hormone-regulated defense and stress response networks contribute to heterosis in Arabidopsis F1 hybrids. Proceedings of the National Academy of Sciences 112, E6397–E6406. https://doi.org/10.1073/pnas.1519926112

Gu, J., Li, Z., Mao, Y., Struik, P.C., Zhang, H., Liu, L., Wang, Z., Yang, J., 2018. Roles of nitrogen and cytokinin signals in root and shoot communications in maximizing of plant productivity and their agronomic applications. Plant Science 274, 320–331. https://doi.org/10.1016/j.plantsci.2018.06.010

Gust, A.A., Biswas, R., Lenz, H.D., Rauhut, T., Ranf, S., Kemmerling, B., Götz, F., Glawischnig, E., Lee, J., Felix, G., Nürnberger, T., 2007. Bacteria-derived Peptidoglycans Constitute Pathogen-associated Molecular Patterns Triggering Innate Immunity in Arabidopsis*. Journal of Biological Chemistry 282, 32338–32348. https://doi.org/10.1074/jbc.M704886200

Habets, M., Offringa, R., 2014. PIN-driven polar auxin transport in plant developmental plasticity: A key target for environmental and endogenous signals. The New phytologist 203. https://doi.org/10.1111/nph.12831

Halkier, B.A., Gershenzon, J., 2006. Biology and biochemistry of glucosinolates. Annu. Rev. Plant Biol. 57, 303–333. https://doi.org/10.1146/annurev.arplant.57.032905.105228

Han, X., Yang, Y., 2021. Phospholipids in Salt Stress Response. Plants 10, 2204. https://doi.org/10.3390/plants10102204

Hander, T., Fernández-Fernández, Á.D., Kumpf, R.P., Willems, P., Schatowitz, H., Rombaut, D., Staes, A., Nolf, J., Pottie, R., Yao, P., Gonçalves, A., Pavie, B., Boller, T., Gevaert, K., Breusegem, F.V., Bartels, S., Stael, S., 2019. Damage on plants activates Ca2+-dependent metacaspases for release of immunomodulatory peptides. Science 363. https://doi.org/10.1126/science.aar7486

Hao, W., Collier, S.M., Moffett, P., Chai, J., 2013. Structural basis for the interaction between the potato virus X resistance protein (Rx) and its cofactor Ran GTPase-activating protein 2 (RanGAP2). J Biol Chem 288, 35868–35876. https://doi.org/10.1074/jbc.M113.517417

Hashimoto-Sugimoto, M., Higaki, T., Yaeno, T., Nagami, A., Irie, M., Fujimi, M., Miyamoto, M., Akita, K., Negi, J., Shirasu, K., Hasezawa, S., Iba, K., 2013. A Munc13-like protein in Arabidopsis mediates H+-ATPase translocation that is essential for stomatal responses. Nat Commun 4, 2215. https://doi.org/10.1038/ncomms3215

He, J.-X., Gendron, J.M., Sun, Y., Gampala, S.S.L., Gendron, N., Sun, C.Q., Wang, Z.-Y., 2005. BZR1 Is a Transcriptional Repressor with Dual Roles in Brassinosteroid

Homeostasis and Growth Responses. Science 307, 1634–1638. https://doi.org/10.1126/science.1107580
Heidstra, R., Sabatini, S., 2014. Plant and animal stem cells: similar yet different. Nat Rev Mol Cell Biol 15, 301–312. https://doi.org/10.1038/nrm3790
Helling, D., Possart, A., Cottier, S., Klahre, U., Kost, B., 2006. Pollen Tube Tip Growth Depends on Plasma Membrane Polarization Mediated by Tobacco PLC3 Activity and Endocytic Membrane Recycling. The Plant Cell 18, 3519–3534. https://doi.org/10.1105/tpc.106.047373
Hervé, C., Marcus, S.E., Knox, J.P., 2011. Monoclonal antibodies, carbohydrate-binding modules, and the detection of polysaccharides in plant cell walls. Methods Mol Biol 715, 103–113. https://doi.org/10.1007/978-1-61779-008-9_7
Higaki, T., Hashimoto-Sugimoto, M., Akita, K., Iba, K., Hasezawa, S., 2014. Dynamics and Environmental Responses of PATROL1 in Arabidopsis Subsidiary Cells. Plant and Cell Physiology 55, 773–780. https://doi.org/10.1093/pcp/pct151
Hind, S., Malinowski, R., Yalamanchili, R., Stratmann, J.W., 2010. Tissue-type specific systemin perception and the elusive systemin receptor. Plant Signaling & Behavior 5, 42–44. https://doi.org/10.4161/psb.5.1.10119
Hirayama, T., Ohto, C., Mizoguchi, T., Shinozaki, K., 1995. A gene encoding a phosphatidylinositol-specific phospholipase C is induced by dehydration and salt stress in Arabidopsis thaliana. Proc Natl Acad Sci U S A 92, 3903–3907. https://doi.org/10.1073/pnas.92.9.3903
Holstein, S.E.H., Oliviusson, P., 2005. Sequence analysis of Arabidopsis thaliana E/ANTH-domain-containing proteins: membrane tethers of the clathrin-dependent vesicle budding machinery. Protoplasma 226, 13–21. https://doi.org/10.1007/s00709-005-0105-7
Hong, Y., Pan, X., Welti, R., Wang, X., 2008. Phospholipase Dα3 Is Involved in the Hyperosmotic Response in Arabidopsis. Plant Cell 20, 803–816. https://doi.org/10.1105/tpc.107.056390
Hong, Y., Zhao, J., Guo, L., Kim, S.-C., Deng, X., Wang, G., Zhang, G., Li, M., Wang, X., 2016. Plant phospholipases D and C and their diverse functions in stress responses. Progress in Lipid Research 62, 55–74. https://doi.org/10.1016/j.plipres.2016.01.002
Hou, S., Liu, Z., Shen, H., Wu, D., 2019. Damage-Associated Molecular Pattern-Triggered Immunity in Plants. Frontiers in Plant Science 10.
Hou, S., Wang, X., Chen, D., Yang, X., Wang, M., Turrà, D., Pietro, A.D., Zhang, W., 2014. The Secreted Peptide PIP1 Amplifies Immunity through Receptor-Like Kinase 7. PLOS Pathogens 10, e1004331. https://doi.org/10.1371/journal.ppat.1004331
Huaping, H., Xiaohui, J., Lunying, W., Junsheng, H., 2017. Chitin elicitor receptor kinase 1 (CERK1) is required for the non-host defense response of Arabidopsis to Fusarium oxysporum f. Sp. cubense. Eur J Plant Pathol 147, 571–578. https://doi.org/10.1007/s10658-016-1026-3
Hückelhoven, R., 2005. Powdery mildew susceptibility and biotrophic infection strategies. FEMS Microbiology Letters 245, 9–17. https://doi.org/10.1016/j.femsle.2005.03.001
Huffaker, A., Pearce, G., Ryan, C.A., 2006. An endogenous peptide signal in Arabidopsis activates components of the innate immune response. PNAS 103, 10098–10103. https://doi.org/10.1073/pnas.0603727103
Hwang, I., Sheen, J., Müller, B., 2012. Cytokinin Signaling Networks. Annual Review of Plant Biology 63, 353–380. https://doi.org/10.1146/annurev-arplant-042811-105503
Ischebeck, T., Seiler, S., Heilmann, I., 2010. At the poles across kingdoms: phosphoinositides and polar tip growth. Protoplasma 240, 13–31. https://doi.org/10.1007/s00709-009-0093-0

Ischebeck, T., Stenzel, I., Hempel, F., Jin, X., Mosblech, A., Heilmann, I., 2011. Phosphatidylinositol-4,5-bisphosphate influences Nt-Rac5-mediated cell expansion in pollen tubes of Nicotiana tabacum. The Plant Journal 65, 453–468. https://doi.org/10.1111/j.1365-313X.2010.04435.x

Ischebeck, T., Werner, S., Krishnamoorthy, P., Lerche, J., Meijón, M., Stenzel, I., Löfke, C., Wiessner, T., Im, Y.J., Perera, I.Y., Iven, T., Feussner, I., Busch, W., Boss, W.F., Teichmann, T., Hause, B., Persson, S., Heilmann, I., 2013. Phosphatidylinositol 4,5-Bisphosphate Influences PIN Polarization by Controlling Clathrin-Mediated Membrane Trafficking in Arabidopsis. The Plant Cell 25, 4894–4911. https://doi.org/10.1105/tpc.113.116582

Itoh, T., Koshiba, S., Kigawa, T., Kikuchi, A., Yokoyama, S., Takenawa, T., 2001. Role of the ENTH Domain in Phosphatidylinositol-4,5-Bisphosphate Binding and Endocytosis. Science 291, 1047–1051. https://doi.org/10.1126/science.291.5506.1047

Jaillais, Y., Fobis-Loisy, I., Miège, C., Rollin, C., Gaude, T., 2006. AtSNX1 defines an endosome for auxin-carrier trafficking in Arabidopsis. Nature 443, 106–109. https://doi.org/10.1038/nature05046

Jaillais, Y., Ott, T., 2020. The Nanoscale Organization of the Plasma Membrane and Its Importance in Signaling: A Proteolipid Perspective1. Plant Physiology 182, 1682–1696. https://doi.org/10.1104/pp.19.01349

Janská, A., Marsík, P., Zelenková, S., Ovesná, J., 2010. Cold stress and acclimation - what is important for metabolic adjustment? Plant Biol (Stuttg) 12, 395–405. https://doi.org/10.1111/j.1438-8677.2009.00299.x

Jeandet, P., 2015. Phytoalexins: Current Progress and Future Prospects. Molecules 20, 2770–2774. https://doi.org/10.3390/molecules20022770

Jelínková, A., Malínská, K., Simon, S., Kleine-Vehn, J., Pařezová, M., Pejchar, P., Kubeš, M., Martinec, J., Friml, J., Zažímalová, E., Petrášek, J., 2010. Probing plant membranes with FM dyes: tracking, dragging or blocking? The Plant Journal 61, 883–892. https://doi.org/10.1111/j.1365-313X.2009.04102.x

Jia, Q., Zhang, S., Lin, Y., Zhang, J., Li, L., Chen, H., Zhang, Q., 2021. Phospholipase Dδ regulates pollen tube growth by modulating actin cytoskeleton organization in Arabidopsis. Plant Signaling & Behavior 16, 1915610. https://doi.org/10.1080/15592324.2021.1915610

Jiang, C.-H., Fan, Z.-H., Xie, P., Guo, J.-H., 2016. Bacillus cereus AR156 Extracellular Polysaccharides Served as a Novel Micro-associated Molecular Pattern to Induced Systemic Immunity to Pst DC3000 in Arabidopsis. Frontiers in Microbiology 7.

Jiang, L., Wu, J., Fan, S., Li, W., Dong, L., Cheng, Q., Xu, P., Zhang, S., 2015. Isolation and Characterization of a Novel Pathogenesis-Related Protein Gene (GmPRP) with Induced Expression in Soybean (Glycine max) during Infection with Phytophthora sojae. PLOS ONE 10, e0129932. https://doi.org/10.1371/journal.pone.0129932

Jin, J.B., Kim, Y.A., Kim, S.J., Lee, S.H., Kim, D.H., Cheong, G.-W., Hwang, I., 2001. A New Dynamin-Like Protein, ADL6, Is Involved in Trafficking from the trans-Golgi Network to the Central Vacuole in Arabidopsis. The Plant Cell 13, 1511–1526. https://doi.org/10.1105/TPC.000534

Johansson, O.N., Fantozzi, E., Fahlberg, P., Nilsson, A.K., Buhot, N., Tör, M., Andersson, M.X., 2014a. Role of the penetration-resistance genes PEN1, PEN2 and PEN3 in the hypersensitive response and race-specific resistance in Arabidopsis thaliana. The Plant Journal 79, 466–476. https://doi.org/10.1111/tpj.12571

Johansson, O.N., Fantozzi, E., Fahlberg, P., Nilsson, A.K., Buhot, N., Tör, M., Andersson, M.X., 2014b. Role of the penetration-resistance genes PEN1, PEN2 and PEN3 in the

hypersensitive response and race-specific resistance in Arabidopsis thaliana. The Plant Journal 79, 466–476. https://doi.org/10.1111/tpj.12571

Jones, D.A., Takemoto, D., 2004. Plant innate immunity - direct and indirect recognition of general and specific pathogen-associated molecules. Curr Opin Immunol 16, 48–62. https://doi.org/10.1016/j.coi.2003.11.016

Jung, J.-Y., Kim, Y.-W., Kwak, J.M., Hwang, J.-U., Young, J., Schroeder, J.I., Hwang, I., Lee, Y., 2002. Phosphatidylinositol 3- and 4-phosphate are required for normal stomatal movements. Plant Cell 14, 2399–2412. https://doi.org/10.1105/tpc.004143

Junková, P., Neubergerová, M., Kalachova, T., Valentová, O., Janda, M., 2021. Regulation of the microsomal proteome by salicylic acid and deficiency of phosphatidylinositol-4-kinases β1 and β2 in Arabidopsis thaliana. Proteomics 21, 2000223. https://doi.org/10.1002/pmic.202000223

Kadotani, N., Akagi, A., Takatsuji, H., Miwa, T., Igarashi, D., 2016. Exogenous proteinogenic amino acids induce systemic resistance in rice. BMC Plant Biology 16, 60. https://doi.org/10.1186/s12870-016-0748-x

Kalachova, T., Janda, M., Šašek, V., Ortmannová, J., Nováková, P., Dobrev, I.P., Kravets, V., Guivarc'h, A., Moura, D., Burketová, L., Valentová, O., Ruelland, E., 2020. Identification of salicylic acid-independent responses in an Arabidopsis phosphatidylinositol 4-kinase beta double mutant. Ann Bot 125, 775–784. https://doi.org/10.1093/aob/mcz112

Kalachova, T., Leontovyčová, H., Iakovenko, O., Pospíchalová, R., Maršík, P., Klouček, P., Janda, M., Valentová, O., Kocourková, D., Martinec, J., Burketová, L., Ruelland, E., 2019. Interplay between phosphoinositides and actin cytoskeleton in the regulation of immunity related responses in Arabidopsis thaliana seedlings. Environmental and Experimental Botany 167, 103867. https://doi.org/10.1016/j.envexpbot.2019.103867

Kalachova, T., Puga-Freitas, R., Kravets, V., Soubigou-Taconnat, L., Repellin, A., Balzergue, S., Zachowski, A., Ruelland, E., 2016. The inhibition of basal phosphoinositide-dependent phospholipase C activity in Arabidopsis suspension cells by abscisic or salicylic acid acts as a signalling hub accounting for an important overlap in transcriptome remodelling induced by these hormones. Environmental and Experimental Botany 123, 37–49. https://doi.org/10.1016/j.envexpbot.2015.11.003

Kalachova, T., Škrabálková, E., Pateyron, S., Soubigou-Taconnat, L., Djafi, N., Collin, S., Sekereš, J., Burketová, L., Potocký, M., Pejchar, P., Ruelland, E., 2022. DIACYLGLYCEROL KINASE 5 participates in flagellin-induced signaling in Arabidopsis. Plant Physiology kiac354. https://doi.org/10.1093/plphys/kiac354

Kamada-Nobusada, T., Sakakibara, H., 2009. Molecular basis for cytokinin biosynthesis. Phytochemistry 70, 444–449. https://doi.org/10.1016/j.phytochem.2009.02.007

Kanai, F., Liu, H., Field, S.J., Akbary, H., Matsuo, T., Brown, G.E., Cantley, L.C., Yaffe, M.B., 2001. The PX domains of p47phox and p40phox bind to lipid products of PI(3)K. Nat Cell Biol 3, 675–678. https://doi.org/10.1038/35083070

Kanehara, K., Yu, C.-Y., Cho, Y., Cheong, W.-F., Torta, F., Shui, G., Wenk, M.R., Nakamura, Y., 2015. Arabidopsis AtPLC2 Is a Primary Phosphoinositide-Specific Phospholipase C in Phosphoinositide Metabolism and the Endoplasmic Reticulum Stress Response. PLOS Genetics 11, e1005511. https://doi.org/10.1371/journal.pgen.1005511

Kang, B.-H., Busse, J.S., Bednarek, S.Y., 2003. Members of the Arabidopsis Dynamin-Like Gene Family, ADL1, Are Essential for Plant Cytokinesis and Polarized Cell Growth[W]. The Plant Cell 15, 899–913. https://doi.org/10.1105/tpc.009670

Kang, B.-H., Nielsen, E., Preuss, M.L., Mastronarde, D., Staehelin, L.A., 2011a. Electron tomography of RabA4b- and PI-4Kβ1-labeled trans Golgi network compartments in Arabidopsis. Traffic 12, 313–329. https://doi.org/10.1111/j.1600-0854.2010.01146.x

Kang, B.-H., Nielsen, E., Preuss, M.L., Mastronarde, D., Staehelin, L.A., 2011b. Electron Tomography of RabA4b- and PI-4Kβ1-Labeled Trans Golgi Network Compartments in Arabidopsis. Traffic 12, 313–329. https://doi.org/10.1111/j.1600-0854.2010.01146.x

Kapp-Barnea, Y., Melnikov, S., Shefler, I., Jeromin, A., Sagi-Eisenberg, R., 2003. Neuronal calcium sensor-1 and phosphatidylinositol 4-kinase beta regulate IgE receptor-triggered exocytosis in cultured mast cells. J Immunol 171, 5320–5327. https://doi.org/10.4049/jimmunol.171.10.5320

Karpets, Yu.V., Kolupaev, Yu.E., Lugovaya, A.A., Oboznyi, A.I., 2014. Effect of jasmonic acid on the pro-/antioxidant system of wheat coleoptiles as related to hyperthermia tolerance. Russ J Plant Physiol 61, 339–346. https://doi.org/10.1134/S102144371402006X

Kawashima, T., Berthet-Colominas, C., Wulff, M., Cusack, S., Leberman, R., 1996. The structure of the Escherichia coli EF-Tu· EF-Ts complex at 2.5 Å resolution. Nature 379, 511–518. https://doi.org/10.1038/379511a0

Kazan, K., 2013. Auxin and the integration of environmental signals into plant root development. Ann Bot 112, 1655–1665. https://doi.org/10.1093/aob/mct229

Ke, M., Ma, Z., Wang, D., Sun, Y., Wen, C., Huang, D., Chen, Z., Yang, L., Tan, S., Li, R., Friml, J., Miao, Y., Chen, X., 2021. Salicylic acid regulates PIN2 auxin transporter hyperclustering and root gravitropic growth via Remorin-dependent lipid nanodomain organisation in Arabidopsis thaliana. New Phytol 229, 963–978. https://doi.org/10.1111/nph.16915

Keto-Timonen, R., Hietala, N., Palonen, E., Hakakorpi, A., Lindström, M., Korkeala, H., 2016. Cold Shock Proteins: A Minireview with Special Emphasis on Csp-family of Enteropathogenic Yersinia. Frontiers in Microbiology 7.

Khokon, Md.A.R., Okuma, E., Hossain, M.A., Munemasa, S., Uraji, M., Nakamura, Y., Mori, I.C., Murata, Y., 2011. Involvement of extracellular oxidative burst in salicylic acid-induced stomatal closure in Arabidopsis. Plant, Cell & Environment 34, 434–443. https://doi.org/10.1111/j.1365-3040.2010.02253.x

Kieber, J.J., Schaller, G.E., 2014. Cytokinins. arbo.j 2014. https://doi.org/10.1199/tab.0168

Klarzynski, O., Descamps, V., Plesse, B., Yvin, J.-C., Kloareg, B., Fritig, B., 2003. Sulfated fucan oligosaccharides elicit defense responses in tobacco and local and systemic resistance against tobacco mosaic virus. Mol Plant Microbe Interact 16, 115–122. https://doi.org/10.1094/MPMI.2003.16.2.115

Kobayashi, K., Endo, K., Wada, H., 2016. Roles of Lipids in Photosynthesis. Subcell Biochem 86, 21–49. https://doi.org/10.1007/978-3-319-25979-6_2

Kocourková, D., Kroumanová, K., Podmanická, T., Daněk, M., Martinec, J., 2021. Phospholipase Dα1 Acts as a Negative Regulator of High Mg2+-Induced Leaf Senescence in Arabidopsis. Front Plant Sci 12, 770794. https://doi.org/10.3389/fpls.2021.770794

Koh, S., André, A., Edwards, H., Ehrhardt, D., Somerville, S., 2005. Arabidopsis thaliana subcellular responses to compatible Erysiphe cichoracearum infections. The Plant Journal 44, 516–529. https://doi.org/10.1111/j.1365-313X.2005.02545.x

Kopylova, E., Noé, L., Touzet, H., 2012. SortMeRNA: fast and accurate filtering of ribosomal RNAs in metatranscriptomic data. Bioinformatics 28, 3211–3217. https://doi.org/10.1093/bioinformatics/bts611

Kraepiel, Y., Barny, M.-A., 2016. Gram-negative phytopathogenic bacteria, all hemibiotrophs after all? Molecular Plant Pathology 17, 313–316. https://doi.org/10.1111/mpp.12345

Krinke, O., Novotná, Z., Valentová, O., Martinec, J., 2007. Inositol trisphosphate receptor in higher plants: is it real? Journal of Experimental Botany 58, 361–376. https://doi.org/10.1093/jxb/erl220

Kumar, K., Verma, P., 2013. Plant Pathogen Interactions: Crop Improvement Under Adverse Conditions. pp. 433–459. https://doi.org/10.1007/978-1-4614-5001-6_16

Kunze, G., Zipfel, C., Robatzek, S., Niehaus, K., Boller, T., Felix, G., 2004. The N Terminus of Bacterial Elongation Factor Tu Elicits Innate Immunity in Arabidopsis Plants. The Plant Cell 16, 3496–3507. https://doi.org/10.1105/tpc.104.026765

Kusano, H., Testerink, C., Vermeer, J.E.M., Tsuge, T., Shimada, H., Oka, A., Munnik, T., Aoyama, T., 2008. The Arabidopsis Phosphatidylinositol Phosphate 5-Kinase PIP5K3 Is a Key Regulator of Root Hair Tip Growth. The Plant Cell 20, 367–380. https://doi.org/10.1105/tpc.107.056119

Kusner, D.J., Barton, J.A., Wen, K.-K., Wang, X., Rubenstein, P.A., Iyer, S.S., 2002. Regulation of Phospholipase D Activity by Actin: Actin exerts bidirectional modulation of mammalian phospolipase d activity in a polymerization-dependent, isoform-specific manner*. Journal of Biological Chemistry 277, 50683–50692. https://doi.org/10.1074/jbc.M209221200

Kutateladze, T.G., 2010. Translation of the phosphoinositide code by PI effectors. Nat Chem Biol 6, 507–513. https://doi.org/10.1038/nchembio.390

Kwon, C., Neu, C., Pajonk, S., Yun, H.S., Lipka, U., Humphry, M., Bau, S., Straus, M., Kwaaitaal, M., Rampelt, H., El Kasmi, F., Jürgens, G., Parker, J., Panstruga, R., Lipka, V., Schulze-Lefert, P., 2008. Co-option of a default secretory pathway for plant immune responses. Nature 451, 835–840. https://doi.org/10.1038/nature06545

Lakehal, A., Bellini, C., 2019. Control of adventitious root formation: insights into synergistic and antagonistic hormonal interactions. Physiol Plant 165, 90–100. https://doi.org/10.1111/ppl.12823

Lambertucci, S., Orman, K.M., Das Gupta, S., Fisher, J.P., Gazal, S., Williamson, R.J., Cramer, R., Bindschedler, L.V., 2019. Analysis of Barley Leaf Epidermis and Extrahaustorial Proteomes During Powdery Mildew Infection Reveals That the PR5 Thaumatin-Like Protein TLP5 Is Required for Susceptibility Towards Blumeria graminis f. sp. hordei. Frontiers in Plant Science 10.

Lee, J., Klessig, D.F., Nürnberger, T., 2001. A harpin binding site in tobacco plasma membranes mediates activation of the pathogenesis-related gene HIN1 independent of extracellular calcium but dependent on mitogen-activated protein kinase activity. Plant Cell 13, 1079–1093. https://doi.org/10.1105/tpc.13.5.1079

Lee, M.W., Huffaker, A., Crippen, D., Robbins, R.T., Goggin, F.L., 2018. Plant elicitor peptides promote plant defences against nematodes in soybean. Molecular Plant Pathology 19, 858–869. https://doi.org/10.1111/mpp.12570

Lee, Yuree, Kim, E.-S., Choi, Y., Hwang, I., Staiger, C.J., Chung, Y.-Y., Lee, Youngsook, 2008. The Arabidopsis phosphatidylinositol 3-kinase is important for pollen development. Plant Physiol 147, 1886–1897. https://doi.org/10.1104/pp.108.121590

Lefevere, H., Bauters, L., Gheysen, G., 2020. Salicylic Acid Biosynthesis in Plants. Frontiers in Plant Science 11.

Lenoir, M., Kufareva, I., Abagyan, R., Overduin, M., 2015. Membrane and Protein Interactions of the Pleckstrin Homology Domain Superfamily. Membranes 5, 646–663. https://doi.org/10.3390/membranes5040646

Leontovyčová, H., Kalachova, T., Trdá, L., Pospíchalová, R., Lamparová, L., Dobrev, P.I., Malínská, K., Burketová, L., Valentová, O., Janda, M., 2019. Actin depolymerization is able to increase plant resistance against pathogens via activation of salicylic acid signalling pathway. Scientific Reports 9, 10397. https://doi.org/10.1038/s41598-019-46465-5

Li, F., Wang, J., Ma, C., Zhao, Y., Wang, Y., Hasi, A., Qi, Z., 2013. Glutamate Receptor-Like Channel3.3 Is Involved in Mediating Glutathione-Triggered Cytosolic Calcium Transients, Transcriptional Changes, and Innate Immunity Responses in Arabidopsis. Plant Physiology 162, 1497–1509. https://doi.org/10.1104/pp.113.217208

Li, J., Brader, G., Palva, E.T., 2004. The WRKY70 Transcription Factor: A Node of Convergence for Jasmonate-Mediated and Salicylate-Mediated Signals in Plant Defense[W]. The Plant Cell 16, 319–331. https://doi.org/10.1105/tpc.016980

Li, J., Zhong, R., Palva, E.T., 2017. WRKY70 and its homolog WRKY54 negatively modulate the cell wall-associated defenses to necrotrophic pathogens in Arabidopsis. PLOS ONE 12, e0183731. https://doi.org/10.1371/journal.pone.0183731

Li, L., He, Y., Wang, Y., Zhao, S., Chen, X., Ye, T., Wu, Yuxuan, Wu, Yan, 2015. Arabidopsis PLC2 is involved in auxin-modulated reproductive development. The Plant Journal 84, 504–515. https://doi.org/10.1111/tpj.13016

Li, L., Shuai, L., Sun, J., Li, C., Yi, P., Zhou, Z., He, X., Ling, D., Sheng, J., Kong, K.-W., Zheng, F., Li, J., Liu, G., Xin, M., Li, Z., Tang, Y., 2020. The Role of 1-Methylcyclopropene in the regulation of ethylene biosynthesis and ethylene receptor gene expression in Mangifera indica L. (Mango Fruit). Food Science & Nutrition 8, 1284–1294. https://doi.org/10.1002/fsn3.1417

Li, L., Xu, J., Xu, Z.-H., Xue, H.-W., 2005. Brassinosteroids Stimulate Plant Tropisms through Modulation of Polar Auxin Transport in Brassica and Arabidopsis. The Plant Cell 17, 2738–2753. https://doi.org/10.1105/tpc.105.034397

Li, M., Qin, C., Welti, R., Wang, X., 2006. Double Knockouts of Phospholipases Dζ1 and Dζ2 in Arabidopsis Affect Root Elongation during Phosphate-Limited Growth But Do Not Affect Root Hair Patterning. Plant Physiology 140, 761–770. https://doi.org/10.1104/pp.105.070995

Li, Q., Zheng, J., Li, S., Huang, G., Skilling, S.J., Wang, L., Li, L., Li, M., Yuan, L., Liu, P., 2017. Transporter-Mediated Nuclear Entry of Jasmonoyl-Isoleucine Is Essential for Jasmonate Signaling. Molecular Plant 10, 695–708. https://doi.org/10.1016/j.molp.2017.01.010

Li, W., Ahn, I.-P., Ning, Y., Park, C.-H., Zeng, L., Whitehill, J.G.A., Lu, H., Zhao, Q., Ding, B., Xie, Q., Zhou, J.-M., Dai, L., Wang, G.-L., 2012. The U-Box/ARM E3 Ligase PUB13 Regulates Cell Death, Defense, and Flowering Time in Arabidopsis. Plant Physiology 159, 239–250. https://doi.org/10.1104/pp.111.192617

Li, W., Li, M., Zhang, W., Welti, R., Wang, X., 2004. The plasma membrane–bound phospholipase Dδ enhances freezing tolerance in Arabidopsis thaliana. Nat Biotechnol 22, 427–433. https://doi.org/10.1038/nbt949

Li, Y., Tessaro, M.J., Li, X., Zhang, Y., 2010. Regulation of the Expression of Plant Resistance Gene SNC1 by a Protein with a Conserved BAT2 Domain. Plant Physiology 153, 1425–1434. https://doi.org/10.1104/pp.110.156240

Liao, D., Cao, Y., Sun, X., Espinoza, C., Nguyen, C.T., Liang, Y., Stacey, G., 2017. Arabidopsis E3 ubiquitin ligase PLANT U-BOX13 (PUB13) regulates chitin receptor LYSIN MOTIF RECEPTOR KINASE5 (LYK5) protein abundance. New Phytologist 214, 1646–1656. https://doi.org/10.1111/nph.14472

Lin, F., Krishnamoorthy, P., Schubert, V., Hause, G., Heilmann, M., Heilmann, I., 2019. A dual role for cell plate-associated PI4Kβ in endocytosis and phragmoplast dynamics

during plant somatic cytokinesis. The EMBO Journal 38, e100303. https://doi.org/10.15252/embj.2018100303
Lin, W., Lu, D., Gao, X., Jiang, S., Ma, X., Wang, Z., Mengiste, T., He, P., Shan, L., 2013. Inverse modulation of plant immune and brassinosteroid signaling pathways by the receptor-like cytoplasmic kinase BIK1. PNAS 110, 12114–12119. https://doi.org/10.1073/pnas.1302154110
Lipka, U., Fuchs, R., Lipka, V., 2008. Arabidopsis non-host resistance to powdery mildews. Current Opinion in Plant Biology, Biotic Interactions 11, 404–411. https://doi.org/10.1016/j.pbi.2008.04.004
Lipka, V., Kwon, C., Panstruga, R., 2007. SNARE-Ware: The Role of SNARE-Domain Proteins in Plant Biology. Annu. Rev. Cell Dev. Biol. 23, 147–174. https://doi.org/10.1146/annurev.cellbio.23.090506.123529
Liu, H., Liu, B., Lou, S., Bi, H., Tang, H., Tong, S., Song, Y., Chen, N., Zhang, H., Jiang, Y., Liu, J., 2021. CHYR1 ubiquitinates the phosphorylated WRKY70 for degradation to balance immunity in Arabidopsis thaliana. New Phytologist 230, 1095–1109. https://doi.org/10.1111/nph.17231
Liu, H.T., Gao, F., Cui, S.J., Han, J.L., Sun, D.Y., Zhou, R.G., 2006. Primary evidence for involvement of IP3 in heat-shock signal transduction in Arabidopsis. Cell Res 16, 394–400. https://doi.org/10.1038/sj.cr.7310051
Liu, J., Liu, B., Chen, S., Gong, B.-Q., Chen, L., Zhou, Q., Xiong, F., Wang, M., Feng, D., Li, J.-F., Wang, H.-B., Wang, J., 2018. A Tyrosine Phosphorylation Cycle Regulates Fungal Activation of a Plant Receptor Ser/Thr Kinase. Cell Host & Microbe 23, 241-253.e6. https://doi.org/10.1016/j.chom.2017.12.005
Liu, J., Magalhaes, J.V., Shaff, J., Kochian, L.V., 2009. Aluminum-activated citrate and malate transporters from the MATE and ALMT families function independently to confer Arabidopsis aluminum tolerance. The Plant Journal 57, 389–399. https://doi.org/10.1111/j.1365-313X.2008.03696.x
Liu, S., Wang, W.-H., Dang, Y.-L., Fu, Y., Sang, R., 2012. Rational design and efficient synthesis of a fluorescent-labeled jasmonate. Tetrahedron Letters 53, 4235–4239. https://doi.org/10.1016/j.tetlet.2012.06.006
Liu, T., Liu, Z., Song, C., Hu, Y., Han, Z., She, J., Fan, F., Wang, J., Jin, C., Chang, J., Zhou, J.-M., Chai, J., 2012. Chitin-Induced Dimerization Activates a Plant Immune Receptor. Science 336, 1160–1164. https://doi.org/10.1126/science.1218867
Löfke, C., Dünser, K., Scheuring, D., Kleine-Vehn, J., 2015. Auxin regulates SNARE-dependent vacuolar morphology restricting cell size. eLife 4, e05868. https://doi.org/10.7554/eLife.05868
Lotze, M.T., Zeh, H.J., Rubartelli, A., Sparvero, L.J., Amoscato, A.A., Washburn, N.R., DeVera, M.E., Liang, X., Tör, M., Billiar, T., 2007. The grateful dead: damage-associated molecular pattern molecules and reduction/oxidation regulate immunity. Immunological Reviews 220, 60–81. https://doi.org/10.1111/j.1600-065X.2007.00579.x
Lou, Y., Ma, H., Lin, W.-H., Chu, Z.-Q., Mueller-Roeber, B., Xu, Z.-H., Xue, H.-W., 2006. The Highly Charged Region of Plant β-type Phosphatidylinositol 4-kinase is Involved in Membrane Targeting and Phospholipid Binding. Plant Mol Biol 60, 729–746. https://doi.org/10.1007/s11103-005-5548-x
Lu, D., Lin, W., Gao, X., Wu, S., Cheng, C., Avila, J., Heese, A., Devarenne, T.P., He, P., Shan, L., 2011. Direct Ubiquitination of Pattern Recognition Receptor FLS2 Attenuates Plant Innate Immunity. Science 332, 1439–1442. https://doi.org/10.1126/science.1204903

Lu, D., Wu, S., Gao, X., Zhang, Y., Shan, L., He, P., 2010. A receptor-like cytoplasmic kinase, BIK1, associates with a flagellin receptor complex to initiate plant innate immunity. Proceedings of the National Academy of Sciences 107, 496–501. https://doi.org/10.1073/pnas.0909705107

Lu, Y.-J., Day, B., 2017. Quantitative Evaluation of Plant Actin Cytoskeletal Organization During Immune Signaling. Methods Mol Biol 1578, 207–221. https://doi.org/10.1007/978-1-4939-6859-6_17

Ludwig-Müller, J., Jülke, S., Geiß, K., Richter, F., Mithöfer, A., Šola, I., Rusak, G., Keenan, S., Bulman, S., 2015. A novel methyltransferase from the intracellular pathogen Plasmodiophora brassicae methylates salicylic acid. Molecular Plant Pathology 16, 349–364. https://doi.org/10.1111/mpp.12185

Luschnig, C., Vert, G., 2014. The dynamics of plant plasma membrane proteins: PINs and beyond. Development (Cambridge, England) 141, 2924–2938. https://doi.org/10.1242/dev.103424

Ma, H., Lou, Y., Lin, W.H., Xue, H.W., 2006. MORN motifs in plant PIPKs are involved in the regulation of subcellular localization and phospholipid binding. Cell Res 16, 466–478. https://doi.org/10.1038/sj.cr.7310058

Ma, X., Xu, G., He, P., Shan, L., 2016. SERKing Coreceptors for Receptors. Trends Plant Sci 21, 1017–1033. https://doi.org/10.1016/j.tplants.2016.08.014

Ma, Y., Walker, R.K., Zhao, Y., Berkowitz, G.A., 2012. Linking ligand perception by PEPR pattern recognition receptors to cytosolic Ca2+ elevation and downstream immune signaling in plants. PNAS 109, 19852–19857. https://doi.org/10.1073/pnas.1205448109

Macaulay, K.M., Heath, G.A., Ciulli, A., Murphy, A.M., Abell, C., Carr, J.P., Smith, A.G., 2017. The biochemical properties of the two Arabidopsis thaliana isochorismate synthases. Biochemical Journal 474, 1579–1590. https://doi.org/10.1042/BCJ20161069

Macho, A.P., Zipfel, C., 2014. Plant PRRs and the Activation of Innate Immune Signaling. Molecular Cell 54, 263–272. https://doi.org/10.1016/j.molcel.2014.03.028

Maffucci, T., Falasca, M., 2001. Specificity in pleckstrin homology (PH) domain membrane targeting: a role for a phosphoinositide–protein co-operative mechanism. FEBS Letters 506, 173–179. https://doi.org/10.1016/S0014-5793(01)02909-X

Maruta, N., Burdett, H., Lim, B.Y.J., Hu, X., Desa, S., Manik, M.K., Kobe, B., 2022. Structural basis of NLR activation and innate immune signalling in plants. Immunogenetics 74, 5–26. https://doi.org/10.1007/s00251-021-01242-5

Mashiguchi, K., Hisano, H., Takeda-Kamiya, N., Takebayashi, Y., Ariizumi, T., Gao, Y., Ezura, H., Sato, K., Zhao, Y., Hayashi, K., Kasahara, H., 2019. Agrobacterium tumefaciens Enhances Biosynthesis of Two Distinct Auxins in the Formation of Crown Galls. Plant and Cell Physiology 60, 29–37. https://doi.org/10.1093/pcp/pcy182

McCarthy, D.J., Chen, Y., Smyth, G.K., 2012. Differential expression analysis of multifactor RNA-Seq experiments with respect to biological variation. Nucleic Acids Res 40, 4288–4297. https://doi.org/10.1093/nar/gks042

McKenna, J.F., Rolfe, D.J., Webb, S.E.D., Tolmie, A.F., Botchway, S.W., Martin-Fernandez, M.L., Hawes, C., Runions, J., 2019. The cell wall regulates dynamics and size of plasma-membrane nanodomains in Arabidopsis. PNAS 116, 12857–12862. https://doi.org/10.1073/pnas.1819077116

Mélida, H., Sopeña-Torres, S., Bacete, L., Garrido-Arandia, M., Jordá, L., López, G., Muñoz-Barrios, A., Pacios, L.F., Molina, A., 2018. Non-branched β-1,3-glucan

oligosaccharides trigger immune responses in Arabidopsis. The Plant Journal 93, 34–49. https://doi.org/10.1111/tpj.13755
Meyers, B.C., Kozik, A., Griego, A., Kuang, H., Michelmore, R.W., 2003. Genome-wide analysis of NBS-LRR-encoding genes in Arabidopsis. Plant Cell 15, 809–834. https://doi.org/10.1105/tpc.009308
Micali, C.O., Neumann, U., Grunewald, D., Panstruga, R., O'Connell, R., 2011. Biogenesis of a specialized plant–fungal interface during host cell internalization of Golovinomyces orontii haustoria. Cellular Microbiology 13, 210–226. https://doi.org/10.1111/j.1462-5822.2010.01530.x
Mishra, G., Zhang, W., Deng, F., Zhao, J., Wang, X., 2006. A Bifurcating Pathway Directs Abscisic Acid Effects on Stomatal Closure and Opening in Arabidopsis. Science 312, 264–266. https://doi.org/10.1126/science.1123769
Monaghan, J., Zipfel, C., 2012. Plant pattern recognition receptor complexes at the plasma membrane. Current Opinion in Plant Biology, Biotic interactions 15, 349–357. https://doi.org/10.1016/j.pbi.2012.05.006
Money, N.P., 2016. Chapter 2 - Fungal Cell Biology and Development, in: Watkinson, S.C., Boddy, L., Money, N.P. (Eds.), The Fungi (Third Edition). Academic Press, Boston, pp. 37–66. https://doi.org/10.1016/B978-0-12-382034-1.00002-5
Mosher, S., Kemmerling, B., 2013. PSKR1 and PSY1R-mediated regulation of plant defense responses. Plant Signaling & Behavior 8, e24119. https://doi.org/10.4161/psb.24119
Moshkanbaryans, L., Chan, L.-S., Graham, M.E., 2014. The Biochemical Properties and Functions of CALM and AP180 in Clathrin Mediated Endocytosis. Membranes 4, 388–413. https://doi.org/10.3390/membranes4030388
Mou, Z., 2017. Extracellular pyridine nucleotides as immune elicitors in arabidopsis. Plant Signaling & Behavior 12, e1388977. https://doi.org/10.1080/15592324.2017.1388977
Mouchel, C.F., Osmont, K.S., Hardtke, C.S., 2006. BRX mediates feedback between brassinosteroid levels and auxin signalling in root growth. Nature 443, 458–461. https://doi.org/10.1038/nature05130
Mueller-Roeber, B., Pical, C., 2002. Inositol Phospholipid Metabolism in Arabidopsis. Characterized and Putative Isoforms of Inositol Phospholipid Kinase and Phosphoinositide-Specific Phospholipase C. Plant Physiology 130, 22–46. https://doi.org/10.1104/pp.004770
Munnik, T., Meijer, H.J.G., Ter Riet, B., Hirt, H., Frank, W., Bartels, D., Musgrave, A., 2000. Hyperosmotic stress stimulates phospholipase D activity and elevates the levels of phosphatidic acid and diacylglycerol pyrophosphate. The Plant Journal 22, 147–154. https://doi.org/10.1046/j.1365-313x.2000.00725.x
Munnik, T., Testerink, C., 2009. Plant phospholipid signaling: "in a nutshell." Journal of Lipid Research 50, S260–S265. https://doi.org/10.1194/jlr.R800098-JLR200
Nakaminami, K., Karlson, D.T., Imai, R., 2006. Functional conservation of cold shock domains in bacteria and higher plants. Proceedings of the National Academy of Sciences 103, 10122–10127. https://doi.org/10.1073/pnas.0603168103
Nam, K.H., Li, J., 2002. BRI1/BAK1, a Receptor Kinase Pair Mediating Brassinosteroid Signaling. Cell 110, 203–212. https://doi.org/10.1016/S0092-8674(02)00814-0
Nawrath, C., Métraux, J.-P., 1999. Salicylic Acid Induction–Deficient Mutants of Arabidopsis Express PR-2 and PR-5 and Accumulate High Levels of Camalexin after Pathogen Inoculation. The Plant Cell 11, 1393–1404. https://doi.org/10.1105/tpc.11.8.1393
Nazar, R., Khan, M.I.R., Iqbal, N., Masood, A., Khan, N.A., 2014. Involvement of ethylene in reversal of salt-inhibited photosynthesis by sulfur in mustard. Physiologia Plantarum 152, 331–344. https://doi.org/10.1111/ppl.12173

Nguyen, Q.-M., Iswanto, A.B.B., Son, G.H., Kim, S.H., 2021. Recent Advances in Effector-Triggered Immunity in Plants: New Pieces in the Puzzle Create a Different Paradigm. Int J Mol Sci 22, 4709. https://doi.org/10.3390/ijms22094709

Nielsen, M.E., Feechan, A., Böhlenius, H., Ueda, T., Thordal-Christensen, H., 2012. Arabidopsis ARF-GTP exchange factor, GNOM, mediates transport required for innate immunity and focal accumulation of syntaxin PEN1. Proceedings of the National Academy of Sciences 109, 11443–11448. https://doi.org/10.1073/pnas.1117596109

Nielsen, M.E., Thordal-Christensen, H., 2012. Recycling of Arabidopsis plasma membrane PEN1 syntaxin. Plant Signal Behav 7, 1541–1543. https://doi.org/10.4161/psb.22304

Niki, T., Mitsuhara, I., Seo, S., Ohtsubo, N., Ohashi, Y., 1998. Antagonistic Effect of Salicylic Acid and Jasmonic Acid on the Expression of Pathogenesis-Related (PR) Protein Genes in Wounded Mature Tobacco Leaves. Plant and Cell Physiology 39, 500–507. https://doi.org/10.1093/oxfordjournals.pcp.a029397

Noack, L.C., Bayle, V., Armengot, L., Rozier, F., Mamode-Cassim, A., Stevens, F.D., Caillaud, M.-C., Munnik, T., Mongrand, S., Pleskot, R., Jaillais, Y., 2022. A nanodomain-anchored scaffolding complex is required for the function and localization of phosphatidylinositol 4-kinase alpha in plants. The Plant Cell 34, 302–332. https://doi.org/10.1093/plcell/koab135

Noack, L.C., Jaillais, Y., 2020. Functions of Anionic Lipids in Plants. Annu Rev Plant Biol 71, 71–102. https://doi.org/10.1146/annurev-arplant-081519-035910

Nomikos, M., Elgmati, K., Theodoridou, M., Calver, B.L., Nounesis, G., Swann, K., Lai, F.A., 2011. Phospholipase Cζ binding to PtdIns(4,5)P2 requires the XY-linker region. Journal of Cell Science 124, 2582–2590. https://doi.org/10.1242/jcs.083485

Normanly, J., Cohen, J.D., Fink, G.R., 1993. Arabidopsis thaliana auxotrophs reveal a tryptophan-independent biosynthetic pathway for indole-3-acetic acid. Proc Natl Acad Sci U S A 90, 10355–10359.

Novák, D., Vadovič, P., Ovečka, M., Šamajová, O., Komis, G., Colcombet, J., Šamaj, J., 2018. Gene Expression Pattern and Protein Localization of Arabidopsis Phospholipase D Alpha 1 Revealed by Advanced Light-Sheet and Super-Resolution Microscopy. Frontiers in Plant Science 9.

Nürnberger, T., Brunner, F., 2002. Innate immunity in plants and animals: emerging parallels between the recognition of general elicitors and pathogen-associated molecular patterns. Current Opinion in Plant Biology 5, 318–324. https://doi.org/10.1016/S1369-5266(02)00265-0

Ohashi, Y., Oka, A., Rodrigues-Pousada, R., Possenti, M., Ruberti, I., Morelli, G., Aoyama, T., 2003. Modulation of Phospholipid Signaling by GLABRA2 in Root-Hair Pattern Formation. Science 300, 1427–1430. https://doi.org/10.1126/science.1083695

Ohlrogge, J., Browse, J., 1995. Lipid biosynthesis. Plant Cell 7, 957–970.

Okazaki, K., Miyagishima, S., Wada, H., 2015. Phosphatidylinositol 4-Phosphate Negatively Regulates Chloroplast Division in Arabidopsis. The Plant Cell 27, 663–674. https://doi.org/10.1105/tpc.115.136234

Okrent, R.A., Brooks, M.D., Wildermuth, M.C., 2009. Arabidopsis GH3.12 (PBS3) Conjugates Amino Acids to 4-Substituted Benzoates and Is Inhibited by Salicylate *. Journal of Biological Chemistry 284, 9742–9754. https://doi.org/10.1074/jbc.M806662200

Ortega-Villasante, C., Burén, S., Barón-Sola, Á., Martínez, F., Hernández, L.E., 2016. In vivo ROS and redox potential fluorescent detection in plants: Present approaches and future perspectives. Methods, Current Methods to unravel Reactive Oxygen Species (ROS) Biology 109, 92–104. https://doi.org/10.1016/j.ymeth.2016.07.009

Ortíz-Castro, R., Valencia-Cantero, E., López-Bucio, J., 2008. Plant growth promotion by Bacillus megaterium involves cytokinin signaling. Plant Signaling & Behavior 3, 263–265. https://doi.org/10.4161/psb.3.4.5204

Ortiz-Morea, F.A., Savatin, D.V., Dejonghe, W., Kumar, R., Luo, Y., Adamowski, M., Begin, J.V. den, Dressano, K., Oliveira, G.P. de, Zhao, X., Lu, Q., Madder, A., Friml, J., Moura, D.S. de, Russinova, E., 2016. Danger-associated peptide signaling in Arabidopsis requires clathrin. PNAS 113, 11028–11033. https://doi.org/10.1073/pnas.1605588113

Osugi, A., Sakakibara, H., 2015. Q&A: How do plants respond to cytokinins and what is their importance? BMC Biology 13, 102. https://doi.org/10.1186/s12915-015-0214-5

Otterhag, L., Sommarin, M., Pical, C., 2001. N-terminal EF-hand-like domain is required for phosphoinositide-specific phospholipase C activity in Arabidopsis thaliana. FEBS Letters 497, 165–170. https://doi.org/10.1016/S0014-5793(01)02453-X

Pajonk, S., Kwon, C., Clemens, N., Panstruga, R., Schulze-Lefert, P., 2008. Activity determinants and functional specialization of Arabidopsis PEN1 syntaxin in innate immunity. J Biol Chem 283, 26974–26984. https://doi.org/10.1074/jbc.M805236200

Pappan, K., Wang, X., 1999. Plant Phospholipase Dα Is an Acidic Phospholipase Active at Near-Physiological Ca2+ Concentrations. Archives of Biochemistry and Biophysics 368, 347–353. https://doi.org/10.1006/abbi.1999.1325

Park, S.-W., Kaimoyo, E., Kumar, D., Mosher, S., Klessig, D.F., 2007. Methyl salicylate is a critical mobile signal for plant systemic acquired resistance. Science 318, 113–116. https://doi.org/10.1126/science.1147113

Parre, E., Ghars, M.A., Leprince, A.-S., Thiery, L., Lefebvre, D., Bordenave, M., Richard, L., Mazars, C., Abdelly, C., Savouré, A., 2007. Calcium signaling via phospholipase C is essential for proline accumulation upon ionic but not nonionic hyperosmotic stresses in Arabidopsis. Plant Physiology 144, 503–512. https://doi.org/10.1104/pp.106.095281

Pearce, G., 2011. Systemin, Hydroxyproline-Rich Systemin and the Induction of Protease Inhibitors. Current Protein and Peptide Science 12, 399–408. https://doi.org/10.2174/138920311796391106

Pearce, G., Munske, G., Yamaguchi, Y., Ryan, C.A., 2010. Structure–activity studies of GmSubPep, a soybean peptide defense signal derived from an extracellular protease. Peptides 31, 2159–2164. https://doi.org/10.1016/j.peptides.2010.09.004

Peng, Y., Yang, J., Li, X., Zhang, Y., 2021. Salicylic Acid: Biosynthesis and Signaling. Annu Rev Plant Biol 72, 761–791. https://doi.org/10.1146/annurev-arplant-081320-092855

Perera, I.Y., Hung, C.-Y., Moore, C.D., Stevenson-Paulik, J., Boss, W.F., 2008. Transgenic Arabidopsis plants expressing the type 1 inositol 5-phosphatase exhibit increased drought tolerance and altered abscisic acid signaling. Plant Cell 20, 2876–2893. https://doi.org/10.1105/tpc.108.061374

Pescador Azofra, L., 2021. Role of nitric oxide signalling in beneficial and pathogenic plant–fungal interactions. Universidad de Granada.

Petrášek, J., Friml, J., 2009. Auxin transport routes in plant development. Development 136, 2675–2688. https://doi.org/10.1242/dev.030353

Pinosa, F., Buhot, N., Kwaaitaal, M., Fahlberg, P., Thordal-Christensen, H., Ellerström, M., Andersson, M.X., 2013. Arabidopsis Phospholipase Dδ Is Involved in Basal Defense and Nonhost Resistance to Powdery Mildew Fungi. Plant Physiology 163, 896–906. https://doi.org/10.1104/pp.113.223503

Pitts, R.J., Cernac, A., Estelle, M., 1998. Auxin and ethylene promote root hair elongation in Arabidopsis. The Plant Journal 16, 553–560. https://doi.org/10.1046/j.1365-313x.1998.00321.x

Platre, M.P., Noack, L.C., Doumane, M., Bayle, V., Simon, M.L.A., Maneta-Peyret, L., Fouillen, L., Stanislas, T., Armengot, L., Pejchar, P., Caillaud, M.-C., Potocký, M., Čopič, A., Moreau, P., Jaillais, Y., 2018. A Combinatorial Lipid Code Shapes the Electrostatic Landscape of Plant Endomembranes. Developmental Cell 45, 465-480.e11. https://doi.org/10.1016/j.devcel.2018.04.011

Pleskot, R., Li, J., Žárský, V., Potocký, M., Staiger, C.J., 2013. Regulation of cytoskeletal dynamics by phospholipase D and phosphatidic acid. Trends in Plant Science 18, 496–504. https://doi.org/10.1016/j.tplants.2013.04.005

Pluhařová, K., Leontovyčová, H., Stoudková, V., Pospíchalová, R., Maršík, P., Klouček, P., Starodubtseva, A., Iakovenko, O., Krčková, Z., Valentová, O., Burketová, L., Janda, M., Kalachova, T., 2019. "Salicylic Acid Mutant Collection" as a Tool to Explore the Role of Salicylic Acid in Regulation of Plant Growth under a Changing Environment. Int J Mol Sci 20, E6365. https://doi.org/10.3390/ijms20246365

Pokotylo, I., Kolesnikov, Y., Kravets, V., Zachowski, A., Ruelland, E., 2014. Plant phosphoinositide-dependent phospholipases C: Variations around a canonical theme. Biochimie, Lipids in Metabolic Diseases 96, 144–157. https://doi.org/Kumar

Pokotylo, I., Kravets, V., Martinec, J., Ruelland, E., 2018. The phosphatidic acid paradox: Too many actions for one molecule class? Lessons from plants. Progress in Lipid Research 71, 43–53. https://doi.org/10.1016/j.plipres.2018.05.003

Pourcher, M., Santambrogio, M., Thazar, N., Thierry, A.-M., Fobis-Loisy, I., Miège, C., Jaillais, Y., Gaude, T., 2010. Analyses of SORTING NEXINs Reveal Distinct Retromer-Subcomplex Functions in Development and Protein Sorting in Arabidopsis thaliana. The Plant Cell 22, 3980–3991. https://doi.org/10.1105/tpc.110.078451

Premkumar, A., Lindberg, S., Lager, I., Rasmussen, U., Schulz, A., 2019. Arabidopsis PLDs with C2-domain function distinctively in hypoxia. Physiologia Plantarum 167, 90–110. https://doi.org/10.1111/ppl.12874

Preuss, M.L., Schmitz, A.J., Thole, J.M., Bonner, H.K.S., Otegui, M.S., Nielsen, E., 2006. A role for the RabA4b effector protein PI-4Kbeta1 in polarized expansion of root hair cells in Arabidopsis thaliana. J Cell Biol 172, 991–998. https://doi.org/10.1083/jcb.200508116

Preuss, M.L., Serna, J., Falbel, T.G., Bednarek, S.Y., Nielsen, E., 2004. The Arabidopsis Rab GTPase RabA4b Localizes to the Tips of Growing Root Hair Cells. Plant Cell 16, 1589–1603. https://doi.org/10.1105/tpc.021634

Pršić, J., Ongena, M., 2020. Elicitors of Plant Immunity Triggered by Beneficial Bacteria. Frontiers in Plant Science 11.

Qin, C., Wang, X., 2002. The Arabidopsis Phospholipase D Family. Characterization of a Calcium-Independent and Phosphatidylcholine-Selective PLDζ1 with Distinct Regulatory Domains. Plant Physiology 128, 1057–1068. https://doi.org/10.1104/pp.010928

Qin, L., Zhou, Z., Li, Q., Zhai, C., Liu, L., Quilichini, T.D., Gao, P., Kessler, S.A., Jaillais, Y., Datla, R., Peng, G., Xiang, D., Wei, Y., 2020. Specific Recruitment of Phosphoinositide Species to the Plant-Pathogen Interfacial Membrane Underlies Arabidopsis Susceptibility to Fungal Infection[OPEN]. The Plant Cell 32, 1665–1688. https://doi.org/10.1105/tpc.19.00970

Qin, W., Pappan, K., Wang, X., 1997. Molecular Heterogeneity of Phospholipase D (PLD): CLONING OF PLDγ AND REGULATION OF PLANT PLDγ, -β, AND -α BY POLYPHOSPHOINOSITIDES AND CALCIUM*. Journal of Biological Chemistry 272, 28267–28273. https://doi.org/10.1074/jbc.272.45.28267

R Core Team, 2018. R: A Language and Environment for Statistical Computing.

Rajashekar, C.B., Zhou, H.-E., Zhang, Y., Li, W., Wang, X., 2006. Suppression of phospholipase Dα1 induces freezing tolerance in Arabidopsis: Response of cold-responsive genes and osmolyte accumulation. Journal of Plant Physiology 163, 916–926. https://doi.org/10.1016/j.jplph.2005.08.006

Rajjou, L., Belghazi, M., Huguet, R., Robin, C., Moreau, A., Job, C., Job, D., 2006. Proteomic Investigation of the Effect of Salicylic Acid on Arabidopsis Seed Germination and Establishment of Early Defense Mechanisms. Plant Physiology 141, 910–923. https://doi.org/10.1104/pp.106.082057

Ramamoorthy, R., Kumar, P.P., 2012. Molecular Genetic Strategies for Enhancing Plant Biomass for Cellulosic Ethanol Production, in: Baskar, C., Baskar, S., Dhillon, R.S. (Eds.), Biomass Conversion: The Interface of Biotechnology, Chemistry and Materials Science. Springer, Berlin, Heidelberg, pp. 237–250. https://doi.org/10.1007/978-3-642-28418-2_8

Raynaud, F.I., Eccles, S., Clarke, P.A., Hayes, A., Nutley, B., Alix, S., Henley, A., Di-Stefano, F., Ahmad, Z., Guillard, S., Bjerke, L.M., Kelland, L., Valenti, M., Patterson, L., Gowan, S., de Haven Brandon, A., Hayakawa, M., Kaizawa, H., Koizumi, T., Ohishi, T., Patel, S., Saghir, N., Parker, P., Waterfield, M., Workman, P., 2007. Pharmacologic Characterization of a Potent Inhibitor of Class I Phosphatidylinositide 3-Kinases. Cancer Research 67, 5840–5850. https://doi.org/10.1158/0008-5472.CAN-06-4615

Rekhter, D., Lüdke, D., Ding, Y., Feussner, K., Zienkiewicz, K., Lipka, V., Wiermer, M., Zhang, Y., Feussner, I., 2019. Isochorismate-derived biosynthesis of the plant stress hormone salicylic acid. Science 365, 498–502. https://doi.org/10.1126/science.aaw1720

Ren, H., Gao, K., Liu, Y., Sun, D., Zheng, S., 2017. The role of AtPLC3 and AtPLC9 in thermotolerance in Arabidopsis. Plant Signaling & Behavior 12, e1162368. https://doi.org/10.1080/15592324.2016.1162368

Retzer, K., Akhmanova, M., Konstantinova, N., Malínská, K., Leitner, J., Petrášek, J., Luschnig, C., 2019. Brassinosteroid signaling delimits root gravitropism via sorting of the Arabidopsis PIN2 auxin transporter. Nat Commun 10, 5516. https://doi.org/10.1038/s41467-019-13543-1

Retzer, K., Weckwerth, W., 2021. The TOR–Auxin Connection Upstream of Root Hair Growth. Plants 10, 150. https://doi.org/10.3390/plants10010150

Rigaill, G., Balzergue, S., Brunaud, V., Blondet, E., Rau, A., Rogier, O., Caius, J., Maugis-Rabusseau, C., Soubigou-Taconnat, L., Aubourg, S., Lurin, C., Martin-Magniette, M.-L., Delannoy, E., 2018. Synthetic data sets for the identification of key ingredients for RNA-seq differential analysis. Brief Bioinform 19, 65–76. https://doi.org/10.1093/bib/bbw092

Rivas-San Vicente, M., Plasencia, J., 2011. Salicylic acid beyond defence: its role in plant growth and development. Journal of Experimental Botany 62, 3321–3338. https://doi.org/10.1093/jxb/err031

Ross, A., Yamada, K., Hiruma, K., Yamashita-Yamada, M., Lu, X., Takano, Y., Tsuda, K., Saijo, Y., 2014. The Arabidopsis PEPR pathway couples local and systemic plant immunity. EMBO J 33, 62–75. https://doi.org/10.1002/embj.201284303

Ruan, J., Zhou, Y., Zhou, M., Yan, J., Khurshid, M., Weng, W., Cheng, J., Zhang, K., 2019. Jasmonic Acid Signaling Pathway in Plants. International Journal of Molecular Sciences 20, 2479. https://doi.org/10.3390/ijms20102479

Ruelland, E., Cantrel, C., Gawer, M., Kader, J.-C., Zachowski, A., 2002. Activation of Phospholipases C and D Is an Early Response to a Cold Exposure in Arabidopsis Suspension Cells. Plant Physiol 130, 999–1007. https://doi.org/10.1104/pp.006080

Ruelland, E., Pokotylo, I., Djafi, N., Cantrel, C., Repellin, A., Zachowski, A., 2014. Salicylic acid modulates levels of phosphoinositide dependent-phospholipase C substrates and products to remodel the Arabidopsis suspension cell transcriptome. Frontiers in Plant Science 5.

Russinova, E., Borst, J.-W., Kwaaitaal, M., Caño-Delgado, A., Yin, Y., Chory, J., Vries, S.C. de, 2004. Heterodimerization and Endocytosis of Arabidopsis Brassinosteroid Receptors BRI1 and AtSERK3 (BAK1). The Plant Cell 16, 3216–3229. https://doi.org/10.1105/tpc.104.025387

Ruzicka, K., Ljung, K., Vanneste, S., Podhorská, R., Beeckman, T., Friml, J., Benková, E., 2007. Ethylene Regulates Root Growth through Effects on Auxin Biosynthesis and Transport-Dependent Auxin Distribution. The Plant cell 19, 2197–212. https://doi.org/10.1105/tpc.107.052126

Ryu, H.-S., Han, M., Lee, S.-K., Cho, J.-I., Ryoo, N., Heu, S., Lee, Y.-H., Bhoo, S.H., Wang, G.-L., Hahn, T.-R., Jeon, J.-S., 2006. A comprehensive expression analysis of the WRKY gene superfamily in rice plants during defense response. Plant Cell Rep 25, 836–847. https://doi.org/10.1007/s00299-006-0138-1

Saboki, E., n.d. Pathogenesis Related (PR) Proteins in Plant Defense Mechanism.

Saini, S., Sharma, I., Kaur, N., Pati, P.K., 2013. Auxin: a master regulator in plant root development. Plant Cell Rep 32, 741–757. https://doi.org/10.1007/s00299-013-1430-5

Sakakibara, H., 2006. CYTOKININS: Activity, Biosynthesis, and Translocation. Annual Review of Plant Biology 57, 431–449. https://doi.org/10.1146/annurev.arplant.57.032905.105231

Sakurai, H.T., Inoue, T., Nakano, A., Ueda, T., 2016. Endosomal RAB effector with PX-domain, an Interacting Partner of RAB5 GTPases, Regulates Membrane Trafficking to Protein Storage Vacuoles in Arabidopsis. The Plant Cell 28, 1490–1503. https://doi.org/10.1105/tpc.16.00326

Sanchez, J.-P., Chua, N.-H., 2001. Arabidopsis PLC1 Is Required for Secondary Responses to Abscisic Acid Signals. The Plant Cell 13, 1143–1154. https://doi.org/10.1105/tpc.13.5.1143

Šašek, V., Janda, M., Delage, E., Puyaubert, J., Guivarc'h, A., López Maseda, E., Dobrev, P.I., Caius, J., Bóka, K., Valentová, O., Burketová, L., Zachowski, A., Ruelland, E., 2014. Constitutive salicylic acid accumulation in pi4kIIIβ1β2 Arabidopsis plants stunts rosette but not root growth. New Phytologist 203, 805–816. https://doi.org/10.1111/nph.12822

Schapire, A.L., Voigt, B., Jasik, J., Rosado, A., Lopez-Cobollo, R., Menzel, D., Salinas, J., Mancuso, S., Valpuesta, V., Baluska, F., Botella, M.A., 2008. Arabidopsis Synaptotagmin 1 Is Required for the Maintenance of Plasma Membrane Integrity and Cell Viability. The Plant Cell 20, 3374–3388. https://doi.org/10.1105/tpc.108.063859

Scheffzek, K., Welti, S., 2012. Pleckstrin homology (PH) like domains – versatile modules in protein–protein interaction platforms. FEBS Letters, Modular Protein Domains 586, 2662–2673. https://doi.org/10.1016/j.febslet.2012.06.006

Schilmiller, A.L., Last, R.L., Pichersky, E., 2008. Harnessing plant trichome biochemistry for the production of useful compounds. The Plant Journal 54, 702–711. https://doi.org/10.1111/j.1365-313X.2008.03432.x

Schindelin, J., Arganda-Carreras, I., Frise, E., Kaynig, V., Longair, M., Pietzsch, T., Preibisch, S., Rueden, C., Saalfeld, S., Schmid, B., Tinevez, J.-Y., White, D.J., Hartenstein, V., Eliceiri, K., Tomancak, P., Cardona, A., 2012. Fiji: an open-source platform for biological-image analysis. Nat Methods 9, 676–682. https://doi.org/10.1038/nmeth.2019

Schmelz, E.A., Carroll, M.J., LeClere, S., Phipps, S.M., Meredith, J., Chourey, P.S., Alborn, H.T., Teal, P.E.A., 2006. Fragments of ATP synthase mediate plant perception of insect attack. Proceedings of the National Academy of Sciences 103, 8894–8899. https://doi.org/10.1073/pnas.0602328103

Seguié-Simarro, J.M., Austin, J.R., II, White, E.A., Staehelin, L.A., 2004. Electron Tomographic Analysis of Somatic Cell Plate Formation in Meristematic Cells of Arabidopsis Preserved by High-Pressure Freezing[W]. The Plant Cell 16, 836–856. https://doi.org/10.1105/tpc.017749

Semeradova, H., Montesinos, J.C., Benkova, E., 2020. All Roads Lead to Auxin: Post-translational Regulation of Auxin Transport by Multiple Hormonal Pathways. Plant Communications, Focus Issue on Plant Hormones (Organizing Editors: Steven Smith, Jan Hejátko, Yonghong Wang, Daoxin Xie) 1, 100048. https://doi.org/10.1016/j.xplc.2020.100048

Shao, D., Smith, D.L., Kabbage, M., Roth, M.G., 2021. Effectors of Plant Necrotrophic Fungi. Frontiers in Plant Science 12.

Shinya, T., Yamaguchi, K., Desaki, Y., Yamada, K., Narisawa, T., Kobayashi, Y., Maeda, K., Suzuki, M., Tanimoto, T., Takeda, J., Nakashima, M., Funama, R., Narusaka, M., Narusaka, Y., Kaku, H., Kawasaki, T., Shibuya, N., 2014. Selective regulation of the chitin-induced defense response by the Arabidopsis receptor-like cytoplasmic kinase PBL27. The Plant Journal 79, 56–66. https://doi.org/10.1111/tpj.12535

Simon, M.L.A., Platre, M.P., Assil, S., van Wijk, R., Chen, W.Y., Chory, J., Dreux, M., Munnik, T., Jaillais, Y., 2014. A multi-colour/multi-affinity marker set to visualize phosphoinositide dynamics in Arabidopsis. The Plant Journal 77, 322–337. https://doi.org/10.1111/tpj.12358

Simon, S., Skůpa, P., Viaene, T., Zwiewka, M., Tejos, R., Klíma, P., Čarná, M., Rolčík, J., De Rycke, R., Moreno, I., Dobrev, P.I., Orellana, A., Zažímalová, E., Friml, J., 2016. PIN6 auxin transporter at endoplasmic reticulum and plasma membrane mediates auxin homeostasis and organogenesis in Arabidopsis. New Phytologist 211, 65–74. https://doi.org/10.1111/nph.14019

Singh, A., Kanwar, P., Pandey, A., Tyagi, A.K., Sopory, S.K., Kapoor, S., Pandey, G.K., 2013. Comprehensive genomic analysis and expression profiling of phospholipase C gene family during abiotic stresses and development in rice. PLoS One 8, e62494. https://doi.org/10.1371/journal.pone.0062494

Singh, R.S., Singh, U.S., 1988. Pathogenesis and host-parasite specificity in plant diseases. Gordon and Breach Science Pub.

Singh, S.K., Fischer, U., Singh, M., Grebe, M., Marchant, A., 2008. Insight into the early steps of root hair formation revealed by the procuste1 cellulose synthase mutant of Arabidopsis thaliana. BMC Plant Biology 8, 57. https://doi.org/10.1186/1471-2229-8-57

Sinha, M., Singh, R.P., Kushwaha, G.S., Iqbal, N., Singh, A., Kaushik, S., Kaur, P., Sharma, S., Singh, T.P., 2014. Current overview of allergens of plant pathogenesis related protein families. ScientificWorldJournal 2014, 543195. https://doi.org/10.1155/2014/543195

Song, J., Lee, M.H., Lee, G.-J., Yoo, C.M., Hwang, I., 2006. Arabidopsis EPSIN1 Plays an Important Role in Vacuolar Trafficking of Soluble Cargo Proteins in Plant Cells via Interactions with Clathrin, AP-1, VTI11, and VSR1. The Plant Cell 18, 2258–2274. https://doi.org/10.1105/tpc.105.039123

Song, W., Forderer, A., Yu, D., Chai, J., 2021. Structural biology of plant defence. New Phytologist 229, 692–711. https://doi.org/10.1111/nph.16906

Souza, C. de A., Li, S., Lin, A.Z., Boutrot, F., Grossmann, G., Zipfel, C., Somerville, S.C., 2017. Cellulose-Derived Oligomers Act as Damage-Associated Molecular Patterns and Trigger Defense-Like Responses. Plant Physiology 173, 2383–2398. https://doi.org/10.1104/pp.16.01680

Spaepen, S., Vanderleyden, J., 2011. Auxin and Plant-Microbe Interactions. Cold Spring Harb Perspect Biol 3, a001438. https://doi.org/10.1101/cshperspect.a001438

Splivallo, R., Fischer, U., Göbel, C., Feussner, I., Karlovsky, P., 2009. Truffles Regulate Plant Root Morphogenesis via the Production of Auxin and Ethylene. Plant Physiology 150, 2018–2029. https://doi.org/10.1104/pp.109.141325

Starodubtseva, A., Kalachova, T., Retzer, K., Jelínková, A., Dobrev, P., Lacek, J., Pospíchalová, R., Angelini, J., Guivarc'h, A., Pateyron, S., Soubigou-Taconnat, L., Burketová, L., Ruelland, E., 2022. An Arabidopsis mutant deficient in phosphatidylinositol-4-phosphate kinases ß1 and ß2 displays altered auxin-related responses in roots. Sci Rep 12, 6947. https://doi.org/10.1038/s41598-022-10458-8

Stegmann, M., Monaghan, J., Smakowska-Luzan, E., Rovenich, H., Lehner, A., Holton, N., Belkhadir, Y., Zipfel, C., 2017. The receptor kinase FER is a RALF-regulated scaffold controlling plant immune signaling. Science 355, 287–289. https://doi.org/10.1126/science.aal2541

Stein, M., Dittgen, J., Sánchez-Rodríguez, C., Hou, B.-H., Molina, A., Schulze-Lefert, P., Lipka, V., Somerville, S., 2006. Arabidopsis PEN3/PDR8, an ATP Binding Cassette Transporter, Contributes to Nonhost Resistance to Inappropriate Pathogens That Enter by Direct Penetration. The Plant Cell 18, 731–746. https://doi.org/10.1105/tpc.105.038372

Stenmark, H., Aasland, R., Toh, B.-H., D'Arrigo, A., 1996. Endosomal Localization of the Autoantigen EEA1 Is Mediated by a Zinc-binding FYVE Finger *. Journal of Biological Chemistry 271, 24048–24054. https://doi.org/10.1074/jbc.271.39.24048

Stenzel, I., Ischebeck, T., König, S., Hołubowska, A., Sporysz, M., Hause, B., Heilmann, I., 2008. The Type B Phosphatidylinositol-4-Phosphate 5-Kinase 3 Is Essential for Root Hair Formation in Arabidopsis thaliana. The Plant Cell 20, 124–141. https://doi.org/10.1105/tpc.107.052852

Stevenson, J.M., Perera, I.Y., Boss, W.F., 1998. A Phosphatidylinositol 4-Kinase Pleckstrin Homology Domain That Binds Phosphatidylinositol 4-Monophosphate. Journal of Biological Chemistry 273, 22761–22767. https://doi.org/10.1074/jbc.273.35.22761

Stintzi, A., Heitz, T., Prasad, V., Wiedemann-Merdinoglu, S., Kauffmann, S., Geoffroy, P., Legrand, M., Fritig, B., 1993. Plant 'pathogenesis-related' proteins and their role in defense against pathogens. Biochimie 75, 687–706. https://doi.org/10.1016/0300-9084(93)90100-7

Strahl, T., Thorner, J., 2007. Synthesis and function of membrane phosphoinositides in budding yeast, Saccharomyces cerevisiae. Biochim Biophys Acta 1771, 353–404. https://doi.org/10.1016/j.bbalip.2007.01.015

Sun, J., Xu, Y., Ye, S., Jiang, H., Chen, Q., Liu, F., Zhou, W., Chen, R., Li, X., Tietz, O., Wu, X., Cohen, J.D., Palme, K., Li, C., 2009. Arabidopsis ASA1 is important for jasmonate-mediated regulation of auxin biosynthesis and transport during lateral root formation. Plant Cell 21, 1495–1511. https://doi.org/10.1105/tpc.108.064303

Sun, T., Zhang, Y., 2021. Short- and long-distance signaling in plant defense. The Plant Journal 105, 505–517. https://doi.org/10.1111/tpj.15068

Sun, T., Zhang, Yaxi, Li, Y., Zhang, Q., Ding, Y., Zhang, Yuelin, 2015. ChIP-seq reveals broad roles of SARD1 and CBP60g in regulating plant immunity. Nat Commun 6, 10159. https://doi.org/10.1038/ncomms10159

Sun, Y., Han, Z., Tang, J., Hu, Z., Chai, C., Zhou, B., Chai, J., 2013a. Structure reveals that BAK1 as a co-receptor recognizes the BRI1-bound brassinolide. Cell Res 23, 1326–1329. https://doi.org/10.1038/cr.2013.131

Sun, Y., Li, L., Macho, A.P., Han, Z., Hu, Z., Zipfel, C., Zhou, J.-M., Chai, J., 2013b. Structural Basis for flg22-Induced Activation of the Arabidopsis FLS2-BAK1 Immune Complex. Science 342, 624–628. https://doi.org/10.1126/science.1243825

Svolacchia, N., Salvi, E., Sabatini, S., 2020. Arabidopsis primary root growth: let it grow, can't hold it back anymore! Current Opinion in Plant Biology, Cell signalling and gene regulation 57, 133–141. https://doi.org/10.1016/j.pbi.2020.08.005

Swarup, R., Parry, G., Graham, N., Allen, T., Bennett, M., 2002. Auxin cross-talk: integration of signalling pathways to control plant development. Plant Mol Biol 49, 411–426. https://doi.org/10.1007/978-94-010-0377-3_12

Szentpetery, Z., Szakacs, G., Bojjireddy, N., Tai, A.W., Balla, T., 2011. Genetic and functional studies of phosphatidyl-inositol 4-kinase type IIIα. Biochimica et Biophysica Acta (BBA) - Molecular and Cell Biology of Lipids 1811, 476–483. https://doi.org/10.1016/j.bbalip.2011.04.013

Szumlanski, A.L., Nielsen, E., 2010. Phosphatidylinositol 4-Phosphate is Required for Tip Growth in Arabidopsis thaliana, in: Munnik, T. (Ed.), Lipid Signaling in Plants, Plant Cell Monographs. Springer, Berlin, Heidelberg, pp. 65–77. https://doi.org/10.1007/978-3-642-03873-0_4

Takahashi, S., Monda, K., Higaki, T., Hashimoto-Sugimoto, M., Negi, J., Hasezawa, S., Iba, K., 2017. Differential Effects of Phosphatidylinositol 4-Kinase (PI4K) and 3-Kinase (PI3K) Inhibitors on Stomatal Responses to Environmental Signals. Front Plant Sci 8, 677. https://doi.org/10.3389/fpls.2017.00677

Takemoto, D., Jones, D.A., Hardham, A.R., 2006. Re-organization of the cytoskeleton and endoplasmic reticulum in the Arabidopsis pen1-1 mutant inoculated with the non-adapted powdery mildew pathogen, Blumeria graminis f. sp. hordei. Molecular Plant Pathology 7, 553–563. https://doi.org/10.1111/j.1364-3703.2006.00360.x

Tang, D., Ade, J., Frye, C.A., Innes, R.W., 2005. Regulation of plant defense responses in Arabidopsis by EDR2, a PH and START domain-containing protein. The Plant Journal 44, 245–257. https://doi.org/10.1111/j.1365-313X.2005.02523.x

Tang, J., Han, Z., Sun, Y., Zhang, H., Gong, X., Chai, J., 2015. Structural basis for recognition of an endogenous peptide by the plant receptor kinase PEPR1. Cell Res 25, 110–120. https://doi.org/10.1038/cr.2014.161

Tasma, I.M., Brendel, V., Whitham, S.A., Bhattacharyya, M.K., 2008. Expression and evolution of the phosphoinositide-specific phospholipase C gene family in Arabidopsis thaliana. Plant Physiology and Biochemistry 46, 627–637. https://doi.org/10.1016/j.plaphy.2008.04.015

Thain, S.C., Vandenbussche, F., Laarhoven, L.J.J., Dowson-Day, M.J., Wang, Z.-Y., Tobin, E.M., Harren, F.J.M., Millar, A.J., Van Der Straeten, D., 2004. Circadian Rhythms of Ethylene Emission in Arabidopsis. Plant Physiology 136, 3751–3761. https://doi.org/10.1104/pp.104.042523

Thordal-Christensen, H., 2003. Fresh insights into processes of nonhost resistance. Current Opinion in Plant Biology 6, 351–357. https://doi.org/10.1016/S1369-5266(03)00063-3

Tierens, K.F.M.-J., Thomma, B.P.H.J., Bari, R.P., Garmier, M., Eggermont, K., Brouwer, M., Penninckx, I.A.M.A., Broekaert, W.F., Cammue, B.P.A., 2002. Esa1, an Arabidopsis mutant with enhanced susceptibility to a range of necrotrophic fungal pathogens, shows a distorted induction of defense responses by reactive oxygen generating

compounds. The Plant Journal 29, 131–140. https://doi.org/10.1046/j.1365-313x.2002.01199.x

Torrens-Spence, M.P., Bobokalonova, A., Carballo, V., Glinkerman, C.M., Pluskal, T., Shen, A., Weng, J.-K., 2019. PBS3 and EPS1 complete salicylic acid biosynthesis from isochorismate in Arabidopsis. https://doi.org/10.1101/601948

Toshchakov, V.Y., Javmen, A., 2020. Targeting the TLR signalosome with TIR domain-derived cell-permeable decoy peptides: the current state and perspectives. Innate Immun 26, 35–47. https://doi.org/10.1177/1753425919844310

Truman, W., Bennett, M.H., Kubigsteltig, I., Turnbull, C., Grant, M., 2007. Arabidopsis systemic immunity uses conserved defense signaling pathways and is mediated by jasmonates. Proceedings of the National Academy of Sciences 104, 1075–1080. https://doi.org/10.1073/pnas.0605423104

Ueda, M., Tsutsumi, N., Fujimoto, M., 2016. Salt stress induces internalization of plasma membrane aquaporin into the vacuole in Arabidopsis thaliana. Biochemical and Biophysical Research Communications 474, 742–746. https://doi.org/10.1016/j.bbrc.2016.05.028

Ulmasov, T., Liu, Z.B., Hagen, G., Guilfoyle, T.J., 1995. Composite structure of auxin response elements. Plant Cell 7, 1611–1623. https://doi.org/10.1105/tpc.7.10.1611

Umemura, K., Tanino, S., Nagatsuka, T., Koga, J., Iwata, M., Nagashima, K., Amemiya, Y., 2004. Cerebroside Elicitor Confers Resistance to Fusarium Disease in Various Plant Species. Phytopathology® 94, 813–818. https://doi.org/10.1094/PHYTO.2004.94.8.813

Underwood, W., Somerville, S., 2008. Focal accumulation of defences at sites of fungal pathogen attack. Journal of experimental botany 59, 3501–8. https://doi.org/10.1093/jxb/ern205

van der Biezen, E.A., Jones, J.D., 1998. The NB-ARC domain: a novel signalling motif shared by plant resistance gene products and regulators of cell death in animals. Curr Biol 8, R226-227. https://doi.org/10.1016/s0960-9822(98)70145-9

van Leeuwen, W., Ökrész, L., Bögre, L., Munnik, T., 2004. Learning the lipid language of plant signalling. Trends in Plant Science 9, 378–384. https://doi.org/10.1016/j.tplants.2004.06.008

Van Leeuwen, W., Vermeer, J.E.M., Gadella Jr, T.W.J., Munnik, T., 2007. Visualization of phosphatidylinositol 4,5-bisphosphate in the plasma membrane of suspension-cultured tobacco BY-2 cells and whole Arabidopsis seedlings. The Plant Journal 52, 1014–1026. https://doi.org/10.1111/j.1365-313X.2007.03292.x

van Loon, L.C., Rep, M., Pieterse, C.M.J., 2006. Significance of inducible defense-related proteins in infected plants. Annu Rev Phytopathol 44, 135–162. https://doi.org/10.1146/annurev.phyto.44.070505.143425

Van Loon, L.C., Van Kammen, A., 1970. Polyacrylamide disc electrophoresis of the soluble leaf proteins from Nicotiana tabacum var. ‘Samsun’ and ‘Samsun NN’: II. Changes in protein constitution after infection with tobacco mosaic virus. Virology 40, 199–211. https://doi.org/10.1016/0042-6822(70)90395-8

Vlot, A.C., Dempsey, D.A., Klessig, D.F., 2009. Salicylic Acid, a Multifaceted Hormone to Combat Disease. Annu. Rev. Phytopathol. 47, 177–206. https://doi.org/10.1146/annurev.phyto.050908.135202

Vogelmann, K., Drechsel, G., Bergler, J., Subert, C., Philippar, K., Soll, J., Engelmann, J.C., Engelsdorf, T., Voll, L.M., Hoth, S., 2012. Early Senescence and Cell Death in Arabidopsis saul1 Mutants Involves the PAD4-Dependent Salicylic Acid Pathway. Plant Physiology 159, 1477–1487. https://doi.org/10.1104/pp.112.196220

Waghmare, S., Lileikyte, E., Karnik, R., Goodman, J.K., Blatt, M.R., Jones, A.M.E., 2018. SNAREs SYP121 and SYP122 Mediate the Secretion of Distinct Cargo Subsets1[OPEN]. Plant Physiol 178, 1679–1688. https://doi.org/10.1104/pp.18.00832

Waldie, T., Leyser, O., 2018. Cytokinin Targets Auxin Transport to Promote Shoot Branching. Plant Physiology 177, 803–818. https://doi.org/10.1104/pp.17.01691

Wan, J., Tanaka, K., Zhang, X.-C., Son, G.H., Brechenmacher, L., Nguyen, T.H.N., Stacey, G., 2012. LYK4, a Lysin Motif Receptor-Like Kinase, Is Important for Chitin Signaling and Plant Innate Immunity in Arabidopsis. Plant Physiology 160, 396–406. https://doi.org/10.1104/pp.112.201699

Wan, J., Zhang, X.-C., Neece, D., Ramonell, K.M., Clough, S., Kim, S., Stacey, M.G., Stacey, G., 2008. A LysM Receptor-Like Kinase Plays a Critical Role in Chitin Signaling and Fungal Resistance in Arabidopsis. The Plant Cell 20, 471–481. https://doi.org/10.1105/tpc.107.056754

Wang, C., Wang, X., 2001. A Novel Phospholipase D of Arabidopsis That Is Activated by Oleic Acid and Associated with the Plasma Membrane. Plant Physiology 127, 1102–1112. https://doi.org/10.1104/pp.010444

Wang, C., Zien, C.A., Afitlhile, M., Welti, R., Hildebrand, D.F., Wang, X., 2000. Involvement of Phospholipase D in Wound-Induced Accumulation of Jasmonic Acid in Arabidopsis. The Plant Cell 12, 2237–2246. https://doi.org/10.1105/tpc.12.11.2237

Wang, D., Amornsiripanitch, N., Dong, X., 2006. A Genomic Approach to Identify Regulatory Nodes in the Transcriptional Network of Systemic Acquired Resistance in Plants. PLOS Pathogens 2, e123. https://doi.org/10.1371/journal.ppat.0020123

Wang, L., Einig, E., Almeida-Trapp, M., Albert, M., Fliegmann, J., Mithöfer, A., Kalbacher, H., Felix, G., 2018. The systemin receptor SYR1 enhances resistance of tomato against herbivorous insects. Nature Plants 4, 152–156. https://doi.org/10.1038/s41477-018-0106-0

Wang, W.-M., Liu, P.-Q., Xu, Y.-J., Xiao, S., 2016. Protein trafficking during plant innate immunity. Journal of Integrative Plant Biology 58, 284–298. https://doi.org/10.1111/jipb.12426

Wang, X., 2002. Phospholipase D in hormonal and stress signaling. Current Opinion in Plant Biology 5, 408–414. https://doi.org/10.1016/S1369-5266(02)00283-2

Wang, X., 2000. Multiple forms of phospholipase D in plants: the gene family, catalytic and regulatory properties, and cellular functions. Progress in Lipid Research 39, 109–149. https://doi.org/10.1016/S0163-7827(00)00002-3

Wang, X., Chory, J., 2006. Brassinosteroids Regulate Dissociation of BKI1, a Negative Regulator of BRI1 Signaling, from the Plasma Membrane. Science. https://doi.org/10.1126/science.1127593

Wang, X., Hou, S., Wu, Q., Lin, M., Acharya, B.R., Wu, D., Zhang, W., 2017. IDL6-HAE/HSL2 impacts pectin degradation and resistance to Pseudomonas syringae pv tomato DC3000 in Arabidopsis leaves. The Plant Journal 89, 250–263. https://doi.org/10.1111/tpj.13380

Wang, X., Kota, U., He, K., Blackburn, K., Li, J., Goshe, M.B., Huber, S.C., Clouse, S.D., 2008. Sequential Transphosphorylation of the BRI1/BAK1 Receptor Kinase Complex Impacts Early Events in Brassinosteroid Signaling. Developmental Cell 15, 220–235. https://doi.org/10.1016/j.devcel.2008.06.011

Wang, X., Li, X., Meisenhelder, J., Hunter, T., Yoshida, S., Asami, T., Chory, J., 2005. Autoregulation and Homodimerization Are Involved in the Activation of the Plant Steroid Receptor BRI1. Developmental Cell 8, 855–865. https://doi.org/10.1016/j.devcel.2005.05.001

Welters, P., Takegawa, K., Emr, S.D., Chrispeels, M.J., 1994. AtVPS34, a phosphatidylinositol 3-kinase of Arabidopsis thaliana, is an essential protein with homology to a calcium-dependent lipid binding domain. Proc Natl Acad Sci U S A 91, 11398–11402. https://doi.org/10.1073/pnas.91.24.11398

Wen, X., Zhang, C., Ji, Y., Zhao, Q., He, W., An, F., Jiang, L., Guo, H., 2012. Activation of ethylene signaling is mediated by nuclear translocation of the cleaved EIN2 carboxyl terminus. Cell Res 22, 1613–1616. https://doi.org/10.1038/cr.2012.145

Werner, T., Schmülling, T., 2009. Cytokinin action in plant development. Current Opinion in Plant Biology, Cell signalling and gene regulation 12, 527–538. https://doi.org/10.1016/j.pbi.2009.07.002

Wierzba, M.P., Tax, F.E., 2016. An Allelic Series of bak1 Mutations Differentially Alter bir1 Cell Death, Immune Response, Growth, and Root Development Phenotypes in Arabidopsis thaliana. Genetics 202, 689–702. https://doi.org/10.1534/genetics.115.180380

Wildermuth, M.C., Dewdney, J., Wu, G., Ausubel, F.M., 2001. Isochorismate synthase is required to synthesize salicylic acid for plant defence. Nature 414, 562–565. https://doi.org/10.1038/35107108

Willmann, R., Lajunen, H.M., Erbs, G., Newman, M.-A., Kolb, D., Tsuda, K., Katagiri, F., Fliegmann, J., Bono, J.-J., Cullimore, J.V., Jehle, A.K., Götz, F., Kulik, A., Molinaro, A., Lipka, V., Gust, A.A., Nürnberger, T., 2011. Arabidopsis lysin-motif proteins LYM1 LYM3 CERK1 mediate bacterial peptidoglycan sensing and immunity to bacterial infection. Proceedings of the National Academy of Sciences 108, 19824–19829. https://doi.org/10.1073/pnas.1112862108

Wiszniewski, A.A.G., Bussell, J.D., Long, R.L., Smith, S.M., 2014. Knockout of the two evolutionarily conserved peroxisomal 3-ketoacyl-CoA thiolases in Arabidopsis recapitulates the abnormal inflorescence meristem 1 phenotype. J Exp Bot 65, 6723–6733. https://doi.org/10.1093/jxb/eru397

Wittstock, U., Halkier, B.A., 2002. Glucosinolate research in the Arabidopsis era. Trends in Plant Science 7, 263–270. https://doi.org/10.1016/S1360-1385(02)02273-2

Wrzaczek, M., Vainonen, J.P., Stael, S., Tsiatsiani, L., Help-Rinta-Rahko, H., Gauthier, A., Kaufholdt, D., Bollhöner, B., Lamminmäki, A., Staes, A., Gevaert, K., Tuominen, H., Van Breusegem, F., Helariutta, Y., Kangasjärvi, J., 2015. GRIM REAPER peptide binds to receptor kinase PRK5 to trigger cell death in Arabidopsis. EMBO J 34, 55–66. https://doi.org/10.15252/embj.201488582

Wu, L., Sadhukhan, A., Kobayashi, Y., Ogo, N., Tokizawa, M., Agrahari, R.K., Ito, H., Iuchi, S., Kobayashi, M., Asai, A., Koyama, H., 2019. Involvement of phosphatidylinositol metabolism in aluminum-induced malate secretion in Arabidopsis. Journal of Experimental Botany 70, 3329–3342. https://doi.org/10.1093/jxb/erz179

Xia, K., Wang, B., Zhang, J., Li, Y., Yang, H., Ren, D., 2017. Arabidopsis phosphoinositide-specific phospholipase C 4 negatively regulates seedling salt tolerance. Plant, Cell & Environment 40, 1317–1331. https://doi.org/10.1111/pce.12918

Xing, J., Li, X., Wang, X., Lv, X., Wang, L., Zhang, L., Zhu, Y., Shen, Q., Baluška, F., Šamaj, J., Lin, J., 2019. Secretion of Phospholipase DΔ Functions as a Regulatory Mechanism in Plant Innate Immunity. The Plant Cell 31, 3015–3032. https://doi.org/10.1105/tpc.19.00534

Xing, J., Zhang, L., Duan, Z., Lin, J., 2021. Coordination of Phospholipid-Based Signaling and Membrane Trafficking in Plant Immunity. Trends in Plant Science 26, 407–420. https://doi.org/10.1016/j.tplants.2020.11.010

Xiong, L., Lee, B.-H., Ishitani, M., Lee, H., Zhang, C., Zhu, J.-K., 2001. FIERY1 encoding an inositol polyphosphate 1-phosphatase is negative regulator of abscisic acid and

stress signaling in Arabidopsis. Genes and Development 15, 1971–1984. https://doi.org/10.1101/gad.891901

Xu, F., Zhu, C., Cevik, V., Johnson, K., Liu, Y., Sohn, K., Jones, J.D., Holub, E.B., Li, X., 2015. Autoimmunity conferred by chs3-2D relies on CSA1, its adjacent TNL-encoding neighbour. Sci Rep 5, 8792. https://doi.org/10.1038/srep08792

Yamaguchi, K., Mezaki, H., Fujiwara, M., Hara, Y., Kawasaki, T., 2017. Arabidopsis ubiquitin ligase PUB12 interacts with and negatively regulates Chitin Elicitor Receptor Kinase 1 (CERK1). PLOS ONE 12, e0188886. https://doi.org/10.1371/journal.pone.0188886

Yamaoka, Y., Shin, S., Lee, Yuree, Ito, M., Lee, Youngsook, Nishida, I., 2021. Phosphatidylserine Is Required for the Normal Progression of Cell Plate Formation in Arabidopsis Root Meristems. Plant and Cell Physiology 62, 1396–1408. https://doi.org/10.1093/pcp/pcab086

Yamaryo, Y., Dubots, E., Albrieux, C., Baldan, B., Block, M.A., 2008. Phosphate availability affects the tonoplast localization of PLDzeta2, an Arabidopsis thaliana phospholipase D. FEBS Lett 582, 685–690. https://doi.org/10.1016/j.febslet.2008.01.039

Yan, H., Yoo, M.-J., Koh, J., Liu, L., Chen, Y., Acikgoz, D., Wang, Q., Chen, S., 2014. Molecular Reprogramming of Arabidopsis in Response to Perturbation of Jasmonate Signaling. J. Proteome Res. 13, 5751–5766. https://doi.org/10.1021/pr500739v

Yang, H., Li, Y., Hua, J., 2006. The C2 domain protein BAP1 negatively regulates defense responses in Arabidopsis. The Plant Journal 48, 238–248. https://doi.org/10.1111/j.1365-313X.2006.02869.x

Yang, L., Qin, L., Liu, G., Peremyslov, V.V., Dolja, V.V., Wei, Y., 2014. Myosins XI modulate host cellular responses and penetration resistance to fungal pathogens. PNAS 111, 13996–14001. https://doi.org/10.1073/pnas.1405292111

Yang, N., Zhang, Y., Chen, L., Wang, W., Liu, R., Gao, R., Zhou, Y., Li, H., 2021. G protein and PLDδ are involved in JA to regulate osmotic stress responses in Arabidopsis thaliana. Biochemistry and Biophysics Reports 26, 100952. https://doi.org/10.1016/j.bbrep.2021.100952

Yang, S., Hua, J., 2004. A Haplotype-Specific Resistance Gene Regulated by BONZAI1 Mediates Temperature-Dependent Growth Control in Arabidopsis. The Plant Cell 16, 1060–1071. https://doi.org/10.1105/tpc.020479

Yang, Y., Han, X., Ma, L., Wu, Y., Liu, X., Fu, H., Liu, G., Lei, X., Guo, Y., 2021. Dynamic changes of phosphatidylinositol and phosphatidylinositol 4-phosphate levels modulate H+-ATPase and Na+/H+ antiporter activities to maintain ion homeostasis in Arabidopsis under salt stress. Molecular Plant 14, 2000–2014. https://doi.org/10.1016/j.molp.2021.07.020

Yeung, T., Heit, B., Dubuisson, J.-F., Fairn, G.D., Chiu, B., Inman, R., Kapus, A., Swanson, M., Grinstein, S., 2009. Contribution of phosphatidylserine to membrane surface charge and protein targeting during phagosome maturation. Journal of Cell Biology 185, 917–928. https://doi.org/10.1083/jcb.200903020

Yu, Z., Duan, X., Luo, L., Dai, S., Ding, Z., Xia, G., 2020. How Plant Hormones Mediate Salt Stress Responses. Trends in Plant Science 25, 1117–1130. https://doi.org/10.1016/j.tplants.2020.06.008

Zaynab, M., Fatima, M., Sharif, Y., Zafar, M.H., Ali, H., Khan, K.A., 2019. Role of primary metabolites in plant defense against pathogens. Microbial Pathogenesis 137, 103728. https://doi.org/10.1016/j.micpath.2019.103728

Zhang, D.-W., Deng, X.-G., Fu, F.-Q., Lin, H.-H., 2015. Induction of plant virus defense response by brassinosteroids and brassinosteroid signaling in Arabidopsis thaliana. Planta 241, 875–885. https://doi.org/10.1007/s00425-014-2218-8

Zhang, J., Zhou, J.-M., 2010. Plant immunity triggered by microbial molecular signatures. Mol Plant 3, 783–793. https://doi.org/10.1093/mp/ssq035

Zhang, Q., van Wijk, R., Shahbaz, M., Roels, W., Schooten, B. van, Vermeer, J.E.M., Zarza, X., Guardia, A., Scuffi, D., García-Mata, C., Laha, D., Williams, P., Willems, L.A.J., Ligterink, W., Hoffmann-Benning, S., Gillaspy, G., Schaaf, G., Haring, M.A., Laxalt, A.M., Munnik, T., 2018. Arabidopsis Phospholipase C3 is Involved in Lateral Root Initiation and ABA Responses in Seed Germination and Stomatal Closure. Plant and Cell Physiology 59, 469–486. https://doi.org/10.1093/pcp/pcx194

Zhang, X.G., Coté, G.G., Crain, R.C., 2002. Involvement of phosphoinositide turnover in tracheary element differentiation in Zinnia elegans L. cells. Planta 215, 312–318. https://doi.org/10.1007/s00425-002-0739-z

Zhang, Yaxi, Yang, Y., Fang, B., Gannon, P., Ding, P., Li, X., Zhang, Yuelin, 2010. Arabidopsis snc2-1D Activates Receptor-Like Protein-Mediated Immunity Transduced through WRKY70[C][W]. Plant Cell 22, 3153–3163. https://doi.org/10.1105/tpc.110.074120

Zhao, J., Devaiah, S.P., Wang, C., Li, M., Welti, R., Wang, X., 2013. Arabidopsis phospholipase Dβ1 modulates defense responses to bacterial and fungal pathogens. New Phytologist 199, 228–240. https://doi.org/10.1111/nph.12256

Zhao, J., Wang, X., 2004. Arabidopsis Phospholipase Dα1 Interacts with the Heterotrimeric G-protein α-Subunit through a Motif Analogous to the DRY Motif in G-protein-coupled Receptors *. Journal of Biological Chemistry 279, 1794–1800. https://doi.org/10.1074/jbc.M309529200

Zhao, Y., Yan, A., Feijó, J.A., Furutani, M., Takenawa, T., Hwang, I., Fu, Y., Yang, Z., 2010. Phosphoinositides Regulate Clathrin-Dependent Endocytosis at the Tip of Pollen Tubes in Arabidopsis and Tobacco[W]. Plant Cell 22, 4031–4044. https://doi.org/10.1105/tpc.110.076760

Zhou, J., Liu, D., Wang, P., Ma, X., Lin, W., Chen, S., Mishev, K., Lu, D., Kumar, R., Vanhoutte, I., Meng, X., He, P., Russinova, E., Shan, L., 2018. Regulation of Arabidopsis brassinosteroid receptor BRI1 endocytosis and degradation by plant U-box PUB12/PUB13-mediated ubiquitination. Proceedings of the National Academy of Sciences 115, E1906–E1915. https://doi.org/10.1073/pnas.1712251115

Zhou, J.-J., Luo, J., 2018. The PIN-FORMED Auxin Efflux Carriers in Plants. International Journal of Molecular Sciences 19, 2759. https://doi.org/10.3390/ijms19092759

Zhou, M., Lu, Y., Bethke, G., Harrison, B.T., Hatsugai, N., Katagiri, F., Glazebrook, J., 2018. WRKY70 prevents axenic activation of plant immunity by direct repression of SARD1. New Phytologist 217, 700–712. https://doi.org/10.1111/nph.14846

Zhou, Y., Yang, Y., Niu, Y., Fan, T., Qian, D., Luo, C., Shi, Y., Li, S., An, L., Xiang, Y., 2020. The Tip-Localized Phosphatidylserine Established by Arabidopsis ALA3 Is Crucial for Rab GTPase-Mediated Vesicle Trafficking and Pollen Tube Growth. Plant Cell 32, 3170–3187. https://doi.org/10.1105/tpc.19.00844

Zhou, Z., Zhao, Y., Bi, G., Liang, X., Zhou, J.-M., 2019. Early signalling mechanisms underlying receptor kinase-mediated immunity in plants. Philosophical Transactions of the Royal Society B: Biological Sciences 374, 20180310. https://doi.org/10.1098/rstb.2018.0310

Zhu, T., 2003. A browser-based functional classification SuperViewer for Arabidopsis genomics.

Zhu, Z., Xu, F., Zhang, Yaxi, Cheng, Y.T., Wiermer, M., Li, X., Zhang, Yuelin, 2010. Arabidopsis resistance protein SNC1 activates immune responses through association with a transcriptional corepressor. Proceedings of the National Academy of Sciences 107, 13960–13965. https://doi.org/10.1073/pnas.1002828107

Ziemann, S., van der Linde, K., Lahrmann, U., Acar, B., Kaschani, F., Colby, T., Kaiser, M., Ding, Y., Schmelz, E., Huffaker, A., Holton, N., Zipfel, C., Doehlemann, G., 2018. An apoplastic peptide activates salicylic acid signalling in maize. Nature Plants 4, 172–180. https://doi.org/10.1038/s41477-018-0116-y

Zimmermann, P., Hirsch-Hoffmann, M., Hennig, L., Gruissem, W., 2004. GENEVESTIGATOR. Arabidopsis Microarray Database and Analysis Toolbox. Plant Physiology 136, 2621–2632. https://doi.org/10.1104/pp.104.046367

Zipfel, C., 2014. Plant pattern-recognition receptors. Trends in Immunology 35, 345–351. https://doi.org/10.1016/j.it.2014.05.004

Zipfel, C., Kunze, G., Chinchilla, D., Caniard, A., Jones, J.D.G., Boller, T., Felix, G., 2006. Perception of the bacterial PAMP EF-Tu by the receptor EFR restricts Agrobacterium-mediated transformation. Cell 125, 749–760. https://doi.org/10.1016/j.cell.2006.03.037

Zürcher, E., Müller, B., 2016. Cytokinin Synthesis, Signaling, and Function—Advances and New Insights, in: Jeon, K.W. (Ed.), International Review of Cell and Molecular Biology, International Review of Cell and Molecular Biology. Academic Press, pp. 1–38. https://doi.org/10.1016/bs.ircmb.2016.01.001

Zwiewka, M., Bilanovičová, V., Seifu, Y.W., Nodzyński, T., 2019. The Nuts and Bolts of PIN Auxin Efflux Carriers. Frontiers in Plant Science 10.

8. ABBREVIATIONS

PI4Ks	phosphatidylinositol 4 kinases
PPI	phosphoinositides
PI	phosphatidylinositol
PI4P	phosphatidylinositol-4-phosphate
PI(4,5)P2	phosphatidylinositol-4,5-bisphosphate
IAA	indole-3-acetic acid
Bgh	*Blumeria graminis* f. sp *hordei*
hpi	hour post inoculation
SA	salicylic acid
PTI	PRR-triggered immunity
ETI	effector-triggered immunity
P. syringae	*Pseudomonas syringae* pv. *tomato* DC3000
ROPs	Rho-like GTPase
PM	plasma membrane
PLCs	phospholipases C
PLDs	phospholipases D
PI(4,5)K	phosphatidylinositol-4,5-kinases
PA	phosphatidic acid
PC	phosphatidylcholine
PS	phosphatidylserine
PE	phosphatidylethanolamine
PG	phosphatidylglycerol
PI3P	phosphatidylinositol-3-phosphate
PI(3,5)P2	phosphatidylinositol-3,5-bisphosphate
TGN	trans-Golgi network
WM	wortmannin
PAO	phenylarsine oxide
LKU	lipid kinase unique
PH	pleckstrin homology
NH	novel homology
UBL	ubiquitin-like domains
GTPases	guanosine triphosphatases
CSCs	cellulose synthase complexes
CESAs	cellulose synthase catalytic subunits
DAG	diacylglycerol
IP3	inositol 1,4,5-trisphosphate
ABA	abscisic acid
CK	cytokinins
Bl	brassinolide
GA	gibberellic acid
IAA	indolacetic acid
ET	ethylene
MeJa	methyl jasmonate
DGK	diacylglycerol kinases
DREB2	dehydration responsive element binding protein 2
WT	wild type
PH	Pleckstrin Homology

PX	Phox homology
ENTH	Epsin N-Terminal Homology
C2	conserved region-2 of protein kinase C
DRPs	dynamin-related proteins
EDR1	enhanced disease resistance
OBP	oxysterol-binding protein
RCC	regulator of chromosome condensation
ANK	ankyrin repeats
BAR	Bin/Amphiphysin/Rvs domain
GED	GTPase Effector Domain
OxysterolBP	oxysterol-binding protein
RhoGAP	Rho GTPase activating protein domain
ARFGAP	ARF GTPase–activating protein
S/T kinases	serine-threonine protein kinase catalytic domains
START	steroidogenic acute regulatory protein-related lipid-transfer
ADL6	Arabidopsis dynamin-like 6
SNX	sorting nexin-like
ANTH	AP180 N-terminal homology
epsinR	epsin-related
SYT1	synaptotagmin 1 protein
PBR	PI(4,5)P2 binding region
JA	jasmonic acid
PAMPs	pathogen associated molecular patterns
PRRs	pattern recognition receptors
NLRs	nucleotide-binding domain leucine-rich repeat receptors
MAMPs	microbe-associated molecular patterns
DAMPs	danger associated molecular patterns
ROS	reactive oxygen species
EF-Tu	Elongation Factor-Tu
CSP	cold shock proteins
RLKs	receptor-like kinases
RLPs	receptor-like proteins
LRR	leucine-rich repeat
LysM	lysin motif
WAK	wall-associated kinase
BRI1	BRASSINOSTEROID INSENSITIVE 1
Pep1	plant elicitor peptide 1
CERK1	chitin elicitor receptor kinase1
LYK	Lysine motif receptor kinase
MAPK	mitogen-activated protein kinase
BAK1	BRI1-associated receptor kinase 1
BR	brassinosteroid
CC	coiled-coil
TIR	Toll/interleukin-1 receptor
SNC1	suppressor of npr1-1, constitutive 1
NPR1	NONEXPRESSOR OF PR GENES1
EDS1	enhanced disease susceptibility1
NDR1	non-race-specific disease resistance 1
IC	isochorismate
PAL	phenylalanine ammonia-lyase

ICS	isochorismate synthase
tCA	trans-cinnamic acid
BA	benzoic acid
TF	transcription factors
PR	pathogenesis-related
CTR1	constitutive triple response 1
PAA	phenylacetic acid
iP	N 6-(Δ2-isopentenyl)adenine
tZ	trans-zeatin
cZ	cis-zeatin
AHPs	*A. thaliana* histidine-containing phosphotransfer proteins
ARRs	*A. thaliana* response regulators
BSU1	BRI1 suppressor1
BSL1-3	BSU1-Like 1-3
BIN2	Brassinosteroid-Insensitive 2
CMV	cucumber mosaic virus
SCN	stem cell niches
DZ	division zone
EZ	elongation zone
DiffZ	differentiation zone
TZ	transition zone
GA	gibberellin
SHY2	*Short hypocotyl2*
BRX	*BRAVIS RADIX*
SAR	systemic acquired resistance
ISR	induced systemic resistance
dpi	days post-inoculation
PEN	PENETRATION
PCR	polymerase chain reaction
qPCR	real-time polymerase chain reaction
RNA-Seq	RNA sequencing
BAP	6-benzylaminopurine